

**Bone Tissue Engineering Using High Permeability Poly- ϵ -caprolactone Scaffolds
Conjugated with Bone Morphogenetic Protein-2**

by

Anna Guyer Mitsak

A dissertation submitted in partial fulfillment
of the requirements for the degree of
Doctor of Philosophy
(Biomedical Engineering)
in The University of Michigan
2012

Doctoral Committee:

Professor Scott J. Hollister, Chair
Professor Paul H. Krebsbach
Assistant Professor Mohamed E. H. El-Sayed
Professor Matthew B. Wheeler, University of Illinois at Urbana-Champaign

© Anna Guyer Mitsak

2012

To my parents, whose love, support and patience have gotten me to where I am today.

ACKNOWLEDGEMENTS

Early on in graduate school, a professor told me that graduate school would be some of the best years of my life. At the time, I was struggling to get my experiments running and frustration was the emotion I experienced most, so I had a hard time believing the professor's words. While frustration was always present due to broken equipment, finicky cells and ELISAs that seemed doomed to failure, these and other challenges taught me how to solve problems, think critically and creatively and to persevere in the face of adversity. My involvement in global health and medical device design rounded out my graduate experience and enabled me to meet many wonderful people. Thus, despite the challenges that come with being a PhD student, I have realized that my years at the University of Michigan have indeed been some of the greatest years of my life. My sincerest gratitude goes out to all of the people who have mentored, supported and believed in me every step of the way.

I'd first like to thank my advisor, Dr. Scott Hollister, for welcoming me into his lab and supporting me through the many twists and turns of project formulation and reformulation. While always there to provide guidance, he also gave me the freedom to create my own research path, which challenged me to think independently and creatively. Thank you for sharing your insight and advice, and for always believing in me and encouraging me to stay positive. My committee members have also been wonderful mentors throughout the PhD process. Thank you to Paul Kresbach, Mohamed El-Sayed

and Matt Wheeler for sharing not only your scientific know-how but also your compassion and support over the past several years. I am honored to have worked with all of you and appreciate your guidance.

Successful research cannot be undertaken independently, and my project would not have been completed without the tremendous support of past and present members of the Scaffold Tissue Engineering Group. Thank you to: Shelley Brown, Sitaram Chivukula, Marta Dias, Alisha Diggs, Andrew Dunn, Colleen Flanagan, Matt Harris, Claire Jeong, Hee Suk Kang, Jessica Kemppainen, Elly Liao, Francesco Migneco, Erin Moffitt, Chan-Ho Park, Janki Patel, Eiji Saito, Auresa Thomas, Frank Winterroth, Darice Wong and Huina Zhang. You all were an incredible support system and were always there when I needed someone to help in the lab or participate in a brainstorming session. Special thanks to Jessica Kemppainen who went out of her way to teach and mentor me when I first joined the lab and to Colleen Flanagan for lending an ear when I needed to vent and placing many an urgent order! To the undergraduate and Master's students who assisted me – Matt Harris, Sitaram Chivukula and Andy Dunn: thank you for enduring long hours of scaffold manufacturing, mechanical testing and cell culturing. My research would not have been completed without all of their help completing these (often tedious) tasks.

I'd like to thank the BME department for their support in handling the logistics of graduate school, especially Maria Steele and Katharine Guarino for working out the many scheduling and funding kinks that are inevitably encountered during the PhD process. Thank you to my fellow LBME occupants, especially the Stegeman, El-Sayed, Putnam, Mayer labs, for lending equipment or a helping hand when needed and creating

an inviting and fun atmosphere to work in. Special thanks to Ram Rao for lending numerous reagents and protocols, both of which helped me tremendously in the last few months of my PhD. I am also grateful to the Orthopedic Research Lab and the Dental School Histology Core for providing necessary resources without which I would not have been able to complete my research.

While most of my time over the past 6 years was spent in the lab, I also spent many hours participating in various extracurricular activities. I am grateful to all of the wonderful people I met through my involvement with M-HEAL, the Center for Global Health, the Graduate Student Advisory Committee and the BME Graduate Student Council. I extend my sincere gratitude to Aileen Huang-Saad, for not only being a wonderful faculty advisor to M-HEAL and my SureSecure design team, but for also being an amazing personal mentor to me as I struggled through research hurdles and career planning. Thank you for always supporting and believing in me.

I would like to thank all of my friends for their unwavering love, support and patience; I am truly lucky to have all of you in my life. To my Michigan friends, especially Becca, Alissa, Nathaniel, Allyson and Erin, you all have been an amazing support system for me and I thank you for all of the wonderful memories cooking, running, swimming, biking, shopping, Glee-watching and dancing. To the “Broads”: thank you for the nights out, the tailgates and brunches and the chipatis, and for always encouraging me through the PhD process. Thank you to my UVA girls – Emily, Erica, Ashley and Katie – for your lasting friendship and all of the emails, phone calls and visits to Ann Arbor that never failed to lift my spirits and bolster my confidence. I’d also like to thank Team Vanguard, my sailing team, for welcoming me to the team and being patient

as I learned how to sail. You all are a great group of people and I am grateful to have shared so many great memories on the water with you!

Finally, I extend my heartfelt appreciation and thanks to my family for their love and support and for always encouraging me to dream big. Thank you to my parents for giving me a strong foundation upon which to grow and for always pushing me to be my best. I appreciate your many visits to Ann Arbor as well as the many care packages and cards that always brought a smile to my face. To Megan, Stevie and Brian, your visits to Ann Arbor were always a fun break from the lab and I thank you for being patient and offering encouragement as I navigated through graduate school. Lastly, thank you to Douglas, for being my biggest fan and believing in me even when I barely believed in myself. Your love and support has meant the world to me and I can't see what the future holds for us!

TABLE OF CONTENTS

Dedication.....	ii
Acknowledgements.....	iii
List of Figures.....	x
List of Tables.....	xi
Abstract.....	xii
Chapter 1 Introduction.....	1
1.1 Problem Statement.....	1
1.2 Clinical State of the Art: Repairing Bone Defects.....	2
1.3 Scaffold Tissue Engineering.....	6
1.4 Thesis Aims.....	9
1.5 Dissertation Contents.....	12
1.6 References.....	14
Chapter 2 Bone: Development, Regeneration and Characteristics.....	18
2.1 Bone Development: Endochondral v. Intramembranous Ossification.....	18
2.2 The Role of Bone Morphogenetic Proteins in Bone Development and Remodeling ..	21
2.3 Bone and Cartilage Gene Expression.....	27
2.4 Conclusion.....	31
2.5 References.....	31
Chapter 3 Scaffold Tissue Engineering: Developing a Complete System for Repairing and Regenerating Bone.....	37
3.1 Introduction.....	37
3.2 Materials for Effective Scaffolds.....	38
3.3 Scaffold Architecture Considerations.....	42
3.4 Additional Factors.....	46
3.5 Conclusion.....	53
3.6 References.....	54
Chapter 4 The Effect of Polycaprolactone Scaffold Permeability on Bone Regeneration <i>In Vivo</i>	63
4.1 Introduction.....	63
4.2 Materials and Methods.....	67
4.3 Results.....	71

4.4	Discussion.....	79
4.5	Conclusions.....	84
4.6	Acknowledgements.....	84
4.7	References.....	84
Chapter 5 <i>In Vitro</i> Differentiation of Human Adipose Derived Stem Cells and Bone Marrow Stromal Cells on PCL Scaffolds Conjugated with rhBMP-2.....		88
5.1	Introduction.....	88
5.2	Materials and Methods.....	93
5.3	Results.....	101
5.4	Discussion.....	112
5.5	Conclusion.....	118
5.6	Acknowledgements.....	119
5.7	References.....	120
Chapter 6 <i>In Vivo</i> Bone Regeneration by Human Adipose Derived Stem Cells and Bone Marrow Stromal Cells on PCL Scaffolds Conjugated with rhBMP-2.....		127
6.1	Introduction.....	127
6.2	Materials and Methods.....	131
6.3	Results.....	135
6.4	Discussion.....	141
6.5	Conclusion.....	148
6.6	Acknowledgements.....	149
6.7	References.....	150
Chapter 7 Evaluating Three Methods of Attaching rhBMP-2 to Polycaprolactone Scaffolds.....		156
7.1	Introduction.....	156
7.2	Materials and Methods.....	160
7.3	Results.....	166
7.4	Discussion.....	174
7.5	Conclusions.....	182
7.6	Acknowledgements.....	183
7.7	References.....	183
Chapter 8 Conclusions and Future Directions.....		187
8.1	Conclusions.....	187
8.2	Future Work.....	197
8.3	References.....	202
Appendix A Mechanical Characterization and Non-linear Elastic Modeling of Poly(glycerol sebacate) for Soft Tissue Engineering.....		204
A.1	Introduction.....	204

A.2	Materials and Methods.....	209
A.3	Results.....	214
A.4	Discussion.....	223
A.5	Conclusion.....	230
A.6	Acknowledgments.....	231
A.7	References.....	231

LIST OF FIGURES

Figure 1.1: Common SFF techniques.	7
Figure 2.1: SMAD pathway activation in response to BMP.....	22
Figure 2.2: Progression of osteogenesis and associated gene expression.....	27
Figure 3.1: Conjugation of His-BMP-2-specific monoclonal antibodies to DBM using sulfo-SMCC.....	50
Figure 3.2: rhBMP-2 conjugation to PCL using sulfo-SMCC.....	51
Figure 3.3: Conjugation to PLGA using heparin.....	52
Figure 4.1: Bone volume and bon in-growth.....	71
Figure 4.2: Micro-CT image slices from the center of representative low and high permeability scaffolds at 4 weeks (A and C) and 8 weeks (B and D).....	72
Figure 4.3: Analysis of mineral content.....	73
Figure 4.4: Schematic of concentric cylinder bone volume analysis.....	74
Figure 4.5: Concentric cylinder bone volume analysis.....	75
Figure 4.6: Construct mechanical properties.....	77
Figure 4.7: Representative histological sections of high permeability (a and b) and low permeability (c and d) scaffolds at 8 weeks.....	78
Figure 5.1: Schematic representation of BMP-2 conjugation using sulfo-SMCC as a crosslinker between amine groups introduced onto PCL scaffold and BMP-2.....	96
Figure 5.2: Calcium content as measured by cresolphthalein complexone methodology.....	104
Figure 5.3: Sulfated-glycosaminoglycan (sGAG) content as measured by dimethylmethylene blue.....	105
Figure 5.4: Osteogenic gene expression.....	107
Figure 5.5: Chondrogenic gene expression.....	109
Figure 6.1: Bone volume as quantified by micro-CT.....	136
Figure 6.2: Penetration of bone into scaffold. Bone volume was measured in four cylindrical shell regions.....	138
Figure 6.3: Micro-CT image slices through the center of PCL scaffolds.....	139
Figure 6.4: Mechanical properties of constructs, evaluated by unconfined compression testing.....	141
Figure 7.1: SLS-manufactured PCL disc (A) and porous scaffold (B).....	160
Figure 7.2: rhBMP-2 conjugation efficiency.....	167
Figure 7.3: rhBMP-2 release from discs.....	167
Figure 7.4: rhBMP-2 conjugation efficiency for PCL scaffolds.....	169
Figure 7.5: rhBMP-2 release from scaffolds.....	170
Figure 7.6: Alkaline phosphatase content.....	172
Figure 7.7: Day 3 alkaline phosphatase staining on discs seeded with C2C12 cells.....	173

LIST OF TABLES

Table 4-1: Scaffold design properties.....	67
Table 5-1: Design parameters for scaffolds designed for this Aim.	94
Table 5-2: Experimental groups.....	97
Table 5-3: Computational and experimental permeability values for scaffolds used in Aim 4 (High Permeability A and Low Permeability A) and used in Aim II (High Permeability B and Low Permeability B).....	102
Table 5-4: Qualitative assessment of the relative expression of osteogenic and chondrogenic markers.....	111
Table 5-5: Qualitative assessment of the relative expression of osteogenic and chondrogenic markers for groups with BMP-2 versus without BMP-2.	112
Table 6-1: Experimental groups for implantation.....	133

ABSTRACT

Bone is the second most commonly transplanted tissue in the United States. Limitations of current bone defect treatment options include morbidity at the autograft harvest site, mechanical failure, and poorly controlled growth factor delivery. Combining synthetic scaffolds with biologics may address these issues and reduce dependency on autografts. The ideal scaffolding system should promote tissue in-growth and nutrient diffusion, control delivery of biologics and maintain mechanical integrity during bone formation. This dissertation evaluates how scaffold permeability, conjugated bone morphogenetic protein-2 (BMP-2) and differentiation medium affect osteogenesis *in vitro* and bone growth *in vivo*.

“High” and “low” permeability polycaprolactone (PCL) scaffolds with regular architectures were manufactured using solid free form fabrication. Bone growth *in vivo* was evaluated in an ectopic mouse model. High permeability scaffolds promoted better 8 week bone growth, supported tissue penetration into the scaffold core, and demonstrated increased mechanical properties due to newly formed bone. Next, the effects of differentiation medium and conjugated BMP-2 on osteogenesis were compared. Conjugation may improve BMP-2 loading efficiency, help localize bone growth and control release. High permeability scaffolds were conjugated with BMP-2 using the crosslinker, sulfo-SMCC. When adipose-derived and bone marrow stromal cells were seeded onto constructs (with or without BMP-2), BMSC expressed more differentiation markers, and differentiation medium affected differentiation more than BMP-2. *In vivo*, scaffolds with ADSC pre-differentiated in osteogenic medium (with and without BMP-2) and scaffolds with only BMP-2 grew the most bone. Bone volume did not differ among these groups, but constructs with ADSC had evenly distributed, scaffold-guided bone growth.

Analysis of two additional BMP-2 attachment methods (heparin and adsorption) showed highest conjugation efficiency for the sulfo-SMCC method. BMP-2 release from all constructs was minimal, proving that BMP-2 was tightly bound to constructs regardless of the attachment method. However, C2C12 myoblasts did not produce alkaline phosphatase when seeded onto heparin- and sulfo-SMCC-conjugated scaffolds suggesting hindrance of BMP-2 bioactivity.

This thesis demonstrated that high permeability PCL scaffolds promote bone growth better than low permeability scaffolds and that *in vitro* pre-differentiation of cells affects osteogenesis more than conjugated BMP-2. Future work will optimize BMP-2 conjugation to ensure maintenance of bioactivity.

CHAPTER 1 Introduction

1.1 Problem Statement

Bone is the second most commonly transplanted organ, with approximately 500,000 bone grafts performed annually in the U.S. and 2.2 million performed each year worldwide [1]. The options for treating conditions such as fracture non-unions, tumor resections and degenerative disc disease include autografts and allografts, bone void fillers and synthetic scaffolds that may include biologics such as BMP-2. The limitations of these treatments include mechanical failure, inadequate growth factor delivery, and, if an autograft is used, donor site morbidity at the graft harvest site. The treatments are also quite costly as demonstrated by the \$1 billion Medicare spent on spine surgery in 2003 [2]. The incidence of bone defects is likely to increase due to an aging population that is susceptible to falls and degenerative diseases, and injured veterans returning from combat with traumatic injuries to the face and limbs. These injuries require more effective, sophisticated and cost effective bone repair techniques. There is a need to develop tissue engineered constructs with defined architecture that support bone in-growth and can deliver biologics such as BMP-2 in a safe, controlled and repeatable way.

1.2 Clinical State of the Art: Repairing Bone Defects

Bone grafts are used when a bone defect cannot or does not heal naturally with casting and/or fixation. In 2008, the market for bone grafts and bone substitutes was estimated at \$1.64 billion, up 14% from 2007. Furthermore, bone substitutes represented almost 52% of the market in 2007, compared to only 29% in 2006, reflecting the shift away from human-tissue-derived products and toward engineered, synthetic products [3]. Bone grafts and substitutes are used to treat fracture non-unions, tumor resections, traumatic injuries and spinal defects. A range of grafting materials exist and fall into three categories: autologous bone grafts and their derivatives, bone substitutes made of synthetic materials and allografts derived from cadaver donors.

Autografts and Allografts

The gold standard for bone grafting is autografting in which the patient's own bone is harvested and used to repair the damaged bone tissue. Since adequate perfusion of the graft is necessary for ensuring graft survival, autografts can be harvested and transplanted along with the associated vasculature to ensure that the transplanted bone is supported by a blood supply. This greatly improves graft survival rates and effectiveness. Autografts possess the three characteristics that are ideal for a bone graft: osteoinductivity, osteoconductivity and osteogenicity. Furthermore, they carry no risk of disease transmission or immune system rejection since the bone is the patient's own tissue. Despite these advantages, there are still drawbacks to using autografts. Two procedures must be performed, one to harvest the autograft and one to implant the bone at the defect site, which increases the total procedure time and cost. Patients often experience pain at the autograft harvest site and there can be a limited amount of bone

that is suitable for grafting, especially in elderly patients. Furthermore, autografts lack geometrical similarity to complex defects and are difficult to shape to the defect contours [4].

Allografts, in which bone is taken from a cadaver donor, account for 15% of all bone grafts [3]. Allografts can be either cortical or cancellous bone and are prepared in fresh, frozen and freeze-dried forms. Fresh-frozen grafts are more osteoinductive and stronger than freeze-dried grafts because the processing maintains biologic and mechanical characteristics. Allografts have several advantages over autografts. Their availability is increasing and they can be manufactured into specific geometries such as dowels, strips, gels and powders [5]. The morbidity associated with harvesting autografts is eliminated and greater bone volumes are available. One drawback to using allografts is the risk of disease transmission, although this risk is greatly diminished with appropriate processing of the graft post-harvest. This processing negatively influences graft effectiveness though, because it decreases the mechanical and biologic properties of the graft. Cost is another barrier to widespread use of allografts. The resources and time needed for sterile harvesting, donor screening, transport, storage, processing, packaging and distribution of allografts is large and may limit scaled-up use of this type of graft.

Synthetic Grafts

Synthetic grafts, also known as bone substitutes, have been developed to address the issues associated with allografts and autografts. Synthetic materials, materials derived from natural tissue, and biologic/synthetic composites exist for various applications. The most common bone substitute materials are calcium-containing ceramics and biodegradable polymers, both of which can be processed into various forms and shapes

for specific applications. Ceramics are osteoconductive materials made of calcium phosphate that have been used in dentistry and orthopedic applications since the 1980s [6]. Hydroxy apatite (HA) and tri-calcium phosphate (TCP) are the most common materials in this category. To optimize the properties of both materials, HA-TCP composites have been developed, often using β -TCP, which has larger pores and greater porosity than traditional TCP. Commercially available products include Orthovita[®]'s Vitoss (β -TCP) bone graft substitute, Stryker's BoneSave bone void filler (HA/TCP) and BIOMET[®] BonePlast[®] (HA-TCP), a bone void filler for non-load bearing sites. HA derived from coralline sources has a structure similar to cortical and cancellous bone and has been developed into the ProOsteon[®] line of bone graft substitutes by BIOMET[®].

Degradable polymers have received a lot of attention in recent years because they can be produced on a large scale and can be manufactured into various forms, including specifically designed architectures. A polymer for bone tissue engineering must be biocompatible, bioresorbable, and have the appropriate mechanical properties to support developing bone. Ideally, it should also be osteoconductive and have the ability for osteoinductive modification. Poly(lactic-co-glycolic acid) (PLGA)[4, 7-9], poly(L-lactic acid) (PLLA)[7, 10-12], poly(caprolactone) (PCL) [13-20] and poly(propylene fumarate) (PPF) [21-24] have been investigated for bone tissue engineering, all of which can be manufactured into scaffolds with specific architectures using solid free form fabrication (SFF) techniques.

Materials derived from natural tissues that are used for bone grafting include collagen and demineralized bone matrix (DBM). Collagen type I is a major component of bone that is involved in mineral deposition, vascular ingrowth and growth factor

binding[1]. It has relatively weak mechanical properties (modulus in the kilopascal range or less) and is mainly used as a delivery agent and not a load-bearing graft. DBM consists of cortical bone allograft that has been stripped of its mineral components such that it retains the trabecular structure of the original tissue. The matrix is osteoconductive and even more osteoinductive than standard allografts because the demineralization renders some of the biological components more available. Biomet[®] DBM Putty is a commercially available product that consists of human DBM loaded into a syringe.

An ideal synthetic graft should mimic both the biologic and the mechanical properties of a natural autograft or allograft. To this end, composites that incorporate a biologic component and a synthetic scaffold have been developed. Common biologics include growth factors such as bone morphogenetic proteins (BMPs), bone marrow aspirate and autologous cells. Growth factors can be directly incorporated into a scaffold product, while aspirate or autologous cells are taken from the patient and added to the graft during the time of implantation. Several products that incorporate growth factors are currently on the market. Medtronic's Infuse[®] Bone Graft consists of recombinant human BMP-2 (rhBMP-2) within an absorbable collagen sponge, which can be used on its own or with the LT-Cage[®] Lumbar Tapered Fusion Device for spinal fusion. Stryker developed OP-1[™] Putty that consists of rhBMP-7 within a moldable collagen I carrier. It has been approved by the FDA under a humanitarian device exemption for spinal fusion to benefit patients whose autograft supply has been compromised by diabetes, smoking and/or osteoporosis. In 2005 the FDA approved BioMimetic's GEM 21S[®] Growth-factor Enhanced Matrix [25], consisting of recombinant human platelet derived growth factor (rhPDGF) and β -TCP. It is meant for treating periodontal defects and is designed to

stimulate wound healing (with rhPDGF) and bone regeneration (with β -TCP) by stimulating a cascade of molecular events upon implantation.

1.3 Scaffold Tissue Engineering

Clinicians and researchers have recognized that alternatives to autografts and allografts are needed to meet the growing demand for bone grafts. Bone tissue engineering emerged as a promising way to develop such alternatives by combining cells, growth factors and a scaffold to create an osteoconductive and osteoinductive environment for regenerating diseased or damaged bone. As mentioned in Section 1.2.3, a few commercially available composite grafts incorporate a biologic with a synthetic carrier or scaffold but the optimal combination of cells, growth factors and scaffold remains elusive.

As discussed in Section 1.2, ceramics, polymers and biologically-derived materials are the three main classes of materials used to create scaffolds and deliver cells and growth factors. Solid free form fabrication (SFF), several common types of which are depicted in Figure 1, is a scaffold manufacturing technique that yields scaffolds with defined porosity, pore size, interconnectivity and pore shape. These diffusion variables are all described by a single variable called permeability, which describes the flow of fluid through a porous medium and can be precisely controlled by SFF. In this dissertation, higher scaffold permeability is hypothesized to promote greater bone regeneration. Higher permeability enhances diffusion of nutrients and removal of waste products, but there is a tradeoff that exists whereby increased scaffold permeability leads to decreased mechanical properties. Thus, these diffusion variables also affect mechanical

properties, which can be regulated by the scaffold design and the scaffold material.

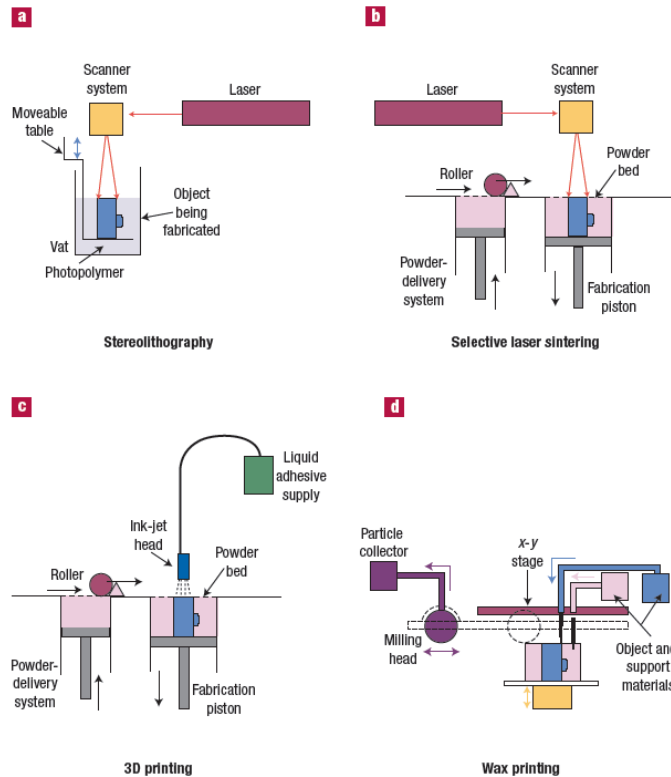


Figure 1.1: Common SFF techniques. The WorldWide Guide to Rapid Prototyping ©Copyright Castle Island Co. All rights reserved. <http://home.att.net/~castleisland/>.

Growth factors and cells are important additions to synthetic grafts because such grafts lack intrinsic osteoinductivity. Bone morphogenetic proteins (BMPs) regulate osteocalcin, osteopontin and other ECM-specific proteins that are important in osteogenesis [26]. When BMP-2 is incorporated within a tissue engineered construct, it can bind to its receptor on cell membranes to initiate the Smad pathway and turn on these osteogenic genes. Several cell types have been examined for bone regeneration. Adult stem cells are readily available from bone marrow aspirate or adipose tissue (lipoaspirate), have the potential to differentiate down a number of lineages, and can be easily expanded and cultured *in vitro* [27-30]. Osteogenesis of these cells is induced by

using cell culture medium containing chondrogenic [31, 32] or osteogenic [33, 34] supplements, although the necessity of differentiation medium for inducing *in vivo* bone growth is debatable. Embryonic stem cells have also been investigated for bone tissue applications [35, 36] as have primary cells such as osteoblasts, although these are difficult to harvest in large numbers and can become senescent in culture, limiting their clinical potential.

The ultimate goal of tissue engineering is to determine the ideal combination of factors that will enhance bone regeneration in a clinical application such as spinal fusion or mandibular reconstruction. Through *in vitro* screening and small animal models, a large number of variables can be screened to determine which ones should be examined more closely in larger animal models. Previous work demonstrated that scaffolds manufactured of the FDA approved polyester poly(ϵ -caprolactone) (PCL) are appropriate for bone tissue engineering [14]. PCL scaffolds with precisely designed architectures can be manufactured on a large scale using selective laser sintering and can be conjugated with growth factors [37, 38]. Covalently linking BMP-2 to a PCL scaffold may be advantageous over physical adsorption because covalent conjugation enables sustained release of the growth factor to better control bone growth. Furthermore, using BMP-2 instead of differentiation medium may represent a feasible, clinically relevant approach to inducing osteogenesis of adult stem cells. The goal of this thesis was to evaluate how scaffold design, growth factor incorporation and differentiation medium affect osteogenesis and bone regeneration of adipose-derived stem cells and bone marrow stromal cells seeded on PCL scaffolds.

1.4 Thesis Aims

This thesis addresses existing limitations of bone tissue engineering by improving the entire system consisting of scaffold, cells and growth factors. This is accomplished through four primary research aims. Aim I addresses biomaterial scaffold design, specifically looking at scaffold permeability effects on bone regeneration. An appropriate scaffold is the first requirement of the tissue engineering triad, with requirements two and three being growth factors and cells. The integration of growth factors within a scaffold construct is addressed in Aims II and III. Aim II looks at the individual and combinatorial effects of differentiation medium and conjugated rhBMP-2 on *in vitro* osteogenesis. Adipose-derived stem cells (ADSC) and bone marrow stromal cells (BMSC) are seeded into high permeability scaffolds chemically conjugated with rhBMP-2, and calcium content, sGAG content and gene expression are evaluated. In Aim III, an ectopic mouse model is used to evaluate the bone growth response of ADSC and BMSC exposed to various combinations of rhBMP-2 and differentiation medium and to determine if *in vitro* behavior translates *in vivo*. Lastly, Aim IV revisits characterization of the chemical conjugation method by examining loading efficiency, release and bioactivity in comparison to two alternative methods of BMP-2 incorporation. The objectives of each aim are summarized as follows:

Aim I: To examine the effect of polycaprolactone scaffold permeability on bone regeneration through comparison of two specifically design scaffolds in an *in vivo* ectopic mouse model.

Aim II: To compare the effects of scaffold-conjugated rhBMP-2 and differentiation medium on the *in vitro* expression of osteogenic and chondrogenic markers by human adipose derived stem cells and bone marrow stromal cells.

Aim III: To compare the effects of scaffold-conjugated rhBMP-2 and differentiation medium on the *in vivo* bone growth response of human adipose derived stem cells and bone marrow stromal cells.

Aim IV: To characterize three methods of attaching rhBMP-2 to PCL constructs – sulfosuccinimidyl-4-(N-maleimidomethyl)cyclohexane-1-carboxylate (sulfo-SMCC) conjugation, heparin conjugation and physical adsorption – by evaluating growth factor conjugation efficiency, growth factor release and bioactivity as assessed by C2C12 alkaline phosphatase activity.

These aims are intimately connected through their focus on the interplay between cells, growth factors and scaffold environment as key in promoting bone regeneration. The first aim isolates the effect of scaffold permeability through the use of two scaffold designs with specifically designed architectures. These scaffolds were designed and manufactured to have a regular architecture that not only enhances mass transport through the scaffold but also maintains mechanical properties, which are crucial for supporting developing bone tissue. By using a well-characterized subcutaneous mouse model [39] that utilizes immune-compromised animals, the influence of other variables was reduced, allowing for isolation of the effect of scaffold permeability alone. **The hypothesis was that a higher permeability scaffold would lead to better bone regeneration by improving mass transport and enabling blood vessel infiltration.**

A suitable scaffold is only one part of the tissue engineering triad of scaffold, cells and growth factors that must be optimized for a successful solution. Aim II addresses the second and third components of this triad by comparing *in vitro* osteogenesis of ADSC and BMSC exposed to various combinations of chemically conjugated rhBMP-2 and differentiation medium. Both growth factors and *in vitro* pre-conditioning of adult stem cells influence their osteogenic capacity. Osteogenic pulsing alone directs cells down an osteogenic path, but combining this pre-conditioning with chemically conjugated rhBMP-2 has not been studied previously and is examined in Aim II. **The combination of conjugated rhBMP-2 and osteogenic medium was hypothesized to significantly increase markers of osteogenesis in both cell types.**

In vitro models enable large scale investigation of many factors that could influence osteogenesis. However, the results of these controlled, simplistic studies are not guaranteed to carry over to an *in vivo* setting. In Aim III, the same groups from Aim II are incorporated into an ectopic mouse model and assessed for bone growth capacity. For this Aim, it was **hypothesized that BMSC would produce more bone than ASDC and that rhBMP-2 would significantly increase bone growth, regardless of the *in vitro* differentiation conditions.**

BMP-2 has been shown to stimulate osteogenesis by various cell types and has been approved for clinical use in certain situations. Despite some clinical success, there are problems controlling BMP-2 delivery and patient safety is compromised when large doses of the protein are used. BMP-2 conjugation to tissue engineered scaffolds may address these issues by improving initial loading efficiency and controlling release while still enabling biologic activity. In Aim IV, three methods to attach rhBMP-2 to PCL are

investigated. Two chemical conjugation methods (one involving a heterobifunctional thiol-amine crosslinker and the other utilizing EDC chemistry and heparin) are compared against physical adsorption of rhBMP-2 onto the scaffold. Conjugation efficiency and release are analyzed by ELISA and the bioactivity of the attached rhBMP-2 is assessed by induction of alkaline phosphatase production by C2C12 myoblasts. **In Aim IV we hypothesized that the heparin conjugation method would result in higher conjugation efficiency and more sustained release of rhBMP-2 as well as better maintenance of the growth factor's biologic effect on cells.**

1.5 Dissertation Contents

Chapters 2 and 3 of this dissertation discuss relevant background topics that establish a context for the experimental work described in Chapters 4 through 7. In Chapter 2, bone development, repair and regeneration are detailed, including sections on intramembranous and endochondral ossification and osteogenic gene expression. The goal is to first understand how bone grows, remodels and repairs in its natural environment, and then apply this knowledge to the creation of effective tissue engineered repair systems. Chapter 3 elaborates on the concept of tissue engineering that was introduced earlier in Chapter 1. A discussion of scaffold material and architecture considerations for bone tissue engineering make up the first half of the chapter, with special emphasis on polycaprolactone and permeability, the two notable scaffold parameters in this thesis. Cells and growth factors for bone tissue engineering are then discussed to emphasize the importance of including these components in a tissue engineered system. Biologics greatly increase the complexity of any tissue engineered system and need to be fully characterized upon introduction.

Chapter 4 marks the first experimental chapter and includes results from the scaffold permeability study comparing bone growth in low permeability PCL scaffolds to bone growth in high permeability PCL scaffolds. In Chapter 5, conjugated rhBMP-2 is introduced onto the PCL scaffolds. The effects of conjugated rhBMP-2 and differentiation medium on *in vitro* osteogenesis of two cell types are analyzed in this chapter. *In vivo* bone growth using the same groups of Chapter 5 is analyzed in Chapter 6 in an effort to determine if *in vitro* osteogenesis translates to *in vivo* bone growth. This Chapter also investigates whether conjugated rhBMP-2 or pre-differentiation *in vitro* has a greater effect on bone growth by the two cell types. In chapter 7, several methods of attaching rhBMP-2 to scaffolds are characterized. The sulfo-SMCC method used in Aims II and III (Chapters 5 and 6, respectively) and two alternative conjugation methods are analyzed in terms of their BMP-2 conjugation efficiency, release profiles and bioactivity. The dissertation closes with a conclusion in Chapter 8 that offers a final summary of the results and suggestions for future directions.

1.6 References

- [1] Giannoudis PV, Dinopoulos H, Tsiridis E. Bone substitutes: An update. *Injury-International Journal of the Care of the Injured*. 2005;36:20-7.
- [2] Tosteson ANA, Lurie JD, Tosteson TD, Skinner JS, Herkowitz H, Albert T, et al. Surgical Treatment of Spinal Stenosis with and without Degenerative Spondylolisthesis: Cost-Effectiveness after 2 Years. *Annals of Internal Medicine*: 149; 2008. p. 845-53.
- [3] Bone grafts and bone substitutes. *Orthopedic Network News*: Mendenhall Associates, Inc.; 2008.
- [4] Huang CK, Huang W, Jarrahy R, Rudkin GH, Ishida K, Yamaguchi DT, et al. Genetic markers of osteogenesis and angiogenesis are altered in processed lipoaspirate cells when cultured on 3D scaffolds. *Plastic and Reconstructive Surgery* 2008. p. 411.
- [5] Boyce T, Edwards J, Scarborough N. Allograft bone - The influence of processing on safety and performance. *Orthopedic Clinics of North America*. 1999;30:571-+.
- [6] Bohner M. Calcium orthophosphates in medicine: from ceramics to calcium phosphate cements. *Injury-International Journal of the Care of the Injured*. 2000;31:S37-S47.
- [7] Tanaka Y, Yamaoka H, Nishizawa S, Nagata S, Ogasawara T, Asawa Y, et al. The optimization of porous polymeric scaffolds for chondrocyte/atelocollagen based tissue-engineered cartilage. *Biomaterials*. 2010;31:4506-16.
- [8] Mooney DJ, Baldwin DF, Suh NP, Vacanti LP, Langer R. Novel approach to fabricate porous sponges of poly(D,L-lactic-co-glycolic acid) without the use of organic solvents. *Biomaterials*. 1996;17:1417-22.
- [9] Saito E, Kang H, Taboas JM, Diggs A, Flanagan CL, Hollister SJ. Experimental and computational characterization of designed and fabricated 50:50 PLGA porous scaffolds for human trabecular bone applications. *Journal of Materials Science-Materials in Medicine*. 2010;21:2371-83.
- [10] Kanczler JM, Barry J, Ginty P, Howdle SM, Shakesheff KM, Oreffo ROC. Supercritical carbon dioxide generated vascular endothelial growth factor encapsulated poly(DL-lactic acid) scaffolds induce angiogenesis in vitro. *Biochemical and Biophysical Research Communications*. 2007;352:135-41.
- [11] Ma PX, Choi JW. Biodegradable polymer scaffolds with well-defined interconnected spherical pore network. *Tissue Engineering*. 2001;7:23-33.
- [12] Yanoso-Scholl L, Jacobson JA, Bradica G, Lerner AL, O'Keefe RJ, Schwarz EM, et al. Evaluation of dense polylactic acid/beta-tricalcium phosphate scaffolds for bone tissue engineering. *Journal of Biomedical Materials Research Part A*. 2010;95A:717-26.

- [13] Ciapetti G, Ambrosio L, Savarino L, Granchi D, Cenni E, Baldini N, et al. Osteoblast growth and function in porous poly- ϵ -caprolactone matrices for bone repair: a preliminary study. *Biomaterials*2003. p. 3815-24.
- [14] Williams JM, Adewunmi A, Schek RM, Flanagan CL, Krebsbach PH, Feinberg SE, et al. Bone tissue engineering using polycaprolactone scaffolds fabricated via selective laser sintering. *Biomaterials*. 2005;26:4817-27.
- [15] Hutmacher DW, Schantz T, Zein I, Ng KW, Teoh SH, Tan KC. Mechanical properties and cell cultural response of polycaprolactone scaffolds designed and fabricated via fused deposition modeling. *Journal of Biomedical Materials Research*. 2001;55:203-16.
- [16] Zein I, Hutmacher DW, Tan KC, Teoh SH. Fused deposition modeling of novel scaffold architectures for tissue engineering applications. *Biomaterials*. 2002;23:1169-85.
- [17] Marra KG, Szem JW, Kumta PN, DiMilla PA, Weiss LE. In vitro analysis of biodegradable polymer blend/hydroxyapatite composites for bone tissue engineering. *Journal of Biomedical Materials Research*. 1999;47:324-35.
- [18] Pitt CG, Chasalow FI, Hibionada YM, Klimas DM, Schindler A. Aliphatic polyesters. I. The degradation of poly(ϵ -caprolactone) in vivo. *Journal of Applied Polymer Science*1981. p. 3779-87.
- [19] Adewunmi B, Williams JM, Flanagan CL, Engel A, Hollister SJ. Mechanical and structural properties of polycaprolactone scaffolds made by selective laser sintering. 7th World Biomaterials Congress. Sydney, Australia2004.
- [20] Fisher JP, Vehof JWM, Dean D, van der Waerden J, Holland TA, Mikos AG, et al. Soft and hard tissue response to photocrosslinked poly(propylene fumarate) scaffolds in a rabbit model. *Journal of Biomedical Materials Research*. 2002;59:547-56.
- [21] Lin C-Y, Schek RM, Mistry AS, Shi S, Mikos AG, Krebsbach PH, et al. Functional bone engineering using ex vivo gene therapy and topology-optimized, biodegradable polymer composite scaffolds. *Tissue Engineering*2005. p. 1589-98.
- [22] Lee K-W, Wang S, Fox BC, Ritman EL, Yaszemski MJ, Lu L. Poly(propylene fumarate) bone tissue engineering scaffold fabrication using stereolithography: Effects of resin formulations and laser parameters. *Biomacromolecules*. 2007;8:1077-84.
- [23] Wang K, Cai L, Hao F, Xu XM, Cui MZ, Wang SF. Distinct Cell Responses to Substrates Consisting of Poly(epsilon-caprolactone) and Poly(propylene fumarate) in the Presence or Absence of Cross-Links. *Biomacromolecules*. 2010;11:2748-59.
- [24] Roosa SMM, Kemppainen JM, Moffitt EN, Krebsbach PH, Hollister SJ. The pore size of polycaprolactone scaffolds has limited influence on bone regeneration in an in vivo model. *Journal of Biomedical Materials Research Part A*. 2010;92A:359-68.

- [25] After First Product Approval, BioMimetic Seeks \$50M IPO. 2006.
- [26] Ducy P, Zhang R, Geoffroy V, Ridall AL, Karsenty G. Osf2/Cbfa1: A transcriptional activator of osteoblast differentiation. *Cell*. 1997;89:747-54.
- [27] Zuk P, Zhu M, Ashjian P, De Ugartea D, Huang J, Mizuno H, et al. Human adipose tissue is a source of multipotent stem cells. *Molecular Biology of the Cell* 2002. p. 4279-95.
- [28] Kern S, Eichler H, Stoeve J, Kluter H, Bieback K. Comparative analysis of mesenchymal stem cells from bone marrow, umbilical cord blood, or adipose tissue. *Stem Cells* 2006. p. 1294-301.
- [29] Long MW, Robinson JA, Ashcraft EA, Mann KG. Regulation of Human Bone Marrow-Derived Osteoprogenitor Cells by Osteogenic Growth Factors. *Journal of Clinical Investigation*. 1995;95:881-7.
- [30] Yamaguchi A, Yokose S, Ikeda T, Katagiri T, Wozney JM, Rosen V, et al. BMP-2 Induces Bone Marrow Stromal Cells to Differentiate into Osteoblasts and Decreases their Capacity to Support Osteoclast Formation. *Journal of Bone and Mineral Research*. 1993;8:S158-S.
- [31] Farrell E, Both SK, Odoerfer KI, Koevoet W, Kops N, O'Brien FJ, et al. In-vivo generation of bone via endochondral ossification by in-vitro chondrogenic priming of adult human and rat mesenchymal stem cells. *Bmc Musculoskeletal Disorders*. 2011;12.
- [32] Farrell E, van der Jaagt O, Koevoet W, Kops N, van Manen C, Hellingman C, et al. Chondrogenic priming of human bone marrow stromal cells: a better route bone repair? *Tissue Engineering Part C* 2009.
- [33] Dudas JR, Marra KG, Cooper GM, Penascino VM, Mooney MP, Jiang S, et al. The osteogenic potential of adipose-derived stem cells for the repair of rabbit calvarial defects. *Annals of Plastic Surgery*. 2006;56:543-8.
- [34] Yoon E, Dhar S, Chun DE, Gharibjanian NA, Evans GRD. In vivo osteogenic potential of human adipose-derived stem cells/poly lactide-co-glycolic acid constructs for bone regeneration in a rat critical-sized calvarial defect model. *Tissue Engineering*. 2007;13:619-27.
- [35] Arpornmaeklong P, Brown SE, Wang Z, Krebsbach PH. Phenotypic Characterization, Osteoblastic Differentiation, and Bone Regeneration Capacity of Human Embryonic Stem Cell-Derived Mesenchymal Stem Cells. *Stem Cells and Development*. 2009;18:955-68.
- [36] Arpornmaeklong P, Wang Z, Pressler MJ, Brown SE, Krebsbach PH. Expansion and Characterization of Human Embryonic Stem Cell-Derived Osteoblast-Like Cells. *Cellular Reprogramming*. 2010;12:377-89.

- [37] Zhang HN, Migneco F, Lin CY, Hollister SJ. Chemically-Conjugated Bone Morphogenetic Protein-2 on Three-Dimensional Polycaprolactone Scaffolds Stimulates Osteogenic Activity in Bone Marrow Stromal Cells. *Tissue Engineering Part A*. 2010;16:3441-8.
- [38] Park YJ, Kim KH, Lee JY, Ku Y, Lee SJ, Min BM, et al. Immobilization of bone morphogenetic protein-2 on a nanofibrous chitosan membrane for enhanced guided bone regeneration. *Biotechnology and Applied Biochemistry*. 2006;43:17-24.
- [39] Schek RM, Wilke EN, Hollister SJ, Krebsbach PH. Combined use of designed scaffolds and adenoviral gene therapy for skeletal tissue engineering. *Biomaterials*. 2006;27:1160-6.

CHAPTER 2 Bone: Development, Regeneration and Characteristics

2.1 Bone Development: Endochondral v. Intramembranous Ossification

Understanding the pathways for normal bone development is imperative for designing a successful tissue engineering construct for bone regeneration at a defect site. Bone tissue forms through endochondral ossification or intramembranous ossification, depending on the type and location of the bone. Long bones develop through endochondral ossification, while the flat bones of the skull and face are formed through intramembranous ossification. Aspects of one or both development pathways could be exploited in a tissue engineering system to produce the best regenerative environment.

2.1.1 Intramembranous Ossification

Intramembranous ossification occurs when mesenchymal cells from the neural crest are directly converted to bone cells. The cells from the neural crest condense to form nodules that then form either capillaries or osteoblasts. The osteoblasts secrete a collagen-proteoglycan matrix that binds calcium and initiates the calcification process of the “pre-bone” osteoid matrix. Osteoblasts line the osteoid region and osteoblasts that become trapped within this region become osteocytes. Bony spicules then radiate outward from where the osteocytes initiate the ossification process, and are surrounded by a compact membrane of mesenchymal cells known as the periosteum. The thickness of the bone increases as layers of osteoid matrix are laid down by osteoblasts [2].

2.1.2 *Endochondral Ossification*

Unlike the intramembranous pathway, which leads to direct formation of bone tissue, endochondral ossification produces bone indirectly, by first forming cartilage that eventually mineralizes to become bone. The process begins with the formation of avascular clusters of chondrocytes that are surrounded by extracellular matrix (ECM). The largest and most mature chondrocytes are located at the center of these nodules and become the center for growth and ossification. This collection of chondrocytes grows into cartilage through typical chondrogenesis: the chondrocytes undergo mitosis and proliferate, the volume of the ECM increases and the cells hypertrophy. There are then multiple stages of ossification, presented here in five stages as described by Streeter [3]. The first stage is the cartilage growth at the center of the chondrocyte mass, as just described. A membrane (the perichondrium) surrounds the cartilage and recruits new cells, directing them toward chondrogenic differentiation. In the second and third stages of ossification, the cells elongate perpendicular to the direction of greatest growth and then become large and cuboidal in shape. In stage 4, large, hypertrophic chondrocytes die and then the ECM is calcified. These hypertrophic chondrocytes release a chemo-attractant molecule that attracts endothelial cells and stimulates angiogenesis. This leads to vascularization of the calcified cartilage, which allows nutrients, osteoblasts and osteoclasts to penetrate and resorb the calcified cartilage that is then replaced by well-vascularized bone tissue (Stage 5).

The intrusion of blood vessels into the region of hypertrophied chondrocytes differentiates mature cartilage from bone. Cartilage is notably avascular, while bone is a highly metabolically active tissue requiring a plentiful blood supply. In endochondral ossification, bone girth is increased by osteoblasts laying down bone on the mineralized

surfaces, while bone length increases by progression of the ossification fronts away from either end of the original nodule. Endochondral ossification is regulated by biologic and mechanical factors. BMPs, growth hormone, and thyroid and parathyroid hormones regulate the initiation and progression of ossification. Mechanical loading is the primary factor that controls bone patterning and also regulates chemical mediators of angiogenesis, cartilage growth and cartilage differentiation [4].

2.1.3 Skeletal Tissue Regeneration

When bone tissue is injured due to trauma or a surgical procedure, natural bone regeneration occurs to repair the damage. While initiation of regeneration after injury is distinct from initiation of the aforementioned developmental pathways, the mechanism through which bone is regenerated can be either intramembranous or endochondral. There is an initial wound healing response in which lysosomal enzymes released by dying cells trigger cell proliferation and differentiation, leading to inflammation and subsequent regeneration. The inflammatory response triggers angiogenesis and the recruitment of endothelial cells, which are a source of pluripotent stem cells. These stem cells differentiate to bone cells given the correct mechanobiological regulation [5]. Conditions that are optimal for bone regeneration include low levels of hydrostatic and shear stress and high vascularity (low vascularity will cause differentiation to chondrocytes instead). Ossification can be intramembranous, endochondral or appositional depending on the levels of stress and strain experienced by the tissue and the degree of vascularity.

2.2 The Role of Bone Morphogenetic Proteins in Bone Development and Remodeling

A number of biologic factors regulate bone development, growth and regeneration. Bone morphogenetic proteins (BMPs) belong to the transforming growth factor beta (TGF- β) superfamily and are critically involved in the proliferation and differentiation of many different cell types [6-8]. BMP-2 through -7 have been found in extracts of demineralized bone matrix [9-11] and their role in regulating osteogenesis [12, 13] and chondrogenesis [8, 10, 14] has garnered much attention in the field over the past several decades. BMPs can be delivered to regeneration sites using a number of techniques, including *ex vivo* cellular transfection using a viral vector [13-16], release from a sponge or gel [17-20], physical adsorption of recombinant protein onto a scaffold surface [21-24] and chemical conjugation to a scaffold surface [25-28]. The mechanisms of action and uses of BMP-2 and BMP-7 in tissue engineering are reviewed here.

2.2.1 BMP-2

BMP-2 is a Hox gene within the TGF- β superfamily that activates downstream target genes to regulate production of osteogenic factors. In its active form, the protein is a disulfide-linked homodimer. Each monomer contains seven cysteines, six of which form intramolecular disulfide bonds that make up the cysteine knot, a structural entity that is a common feature in all members of the TGF- β family and is important in BMP-2 signaling [29, 30]. The remaining free cysteine of each monomer forms a disulfide bond to create the dimerized, active form of BMP-2. The signaling cascade, which eventually activates the Smad pathway (Figure 1), is induced when BMP-2 binds to a type II receptor in the cell membrane. This binding activates the type I receptor which then

phosphorylates R-smads 1, 5 and 8. These activated R-smads form complexes with co-

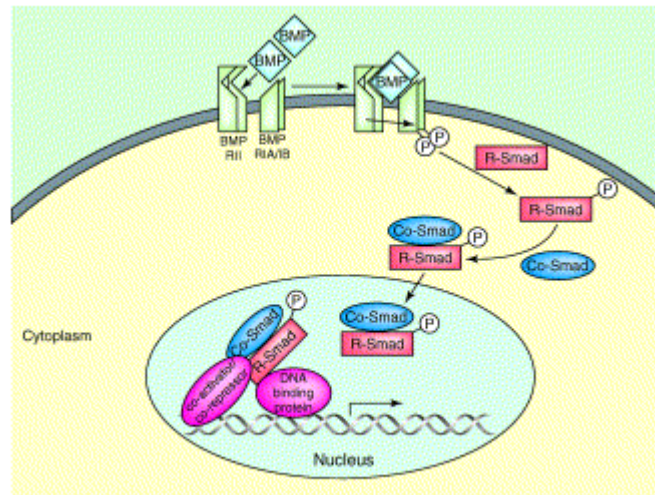


Figure 2.1: SMAD pathway activation in response to BMP [1].

smads and translocate to the nucleus for transcriptional regulation of target genes. The main Smad pathway-activated BMP-2 target gene is Runx2, which activates the genes for osteocalcin, osteopontin and other ECM-specific proteins [31]. Aside from its osteogenic targets, BMP-2 has also been shown to have an angiogenic effect on osteoblasts, inducing them to secrete VEG-F and stimulate blood vessel invasion during endochondral ossification [32, 33].

The osteogenic effect of BMP-2 is well-documented but there is also evidence that the protein has a chondrogenic effect as well. Sellers et al found that both subchondral bone and cartilage were regenerated when recombinant human BMP-2 (rhBMP-2) within a collagen sponge was used to treat full thickness cartilage defects in rabbits [34]. Cartilage maintenance and cessation of endochondral ossification was most likely due to biomechanical factors and other factors including cartilage-derived morphogenetic proteins whose effects were enabled by the proximity of the implant to

native cartilage [34]. BMP-2 may be advantageous to both osteogenesis and chondrogenesis and many factors (implantation site, the presence of cells within the implanted construct, construct material and construct architecture) influence the tissue that is ultimately regenerated. Thus, there is a need to further explore in what capacity this protein can and should be used to regenerate tissue in a controlled, repeatable manner.

Recombinant BMP-2 was first produced in Chinese hamster ovary (CHO) cells as reported by Wang et al in 1990 [35]. When 0.5-115 µg doses were implanted in rats ectopically, cartilage was observed by day 7 and bone by day 14. Since that first report of recombinant human BMP-2 (rhBMP-2), it has also been produced in *Escherichia coli* (*e. coli*) [36] and both forms are commercially available. rhBMP-2 is widely used in many research fields, from molecular biology to tissue engineering and is a component of a Medtronic's INFUSE spinal fusion device. Slight differences exist between CHO-derived rhBMP-2 and *e. coli*-derived rhBMP-2. The CHO-derived form is glycosylated upon production, producing a protein that is more susceptible to hydrolysis than the *e. coli*-derived version. This difference in solubility could be exploited depending on the delivery method and desired release profile of the protein. Due to its lack of glycosylation, *e. coli*-derived rhBMP-2 may be more stable when incorporated into scaffold systems, resulting in more controlled release.

rhBMP-2 is used in both *in vitro* and *in vivo* systems and can be delivered in a number of ways. The simplest way to deliver rhBMP-2 to cells is to solubilize it in cell culture medium [37, 38]. While this method is advantageous for studying the bioactivity of rhBMP-2 and its effect on cultured cells, it is not particularly relevant for clinical

applications since it can't be translated to an *in vivo* setting. Another way to deliver rhBMP-2 is by encapsulating the growth factor in a hydrogel or microspheres [19, 20, 39, 40]. With this method, the release profile can be controlled by varying the degradation characteristics of the polymer that encapsulates the rhBMP-2. Physical adsorption is used to attach rhBMP-2 to more rigid scaffolds, such as the collagen sponge used for the INFUSE bone graft [34]. Bonding occurs through electrostatic interactions and the strength of this bond can be affected by altering the substrate surface or adjusting the pH of the adsorption solution to increase the charge on the growth factor. This type of incorporation typically results in a "burst" release of the protein that yields poor temporal distribution and has resulted in adverse events in patients [41, 42]. Delivery of growth factors using a viral vector involves transducing cells with a virus whose DNA encodes for the growth factor [13, 43]. When BMP is introduced by this method, transfected cells produce large amounts of bone in a relatively short time period [14, 16]. Viral vector delivery of rhBMP-7 is used in Aim 1 of this thesis as a well-characterized and reliable way to induce ectopic bone formation. Using this model enabled better isolation of the effect of scaffold permeability on bone regeneration.

Chemical conjugation of growth factors was developed to improve the bonding strength between the protein and the biomaterial substrate, resulting in a more sustained release profile and better localization of bone growth. Chemical reactions employing 1-Ethyl-3-(3-dimethylaminopropyl)carbodiimide (EDC) chemistry, heparin, sulfosuccinimidyl-4-(N-maleimidomethyl)cyclohexane-1-carboxylate (sulfo-SMCC), poly(ethylene-glycol) (PEG) and collagen are commonly used to covalently link growth factors to scaffold surfaces. Methods to covalently link rhBMP-2 to scaffolds exploit both

the surface chemistry of the scaffold surface and the available functional groups on the rhBMP-2. All of the methods presented here require the existence of primary amines on the scaffold surface, which can be introduced by simple surface modification of the polymer. Heparin is a polysaccharide associated with the cell surface and extracellular matrix that binds directly to rhBMP-2. Heparin has been shown to positively influence BMP-2's osteogenic effect and improves its stability [44]. Binding between heparin and rhBMP-2 occurs through electrostatic interactions between heparin's negatively charged sulfate groups and the protein's positively charged amino acid residues. Many growth factors, including BMP-2 and VEG-F, have a specific N-terminal heparin binding site, which provides stronger attachment than typical adsorption, protects the growth factor from degradation and may improve the growth factor's bioavailability [44-46]. To link heparin to an aminated scaffold, 1-Ethyl-3-(3-dimethylaminopropyl)carbodiimide (EDC) is used to activate the carboxylic groups of heparin which then interact with the primary amine groups on the scaffold surface [39]. EDC chemistry has also been demonstrated for direct linkage between rhBMP-2 and poly(lactide-co-glycolide acid) or polycaprolactone [47]. Collagen tethering is another method for linking rhBMP-2 to scaffolds [48]. Although this method involves more reaction steps, it allows for conjugation of many different growth factors due to collagen's many reactive terminal and side chain residues. Sulfo-SMCC has been used for incorporating antibodies into polymeric delivery systems [49] and linking bisphosphonates to a glycoprotein for enhancing the protein's affinity to bone [50]. Based on previous work by our lab and others [28, 51] we used sulfo-SMCC to conjugate rhBMP-2 to PCL scaffolds. We hypothesized that this covalent conjugation

method as well as the use of non-glycosylated *e. coli*-derived rhBMP-2 would promote greater growth factor retention on the scaffold and lead to more controlled release.

2.2.2 BMP-7

BMP-7 is another protein in the TGF- β family that has effects on both cartilage and bone development, although it exhibits stronger anabolic effects on cartilage growth than BMP-2 does [52, 53]. Still, there have been contradicting reports of BMP-7's influence on tissue growth and it may be a potent inducer of either chondrogenesis or osteogenesis, depending upon the surrounding environment. Like BMP-2, BMP-7 induces expression of Runx-2, the earliest transcription factor expressed during osteogenesis. BMP-7 acts through endochondral ossification [53] but its effect on either chondrogenesis or osteogenesis (or both) can vary based on what it is acting upon, be it cells, *in vivo* tissue or explanted tissue rudiments. Like BMP-2, recombinant forms of BMP-7 (rhBMP-7) have been developed, stimulating its wide use in research settings. rhBMP-7 stimulated alkaline phosphatase production, osteocalcin production and mineralization when used in long term (11-17 day) cultures of osteoblasts supplemented with osteogenic factors [54]. In ectopic sites using fibroblasts transfected with rhBMP-7, the protein induced bone formation in scaffold constructs [43, 55], but when used to stimulate mouse embryonic long bone rudiments [56], BMP-7 stimulated chondrogenesis while inhibiting osteogenesis. Since the primary concern of Aim 1 was evaluating scaffold design, a well-characterized and reliable method of bone induction was desired, which was the motivation for delivering rhBMP-7 via a viral vector system [55].

2.3 Bone and Cartilage Gene Expression

Bone matrix consists of two phases, a mineral phase that provides stiffness, and an organic phase composed almost entirely of type I collagen fibers, which give bone its ductility and toughness. Many genes are involved in the development of this complex matrix and it is possible to assess the stage of bone tissue development by examining gene markers for early, intermediate and late stages of osteogenic differentiation and matrix mineralization. These stages of bone development have been categorized into three phases: proliferation with matrix secretion, matrix maturation, and matrix mineralization [57]. This temporal distribution of gene expression, shown schematically in Figure 2 [57], begins with Collagen I expression, stimulated by the differentiation of

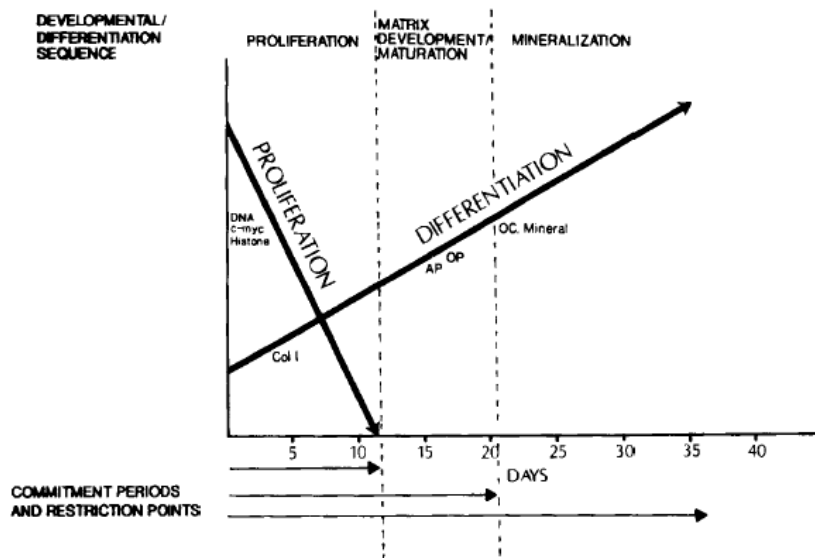


Figure 2.2: Progression of osteogenesis and associated gene expression.

pre-osteoblasts down an osteogenic lineage. Next, proliferation decreases as the matrix matures and prepares for mineralization. Differentiation of cells into osteoblasts occurs and is coupled with a peak in osteopontin and alkaline phosphatase expression, which is responsible for calcium phosphate mineral formation [58]. Lastly, mature bone is marked

by completion of matrix mineralization and upregulation of osteocalcin [59]. In this thesis, *in vitro* alkaline phosphatase, collagen I and osteocalcin gene expression is analyzed using quantitative polymerase chain reaction (qPCR). It has been shown that the expression of these genes is upregulated by rat bone marrow stromal cells seeded on PCL scaffolds with chemically conjugated rhBMP-2, as compared to cells on physically adsorbed rhBMP-2 [25]. In this work, the same scaffold system is used to examine the effect of culture medium and conjugated rhBMP-2 on the expression of these markers in two human adult stem cell types.

2.3.1 *Collagen Type I*

Type I collagen represents 95% of the total collagen content in bone, composing most of the organic phase of the highly organized bone extracellular matrix. The collagen phase of the matrix is required for formation of the mineral phase, which consists of hydroxyapatite nanocrystals distributed on and within the interwoven complex of collagen fibrils. Collagen fibrils are composed of three polypeptide α -chains arranged in a triple helix and, in bone, are deposited by osteoblasts into parallel sheets called lamellae. These lamellae form osteons in compact bone and trabeculae in spongy bone. A period of osteoblast proliferation immediately precedes peak collagen I expression. This proliferative period supports collagen synthesis and deposition; collagen is required for subsequent events that make the matrix ready for mineralization [3]. Collagen fibers play a large role in bone mechanical properties and are responsible for bone tissue's ductility and toughness.

2.3.2 Alkaline Phosphatase

Alkaline phosphatase (ALP), while not specific to bone tissue [60], is expressed at high levels by pre-osteoblasts and osteoblasts and is responsible for calcium phosphate mineral formation. ALP correlates with the rate of bone formation and can act as an index of osteoblast activity during appositional bone growth. Studies have shown an increase in expression of osteogenic markers, including ALP, for cells cultured in constructs made of osteoconductive materials versus non-osteoconductive materials [61]. ALP expression precedes expression of the matrix protein osteocalcin [61, 62], indicating that ALP acts before mineralization occurs to prepare the matrix for mineralization events.

Hypertrophic chondrocytes also express ALP, which further supports the notion that ALP is a very early marker of differentiation, since hypertrophied chondrocytes signal the beginning of endochondral ossification. In this thesis, the effect of cell type and *in vitro* pulsing conditions on ALP gene expression is evaluated by PCR. To address the fact that PCL is not an innately osteoconductive material, rhBMP-2 was incorporated onto the surface of the scaffolds to increase the constructs' propensity for forming localized bone. By comparing the expression of ALP between multiple *in vitro* pulsing conditions, both with and without BMP-2 present, we may be able to shed light on its involvement in ossification in an osteogenic versus a chondrogenic environment.

2.3.3 Osteocalcin

Osteocalcin (OCN), also known as bone Gla protein (BGlaP) is a small, non-collagenous protein (49 amino acids, 5.8 kDa) that is produced by osteoblasts and makes up 20% of non-collagenous bone tissue [63]. It is unique to bone tissue, reflects osteoblastic activity, which is a marker of bone formation, and is responsible for

mineralization of the matrix. OCN is only expressed in osteoblasts that are in contact with bone and osteocytes, indicating that it is a later marker of bone maturation, and is expressed after peak expression of ALP occurs [62]. Expression of OCN is closely linked to the deposition of hydroxyapatite within the bone matrix and without this mineralization, OCN is not expressed. Therefore, OCN expression and mineralization are correlated [64]. Studies have also shown a direct, strong correlation between serum-osteocalcin levels and trabecular bone volume, osteoid surface area and osteoblastic surface area in healthy patients [65]. For tissue engineers, the interest in OCN expression stems from a desire to direct the differentiation of adult stem cells down the osteogenic lineage *before* implanting them *in vivo*. High expression of OCN at the end of *in vitro* pre-culture would suggest that the cells have not only differentiated to osteoblasts, but are also at a later stage of differentiation and are likely to form bone once implanted *in vivo*.

2.3.4 Chondrogenic Gene Expression

Examining chondrogenic gene expression in addition to osteogenic gene expression enables us to determine if cellular differentiation was unique to the osteogenic lineage or if certain factors supported chondrogenesis as well. As is the case for osteogenesis, a number of genes regulate the development of cartilage and these genes are expressed in a temporal manner as differentiation and tissue maturation progress. The articular cartilage of joints reduces friction at the ends of long bones by providing a cushioned surface for the bones to move against. It is an avascular tissue composed primarily of water and characterized by chondrocytes embedded in a matrix of collagen (mainly collagen type II) and proteoglycans such as aggrecan. The collagen component of the cartilage matrix provides structure, shape and functionality while the proteoglycans

support mechanical load. For the studies presented in this thesis, BMSC and ADSC expression of collagen II and aggrecan is quantified after two weeks of control, osteogenic or chondrogenic medium to see what effect pulsing has on the cells' expression of a cartilage phenotype.

2.4 Conclusion

Bone is a complex tissue whose growth and repair are highly regulated through temporal expression of various osteogenic genes. Endochondral ossification has been proposed as the mechanism through which bone is regenerated in response to BMPs, which motivated an examination of both osteogenic and chondrogenic markers in the studies presented here. The goal of tissue engineering is to design a scaffold system that mimics the *in vivo* bone environment and induces natural bone regeneration. This dissertation discusses the incorporation of rhBMP-2 onto a highly permeable polymer scaffold for inducing osteogenesis of adult stem cells and eventual bone growth *in vivo*.

2.5 References

- [1] Varas A, Hager-Theodorides AL, Sacedon R, Vicente A, Zapata AG, Crompton T. The role of morphogens in T-cell development. *Trends in Immunology*. 2003;24:197-206.
- [2] Gilbert SF. *Developmental Biology*. 6 ed. Sunderland, MA: Sinauer Associates; 2000.
- [3] Streeter G. Developmental horizons in human embryos. *Contrib Embryol Carnegie Inst*1949. p. 165-96.
- [4] Carter DC, Beaupre GS. *Skeletal Function and Form*. New York, NY: Cambridge University Press; 2001.
- [5] Shapiro F. Bone development and its relation to fracture repair. The role of mesenchymal osteoblasts and surface osteoblasts. *European Cells & Materials*. 2008;15:53-76.

- [6] Kawabata M, Chytil A, Moses HL. Cloning of a novel type II serine/threonine kinase receptor through interaction with the type I transforming growth factor-beta receptor. *Journal of Biological Chemistry*1995. p. 5625-30.
- [7] Kingsley DM. The TGF-beta superfamily: new members, new receptors, and new genetic tests of function in different organisms. *Genes and Development*1994. p. 133-46.
- [8] Lyons KM, Pelton RW, Hogan BLM. Organogenesis and Pattern Formation in the Mouse - RNA Distribution Patterns Suggest a Role for Bone Morphogenetic Protein-2A (BMP-2A). *Development*. 1990;109:833-44.
- [9] Celeste AJ, Iannazzi JA, Taylor RC, Hewick RM, Rosen V, Wang EA, et al. Identification of transforming growth factor beta family members present in bone-inductive protein purified from bovine bone. *Proceedings of the National Academy of Science*1990. p. 9843-7.
- [10] Rosen V, Wozney JM, Wang EA, Cordes P, Celeste A, McQuaid D, et al. Purification and Molecular Cloning of a Novel Group of BMPs and Localization of BMP Messenger-RNA in Developing Bone. *Connective Tissue Research*. 1989;20:313-9.
- [11] Wozney JM, Rosen V, Celeste AJ, Mitsock LM, Whitters MJ, Kriz RW, et al. Novel regulators of bone formation: molecular clones and activities. *Science*1988. p. 1528-34.
- [12] Wozney JM, Li RH. Delivering on the promise of bone morphogenetic proteins. *Trends in Biotechnology*2001. p. 255-65.
- [13] Dragoo JL, Choi JY, Lieberman JR, Huang J, Zuk PA, Zhang J, et al. Bone induction by BMP-2 transduced stem cells derived from human fat. *Journal of Orthopedic Research*2003. p. 622-9.
- [14] Roosa SMM, Kemppainen JM, Moffitt EN, Krebsbach PH, Hollister SJ. The pore size of polycaprolactone scaffolds has limited influence on bone regeneration in an in vivo model. *Journal of Biomedical Materials Research Part A*. 2010;92A:359-68.
- [15] Williams JM, Adewunmi A, Schek RM, Flanagan CL, Krebsbach PH, Feinberg SE, et al. Bone tissue engineering using polycaprolactone scaffolds fabricated via selective laser sintering. *Biomaterials*. 2005;26:4817-27.
- [16] Koh JT, Zhao Z, Wang Z, Lewis IS, Krebsbach PH, Franceschi RT. Combinatorial gene therapy with BMP2/7 enhances cranial bone regeneration. *Journal of Dental Research*. 2008;87:845-9.
- [17] Schek RM, Hollister SJ, Krebsbach PH. Delivery and protection of adenoviruses using biocompatible hydrogels for localized gene therapy. *Molecular Therapy*. 2004;9:130-8.
- [18] Basmanav FB, Kose GT, Hasirci V. Sequential growth factor delivery from complexed microspheres for bone tissue engineering. *Biomaterials*. 2008;29:4195-204.

- [19] Chong Y-I, Ahn K-M, Jeon S-H, Lee S-Y, Lee J-H, Tae G. Enhanced bone regeneration with BMP-2 loaded functional nanoparticle–hydrogel complex. *Journal of Controlled Release* 2007. p. 91-9.
- [20] Jeon O, Song SJ, Yang HS, Bhang S-H, Kang S-W, Sung MA, et al. Long-term delivery enhances in vivo osteogenic efficacy of bone morphogenetic protein-2 compared to short-term delivery. *Biochemical and Biophysical Research Communications*. 2008;369:774-80.
- [21] Schmidmaier G, Schwabe P, Strobel C, Wildemann B. Carrier systems and application of growth factors in orthopaedics. *Injury-International Journal of the Care of the Injured*. 2008;39:S37-S43.
- [22] Dong XL, Wang Q, Wu T, Pan HH. Understanding adsorption-desorption dynamics of BMP-2 on hydroxyapatite (001) surface. *Biophysical Journal*. 2007;93:750-9.
- [23] Draenert F, Nonnenmacher A-L, Kämmerer P, Goldschmitt J, Wagner W. BMP-2 and bFGF release and in vitro effect on human osteoblasts after adsorption to bone grafts and biomaterials. *Clinical Oral Implants Research* 2012. p. 1-8.
- [24] Liu Y, Huse RO, de Groot K, Buser D, Hunziker EB. Delivery mode and efficacy of BMP-2 in association with implants. *Journal of Dental Research*. 2007;86:84-9.
- [25] Zhang HN, Migneco F, Lin CY, Hollister SJ. Chemically-Conjugated Bone Morphogenetic Protein-2 on Three-Dimensional Polycaprolactone Scaffolds Stimulates Osteogenic Activity in Bone Marrow Stromal Cells. *Tissue Engineering Part A*. 2010;16:3441-8.
- [26] Karageorgiou V, Meinel L, Hofmann S, Malhotra A, Volloch V, Kaplan D. Bone morphogenetic protein-2 decorated silk fibroin films induce osteogenic differentiation of human bone marrow stromal cells. *Journal of Biomedical Materials Research Part A*. 2004;71A:528-37.
- [27] Pohl TLM, Boergermann JH, Schwaerzer GK, Knaus P, Cavalcanti-Adam EA. Surface immobilization of bone morphogenetic protein 2 via a self-assembled monolayer formation induces cell differentiation. *Acta Biomaterialia*. 2012;8:772-80.
- [28] Zhao Y, Zhang J, Wang X, Chen B, Xiao Z, Shi C, et al. The osteogenic effect of bone morphogenetic protein-2 on the collagen scaffold conjugated with antibodies. *Journal of Controlled Release*. 2010;141:30-7.
- [29] Hillger F, Herr G, Rudolph R, Schwarz E. Biophysical comparison of BMP-2, ProBMP-2, and the free pro-peptide reveals stabilization of the pro-peptide by the mature growth factor. *Journal of Biological Chemistry*. 2005;280:14974-80.
- [30] Rider CC, Mulloy B. Bone morphogenetic protein and growth differentiation factor cytokine families and their protein antagonists. *Biochemical Journal*. 2010;429:1-12.

- [31] Ducy P, Zhang R, Geoffroy V, Ridall AL, Karsenty G. *Osf2/Cbfa1*: A transcriptional activator of osteoblast differentiation. *Cell*. 1997;89:747-54.
- [32] Moutsatsos IK, Turgeman G, Zhou SH, Kurkalli BG, Pelled G, Tzur L, et al. Exogenously regulated stem cell-mediated gene therapy for bone regeneration. *Molecular Therapy*. 2001;3:449-61.
- [33] Gerber HP, Vu TH, Ryan AM, Kowalski J, Werb Z, Ferrara N. VEGF couples hypertrophic cartilage remodeling, ossification and angiogenesis during endochondral bone formation. *Nature Medicine*. 1999;5:623-8.
- [34] Sellers RS, Peluso D, Morris EA. The effect of recombinant human bone morphogenetic protein-2 (rhBMP-2) on the healing of full-thickness defects of articular cartilage. *Journal of Bone and Joint Surgery-American Volume*. 1997;79A:1452-63.
- [35] Wang EA, Rosen V, Dalessandro JS, Bauduy M, Cordes P, Harada T, et al. Recombinant Human Bone Morphogenetic Protein Induces Bone Formation. *Proceedings of the National Academy of Sciences of the United States of America*. 1990;87:2220-4.
- [36] Kuebler NR, Reuther JF, Faller G, Kirchner T, Ruppert R, Sebald W. Inductive properties of recombinant human BMP-2 produced in a bacterial expression system. *International Journal of Oral and Maxillofacial Surgery*. 1998;27:305-9.
- [37] Melhorn AT, Niemeyer P, Kaschte K, Muller L, Finkenzeller G, Hartl D, et al. Differential effects of BMP-2 and TGF- β 1 on chondrogenic differentiation of adipose derived stem cells. 2007. p. 809-23.
- [38] Huang WB, Carlsen B, Wulur I, Rudkin G, Ishida K, Wu B, et al. BMP-2 exerts differential effects on differentiation of rabbit bone marrow stromal cells grown in two-dimensional and three-dimensional systems and is required for in vitro bone formation in a PLGA scaffold. *Experimental Cell Research*. 2004;299:325-34.
- [39] Jeon O, Song SJ, Kang S-W, Putnam AJ, Kim B-S. Enhancement of ectopic bone formation by bone morphogenetic protein-2 released from a heparin-conjugated poly(Llactic- co-glycolic acid) scaffold. *Biomaterials* 2007. p. 2763-71.
- [40] Kim HD, Valentini RF. Retention and activity of BMP-2 in hyaluronic acid-based scaffolds in vitro. *Journal of Biomedical Materials Research*. 2002;59:573-84.
- [41] Perri B, Cooper M, Laurysen C, Anand N. Adverse swelling associated with use of rh-BMP-2 in anterior cervical discectomy and fusion: a case study. *Spine Journal*. 2007;7:235-9.
- [42] Dickerman RD, Reynolds AS, Morgan BC, Tompkins J, Cattorini J, Bennett M. rh-BMP-2 can be used safely in the cervical spine: dose and containment are the keys! *Spine Journal*. 2007;7:508-9.

- [43] Schek RM, Wilke EN, Hollister SJ, Krebsbach PH. Combined use of designed scaffolds and adenoviral gene therapy for skeletal tissue engineering. *Biomaterials*. 2006;27:1160-6.
- [44] Zhao B, Katagiri T, Toyoda H, Takada T, Yanai T, Fukuda T, et al. Heparin potentiates the in vivo ectopic bone formation induced by bone morphogenetic protein-2. *Journal of Biological Chemistry*. 2006;281:23246-53.
- [45] Rider C. Heparin/heparan sulphate binding in the TGF- β cytokine superfamily. *Biochemical Society Transactions* 2006. p. 458-60.
- [46] Ruppert R, Hoffmann E, Sebald W. Human bone morphogenetic protein 2 contains a heparin-binding site which modifies its biological activity. *European Journal of Biochemistry*. 1996;237:295-302.
- [47] Gharibjanian NA, Chua WC, Dhar S, Scholz T, Shibuya TY, Evans GRD, et al. Release Kinetics of Polymer-Bound Bone Morphogenetic Protein-2 and Its Effects on the Osteogenic Expression of MC3T3-E1 Osteoprecursor Cells. *Plastic and Reconstructive Surgery*. 2009;123:1169-77.
- [48] Liu H-W, Chen C-H, Tsai C-L, Hsiue G-H. Targeted delivery system for juxtacrine signaling growth factor based on rhBMP-2-mediated carrier-protein conjugation. *Bone*. 2006;39:825-36.
- [49] Patri AK, Myc A, Beals J, Thomas TP, Bander NH, Baker JR. Synthesis and in vitro testing of J591 antibody-dendrimer conjugates for targeted prostate cancer therapy. *Bioconjugate Chemistry*. 2004;15:1174-81.
- [50] Gittens SA, Matyas JR, Zernicke RF, Uludag H. Imparting bone affinity to glycoproteins through the conjugation of bisphosphonates. *Pharmaceutical Research*. 2003;20:978-87.
- [51] Park YJ, Kim KH, Lee JY, Ku Y, Lee SJ, Min BM, et al. Immobilization of bone morphogenetic protein-2 on a nanofibrous chitosan membrane for enhanced guided bone regeneration. *Biotechnology and Applied Biochemistry*. 2006;43:17-24.
- [52] Chubinskaya S, Kuettner KE. Regulation of osteogenic proteins by chondrocytes. *International Journal of Biochemistry & Cell Biology*. 2003;35:1323-40.
- [53] Schek RM, Taboas JM, Segvich SJ, Hollister SJ, Krebsbach PH. Engineered osteochondral grafts using biphasic composite solid free-form fabricated scaffolds. *Tissue Engineering*. 2004;10:1376-85.
- [54] Sampath TK, Maliakal JC, Hauschkatn PV, Jones WK, Sasak H, Tucker RF, et al. Recombinant Human Osteogenic Protein- 1 (hOP- 1) Induces New Bone Formation in Vivow ith a Specific Activity Comparablew ith Natural Bovine Osteogenic Protein and StimulatesO steoblast Proliferation and Differentiation in Vitro. *Journal of Biological Chemistry* 1992. p. 20352-62.

- [55] Krebsbach PH, Gu K, Franceschi RT, Rutherford RB. Gene therapy-directed osteogenesis: BMP-7-transduced human fibroblasts form bone in vivo. *Human Gene Therapy*. 2000;11:1201-10.
- [56] Dieudonné S, Semeins C, Goei S, Vukicevic S, Nulend K, Sampath T, et al. Opposite effects of osteogenic protein and transforming growth factor beta on chondrogenesis in cultured long bone rudiments. *Journal of Bone and Mineral Research*2009. p. 771-80.
- [57] Owen TA, Aranow M, Shalhoub V, Barone LM, Wilzig L, Tassinari MS, et al. Progressive development of the rat osteoblast phenotype in vitro: reciprocal relationships in expression of genes associated with osteoblast proliferation and differentiation during formation of the bone extracellular matrix. *Journal of Cell Physiology*1990. p. 420-30.
- [58] Gelinsky M. Mineralised Collagen as Biomaterial and Matrix for Bone Tissue Engineering. In: Meyer U, Meyer T, Handschel J, Wiesman HP, editors. *Fundamentals of Tissue Engineering and Regenerative Medicine*: Springer Berlin Heidelberg; 2009. p. 485-93.
- [59] Huang C, Huang W, Zuk P, Jarrahy R, Rudkin G, Ishida K, et al. Genetic markers of osteogenesis and angiogenesis are altered in processed lipoaspirate cells when cultured on three-dimensional scaffolds. *Plastic and Reconstructive Surgery*2008. p. 411.
- [60] Kirkham GR, Cartmell SH. Genes and proteins involved in the regulation of osteogenesis. *Topics in Tissue Engineering*2007.
- [61] Inanc B, Elcin AE, Elcin YM. Osteogenic induction of human periodontal ligament fibroblasts under two- and three-dimensional culture conditions. *Tissue Engineering*. 2006;12:257-66.
- [62] Weinreb M, Shinar D, Rodan GA. Different pattern of alkaline phosphatase, osteopontin and osteocalcin expression in developing rat bone visualized by in situ hybridization. *Journal of Bone and Mineral Research*1990. p. 831-42.
- [63] Ljunghall S, Lindh E. Assessment of bone turnover with biochemical markers. *Journal of Internal Medicine*1989. p. 219-20.
- [64] Collin P, Nefussi JR, Wetterwald A, Nicolas V, Boy-Lefevre M-L, Fleisch H, et al. Expression of collagen, osteocalcin, and bone alkaline phosphatase in a mineralizing rat osteoblastic cell culture. *Calcified Tissue International*1992. p. 175-83.
- [65] Garcia-Carrasco M, Gruson M, de Vernejoul MC, Denne MA, Miravet L. Osteocalcin and Bone Morphometric Parameters in Adults Without Bone Disease. *Calcified Tissue International*1988. p. 13-7.

CHAPTER 3 Scaffold Tissue Engineering: Developing a Complete System for Repairing and Regenerating Bone

3.1 Introduction

Bone tissue engineering has emerged as an alternative to traditional bone autografts and allografts. The goal of tissue engineering is to create an osteoconductive and osteoinductive environment for regenerating diseased or damaged bone by combining a biomaterial scaffold with cells and growth factors. Tissue engineering has existed within the field of biomedical engineering for the past several decades, and while hundreds of thousands of research articles have been published in the field of tissue engineering, few complete systems are clinically available. Progress has been made in the form of commercially available composite grafts that incorporate a biologic with a synthetic carrier or scaffold, as discussed in Section 1.2. However, these systems are not perfect and the optimal combination of cells, growth factors and scaffold still has not been achieved. Problems still exist, especially with growth factor delivery, an issue that attracted unwanted attention when patient safety was threatened by poorly controlled recombinant human bone morphogenetic protein-2 (rhBMP-2) delivery during spinal fusion [2-4]. A successful solution must be feasible from both a scientific and commercial standpoint and would combine cells, factors and scaffold such that these three components complement one another to provide an appropriate environment for

bone regeneration. Here we discuss each of these components and evaluate the advantages and disadvantages of various approaches.

3.2 Materials for Effective Scaffolds

A material for bone tissue engineering must be biodegradable, biocompatible, have appropriate mechanical properties, and be osteoconductive. Ideally the material can also be modified to become osteoinductive so that once implanted, immature cells are recruited to the scaffold and stimulated to develop into pre-osteoblasts. Scaffolds can be made of ceramics, bioactive glass, polymers, biologically-derived materials or a combination of these. These materials all have advantages and disadvantages for particular applications and are often used in combination to exploit a particular material's strengths.

Ceramics are osteoconductive materials derived from calcium phosphate [6]. The most common are tri-calcium phosphate (TCP) and hydroxy apatite (HA), which have different biological and degradation properties *in vivo* but can be incorporated into composites to offer a range of properties. The chemical makeup of porous TCP is similar to amorphous bone precursors, leading to its osteoconductivity. TCP degrades relatively quickly and is removed from the implant site as bone tissue is deposited, but small pore sizes limit the amount of bone integration that can take place before this degradation occurs. β -TCP, a modified version of TCP, has larger, well connected pores, which encourage vascular and bone in-growth, making β -TCP an ideal material for a bone void filler. Bone cements of β -TCP were tested in canine alveolar bone defects and were completely resorbed and replaced by bone at 6 months [7].

HA has a similar chemical composition as the mineral component of bone [8]. It degrades much more slowly than TCP, at a rate of 5-15% per year [9], and tends to be brittle which can cause stress shielding at an implant site. To exploit the advantageous properties of both materials, HA-TCP composites have been developed, often using β -TCP, which has larger pores and greater porosity than traditional TCP. Ceramics have been manufactured to create scaffolds with defined architecture, and these architectures have been shown to have a direct effect on both mechanical properties and bone regeneration capability [10, 11]. Jin et al manufactured HA constructs from porous particles, porous blocks and honeycomb-shaped particles to create scaffolds with three different pore morphologies. The mode of ossification, either endochondral or direct apposition, depended upon the pore morphology, with the more open pore structures supporting direct apposition of bone onto the scaffold surface [11]. This illustrates how both scaffold architecture and material can direct bone formation. Scaffold architecture effects will be discussed in more detail in section 3.2.

Naturally-derived materials are an attractive choice for bone tissue engineering applications because they possess characteristics of native tissue. Collagen type I is the major protein component of bone tissue, contributing to mineralization, blood vessel infiltration and growth factor binding. It can be isolated from animal sources, most commonly bovine, and manufactured in a range of forms, yielding a range of mechanical properties from very soft foams and gels to stiffer, porous scaffolds. Even in scaffold form, the mechanical properties of collagen are orders of magnitude below those of bone, limiting its use as a bone graft substitute. Collagen is usually used in combination with stronger materials (ceramics, polymers) as a delivery vehicle for growth factors and/or

cells. Demineralized bone matrix (DBM) is decalcified cortical bone that is processed to reduce the risk of infection and immunogenic response in the host. DBM is an intuitive choice for a scaffold since it retains the porous trabecular structure of natural bone. It also possesses osteogenic growth factors that are important for bone regeneration. These factors are actually *more* bioavailable following the processing of DBM that is performed to lessen the risk of disease transmission and immune rejection. Although DBM retains its morphologic and biologic characteristics, it does not possess mechanical properties that can support load or development of new bone tissue. As such, it is typically manufactured as moldable gels, pastes or putties and used as a bone graft extender in complex with more rigid scaffolds.

Synthetic polymers are synthesized from one or more monomer components to produce networks of cross-linked polymer chains, the properties of which can be changed by varying the curing condition or monomer component ratio. Polymers are unique in that their degradation rate and mechanical properties can be precisely controlled by adjusting molecular weight and the block design of the monomers. This ability to tune degradation rate and mechanical properties is a useful tool for tissue engineers [12, 13] and a representative material characterization study appears in Appendix A. While tuning PCL's mechanical and degradation properties is outside the specific scope of this thesis, the concept was incorporated into the scaffold design. Smart scaffold design can balance the need to support developing and surrounding tissues with the desire to have the polymer degrade away once sufficient bone tissue has developed. Polymers that have been investigated for bone tissue engineering include poly(L-lactic acid) (PLLA) [14-18], poly(lactic-co-glycolic acid) (PLGA) [18-20], polycaprolactone (PCL) [21-28], and

poly(propylene fumarate) (PPF) [29-32]. These materials can be manufactured into a variety of forms and support cell growth and incorporation of growth factors.

PLA, PGA and PLGA were some of the first polymers to be granted FDA approval for use in implanted medical devices. The degradation products of these polymers, lactic acid and glycolic acid, are metabolized by natural pathways in the body. These materials can be processed using many techniques to yield constructs with a wide range of properties. The simplest method for creating random pore architecture is porogen leaching. Ma et al [16] used bonded paraffin spheres as porogens for PLLA and PLGA scaffolds. Porosity and pore size were changed by altering the polymer concentration, the number of casting steps and the size of the paraffin spheres. Solid free form fabrication (SFF) techniques take this concept of an open pore structure one step further to create regular pore architectures within scaffolds. One such technique, selective laser sintering (SLS), creates a 3-D structure through deposition of successive layers of polymer particles that are sintered together with a laser beam. This technique has been used to manufacture PLLA scaffolds [14] with a variety of shapes and architectures and was used to create PCL scaffolds for Aims II and III of this thesis. Three-dimensional printing combined with direct polymer casting was used to manufacture scaffolds for Aim I.

PCL is an FDA-approved polyester that degrades in the body via hydrolysis of its ester linkages during the tricarboxylic acid (TCA) cycle. While PCL can support *in vitro* and *in vivo* cell and tissue growth [24, 33], it is naturally hydrophobic and modifications can be made to improve its cell-friendliness. A surfactant can be incorporated into the manufacturing process to increase the hydrophilicity and improve cell attachment on the

surface [21]. Composite materials can be made by combining PCL with ceramics such as HA. These materials are osteoconductive and have greater compressive modulus and strength, making them better for load bearing applications. The incorporation of a ceramic material into PCL constructs has also been shown to improve cell viability and increase osteogenic gene expression [22, 26]. SLS is a popular manufacturing method for PCL scaffolds and can produce scaffolds with moduli ranging from 1-5000 MPa and 0.2% offset yield strength between 0.1-27.3 MPa, which are within the lower range of human trabecular bone [23]. Differences in mechanical properties were created by altering porosity from 0% to 79%. Hutmacher et al [24] showed that scaffolds manufactured by fused deposition modeling to have the same (61%) porosity but different architectures, had significantly different mechanical properties. These examples further illustrate that architecture effects on mechanical properties are complex and warrant in-depth examination. In this thesis, we chose to use PCL scaffolds for several reasons. First, as previously mentioned PCL is FDA approved and has a history of use in bone tissue engineering research. Secondly, we were able to use SFF techniques (both melt casting and SLS) to manufacture scaffolds with specific architectures to test our hypotheses concerning scaffold permeability and bone regeneration. Lastly, PCL can be modified to incorporate growth factors, which is addressed in Aims II through IV of this dissertation.

3.3 Scaffold Architecture Considerations

A scaffold's internal architecture affects the construct's mechanical properties, degradation profile and ability to support cellular infiltration and bone in-growth. Degradation and tissue infiltration are primarily affected by the mass transport properties

of the scaffold, which determine the rate and path of fluid flow through the scaffold pores. These properties can vary depending upon the environment (*in vitro* vs. *in vivo*), the cell type used and the addition of other factors to the tissue engineering system. The simplest scaffolds can be made from a number of polymeric materials using porogen leaching [34], resulting in scaffolds with a defined porosity but with random pore architecture and a range of pore sizes. SFF techniques (introduced in section 3.1) produce scaffolds with defined pore architectures by enabling precise control over a range of diffusion variables including porosity, pore size, interconnectivity and pore shape. Determining the optimal scaffold design for enabling tissue and blood vessel infiltration but also maintaining adequate mechanical properties continues to be a design challenge for bone tissue engineers. In this section, the variables that contribute to scaffold architecture are discussed along with their implications for scaffold mechanical properties and bone growth.

Whenever a scaffold is designed and manufactured, the pore structure is analyzed to determine pore size, porosity and other architectural variables that may influence tissue in-growth and mechanical properties. A lot of research has been devoted to determining the best pore size for tissue in-growth and bone regeneration. SFF techniques have enabled production of scaffolds with a uniform pore size, which is an improvement over other techniques that yield a range of pore sizes [21, 33, 35]. Fisher et al reported that 380-405 μm pores were best for chondrocyte and osteocyte cell growth but smaller pores (290-310 μm) showed faster new bone formation [29]. Minimum pore sizes of 150 μm [29] or 350 μm [36] have been reported for ensuring bone in-growth, but others have also reported no effect of pore size on bone in-growth [29, 35, 37]. The pore sizes used in

these studies may have been greater than the threshold size needed for bone in-growth, resulting in no significant effect between pore sizes. The confusion over whether pore size significantly affects bone in-growth suggests that other architectural features may influence bone growth regardless of pore size. Further investigation into pore size revealed that *accessible* pore size, defined by Jones et al as the size of the largest sphere that can invade from the scaffold edge into a particular pore [38], is what really affects tissue in-growth and that there is a strong correlation between accessible pore size and bone in-growth. This accessible pore size (also referred to as throat size, which is the size of the connections between pores in a scaffold) must be at least 100 μm for bone in-growth to occur.

Porosity is the amount of void space within a construct [35] and the general consensus is that higher porosity promotes better tissue infiltration. However, there is a trade-off between porosity and mechanical properties whereby increasing porosity decreases mechanical properties. Thus scaffolds must be designed to maximize void space while also maintaining adequate mechanical properties to support existing and developing tissue. While porosity and pore size are important variables to consider, they do not fully describe a scaffold's internal architecture. Williams et al [23] found that lowering the porosity of PCL constructs led to lower mechanical properties. However, the authors did not find a strong correlation between modulus and void space, indicating that other factors such as strut size, pore shape and pore morphology are involved in lowering the modulus. A similar result was found using PCL scaffolds manufactured by fused deposition modeling to have either a two-angle laydown pattern (0/90°) or a three-angle laydown pattern (0/60/120°). The two designs had identical porosities (~55%) but the

two-angle pattern had significantly greater mechanical properties [24]. These examples demonstrate how pore morphology can affect mechanical properties. Furthermore, pore morphology can also influence tissue in-growth as shown by Jin et al who directed cells down the endochondral bone development pathway using HA with honeycomb-shaped pores and down a direct ossification pathway using block design HA constructs [11].

Observations such as those listed above have motivated researchers to figure out why different architectures lead to varying degrees and modes of tissue formation. Hui et al examined permeability in cancellous bone grafts and postulated that a threshold conductance (defined as permeability normalized by graft size and the viscosity of saline) of $1.5 \times 10^{-10} \text{ m}^3/\text{sec} \cdot \text{Pa}$ is required for vascularization and mineralization to occur within the grafts [39]. Permeability is only dependent on the material properties of the graft, which may include the pore volume and trabecular structure. This is one of the earliest indications that pore morphology (and not just void space) has a critical effect on mass transport. Permeability defines the physical property of mass transport and refers to the ease with which a fluid flows through a porous material or construct [40]. Permeability acts as an umbrella variable for a number of architectural variables including porosity, tortuosity, pore size and interconnectivity and should be considered as an independent design variable [41], which is done in Aim I of this thesis using PCL scaffolds.

Several studies have demonstrated how a range of scaffold permeabilities and mechanical properties can be created for a given porosity by altering the scaffold architecture [24]. This further supports the hypothesis that it is permeability and not porosity that defines a scaffold's internal architecture. Furthermore, since scaffold permeability determines nutrient diffusion through the construct, it can have significant

effects on tissue in-growth and survival, and scaffold degradation. Higher permeability may lessen mechanical properties, but it can also decrease degradation and maintain existing mechanical properties over time. This is due to a decrease in autocatalytic degradation for high permeability constructs, inhibited since waste products are flushed out of the scaffold area more efficiently. Diffusion of materials through the scaffold also has implications for growth factor delivery. Increased tortuosity within a scaffold decreases its permeability, but higher tortuosity may be better for growth factor retention and sustained release [21]. Thus, if growth factors are incorporated into a scaffold, the scaffold design should have high enough tortuosity to support retention of the growth factor, but also have high permeability for promoting tissue and vessel in-growth and nutrient delivery. The concept of permeability as determined by scaffold architecture is complex when considered within the context of a complete tissue engineering solution. As such, it should be incorporated into the design process and studied as a unique variable. To this end, scaffolds in Aim I of this thesis were designed to have either a “high” or “low” permeability [42] while keeping pore shape and pore size constant and porosity within a set range.

3.4 Additional Factors

Inclusion of growth factors is important for synthetic grafts that lack intrinsic osteoinductivity. Growth factors used in bone tissue engineering can have a range of effects, from osteogenic effects to mitogenic and angiogenic effects. The challenge is to determine the best growth factor(s) and engineer a clinically relevant delivery system that is both safe and effective. Bone morphogenetic proteins (BMPs) are part of the TGF- β superfamily of ligands and are involved in osteogenesis through activation of the SMAD

pathway. BMP-2 binds to the BMP type II receptor, which then activates R-SMADS that translocate to the nucleus to regulate expression of genes such as *cbfa1/RUNX-2*.

RUNX-2 regulates production of osteocalcin, osteopontin and other ECM-specific proteins that are important in osteogenesis [43]. Wound healing growth factors such as PDGF may be important for enhancing healing of soft tissues surrounding bone grafts. Angiogenic growth factors such as vascular endothelial growth factor (VEGF) may complement a highly permeable scaffold by recruiting endothelial cells to the graft and improving vascularization.

BMPs are potent inducers of osteogenesis that are extracted from demineralized bone matrix and have been studied in various *in vitro* and *in vivo* models. Recombinant forms of several human BMPs, most notably BMP-2 and BMP-7, have been developed, increasing their use in both research and clinical settings. Human BMP-2 has been expressed in Chinese hamster ovary (CHO) [44] cell and *Escherichia coli* (*e. coli*) [45] and subsequently purified to produce commercially available BMP-2. BMP-2 upregulates production of osteogenic markers in many cell types, yet its behavior in complex, tissue engineering settings has not been fully characterized. Having passed the largest hurdle to commercialization by obtaining FDA approval for lumbar spine fusion, BMP-2 holds promise for widespread clinical use. The keys to BMP-2's clinical success are suppressing overstimulation of BMP-2-induced bone growth and developing a consistent, controlled conjugation method.

Growth factors can be incorporated into a tissue engineering system via several methods. Culture medium supplementation [46-49], gel and microsphere encapsulation [8, 50-52], gene therapy, physical adsorption to scaffolds and chemical conjugation [1,

53-59] to scaffolds have all been employed and offer various release profiles. The simplest method of exposing cells and scaffolds to growth factors *in vitro* is by supplementing the cell culture medium that the constructs are submerged in. This method has been employed with adult stem cells (adipose- or bone marrow-derived) and various growth factors (BMP-2, BMP-7, TGF- β) [48, 60]. Alkaline phosphatase (ALP) expression was upregulated when cells were exposed to BMP-2, while both BMP-2 and TGF- β were needed for upregulation of chondrogenic genes [60]. Experiments looking at duration of growth factor exposure (fifteen minutes versus four days) showed better upregulation of osteogenic genes with short-term BMP-2 exposure, while short-term BMP-7 exposure resulted in upregulation of chondrogenic genes [48]. Adding growth factors to the medium is a simple way to impact the differentiation of adult stem cells. However, the method is only appropriate for *in vitro* studies and is not easily translatable to long-term *in vivo* growth factor stimulation. Furthermore, this method does not produce localized growth factor delivery and requires larger amounts of the growth factor to achieve the desired effect.

There are several gene therapy methods for delivering growth factors, the two most common being *ex vivo* delivery and *in vivo* delivery. For *ex vivo* delivery, cells are transfected *in vitro* with a virus encoded for the growth factor of interest and then implanted *in vivo*. For *in vivo* growth factor delivery, the virus is directly injected into the *in vivo* environment. Schek et al showed that the *ex vivo* method is far more effective at inducing bone regeneration *in vivo*, probably because the cells begin expressing the growth factor at an earlier time point and are exposed to the virus in a controlled, *in vitro* environment that is optimal for virus transfection [61]. Virus delivery offers more

localized, directed delivery of the growth factor. Viral delivery of rhBMP-2 to adipose-derived stem cells has been used to repair bone defects in mini-pig ulnar defects[62] and rat femoral defects [63] and it remains a popular method of growth factor incorporation. However, concerns with using a live virus have led researchers to develop other techniques for controlled growth factor release.

Chemically conjugating growth factors to scaffolds has emerged as a way to ensure controlled release of the growth factor over several weeks. Covalent conjugation of rhBMP-2 using a crosslinker has been utilized with PLGA, PCL, and chitosan scaffolds [58, 59, 64, 65]. There are several methods for chemically conjugating rhBMP-2 on scaffolds, the most common being direct conjugation with a chemical crosslinker, or conjugation using molecules such as heparin or polyethylene glycol (PEG). For conjugation with a crosslinker, the heterobifunctional amine to sulfhydryl crosslinker sulfosuccinimidyl-4-(N-maleimidomethyl)cyclohexane-1-carboxylate (sulfo-

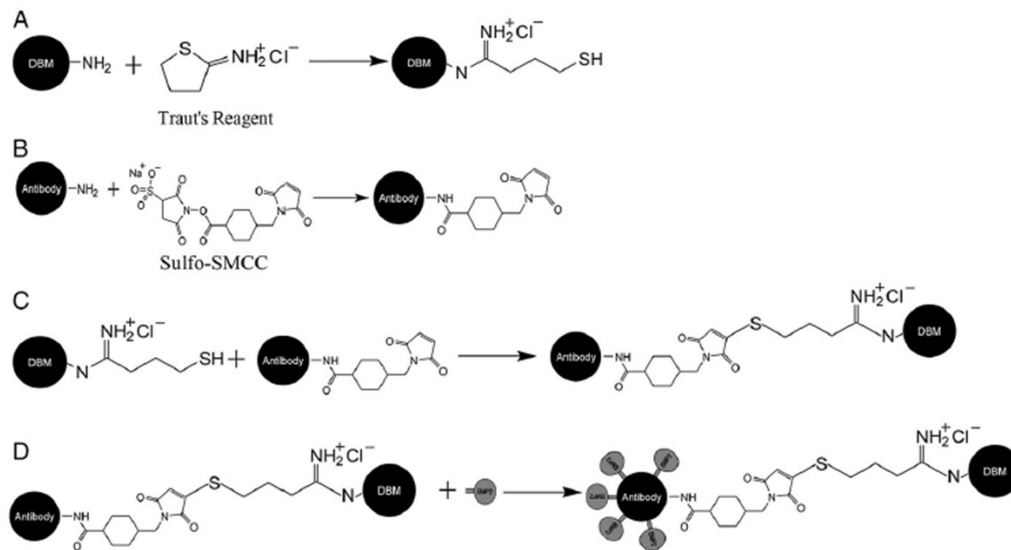


Figure 3.1: Conjugation of His-BMP-2-specific monoclonal antibodies to DBM using sulfo-SMCC. A. Introduction of sulfhydryl groups on DBM using Traut's reagent. B. Conjugation of sulfo-SMCC to antibody. C. Linkage of sulfhydryl-modified DBM and sulfo-SMCC-modified antibody. D. Direct attachment of His-BMP-2 to monoclonal antibody[5].

SMCC) has been used [5, 58, 66]. One way to utilize sulfo-SMCC is to first modify scaffold surfaces with Traut's reagent to introduce sulfhydryl groups. The sulfo-SMCC then interacts with these sulfhydryl groups and amine groups on the BMP-2, as shown in Figure 1. The conjugation scheme depicted in Figure 1 shows demineralized bone matrix (DBM) conjugated with antibodies using sulfo-SMCC. These antibodies then specifically bind BMP-2, representing an indirect conjugation since sulfo-SMCC does not directly interact with the BMP-2. These constructs achieved controlled release *in vitro* and demonstrated better ectopic bone formation compared to controls [5]. This method was also used to directly attach BMP-2 to collagen scaffolds [67]. Direct conjugation using sulfo-SMCC has also been demonstrated with chitosan constructs [59] that showed better loading efficiency than BMP-2 conjugated by physical adsorption. This study did not discuss the specific reaction scheme that the sulfo-SMCC participated in, but since dimerized rhBMP-2 lacks a free cysteine group, the sulfo-SMCC would have no

sulfhydryls to react with. Instead, it likely linked amine groups on the chitosan to amine groups on rhBMP-2, an un-favored reaction that proceeds in the absence of sulfhydryl groups [68]. This method, depicted in Figure 2, was also used previously to conjugate BMP-2 to collagen and to PCL (by our group) [58] and is utilized in this thesis.

The heparin conjugation method, depicted in Figure 3, enables conjugation of many different growth factors, besides rhBMP-2, enabling creation of a platform technology for sustained growth factor delivery. This method was used to conjugate BMP-2 to PLGA scaffolds, with sustained release up to 14 days, increased ALP production by osteoblasts in vitro and better bone formation than scaffolds without BMP-2 or with BMP-2 attached without heparin [1]. Liu et al conjugated rhBMP-2 to PLGA using PEG and reported a conjugation efficiency of 79.8-83.4% [65], and sustained release for 8 days followed by gradual release up to 28 days. Furthermore, the PEG-

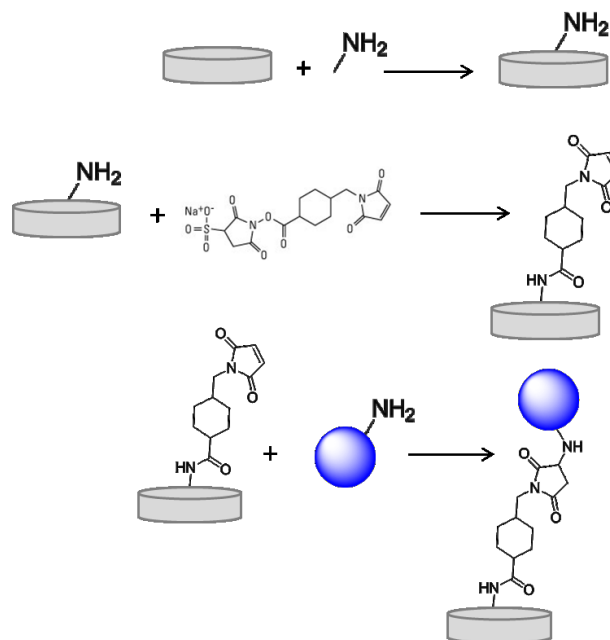


Figure 3.2: rhBMP-2 conjugation to PCL using sulfo-SMCC.

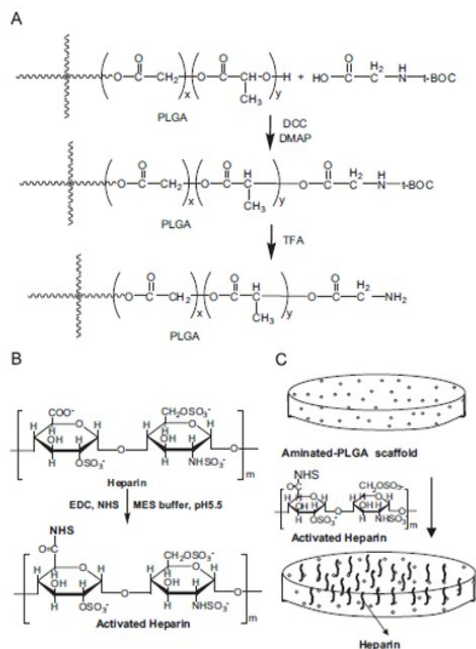


Figure 3.3: Conjugation to PLGA using heparin [1].

tethered PLGA/BMP-2 constructs seeded with BMSCs enhanced de novo bone formation in rabbit cranial defects.

A bone graft should encourage and support the infiltration of surrounding host cells. However, it may also be advantageous to initially seed the graft with some of the patient's own cells that could be pre-cultured to stimulate osteogenesis. Adult stem cells are good candidates for this approach because they are readily available from bone marrow aspirate or lipoaspirate, have the potential to differentiate down a number of lineages, and can be easily expanded and cultured *in vitro*. Both adipose derived stem cells (ADSC) [48, 62, 63, 69-76] and bone marrow stromal cells (BMSC) [47, 77-82] have been used in tissue engineering research. Donor-to-donor variability in osteogenic capacity has been reported for these cells and their response to osteogenic supplements or growth factors such as BMP-2 varies depending on the species. Because of these discrepancies, there is no consensus on which cell type is better for generating bone.

There is thus a need to further investigate the response of human ADSC and BMSC to various osteogenic stimulants. Human embryonic stem cells (hESC) have also been investigated for bone tissue applications [83-85] and have been successfully differentiated toward bone using a number of methods. Arpornmaeklong et al presented a novel method for producing a large number of osteoprogenitor cells from hESC. This method is simpler, more time effective and yields a greater number of osteogenically-primed mesenchymal stem cells than other methods, making it a promising cell production method for scaffold tissue engineering applications. Primary cells have been used in clinical cell therapy techniques to repair cartilage (Carticel) and skin (Apligraf). However, osteoblasts are difficult and painful to harvest, especially in large numbers, and can become senescent in culture, limiting their potential for tissue engineering applications requiring large numbers of active cells. Most research in the field is shifting toward using progenitor cells as opposed to primary cells. In this work, both adipose derived stem cells and bone marrow stromal cells are used to compare their osteogenic response to rhBMP-2 incorporated into PCL scaffolds.

3.5 Conclusion

A complete bone tissue engineered system consists of a scaffold, cells and growth factors, designed to stimulate the growth of new bone when implanted into a defect site. Systematic optimization of each of these factors is imperative for developing a generally appropriate solution and further refinement is needed to address the particulars of a specific application such as mandibular reconstruction or spinal fusion. In this thesis, the scaffold is the primary focus, initially defined by its permeability and later conjugated with BMP-2 in an effort to stimulate bone formation by human ADSC and BMSC. The

goal is to finalize a platform scaffold that can then be used for specific applications by altering the bulk scaffold shape and incorporating additional stimulatory factors if needed.

3.6 References

[1] Jeon O, Song SJ, Kang S-W, Putnam AJ, Kim B-S. Enhancement of ectopic bone formation by bone morphogenetic protein-2 released from a heparin-conjugated poly(L-lactic-co-glycolic acid) scaffold. *Biomaterials* 2007. p. 2763-71.

[2] Shields LBE, Raque GH, Glassman SD, Campbell M, Vitaz T, Harpring J, et al. Adverse effects associated with high-dose recombinant human bone morphogenetic protein-2 use in anterior cervical spine fusion. *Spine*. 2006;31:542-7.

[3] Dickerman RD, Reynolds AS, Morgan BC, Tompkins J, Cattorini J, Bennett M. rh-BMP-2 can be used safely in the cervical spine: dose and containment are the keys! *Spine Journal*. 2007;7:508-9.

[4] Chen N, Smith Z, Stiner E, Armin S, Sheikh H, Khoo L. Symptomatic ectopic bone formation after off-label use of recombinant human bone morphogenetic protein-2 in transforaminal lumbar interbody fusion. *Journal of Neurosurgery: Spine: American Association of Neurosurgery*; 2010. p. 40-6.

[5] Zhao Y, Zhang J, Wang X, Chen B, Xiao Z, Shi C, et al. The osteogenic effect of bone morphogenetic protein-2 on the collagen scaffold conjugated with antibodies. *Journal of Controlled Release*. 2010;141:30-7.

[6] Bohner M. Calcium orthophosphates in medicine: from ceramics to calcium phosphate cements. *Injury-International Journal of the Care of the Injured*. 2000;31:S37-S47.

[7] Sugawara A, Fujikawa K, Hirayama S, Takagi S, Chow LC. In Vivo Characteristics of Premixed Calcium Phosphate Cements When Implanted in Subcutaneous Tissues and Periodontal Bone Defects. *Journal of Research of the National Institute of Standards and Technology*. 2010;115:277-90.

- [8] Woodard JR, Hilldore AJ, Lan SK, Park CJ, Morgan AW, Eurell JAC, et al. The mechanical properties and osteoconductivity of hydroxyapatite bone scaffolds with multi-scale porosity. *Biomaterials*. 2007;28:45-54.
- [9] Fleming JE, Cornell CN, Muschler GE. Bone cells and matrices in orthopedic tissue engineering. *Orthopedic Clinics of North America*. 2000;31:357-+.
- [10] Chu TMG, Orton DG, Hollister SJ, Feinberg SE, Halloran JW. Mechanical and in vivo performance of hydroxyapatite implants with controlled architectures. *Biomaterials*. 2002;23:1283-93.
- [11] Jin QM, Takita H, Kohgo T, Atsumi K, Itoh H, Kuboki Y. Effects of geometry of hydroxyapatite as a cell substratum in BMP-induced ectopic bone formation. *Journal of Biomedical Materials Research*. 2000;52:491-9.
- [12] Jeong CG, Hollister SJ. Mechanical, Permeability, and Degradation Properties of 3D Designed Poly(1,8 Octanediol-co-Citrate) Scaffolds for Soft Tissue Engineering. *Journal of Biomedical Materials Research Part B-Applied Biomaterials*. 2010;93B:141-9.
- [13] Kemppainen JM, Hollister SJ. Tailoring the mechanical properties of 3D-designed poly(glycerol sebacate) scaffolds for cartilage applications. *Journal of Biomedical Materials Research Part A*. 2010;94A:9-18.
- [14] Roberts SJ, Howard D, BATTERY LD, Shakesheff KM. Clinical applications of musculoskeletal tissue engineering. *British Medical Bulletin*. 2008;86:7-22.
- [15] Kanczler JM, Barry J, Ginty P, Howdle SM, Shakesheff KM, Oreffo ROC. Supercritical carbon dioxide generated vascular endothelial growth factor encapsulated poly(DL-lactic acid) scaffolds induce angiogenesis in vitro. *Biochemical and Biophysical Research Communications*. 2007;352:135-41.
- [16] Ma PX, Choi JW. Biodegradable polymer scaffolds with well-defined interconnected spherical pore network. *Tissue Engineering*. 2001;7:23-33.
- [17] Yanoso-Scholl L, Jacobson JA, Bradica G, Lerner AL, O'Keefe RJ, Schwarz EM, et al. Evaluation of dense polylactic acid/beta-tricalcium phosphate scaffolds for bone tissue engineering. *Journal of Biomedical Materials Research Part A*. 2010;95A:717-26.

- [18] Tanaka Y, Yamaoka H, Nishizawa S, Nagata S, Ogasawara T, Asawa Y, et al. The optimization of porous polymeric scaffolds for chondrocyte/atelocollagen based tissue-engineered cartilage. *Biomaterials*. 2010;31:4506-16.
- [19] Mooney DJ, Baldwin DF, Suh NP, Vacanti LP, Langer R. Novel approach to fabricate porous sponges of poly(D,L-lactic-co-glycolic acid) without the use of organic solvents. *Biomaterials*. 1996;17:1417-22.
- [20] Saito E, Kang H, Taboas JM, Diggs A, Flanagan CL, Hollister SJ. Experimental and computational characterization of designed and fabricated 50:50 PLGA porous scaffolds for human trabecular bone applications. *Journal of Materials Science-Materials in Medicine*. 2010;21:2371-83.
- [21] Oh SH, Park IK, Kim JM, Lee JH. In vitro and in vivo characteristics of PCL scaffolds with pore size gradient fabricated by a centrifugation method. *Biomaterials*. 2007;28:1664-71.
- [22] Ciapetti G, Ambrosio L, Savarino L, Granchi D, Cenni E, Baldini N, et al. Osteoblast growth and function in porous poly- ϵ -caprolactone matrices for bone repair: a preliminary study. *Biomaterials*2003. p. 3815-24.
- [23] Williams JM, Adewunmi A, Schek RM, Flanagan CL, Krebsbach PH, Feinberg SE, et al. Bone tissue engineering using polycaprolactone scaffolds fabricated via selective laser sintering. *Biomaterials*. 2005;26:4817-27.
- [24] Hutmacher DW, Schantz T, Zein I, Ng KW, Teoh SH, Tan KC. Mechanical properties and cell cultural response of polycaprolactone scaffolds designed and fabricated via fused deposition modeling. *Journal of Biomedical Materials Research*. 2001;55:203-16.
- [25] Zein I, Hutmacher DW, Tan KC, Teoh SH. Fused deposition modeling of novel scaffold architectures for tissue engineering applications. *Biomaterials*. 2002;23:1169-85.
- [26] Marra KG, Szem JW, Kumta PN, DiMilla PA, Weiss LE. In vitro analysis of biodegradable polymer blend/hydroxyapatite composites for bone tissue engineering. *Journal of Biomedical Materials Research*. 1999;47:324-35.
- [27] Pitt CG, Chasalow FI, Hibionada YM, Klimas DM, Schindler A. Aliphatic polyesters. I. The degradation of poly(ϵ -caprolactone) in vivo. *Journal of Applied Polymer Science*1981. p. 3779-87.

- [28] Adewunmi B, Williams JM, Flanagan CL, Engel A, Hollister SJ. Mechanical and structural properties of polycaprolactone scaffolds made by selective laser sintering. 7th World Biomaterials Congress. Sydney, Australia 2004.
- [29] Fisher JP, Vehof JWM, Dean D, van der Waerden J, Holland TA, Mikos AG, et al. Soft and hard tissue response to photocrosslinked poly(propylene fumarate) scaffolds in a rabbit model. *Journal of Biomedical Materials Research*. 2002;59:547-56.
- [30] Lin C-Y, Schek RM, Mistry AS, Shi S, Mikos AG, Krebsbach PH, et al. Functional bone engineering using ex vivo gene therapy and topology-optimized, biodegradable polymer composite scaffolds. *Tissue Engineering* 2005. p. 1589-98.
- [31] Lee K-W, Wang S, Fox BC, Ritman EL, Yaszemski MJ, Lu L. Poly(propylene fumarate) bone tissue engineering scaffold fabrication using stereolithography: Effects of resin formulations and laser parameters. *Biomacromolecules*. 2007;8:1077-84.
- [32] Wang K, Cai L, Hao F, Xu XM, Cui MZ, Wang SF. Distinct Cell Responses to Substrates Consisting of Poly(epsilon-caprolactone) and Poly(propylene fumarate) in the Presence or Absence of Cross-Links. *Biomacromolecules*. 2010;11:2748-59.
- [33] Roosa SMM, Kemppainen JM, Moffitt EN, Krebsbach PH, Hollister SJ. The pore size of polycaprolactone scaffolds has limited influence on bone regeneration in an in vivo model. *Journal of Biomedical Materials Research Part A*. 2010;92A:359-68.
- [34] Murphy WL, Dennis RG, Kileny JL, Mooney DJ. Salt fusion: An approach to improve pore interconnectivity within tissue engineering scaffolds. *Tissue Engineering*. 2002;8:43-52.
- [35] Ayers RA, Wolford LM, Bateman TA, Ferguson VL, Simske SJ. Quantification of bone ingrowth into porous block hydroxyapatite in humans. *Journal of Biomedical Materials Research*. 1999;47:54-9.
- [36] Hulbert SF, Young FA, Mathews RS, Klawitter JJ, Talbert CD, Stelling FH. POTENTIAL OF CERAMIC MATERIALS AS PERMANENTLY IMPLANTABLE SKELETAL PROSTHESES. *Journal of Biomedical Materials Research*. 1970;4:433-56.
- [37] Robinson BP, Hollinger JO, Szachowicz EH, Brekke J. CALVARIAL BONE REPAIR WITH POROUS D,L-POLYLACTIDE. *Otolaryngology-Head and Neck Surgery*. 1995;112:707-13.

- [38] Hollister SJ, Lin CY, Saito E, Schek RD, Taboas JM, Williams JM, et al. Engineering craniofacial scaffolds. *Orthodontics & craniofacial research*. 2005;8:162-73.
- [39] Hui PW, Leung PC, Sher A. Fluid conductance of cancellous bone graft as a predictor for graft-host interface healing. *Journal of Biomechanics*. 1996;29:123-32.
- [40] Jones AC, Arns CH, Sheppard AP, Hutmacher DW, Milthorpe BK, Knackstedt MA. Assessment of bone ingrowth into porous biomaterials using MICRO-CT. *Biomaterials*. 2007;28:2491-504.
- [41] Agrawal CM, McKinney JS, Lanctot D, Athanasiou KA. Effects of fluid flow on the in vitro degradation kinetics of biodegradable scaffolds for tissue engineering. *Biomaterials*. 2000;21:2443-52.
- [42] Kemppainen JM, Hollister SJ. Differential effects of designed scaffold permeability on chondrogenesis by chondrocytes and bone marrow stromal cells. *Biomaterials*. 2010;31:279-87.
- [43] Li SH, de Wijn JR, Li JP, Layrolle P, de Groot K. Macroporous biphasic calcium phosphate scaffold with high permeability/porosity ratio. *Tissue Engineering*. 2003;9:535-48.
- [44] Israel DI, Nove J, Kerns KM, Moutsatsos IK, Kaufman RJ. Expression and characterization of bone morphogenetic protein-2 in Chinese hamster ovary cells. *Growth factors (Chur, Switzerland)*. 1992;7:139-50.
- [45] Ruppert R, Hoffmann E, Sebald W. Human bone morphogenetic protein 2 contains a heparin-binding site which modifies its biological activity. *European Journal of Biochemistry*. 1996;237:295-302.
- [46] Katagiri T, Yamaguchi A, Komaki M, Abe E, Takahashi N, Ikeda T, et al. Bone Morphogenetic Protein-2 Converts the Differentiation Pathway OF C2C12 Myoblasts into the Osteoblast Lineage. *Journal of Cell Biology*. 1994;127:1755-66.
- [47] Huang WB, Carlsen B, Wulur I, Rudkin G, Ishida K, Wu B, et al. BMP-2 exerts differential effects on differentiation of rabbit bone marrow stromal cells grown in two-dimensional and three-dimensional systems and is required for in vitro bone formation in a PLGA scaffold. *Experimental Cell Research*. 2004;299:325-34.

- [48] Knippenberg M, Helder MN, Doulabi BZ, Wuisman P, Klein-Nulend J. Osteogenesis versus chondrogenesis by BMP-2 and BMP-7 in adipose stem cells. *Biochemical and Biophysical Research Communications*. 2006;342:902-8.
- [49] Noel D, Gazit D, Bouquet C, Apparailly F, Bony C, Ponce P, et al. Short-term BMP-2 expression is sufficient for in vivo osteochondral differentiation of mesenchymal stem cells. *Stem Cells*. 2004;22:74-85.
- [50] Basmanav FB, Kose GT, Hasirci V. Sequential growth factor delivery from complexed microspheres for bone tissue engineering. *Biomaterials*. 2008;29:4195-204.
- [51] Jeon O, Song SJ, Yang HS, Bhang S-H, Kang S-W, Sung MA, et al. Long-term delivery enhances in vivo osteogenic efficacy of bone morphogenetic protein-2 compared to short-term delivery. *Biochemical and Biophysical Research Communications*. 2008;369:774-80.
- [52] Kim S, Kang YQ, Krueger CA, Sen ML, Holcomb JB, Chen D, et al. Sequential delivery of BMP-2 and IGF-1 using a chitosan gel with gelatin microspheres enhances early osteoblastic differentiation. *Acta Biomaterialia*. 2012;8:1768-77.
- [53] Cabric S, Sanchez J, Johansson U, Larsson R, Nilsson B, Korsgren O, et al. Anchoring of Vascular Endothelial Growth Factor to Surface-Immobilized Heparin on Pancreatic Islets: Implications for Stimulating Islet Angiogenesis. *Tissue Engineering Part A*. 2010;16:961-70.
- [54] Koo K, Yeo D, Ahn J, Kim B-S, Kim C-S, Im G-I. Lumbar posterolateral fusion using heparin-conjugated fibrin for sustained delivery of BMP2 in a rabbit model. *Artificial Organs* 2012.
- [55] He Q, Zhao Y, Chen B, Xiao Z, Zhang J, Chen L, et al. Improved cellularization and angiogenesis using collagen scaffolds chemically conjugated with vascular endothelial growth factor. *Acta Biomaterialia*. 2011;7:1084-93.
- [56] Masters KS. Covalent Growth Factor Immobilization Strategies for Tissue Repair and Regeneration. *Macromolecular Bioscience*. 2011;11:1149-63.
- [57] Pohl TLM, Boergermann JH, Schwaerzer GK, Knaus P, Cavalcanti-Adam EA. Surface immobilization of bone morphogenetic protein 2 via a self-assembled monolayer formation induces cell differentiation. *Acta Biomaterialia*. 2012;8:772-80.

- [58] Zhang HN, Migneco F, Lin CY, Hollister SJ. Chemically-Conjugated Bone Morphogenetic Protein-2 on Three-Dimensional Polycaprolactone Scaffolds Stimulates Osteogenic Activity in Bone Marrow Stromal Cells. *Tissue Engineering Part A*. 2010;16:3441-8.
- [59] Park YJ, Kim KH, Lee JY, Ku Y, Lee SJ, Min BM, et al. Immobilization of bone morphogenetic protein-2 on a nanofibrous chitosan membrane for enhanced guided bone regeneration. *Biotechnology and Applied Biochemistry*. 2006;43:17-24.
- [60] Melhorn AT, Niemeyer P, Kaschte K, Muller L, Finkenzeller G, Hartl D, et al. Differential effects of BMP-2 and TGF- β 1 on chondrogenic differentiation of adipose derived stem cells. 2007. p. 809-23.
- [61] Schek RM, Wilke EN, Hollister SJ, Krebsbach PH. Combined use of designed scaffolds and adenoviral gene therapy for skeletal tissue engineering. *Biomaterials*. 2006;27:1160-6.
- [62] Chen QA, Yang ZL, Sun SJ, Huang H, Sun XJ, Wang ZG, et al. Adipose-derived stem cells modified genetically in vivo promote reconstruction of bone defects. *Cytotherapy*. 2010;12:831-40.
- [63] Peterson B, Zhang J, Iglesias R, Kabo M, Hedrick M, Benhaim P, et al. Healing of critically sized femoral defects, using genetically modified mesenchymal stem cells from human adipose tissue. *Tissue Engineering*. 2005;11:120-9.
- [64] Pereira CT, Huang W, Sayer G, Jarrahy R, Rudkin G, Miller TA. Osteogenic Potential of Polymer-Bound Bone Morphogenetic Protein-2 on MC3T3-E1 Two-Dimensional Cell Cultures. *Plastic and Reconstructive Surgery*. 2009;124:2199-200.
- [65] Liu H-W, Chen C-H, Tsai C-L, Hsiue G-H. Targeted delivery system for juxtacrine signaling growth factor based on rhBMP-2-mediated carrier-protein conjugation. *Bone*. 2006;39:825-36.
- [66] Gittens SA, Matyas JR, Zernicke RF, Uludag H. Imparting bone affinity to glycoproteins through the conjugation of bisphosphonates. *Pharmaceutical Research*. 2003;20:978-87.
- [67] Zhang Q, He Q-F, Zhang T-H, Yu X-L, Liu Q, Deng F. Improvement in the delivery system of bone morphogenetic protein-2: a new approach to promote bone formation. *Biomedical Materials* 2012.

- [68] Hermanson GT. *Bioconjugate Techniques*. 2 ed: Elsevier; 2008.
- [69] Bionaz M, Mkrtschjan M, Kyrouac D, Hollister SJ, Wheeler MB. In Vitro Migration of Adipose-Derived Stem Cells From GFP Pigs Into Polycaprolactone Scaffolds Treated With FGF Or BMP2. *Reproduction Fertility and Development*. 2012;24:219-.
- [70] Chou Y-F, Zuk PA, Chang T-L, Benhaim P, Wu BM. Adipose-Derived stem cells and BMP-2: Part 1. BMP2-treated adipose derived stem cells do not improve repair of segmental femoral defects. *Connective Tissue Research*2011. p. 109-18.
- [71] Dudas JR, Marra KG, Cooper GM, Penascino VM, Mooney MP, Jiang S, et al. The osteogenic potential of adipose-derived stem cells for the repair of rabbit calvarial defects. *Annals of Plastic Surgery*. 2006;56:543-8.
- [72] Flynn LE, Prestwich GD, Semple JL, Woodhouse KA. Proliferation and differentiation of adipose-derived stem cells on naturally derived scaffolds. *Biomaterials*. 2008;29:1862-71.
- [73] Kim HP, Ji Y-h, Rhee SC, Dhong ES, Park SH, Yoon E-S. Enhancement of Bone Regeneration Using Osteogenic-Induced Adipose-Derived Stem Cells Combined with Demineralized Bone Matrix in a Rat Critically-Sized Calvarial Defect Model. *Current Stem Cell Research & Therapy*. 2012;7:165-72.
- [74] Mesimaki K, Lindroos B, Tornwall J, Mauno J, Lindqvist C, Kontio R, et al. Novel maxillary reconstruction with ectopic bone formation by GMP adipose stem cells. *International Journal of Oral and Maxillofacial Surgery*. 2009;38:201-9.
- [75] Panetta NJ, Gupta DM, Lee JK, Wan DC, Commons GW, Longaker MT. Human Adipose-Derived Stromal Cells Respond to and Elaborate Bone Morphogenetic Protein-2 during In Vitro Osteogenic Differentiation. *Plastic and Reconstructive Surgery*. 2010;125:483-93.
- [76] Zuk P, Chou Y, Mussano F, Benhaim P, Wu B. Adipose derived stem cells and BMP-2: Part 2. BMP-2 may not influence the osteogenic fate of human adipose-derived stem cells. *Connective Tissue Research*2011. p. 119-32.
- [77] Kim D, Monaco E, Maki A, de Lima AS, Kong HJ, Hurley WL, et al. Morphologic and transcriptomic comparison of adipose- and bone-marrow-derived porcine stem cells cultured in alginate hydrogels. *Cell and Tissue Research*. 2010;341:359-70.

[78] Farrell E, Both SK, Odoerfer KI, Koevoet W, Kops N, O'Brien FJ, et al. In-vivo generation of bone via endochondral ossification by in-vitro chondrogenic priming of adult human and rat mesenchymal stem cells. *Bmc Musculoskeletal Disorders*. 2011;12.

[79] Kasten P, Vogel J, Luginbuhl R, Niemeyer P, Tonak M, Lorenz H, et al. Ectopic bone formation associated with mesenchymal stem cells in a resorbable calcium deficient hydroxyapatite carrier. *Biomaterials*. 2005;26:5879-89.

[80] Liu H-W, Chen C-H, Tsai C-L, Lin IH, Hsiue G-H. Heterobifunctional poly(ethylene glycol)-tethered bone morphogenetic protein-2-stimulated bone marrow mesenchymal stromal cell differentiation and osteogenesis. *Tissue Engineering*. 2007;13:1113-24.

[81] Yamaguchi A, Yokose S, Ikeda T, Katagiri T, Wozney JM, Rosen V, et al. BMP-2 Induces Bone Marrow Stromal Cells to Differentiate into Osteoblasts and Decreases their Capacity to Support Osteoclast Formation. *Journal of Bone and Mineral Research*. 1993;8:S158-S.

[82] Ter Brugge PJ, Jansen JA. In vitro osteogenic differentiation of rat bone marrow cells subcultured with and without dexamethasone. *Tissue Engineering*. 2002;8:321-31.

[83] Arpornmaeklong P, Wang Z, Pressler MJ, Brown SE, Krebsbach PH. Expansion and Characterization of Human Embryonic Stem Cell-Derived Osteoblast-Like Cells. *Cellular Reprogramming*. 2010;12:377-89.

[84] Ward BB, Brown SE, Krebsbach PH. Bioengineering strategies for regeneration of craniofacial bone: a review of emerging technologies. *Oral Diseases*. 2010;16:709-16.

[85] Arpornmaeklong P, Brown SE, Wang Z, Krebsbach PH. Phenotypic Characterization, Osteoblastic Differentiation, and Bone Regeneration Capacity of Human Embryonic Stem Cell-Derived Mesenchymal Stem Cells. *Stem Cells and Development*. 2009;18:955-68.

CHAPTER 4 The Effect of Polycaprolactone Scaffold Permeability on Bone Regeneration *In Vivo*

4.1 Introduction

Biomaterial scaffolds delivering osteogenic factors are a potential alternative to traditional techniques for repairing bone defects resulting from trauma, tumor resection and developmental anomalies. Defining the optimal scaffold for these purposes requires determination of key parameters that have the greatest influence on bone regeneration. For defects of clinically relevant size and shape, the scaffold should allow sufficient nutrient diffusion and waste removal while simultaneously providing adequate load bearing capabilities. Generally speaking, there is a trade-off between these two requirements, as scaffold architectures designed to maximize nutrient diffusion typically result in decreased scaffold mechanical strength. Optimization of scaffold design to satisfy both of these constraints remains a challenge. Therefore, it is important to understand the impact that each of these putative design requirements have on bone regeneration.

Porosity, pore size and permeability are interrelated architectural properties that have been shown to influence both diffusion and scaffold mechanical properties [1, 2]. Unlike porosity, pore size and a number of other structural parameters that have been studied in regards to bone growth [3-5], permeability defines the physical property of

mass transport, which inherently describes the effects that these structural design properties have on fluid transport into and out of a construct. The effects that scaffold permeability has on bone tissue regeneration have not been studied in depth using rigorously controlled porous architectures with reproducibly designed effective permeability. In this work, scaffolds are designed such that permeability changes while pore shape, pore size and pore interconnectivity are held constant between groups in order to specifically compare the effects of increasing permeability on bone growth. Image based design (IBD) combined with solid free form fabrication (SFF) enables the creation of scaffolds that have precise permeability characteristics resulting from rigorously controlled 3D architecture. By using these techniques, the effects that permeability has on the growth of bone tissue into a scaffold can be investigated, providing important considerations for developing optimized constructs.

In recent literature, the range of variables examined for their effect on bone growth extends beyond scaffold design to include cell type, growth factors and scaffold material. Common cell types studied for bone regeneration include fibroblasts, osteoblasts and stem cells, often combined with one or more growth factors such as insulin-like growth factor (IGF), transforming growth factor beta (TGF- β) or bone morphogenetic proteins (BMP). These cells and growth factors are housed within scaffolds made of a variety of materials. Polypropylene fumarate (PPF) [6, 7], poly- ϵ -caprolactone (PCL) [4, 8, 9], polylactic acid (PLA) [10, 11], and poly(lactic-co-glycolic) acid (PLGA) [12, 13] are bioresorbable polymers that have all been investigated, alone or in combination, for bone applications, as have osteoconductive materials such as

tricalcium phosphate (TCP) [10], hydroxy apatite (HA) [14], and calcium phosphate (CaP) [15, 16].

This work uses PCL scaffolds seeded with bone morphogenetic protein-7(BMP-7)-transduced human gingival fibroblasts to study the effects that permeability has on bone tissue regeneration. PCL has been used extensively for tissue engineering applications [4, 8-10, 17, 18]. The degradation profile and mechanical properties of this polymer support its use for bone tissue engineering. PCL scaffolds can be manufactured using a variety of SFF techniques, making PCL a favorable material for studying scaffold architecture effects on tissue regeneration and for subsequent use in clinical tissue engineering applications. Examples of SFF techniques that have been used to create PCL scaffolds include selective laser sintering (SLS) [9], fused deposition modeling [17], photopolymerization of PCL monomer [18] and three dimensional printing (3DP) [10]. Specifically for the purposes of this study, PCL is compatible with the image based design (IBD) and 3DP-direct casting techniques we have used to fabricate consistent, reproducible scaffolds with designed architectures. BMP-7-transduced fibroblasts were utilized as a cell source known to reproducibly generate bone in ectopic sites [4, 19].

Various studies have investigated scaffold architectures that may or may not affect bone growth, with many hypothesizing that results are dependent on the fluid flow and nutrient/waste diffusion properties imposed by the design parameters [1, 2, 18]. Roosa et al [4] determined that different pore sizes (350, 500 and 800 μm) had little effect on *in vivo* bone growth using PCL scaffolds. Others have concluded that increased scaffold porosity is important for cell delivery [20] and sufficient diffusion of nutrients and waste into and out of the scaffold. While studies may support or refute the

requirement of specific pore sizes and shapes, strut/fiber diameters, interconnectivity, or porosities for optimal bone growth, it is important to acknowledge that these design parameters 1) are related to and contingent on one another, and 2) may have a profound effect on the mechanical properties of scaffolds. This work primarily addresses the first challenge by proposing a more definitive way to examine impacts that scaffold architectures may have on tissue growth. This is done by studying the effects of scaffold permeability, a design parameter which, in terms of fluid flow, incorporates all of these design variables.

This work also addresses the second concern of maintaining sufficient mechanical properties to support developing tissue while optimizing scaffold architecture for enhanced bone regeneration. By inference, if permeability is shown to affect the amount of bone generated on PCL scaffolds, structural parameters such as pore size and shape, interconnectivity, strut size and shape, and porosity can be manipulated to meet biomechanical requirements while maintaining permeability within desired ranges. Alternatively, if permeability is shown to have no effect on bone regeneration, these structural parameters can be optimized strictly for mechanical or other desired properties. Furthermore, the work determines the mechanical properties of the scaffold architectures used and compares their modulus and strength to that of native bone as a proof of concept for using PCL to fabricate scaffolds for bone tissue applications.

This study specifically addresses the importance of scaffold permeability as a design parameter and the need for balancing pore geometry with mechanical properties to create scaffolds that allow for bone regeneration, support load, and can be easily manufactured. By utilizing two scaffold designs that held pore shape, pore size, and pore

interconnectivity constant yet resulted in differing permeability, the effect that the latter parameter has on bone regeneration was evaluated in terms of 1) volume, mineral density and mineral content of bone within the entire scaffold, assessed by micro-computed tomography (μ CT) and histology, 2) penetration of bone through the interior of the scaffold, assessed by μ CT analysis with concentric regions of interest, and 3) compressive modulus and strength of resultant bone-polymer constructs, assessed by unconfined compression testing at 4 and 8 weeks in a previously characterized immune-compromised mouse model [4, 19, 21].

4.2 Materials and Methods

4.2.1 Scaffold Fabrication

“Low” and “High” permeability scaffolds were previously designed that have a permeability (determined by computational methods based on Stoke’s flow) of 8.23×10^{-10} or 6.44×10^{-9} (m^2), respectively. The low and high permeability designs have

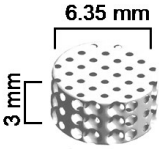
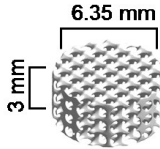
	Low Permeability	High Permeability
		
Permeability (m^2)	8.23×10^{-10}	6.44×10^{-9}
Porosity (%)	53.46	70
Surface Area (mm^2)	317.69	260.52

Table 4-1: Scaffold design properties.

porosities of 53.46% and 70%, and surface areas of 317.69 mm² and 260.52 mm², respectively. The designs and associated properties are displayed in Table 1. Inverse wax molds were built on a Solidscape Model Maker II machine (Solidscape, Inc., Merrimack, NH) and subsequently melt cast into PCL powder (43-50 kDa, Polysciences, Warrington, PA) at 115°C. The cast scaffolds were cooled and hardened overnight in a Teflon mold, placed in 100% ethanol to dissolve the wax mold, trimmed and cleaned with wire. Prior to cell seeding, the scaffolds were sterilized by placing them in 70% ethanol for 24 hours, followed by sterile water for 24 hours and serum-free medium overnight.

4.2.2 Cell Culture and Subcutaneous Implantation Procedure

Human gingival fibroblasts (ScienCell Research Laboratories, Carlsbad, CA) were cultured in Dulbecco's Modified Eagle Medium, supplemented with 10% fetal calf serum and 5% penicillin/streptomycin (all reagents from Gibco, Carlsbad, CA). Four week and eight week studies were carried out separately. For each study, cells were cultured until a sufficient number of cells was reached. The day before implantation, the cells were transduced with Ad-BMP-7 (Vector Core, University of Michigan, Ann Arbor, MI) as previously described [21] at a concentration of 500 pfu/cell. On the day of implantation, 0.75×10^6 cells were seeded into each scaffold (6.35 mm diameter, 3 mm height) using a 1:20 thrombin:fibrinogen gel for cell encapsulation. Seeded scaffolds (n = 18 per low and high permeability design, for each time point) were kept on ice prior to subcutaneous implantation in the backs of NIH3-bg-nu-xid mice (Harlan Laboratories, Indianapolis, IN). Scaffolds infiltrated with a 1:20 thrombin/fibrinogen gel alone (no cells) were used as controls. After four or eight weeks, mice were euthanized and

scaffolds were removed, then placed in Z-Fix overnight, in water for 2 hours and stored in 70% ethanol. Fourteen specimens were excluded from analysis (2 low permeability/four weeks, 7 low permeability/eight weeks and 5 low permeability/eight weeks) due to the death of three animals and difficulties encountered in scaffold processing. This study was conducted in accordance with the regulations set forth by the University Committee on Use and Care of Animals at the University of Michigan.

4.2.3 *Micro-computed Tomography (μ CT) Analysis*

Explanted, fixed scaffolds were scanned in water with a high resolution μ CT scanner (GE Medical Systems, Toronto, CAN) at 75 kV and 75 mA. Bone volume analysis was performed using GEMS Microview software (GE Medical Systems, Toronto, CAN) to obtain bone volume (BV), tissue mineral density (TMD) and tissue mineral content (TMC) data, using a bone threshold value of 1100. TMD measures the *degree* of mineralization of tissue that has been designated bone by the μ CT threshold analysis value (1100) within a given volume, and has units of mass of hydroxyapatite per volume (mg HyAp/ml). TMC quantifies the *amount* of mineralized tissue in the given region of interest (ROI) and has units of mass of hydroxyapatite (mg HyAp). A cubic ROI exceeding scaffold boundaries, was used for “total bone volume” values (includes bone grown inside and outside scaffold boundaries). A cylindrical ROI with fixed x and y dimensions of 6.3455 mm and an average z dimension of 2.5786 ± 0.3963 was used to calculate the total volume of bone generated within scaffold boundaries (“scaffold bone volume”), as well as the percentage of available pore space occupied by bone (“percent occupied pore space”). Pore volume fractions of 0.574 and 0.738 (for the low and high

permeability designs, respectively) were multiplied by bounding scaffold dimensions to calculate available pore volume.

4.2.4 Unconfined Compression Testing

Explanted, fixed experimental and control scaffolds were mechanically tested in unconfined compression using an MTS Alliance RT30 electromechanical test frame (MTS Systems Corp., Minneapolis, MN). Specimens were compressed to 40% strain between two fixed steel platens at a rate of 1.0 mm/min after a 0.5 lbf preload was applied. Data were collected and analyzed using TestWorks4 software (MTS Systems Corp., Minneapolis, MN). Compressive modulus was defined as the slope of the tangent line to the stress-strain curve at 12.5% strain. Compressive yield strength was calculated as the load carried at the 0.2% offset point divided by the original scaffold cross-sectional area.

4.2.5 Histology

At each time point, two fixed scaffolds from each group were sectioned and stained with hematoxylin and eosin to visualize tissue morphology. Sections were viewed under a light microscope and images were obtained at 200X and 400X magnification.

4.2.6 Statistics

Multiple linear regression, performed using SPSS software (SPSS for Windows, Rel 14.0. 2005, SPSS, Inc., Chicago, IL), was used to determine which factors had a significant effect on a given response variable.

4.3 Results

4.3.1 Micro-CT

a) Entire Scaffold Analysis

Micro-CT analysis demonstrated that total bone volume (scaffold bone volume plus bone surrounding the scaffold) did not differ between the low and high permeability

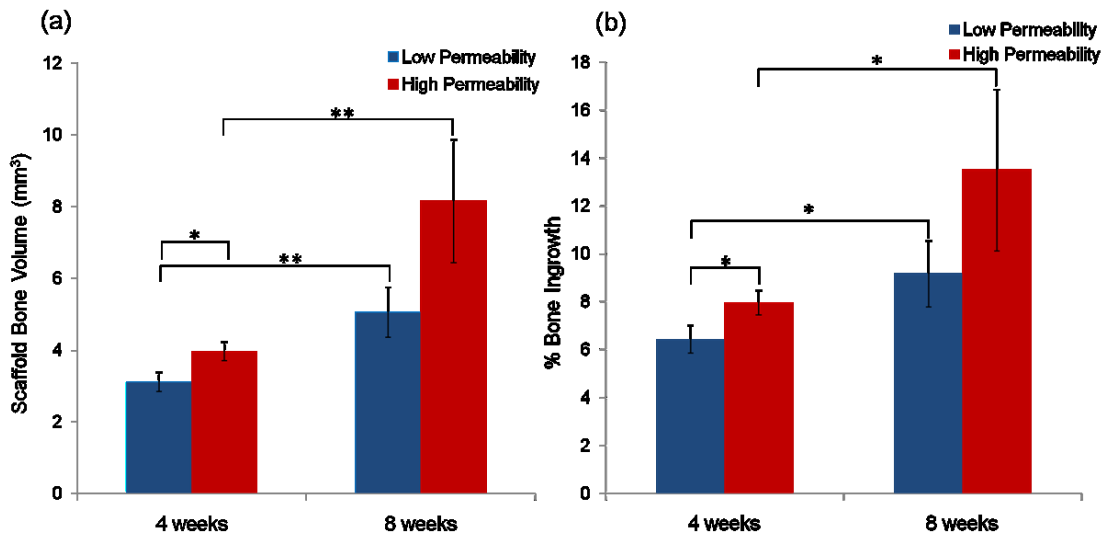


Figure 4.1: a) Bone volume inside the scaffold ROI at 4 and 8 weeks. b) Bone in-growth for the scaffold ROI at 4 and 8 weeks. * $p \leq 0.05$. ** $p \leq 0.01$.

scaffold designs at either time point. However, scaffold bone volume did differ between designs (see Figure 1a). Scaffold bone volume was significantly greater for the high permeability design ($p \leq 0.05$) as compared to the low permeability design at four weeks and was also greater for the high permeability design at eight weeks, although this difference was not significant ($p = 0.11$). Both designs demonstrated a statistically significant increase in scaffold bone volume at eight weeks as compared to four weeks ($p \leq 0.01$). Bone in-growth (Figure 1b) significantly increased with time ($p \leq 0.05$) for both

designs. Also, the high permeability design showed greater bone in-growth as compared to the low permeability design at four weeks ($p \leq 0.05$). At eight weeks, the high permeability scaffolds again averaged a higher bone in-growth than low permeability scaffolds, but this difference was not significant ($p = 0.25$). Micro-CT slices through the middle of a high and a low permeability scaffold after eight weeks *in vivo* (Figure 2b and 2d) show that there appears to be more mineralized tissue in the center of the high permeability scaffolds, compared to the low permeability scaffolds. The concentric cylinder analysis further demonstrated this phenomenon (see below).

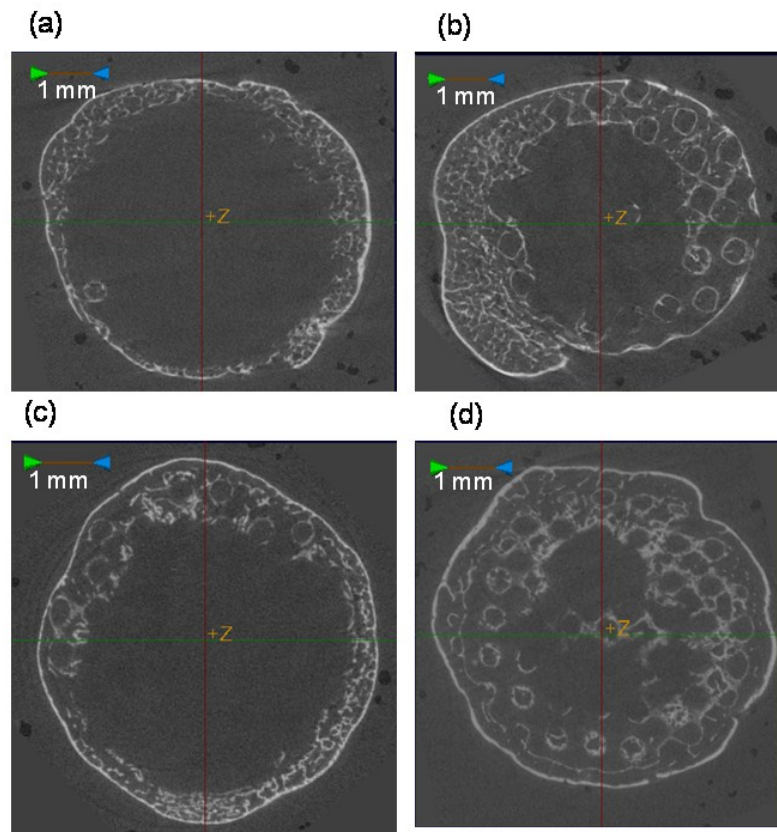


Figure 4.2: Micro-CT image slices from the center of representative low and high permeability scaffolds at 4 weeks (A and C) and 8 weeks (B and D). Scale bars: 1 mm.

TMC values within the scaffold space for four and eight weeks are displayed in Figure

3a. Time had a greater influence on TMC than scaffold design did, with significant increases in TMC from four to eight weeks for both scaffold designs ($p \leq 0.05$). TMC

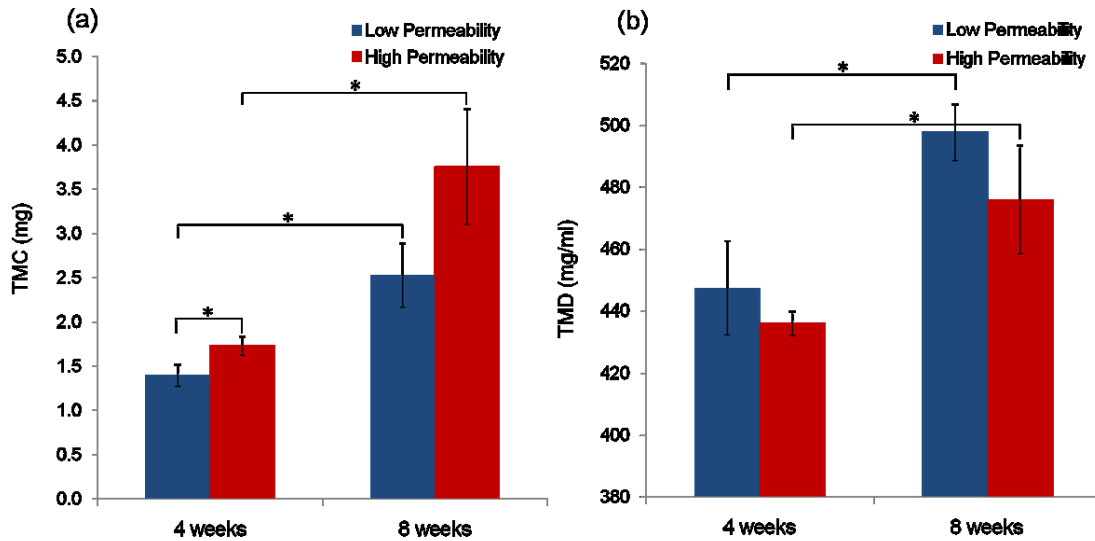


Figure 4.3: (a) Tissue Mineral Content (TMC) and (b) Tissue Mineral Density (TMD) at 4 and 8 weeks.

was also greater for high permeability scaffolds compared to low permeability scaffolds at 4 weeks ($p \leq 0.05$). Average TMD values for bone grown on each design at both four and eight weeks (range = 360-600 mg/ml) fell within the ranges of normal human trabecular and cortical bone [22] and are displayed in Figure 3b. Time *in vivo* had a greater influence on TMD values than scaffold design did. No significant differences in TMD were seen between scaffold design at either time point, but TMD increased

significantly from four to eight weeks for both scaffold designs ($p \leq 0.05$).

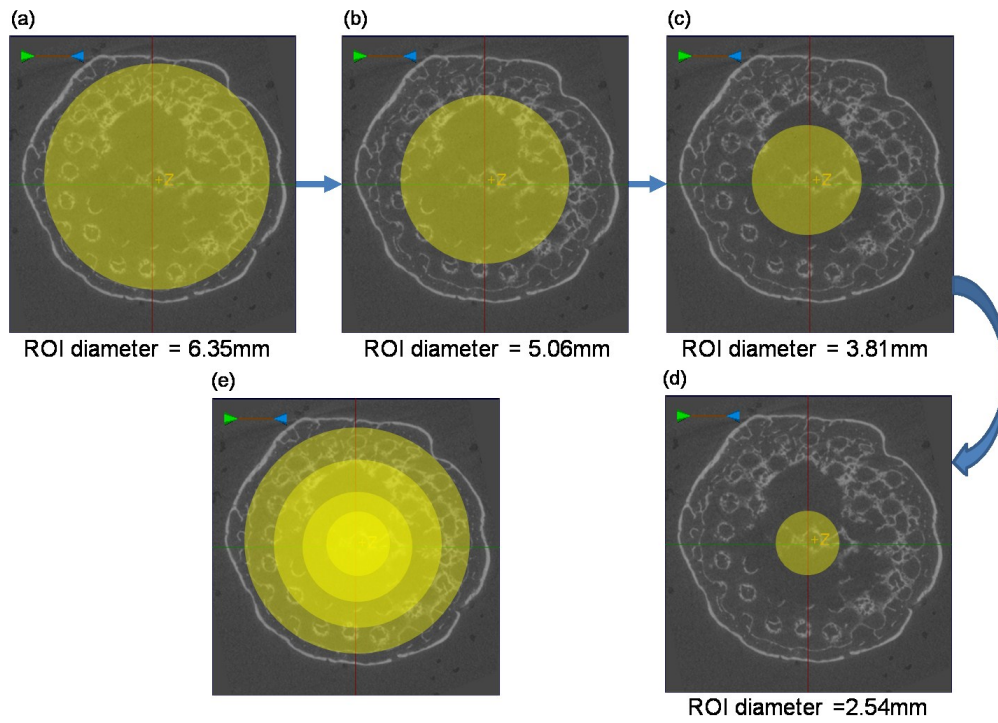


Figure 4.4: Schematic of concentric cylinder bone volume analysis.

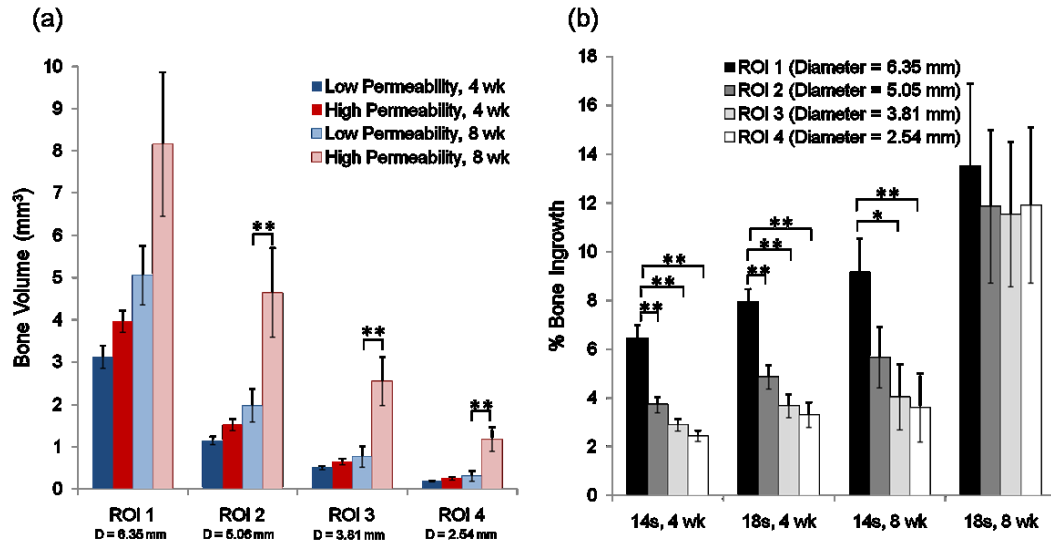


Figure 4.5: Concentric cylinder bone volume analysis. (a) Bone Volume and (b) bone in-growth for high and low permeability scaffolds and 4 and 8 weeks, for four cylindrical regions of interest (ROIs).
* $p \leq 0.05$. ** $p \leq 0.01$.

b) Concentric Cylinder Analysis

The diameters of the cylindrical ROIs were decreased by 1.29 mm each time to create a set of four, concentric ROIs, as shown in Figure 4. For each of these regions, the high permeability scaffolds at 8 weeks contained more bone volume than their low permeability counterparts, with significant differences ($p \leq 0.01$) for ROI 2, ROI 3 and ROI 4 (ROI 1 did not show significance at a 0.05 level, although the p-value was still relatively low, at $p = 0.1$), as shown in Figure 5a. This shows that bone penetrated into the center of the scaffold and was not confined to the edges of the scaffold. For bone in-growth, the most interesting comparisons were those between ROIs for each scaffold design group, as shown in Figure 5b. For both scaffold designs at four weeks and for the low permeability design at eight weeks, in-growth significantly decreased going from the entire scaffold ROI to smaller ROIs. This would suggest that for these groups, in-growth is not maintained throughout the scaffold. However, for the high permeability scaffolds at

eight weeks, this decrease is not observed, demonstrating that in-growth of bone is seen throughout the entire scaffold progressing through the center of the scaffold.

4.3.2 *Compression Testing*

Tangent modulus at 12.5% strain and compressive yield strength at the 0.2% offset yield point are shown in Figure 6 for both scaffold designs and both time points. Modulus and compressive yield strength values of low permeability scaffolds were significantly higher than those for high permeability scaffolds at zero, four and eight weeks ($p \leq 0.01$). Time *in vivo* did not significantly affect tangent modulus values of scaffold-bone constructs for the low permeability design. However, for the high permeability design, there is a significant increase ($p \leq 0.01$) in modulus at eight weeks. Similarly, compressive yield strength (Figure 6b) increases significantly ($p \leq 0.05$) from zero to four and from four to eight weeks for the high permeability design. Average yield strength of low permeability constructs also increased between zero and four weeks ($p \leq 0.01$), but a decrease was seen between four and eight weeks ($p \leq 0.01$).

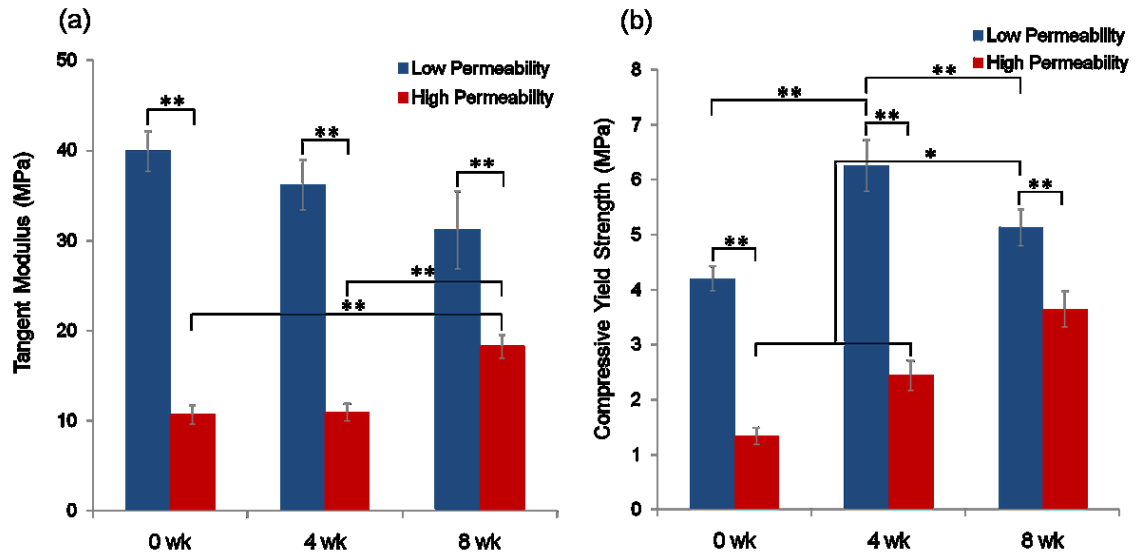


Figure 4.6: (a) Tangent modulus at 12.5% strain, 4 and 8 weeks. (b) Compressive yield strength at 0.2% offset. * $p \leq 0.05$. ** $p \leq 0.01$.

Histological analysis confirmed bone growth (reported quantitatively through μ CT assessment) in and around scaffold pores. Figure 7 shows representative histological sections from an eight week, high permeability scaffold at 50X and 400X (panels (a) and (b), respectively), and an eight week, low permeability scaffold at 50X and 400X (panels (c) and (d), respectively). In the low magnification images, the dark pink staining representing bone is indicated by the arrows and is visible in the pore spaces of the representative high permeability scaffold (a). For the low permeability scaffold (c), this dark pink staining is mainly seen toward the outer edges of the construct. Marrow space

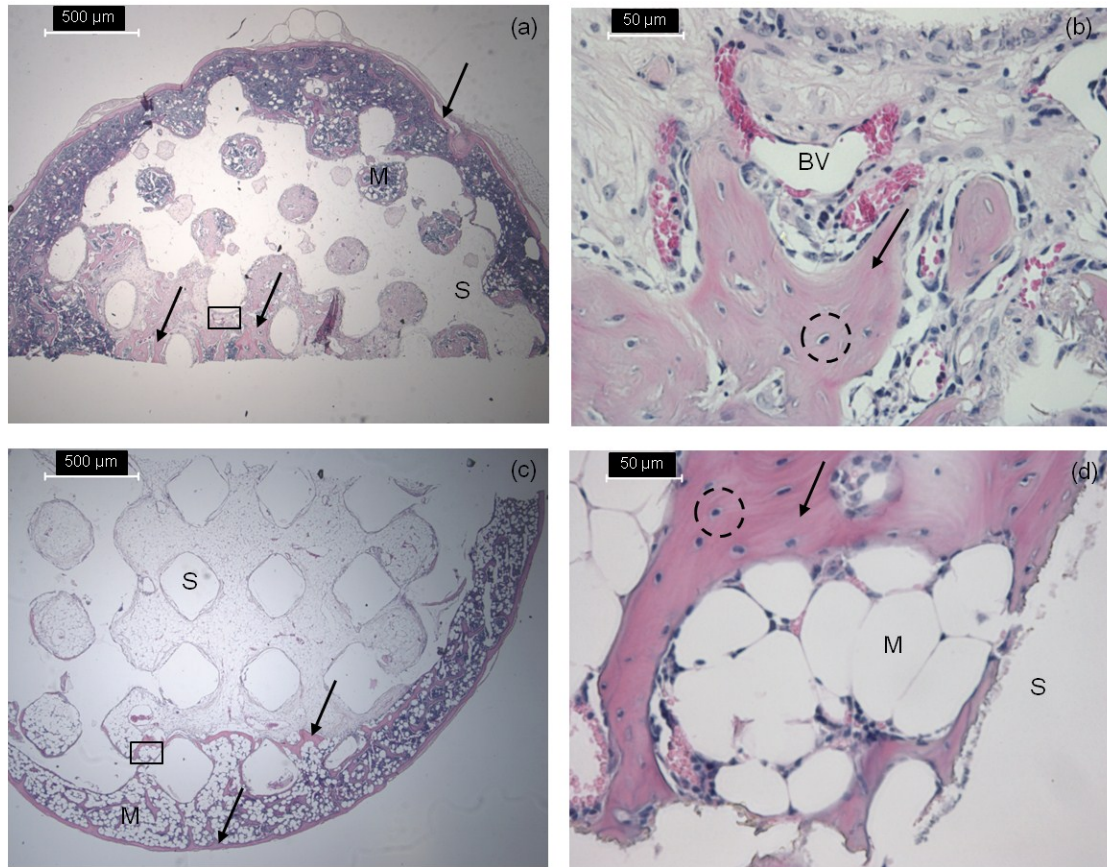


Figure 4.7: Representative histological sections of high permeability (a and b) and low permeability (c and d) scaffolds at 8 weeks. B and D are higher magnification images of rectangular insets indicated in A and C. Bone growth in and around the scaffold is indicated by the dark pink staining and arrows. Osteocytes in lacunae are seen in both high and low permeability scaffolds (indicated by dashed circles) as is marrow space ('M'). Blood vessels are also seen in the high permeability scaffold ('BV').

is indicated in the images by the letter 'M', osteocytes in lacunae are circled and blood vessel infiltration is indicated by 'BV'. All scaffolds displayed a thin layer of bone around the outside of the scaffold. Compared to lower permeability scaffolds, the higher permeability scaffolds showed more evidence of bone spicules growing within the pore space, as shown by greater areas of dark pink staining.

4.4 Discussion

The ultimate goal of utilizing biomaterial scaffolds for bone tissue engineering applications is to develop constructs that support or even enhance bone regeneration while having the capability to bear appropriate amounts of load. To achieve this, the construct must allow sufficient nutrient infiltration to sustain cell recruitment, differentiation and tissue remodeling after implantation. The scaffold must also provide adequate strength to support surrounding tissue and new tissue during development. It is well accepted that such requirements can be achieved using porous scaffolds as the basis of the tissue engineered construct, however there is no data that identify how permeable these constructs must be to support or enhance bone regeneration. In this work, permeability effects on bone growth *in vivo* were determined with scaffolds of low and high (5.8x low) permeability.

The utilization of SFF techniques allows more rigorous control of scaffold architecture compared to previous studies where salt leached [18], gas foamed, or emulsion constructs demonstrated that higher porosity enhances osteogenesis [5, 23]. For this work, pore size (1mm), pore shape (spherical) and pore interconnectivity (100%) were kept constant between the two permeability designs (high and low). Variation in permeability was created by changing the amount of overlap between spherical pores, which resulted in differences in porosity, throat size and surface area, as these design features are interrelated. Higher porosity often results in higher scaffold surface area, which enhances ion exchange and bone-inducing factor adsorption, provided that the scaffold material is hydrophilic and cell-friendly. However, increased porosity doesn't

necessarily result in increased surface area, as demonstrated by the higher porosity scaffolds utilized in this work that had lower surface area than the lower porosity scaffolds. It is possible that this decreased surface area may have been advantageous for cell infiltration due to the hydrophobicity of the PCL scaffold material used here.

Numerous studies (described below) demonstrate that pore size, interconnectivity and porosity affect bone tissue regeneration and these three design features appear to be the most important structural variables in an initial scaffold screening algorithm developed by Van Cleynenbreugel et al [23] for bone tissue engineering applications. It is difficult to keep all three of these variables constant and create two scaffolds of differing permeability that can be built successfully. The scaffolds used here were successfully designed to hold two out of the three variables constant, pore size and interconnectivity, in order to elucidate changes in bone growth caused only by variations in permeability. Pore and throat size, mutually and collectively, influence the diffusion of materials through a scaffold and thus affect nutrient delivery and cell infiltration. Gross pore size alone influences the mode of bone tissue development. A minimum pore size of 300 μm is required for microvessel formation, which greatly improves the flow of nutrients to the interior of the scaffold [24]. Larger pores ($>300 \mu\text{m}$) lead to direct osteogenesis as opposed to endochondral ossification. Jones et al. [2] argue that accessible pore size is the most relevant design variable to consider for bone infiltration into a scaffold, and that it must be at least 100 μm . Scaffolds used in this work were designed with a pore size of 1000 μm , allowing ample space for cells and vessels to infiltrate and bone tissue to develop. The larger pore size also enabled manufacturing of regular pore architecture by solid free form fabrication. However, large pore size does not guarantee successful tissue

regeneration since the overall pore architecture affects accessibility of internal scaffold pores. Throat size and accessible pore size, together, enable initial cell penetration and nutrient and waste diffusion. Otsuki et al [25] found that 52 μm is the minimum throat size allowable for adequate bone and tissue in-growth *in vivo*. Micro-CT quantification and histology in this work illustrate the effectiveness of larger throat sizes (390 μm and 610 μm for the low and high permeability designs, respectively), as bone penetrated into the center of both scaffold design groups.

There have been few studies that directly examined construct permeability and its effect on bone regeneration. Hui et al. [26] proposed that below a threshold fluid conductance, vascularization into cancellous autograft constructs was poor and bone regeneration minimal. However, when interpreting fluid conductance (permeability times construct area divided by construct length) data, it is unclear whether the intrinsic permeability is limiting bone in-growth or whether the size of the construct requires a longer time for “creeping” substitution of bone. Jones et al. [2] proposed that the fluid conductance data of Hui et al [26] along with their own data suggest a minimum intrinsic permeability of $3 \times 10^{-8} \text{ m}^4/\text{Ns}$ to allow bone in-growth independent of the time period. The permeabilities of scaffolds used in this study were 6.9 and $39.9 \times 10^{-8} \text{ m}^4/\text{Ns}$, well above the threshold permeability proposed by Jones et al. [2]. To further examine how the scaffold designs used here affected the growth of bone into interior void spaces, percent increases in scaffold bone volume from four to eight weeks were calculated for each scaffold design group. The high permeability scaffolds showed an average increase in scaffold bone volume of 106%, while low permeability scaffolds had only a 62.3% increase. Granted, these average values do not account for variability, but they suggest

that, in this model, increasing permeability may increase the rate and penetration of bone in-growth into the interior void spaces of scaffolds. Advantageous to tissue engineering applications that employ such findings, the variable of permeability is not confined by a particular pore size or shape to achieve desired properties, enabling optimization of mechanical properties or other tissue regeneration constraints in light of permeability requirements.

It has been postulated that scaffolds for bone regeneration should have a minimum compressive strength of 2 MPa and a minimum modulus of 50 MPa, which are at the low range of properties for trabecular bone. Strength values reported here for both scaffold designs are well within this suggested value. Moduli for the low permeability scaffolds reached 50 MPa, while those of the high permeability design did not. This is not particularly concerning though, since the 50 MPa modulus value refers to mature bone, and the scaffold will primarily be supporting immature, developing bone. The results suggest that the modulus of the high permeability scaffold/tissue construct will continue to increase as more bone penetrates the void space and becomes mineralized. It would be prudent to also evaluate stiffer materials for their ability to regenerate bone successfully, but with any material, a tradeoff exists between mechanical properties and diffusion characteristics, as discussed below.

There is a balance that must be met between increasing mass transport characteristics (in this case permeability) and providing adequate scaffold mechanical properties, both of which are dependent on scaffold internal architecture and material. For a given material, increasing permeability requires increasing void space in the scaffold, thereby decreasing mechanical properties. Expectedly, the two PCL scaffold designs (low

and high permeability) utilized in this work resulted in two different mechanical property profiles. Low permeability scaffolds had a significantly higher ($p \leq 0.01$) average modulus than high permeability scaffolds. This trend endured through the eighth week of *in vivo* implantation, suggesting that the greater amount of PCL scaffold material in these scaffolds was still supporting most of the mechanically applied load during testing. For the high permeability design there was a significant increase ($p \leq 0.05$) in mechanical properties at 8 weeks, which is evident for both modulus and compressive yield strength. This suggests that for this scaffold design, the bone in-growth and penetration into the inside of the scaffold at 8 weeks is contributing to the mechanical strength and beginning to bear more load than the PCL scaffold itself. High permeability scaffolds exhibited an increasing modulus trend from four to eight weeks, which can be explained by the 117% increase in mineralized tissue content (TMC) from four to eight weeks for this design. This mature bone is capable of bearing significant amounts of load during compressive testing and appears to have a large influence on the mechanical properties of the bone-PCL construct. This phenomenon was not observed for the low permeability design, which may be due to the lesser degree of bone in-growth and scaffold degradation due to the presence of thicker struts. This suggests that a high permeability scaffold design may be beneficial for, not only enhancing new bone growth as compared to less permeable designs, but also for providing adequate mechanical properties to support this developing tissue and surrounding tissues at the implantation site.

4.5 Conclusions

In this study, scaffolds were created with rigorously controlled architectures designed to specifically study the influence of permeability on bone regeneration. Results presented here show that higher permeability scaffolds support greater amounts of bone in-growth in a model that utilizes BMP-7-transduced HGFs seeded into PCL scaffolds and implanted in nude mice for up to eight weeks. Bone in-growth in high permeability scaffolds, in turn, increased the mechanical properties of these PCL-bone constructs from zero to eight weeks. Future studies may include 1) longer time *in vivo* to examine the effect of PCL degradation on construct fidelity and to better understand the balance of tissue in-growth and scaffold degradation over time, 2) expansion of permeability ranges evaluated, and 3) testing of size-appropriate constructs in the orthotopic sites of large animals. From the analyses presented here, we conclude that a more permeable scaffold environment is more favorable for bone growth using PCL scaffolds in our *in vivo* mouse model.

4.6 Acknowledgements

Thank you to Eiji Saito for his assistance with animal surgeries and to Colleen Flanagan for her assistance with micro-CT. This work was funded by NIH RO1 AR 053379.

4.7 References

[1] Karande TS, Ong JL, Agrawal CM. Diffusion in musculoskeletal tissue engineering scaffolds: Design issues related to porosity, permeability, architecture, and nutrient mixing. *Annals of Biomedical Engineering*. 2004;32:1728-43.

[2] Jones AC, Arns CH, Hutmacher DW, Milthorpe BK, Sheppard AP, Knackstedt MA. The correlation of pore morphology, interconnectivity and physical properties of 3D ceramic scaffolds with bone ingrowth. *Biomaterials*. 2009;30:1440-51.

[3] Ripamonti U, Ma S, Reddi AH. The Critical Role of Geometry of Porous Hydroxyapatite Delivery System in Induction of Bone by Osteogenin, a Bone Morphogenetic Protein. *Matrix*. 1992;12:202-12.

[4] Roosa SMM, Kempainen JM, Moffitt EN, Krebsbach PH, Hollister SJ. The pore size of polycaprolactone scaffolds has limited influence on bone regeneration in an in vivo model. *Journal of Biomedical Materials Research Part A*. 2010;92A:359-68.

[5] Karageorgiou V, Kaplan D. Porosity of 3D biomaterial scaffolds and osteogenesis. *Biomaterials* 2005. p. 5474-91.

[6] Lee K-W, Wang S, Fox BC, Ritman EL, Yaszemski MJ, Lu L. Poly(propylene fumarate) bone tissue engineering scaffold fabrication using stereolithography: Effects of resin formulations and laser parameters. *Biomacromolecules*. 2007;8:1077-84.

[7] Wang K, Cai L, Hao F, Xu XM, Cui MZ, Wang SF. Distinct Cell Responses to Substrates Consisting of Poly(epsilon-caprolactone) and Poly(propylene fumarate) in the Presence or Absence of Cross-Links. *Biomacromolecules*. 2010;11:2748-59.

[8] Ciapetti G, Ambrosio L, Savarino L, Granchi D, Cenni E, Baldini N, et al. Osteoblast growth and function in porous poly-epsilon-caprolactone matrices for bone repair: a preliminary study. *Biomaterials* 2003. p. 3815-24.

[9] Williams JM, Adewunmi A, Schek RM, Flanagan CL, Krebsbach PH, Feinberg SE, et al. Bone tissue engineering using polycaprolactone scaffolds fabricated via selective laser sintering. *Biomaterials*. 2005;26:4817-27.

[10] Yanoso-Scholl L, Jacobson JA, Bradica G, Lerner AL, O'Keefe RJ, Schwarz EM, et al. Evaluation of dense polylactic acid/beta-tricalcium phosphate scaffolds for bone tissue engineering. *Journal of Biomedical Materials Research Part A*. 2010;95A:717-26.

[11] Tanaka Y, Yamaoka H, Nishizawa S, Nagata S, Ogasawara T, Asawa Y, et al. The optimization of porous polymeric scaffolds for chondrocyte/atelocollagen based tissue-engineered cartilage. *Biomaterials*. 2010;31:4506-16.

- [12] Mooney DJ, Baldwin DF, Suh NP, Vacanti LP, Langer R. Novel approach to fabricate porous sponges of poly(D,L-lactic-co-glycolic acid) without the use of organic solvents. *Biomaterials*. 1996;17:1417-22.
- [13] Saito E, Kang H, Taboas JM, Diggs A, Flanagan CL, Hollister SJ. Experimental and computational characterization of designed and fabricated 50:50 PLGA porous scaffolds for human trabecular bone applications. *Journal of Materials Science-Materials in Medicine*. 2010;21:2371-83.
- [14] Hollister SJ, Lin CY, Saito E, Schek RD, Taboas JM, Williams JM, et al. Engineering craniofacial scaffolds. *Orthodontics & craniofacial research*. 2005;8:162-73.
- [15] Wilson CE, van Blitterswijk CA, Verbout AJ, Dhert WJA, de Bruijn JD. Scaffolds with a standardized macro-architecture fabricated from several calcium phosphate ceramics using an indirect rapid prototyping technique. *Journal of Materials Science-Materials in Medicine*. 2011;22:97-105.
- [16] Sugawara A, Fujikawa K, Hirayama S, Takagi S, Chow LC. In Vivo Characteristics of Premixed Calcium Phosphate Cements When Implanted in Subcutaneous Tissues and Periodontal Bone Defects. *Journal of Research of the National Institute of Standards and Technology*. 2010;115:277-90.
- [17] Zein I, Hutmacher DW, Tan KC, Teoh SH. Fused deposition modeling of novel scaffold architectures for tissue engineering applications. *Biomaterials*. 2002;23:1169-85.
- [18] Kweon H, Yoo MK, Park IK, Kim TH, Lee HC, Lee HS, et al. A novel degradable polycaprolactone networks for tissue engineering. *Biomaterials*. 2003;24:801-8.
- [19] Krebsbach PH, Gu K, Franceschi RT, Rutherford RB. Gene therapy-directed osteogenesis: BMP-7-transduced human fibroblasts form bone in vivo. *Human Gene Therapy*. 2000;11:1201-10.
- [20] Suh SW, Shin JY, Kim JH, Kim JG, Beak CH, Kim DI, et al. Effect of different particles on cell proliferation in polymer scaffolds using a solvent-casting and particulate leaching technique. *Asaio Journal*. 2002;48:460-4.

- [21] Schek RM, Wilke EN, Hollister SJ, Krebsbach PH. Combined use of designed scaffolds and adenoviral gene therapy for skeletal tissue engineering. *Biomaterials*. 2006;27:1160-6.
- [22] Chen QX, Kaji H, Iu MF, Nomura R, Sowa H, Yamauchi M, et al. Effects of an excess and a deficiency of endogenous parathyroid hormone on volumetric bone mineral density and bone geometry determined by peripheral quantitative computed tomography in female subjects. *Journal of Clinical Endocrinology & Metabolism*. 2003;88:4655-8.
- [23] Van Cleynenbreugel T, Schrooten J, Van Oosterwyck H, Sloten JV. Micro-CT-based screening of biomechanical and structural properties of bone tissue engineering scaffolds. *Medical & Biological Engineering & Computing*. 2006;44:517-25.
- [24] van Tienen TG, Heijkants R, Buma P, de Groot JH, Pennings AJ, Veth RPH. Tissue ingrowth polymers and degradation of two biodegradable porous with different porosities and pore sizes. *Biomaterials*. 2002;23:1731-8.
- [25] Otsuki B, Takemoto M, Fujibayashi S, Neo M, Kokubo T, Nakamura T. Pore throat size and connectivity determine bone and tissue ingrowth into porous implants: Three-dimensional micro-CT based structural analyses of porous bioactive titanium implants. *Biomaterials*. 2006;27:5892-900.
- [26] Hui PW, Leung PC, Sher A. Fluid conductance of cancellous bone graft as a predictor for graft-host interface healing. *Journal of Biomechanics*. 1996;29:123-32.

CHAPTER 5 *In Vitro* Differentiation of Human Adipose Derived Stem Cells and Bone Marrow Stromal Cells on PCL Scaffolds Conjugated with rhBMP-2

5.1 Introduction

Chapter 4 showed that high permeability PCL scaffolds promoted more bone growth *in vivo* than their low permeability counterparts. In this Chapter, a high permeability scaffold is combined with human mesenchymal stem cells and rhBMP-2 in an effort to ascertain advantageous combinations of osteogenic factors and cells for promoting osteogenesis *in vitro*. Cells that are within a scaffold construct respond to and produce osteogenic factors to recruit host cells and direct their differentiation into osteoblasts. While there are many cell types that could be incorporated into a scaffold to promote bone regeneration *in vivo*, an ideal cell type should respond positively to osteogenic signals, be easily harvested and behave in a reliable and predictable manner. One way to direct osteogenesis is by exposing cells to growth factors such as bone morphogenetic proteins (BMPs). BMP-2 is a growth factor from the TGF- β family that plays an important role in osteogenic differentiation [1]. When a cell interacts with BMP-2, via binding to types I and II serine/threonine kinase receptors, the Smad 1/5/8 pathway is activated, initiating a signaling cascade that results in expression of Runx-2, and subsequent expression of many osteogenic genes. Determining how best to incorporate BMP-2 into a scaffold tissue engineering system is a challenge because a cell's response to the protein depends on both its innate pre-programmed behavior as well as the way in

which the BMP-2 is delivered. Recombinant human BMP-2 (rhBMP-2) can be delivered in soluble form [2-6], be tethered to materials [7-10] or be encapsulated in microspheres [11-16]. The delivery method can affect bone growth distribution by influencing where and for how long the active BMP-2 resides, be it within the scaffold or distal to it.

There are thus two challenges to be addressed when incorporating a growth factor such as rhBMP-2 into a scaffold tissue engineering system: 1) determining a cell type to use that is clinically feasible and elicits a strong osteogenic and eventual bone formation response, and 2) developing and analyzing a growth factor delivery system that maintains bioactivity and encourages localized bone growth. In this Chapter, the effect of chemically conjugated rhBMP-2 on the differentiation of two cell types, human adipose derived stem cells (ADSC) and bone marrow stromal cells (BMSC), is analyzed. Since it is common practice to expose mesenchymal stem cells to differentiation medium to induce differentiation, this chapter also examines how the combination of these differentiation factors with conjugated rhBMP-2 affects cell behavior. These studies utilized a controlled *in vitro* environment in an effort to illuminate the complex interactions between chemically conjugated rhBMP-2 and clinically relevant human adult stem cells.

The first *in vitro* studies with rhBMP-2 examined the effect of soluble rhBMP-2 on cellular differentiation [4, 17-19]. Studies utilizing pre-osteoblastic cells demonstrated that rhBMP-2 can affect cells differently, depending on the type of cell and the environment in which the growth factor is introduced [20]. While many osteoblastic cell lines respond positively to rhBMP-2 [20-23] *in vitro* by producing bone precursor products, their expression of osteogenic markers varies, indicating that osteogenic

induction is a complex, cell specific process. Pre-osteoblasts are already somewhat committed to the osteogenic pathway, which may augment their ability to respond positively to rhBMP-2, but non-osteoblastic cells have also been stimulated by rhBMP-2 to proceed down an osteogenic path [5, 17, 24]. This suggests that rhBMP-2 is a powerful mediator of osteogenesis among a wide range of uncommitted cell types.

The discovery that rhBMP-2 directs non-osteoblastic cells to undergo osteogenesis led researchers to investigate the ability of BMSC and ADSC to differentiate in response to rhBMP-2. Both cell types are derived from mesenchymal tissue and have the ability to differentiate along a number of lineages. BMSC are the traditional adult stem cell choice, but ADSC are an attractive alternative because harvesting is easier and less painful and yields higher cell numbers [25]. Both of these multipotent cell types are more clinically relevant than pre-osteoblastic cell lines, but there have been conflicting reports concerning the osteogenic capacity of these cells in response to rhBMP-2. After exposure to rhBMP-2, ADSC have shown greater potential to produce bone precursor products compared to controls [26, 27]. Compared to BMSC, ADSC have showed both greater [28] and equal osteogenic [29, 30] potential. rhBMP-2 can induce osteogenesis in both cell types, but there is also evidence that rhBMP-2 may not have a consistent or significant effect on osteogenic gene expression *in vitro* [31] or bone repair *in vivo* [32]. Clearly there are conflicting reports of human adult stems cells' ability to differentiate in response to rhBMP-2. Furthermore, comparing between studies is difficult due to the large degree of variability in experimental parameters such as substrate material and geometry, cell species, rhBMP-2 delivery method and whether the experiment is performed *in vitro* or *in vivo*. This study presents a side-by-side study of

BMSC and ADSC cultured in identical settings and evaluated for both osteogenesis and chondrogenesis.

Growth factor incorporation into scaffolds has been accomplished using a number of methods including viral vector delivery [33, 34], gel encapsulation [12, 35], physical adsorption [9, 36-38] and direct conjugation [37, 39, 40]. The mode of growth factor delivery can affect how much rhBMP-2 is initially needed to produce a cellular response and may influence bone growth distribution. One of the goals for many bone regeneration applications is to restrict bone growth to a defined region, which is especially important for spinal and craniofacial applications where bone growth outside of this region can damage delicate surrounding tissues. Therefore, the goal for rhBMP-2 delivery is to retain the rhBMP-2 within the scaffold region for an extended period of time. This should control the spatial distribution of bone growth and may prolong the interaction between cells and rhBMP-2 to control temporal bone distribution as well.

When rhBMP-2 is directly conjugated to polymer scaffolds, the interaction between the growth factor and the polymer material occurs through either a covalent bond or electrostatic interactions with a specific functional group on the surface of the polymer. Collagen [41] and heparin [13, 42, 43] conjugation methods rely on electrostatic interactions, while conjugation with a chemical crosslinker [9, 40] results in a covalent bond. Depending on the choice of crosslinker, covalent linkage may offer additional control over growth factor release by introducing a bond that is not easily broken, resulting in release that occurs primarily through polymer degradation. Here we use the crosslinker sulfosuccinimidyl-4-(N-maleimidomethyl)cyclohexane-1-carboxylate (sulfo-SMCC) [8, 10, 37] to covalently attach rhBMP-2 to the surface of PCL scaffolds.

rhBMP-2 tethered to PCL scaffolds using this conjugation method has been previously shown by our group to elicit an osteogenic response from rat BMSC *in vitro* [9] and resulted in bone growth *in vivo*, as reported in unpublished findings from our group.

Most studies utilizing conjugated rhBMP-2 do not consider the effect that additional soluble factors may have on differentiation. The traditional method of inducing mesenchymal stem cell differentiation *in vitro* is to supplement cell culture medium with the appropriate soluble factors, which include β -glycerophosphate and ascorbic acid for osteogenesis and insulin, transforming growth factor beta (TGF- β) and dexamethasone for chondrogenesis. This method requires a period of days for induction to occur and cannot be continued *in vivo* which is why differentiation by rhBMP-2 alone is an attractive alternative since the protein could be incorporated into scaffolds that are then implanted. It has been shown that combining osteogenic medium with rhBMP-2 delivery does not improve osteogenesis compared to osteogenic medium or rhBMP-2 alone, suggesting that differentiation by one or the other method is sufficient [44]. However, this has not been studied using conjugated rhBMP-2 or in a format that directly compares ADSC and BMSC. Furthermore, there are few studies looking at rhBMP-2-induced chondrogenic differentiation, a phenomenon that has implications for *in vivo* endochondral ossification, which may be the pathway through which bone growth proceeds in response to rhBMP-2 [45-47]. In the work presented in this Chapter, we specifically investigate how traditional osteogenic and chondrogenic medium supplements combined with conjugated rhBMP-2 affect the response of ADSC and BMSC.

The goals of this study were to examine how the response to rhBMP-2 differs between BMSC and ADSC *in vitro* and to look at the differential effects of differentiation medium (osteogenic or chondrogenic) versus rhBMP-2 alone. Since endochondral ossification has been proposed as a mode of new bone formation favored by mesenchymal stem cells, we chose to examine both chondrogenic and osteogenic markers, including calcium content, sGAG content and osteogenic and chondrogenic gene expression. This *in vitro* examination provides a controlled system for studying how cells respond to chemically conjugated rhBMP-2, which is important to understand prior to performing similar work *in vivo*.

5.2 Materials and Methods

5.2.1 Scaffold Design and Fabrication

Cylindrical scaffolds with regular internal architecture were designed using Interactive Data Language (IDL, Exelis VIS). Low and high permeability scaffolds were designed and characterized to confirm similarities to scaffolds used in Chapter 4, but only the high permeability scaffold design was used for *in vitro* studies. The low permeability scaffold has 2.02 mm spherical pores and the high permeability scaffold has 2.15 mm spherical pores. Complete scaffold parameters are shown in Table 1. Scaffolds were manufactured out of poly- ϵ -caprolactone (with 4% hydroxyapatite incorporated as a flow agent) using a Formiga P100 laser plastic sintering machine (EOS, Krailling, Germany). High permeability scaffolds for *in vitro* (cell culture and permeability measurements)

experiments had a diameter of 6.35 mm and a 4 mm height.

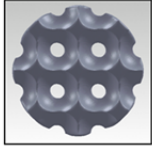
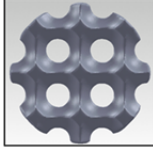
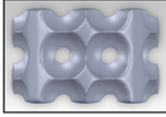
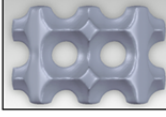


	Low Permeability	High Permeability
Top View		
Side View		
PCL Scaffold		
Permeability (m²)	8.47E-10	5.34E-09
Porosity (%)	54	63
Surface Area (mm²)	175.32	200.10

Table 5-1: Design parameters for scaffolds designed for this Aim.

5.2.2 Scaffold Permeability Analysis – Computational and Experimental

Scaffold permeability was analyzed for comparison to the scaffolds used in Chapter 4. Computational permeability was determined using a custom designed computational tool that uses homogenization theory applied to Stoke’s flow [48]. Experimental scaffold permeability was determined using a custom-designed permeability chamber, with data collection via Labview [49, 50]. The goal of analyzing permeability was to confirm similarities between the scaffolds used in this study (“high permeability B” in Table 3) and those used in Chapter 4 (“A” designs in Table 3).

5.2.3 *rhBMP-2 Conjugation*

rhBMP-2 (Genscript, Inc., Piscataway, NJ) was conjugated to PCL scaffolds using the crosslinker sulfosuccinimidyl-4-(N-maleimidomethyl)cyclohexane-1-carboxylate (sulfo-SMCC, Pierce, Thermo Scientific, Rockford, IL), as shown schematically in Figure 1. Amine groups were introduced onto the surface of the scaffolds by submerging the scaffolds in a 10% w/v solution of 1,6-hexanediamine in isopropanol under vacuum for 1 hour at 37°C. Scaffolds were then thoroughly washed in deionized, distilled water and dried under vacuum for 24 hours. For sulfo-SMCC conjugation, scaffolds were washed at room temperature in activation buffer (BuPH phosphate buffered saline, Pierce, Thermo Scientific, Rockford, IL) three times, under vacuum for 20 minutes each. A 4 mg/ml solution of sulfo-SMCC in activation buffer was then added to each scaffold for 1 hour, under vacuum at room temperature. Scaffolds were then washed twice in activation buffer and once in conjugation buffer (activation buffer containing 0.1M EDTA). A 50 µg/ml solution of rhBMP-2 in conjugation buffer (400 µl total volume) was then added to the scaffolds in an ultra low-attachment plate (Corning, Tewksbury, MA) for 18 hours at 4°C with gentle shaking. After the incubation with rhBMP-2, scaffolds were washed three times in deionized, distilled water and dried under vacuum for 24 hours.

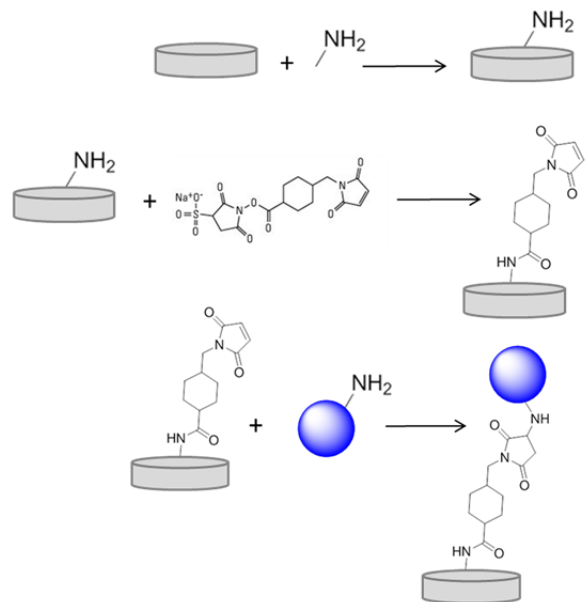


Figure 5.1: Schematic representation of BMP-2 conjugation using sulfo-SMCC as a crosslinker between amine groups introduced onto PCL scaffold and BMP-2.

5.2.4 Cell culture and scaffold cell seeding for *In Vitro* Study

Human adipose derived stem cells (ADSC) and bone marrow stromal cells (BMSC) (Lonza, Walkersville, MD) were cultured in growth medium consisting of either low glucose Dulbecco's Modified Eagle Medium (ADSC) or Modified Essential Medium Alpha (BMSC), supplemented with 10% fetal bovine serum and 5% penicillin/streptomycin (all reagents from Gibco, Carlsbad, CA). Cells were cultured until

	Cells	Medium	BMP-2?
1	ADSC	Growth	No
2	ADSC	Osteogenic	No
3	ADSC	Chondrogenic	No
4	ADSC	Growth	Yes
5	ADSC	Osteogenic	Yes
6	ADSC	Chondrogenic	Yes
7	BMSC	Growth	No
8	BMSC	Osteogenic	No
9	BMSC	Chondrogenic	No
10	BMSC	Growth	Yes
11	BMSC	Osteogenic	Yes
12	BMSC	Chondrogenic	Yes

Table 5-2: Experimental groups.

80% confluency was reached (3-4 days) and then passaged repeatedly to amass required cell numbers to carry out experiments in scaffolds (cells at passage 5 or 6 were used in experiments). The twelve experimental groups are shown in Table 2. Osteogenic medium consisted of growth medium plus 10mM beta-glycerophosphate, 50 µg/ml ascorbic 2-phosphate and 10 nM dexamethasone. Chondrogenic medium consisted of growth medium plus 0.1 mM Non-essential amino acids, 50 µg/ml 2-phospho-L-ascorbic acid, 0.4 mM proline, 5 µg/ml insulin, 10ng/ml TGF-β and 0.1 µM dexamethasone. For each condition, 16 scaffolds were seeded, each with one million cells. The scaffolds were sterilized using two 30 minute washes in 70% ethanol and then thoroughly rinsed with phosphate buffered saline and placed in serum free medium for at least one hour prior to cell seeding. Just before seeding, the scaffolds were removed from the medium, placed in PBS to rinse, blotted dry on sterile gauze and then placed in a sterile Teflon mold, specifically designed for cell seeding purposes. Cells were trypsinized, counted and resuspended in 5 mg/ml fibrinogen. 70 µl of cells + fibrinogen were added to each

scaffold, followed immediately by 7 μ l thrombin and then the Teflon mold containing the scaffolds was placed in a 37°C cell culture incubator for 30 minutes for gelation to occur. Scaffolds were removed from the Teflon mold and placed in a low-attachment cell culture plate with 1.5 ml appropriate medium. Cells in scaffolds were maintained in culture for two weeks, with medium changes every three days.

5.2.5 In Vitro Quantification of Calcium Content (*Calcium Assay*)

To analyze the total amount of calcium contained within the scaffold construct, total calcium was measured using cresolphthalein complexone methodology [51-53]. Scaffolds (N=6 per group) were rinsed twice with PBS, chopped into small pieces (1-1.5 mm³), placed in 300 μ l 1N acetic acid and placed at 4°C with shaking for 24 hours. After 10 μ l of each sample was added in triplicate to a 96-well plate, 300 μ l of the cresolphthalein complexone working solution (five parts of 14.8 M ethanolamine/boric acid buffer, five parts cresolphthalein complexone, two parts hydroxyquinoline and eighty-eight parts deionized-distilled water) was added to each well. After incubation at room temperature for 10 minutes, absorbance was measured at 565 nm using a plate reader (Thermo Multiskan Spectrum, Thermo Scientific, Inc.). Calcium concentration (μ g/ml) was calculated by comparison to a calcium standard curve prepared using a 1 mg/ml calcium chloride standard.

5.2.6 In Vitro Quantification of sulfated-glycosaminoglycans (sGAGs) (*Dimethylmethylene blue Assay*)

The amount of sGAGs within each construct was quantified using a dimethylmethylene blue (DMMB) assay [49, 54]. After two weeks in culture, scaffolds (n =6 per group) were rinsed twice with PBS, chopped into small pieces (1-1.5 mm³) and

placed in 1 ml papain solution: 10 U/ml papain (Sigma Aldrich, St. Louis, MO), 5 mM cysteine (Sigma Aldrich, St. Louis, MO) and 5mM EDTA in PBS, pH 6.0. Samples were placed at 37 °C for 24 hours with manual shaking approximately every hour. After the incubation period, the samples were frozen at -20°C for storage or the DMMB assay was immediately performed.

The DMMB solution consisted of 8 mg 1,9 dimethyl-methylene blue dye (Sigma Aldrich, St. Louis, MO), 1.52 g glycine, 1.185 g NaCl, and 47.5 ml 0.1 HCl in 500 ml distilled water (pH 3.0). Standards of shark chondroitin-6-sulfate were prepared (0.125 mg/ml, 0.0625 mg/ml, 0.03125 mg/ml, 0.015625 mg/ml, 0.0078125 mg/ml, 0.00390625 mg/ml, 0.001953125 mg/ml). 200 µl of DMMB reagent was aliquoted into each well of a 96-well plate along with 20 µl of standard or sample. The absorbance was measured at 525 nm using a plate reader (Thermo Multiskan Spectrum, Thermo Scientific, Inc.). sGAG values were normalized by DNA content, as described in the following section.

5.2.7 *In Vitro DNA Quantification*

DNA quantification was performed following papain digestion (as described above) using a DNA quantitation fluorescent assay (Sigma Aldrich, St. Louis, MO). Previously frozen samples were placed on ice (N=6 per group, same as analyzed for sGAGs) and 100 µg/ml and 10 µg/ml DNA standard and bisBenzimide H33258 solutions were prepared according to kit protocols. Standard DNA solutions (50,100, 200, 500, 1000, 2000 ng) were also prepared according to kit protocols. A 2 µg /ml solution of H33258 was prepared using 0.2 % (v/v), 1 mg/ml H33258, 10% (v/v) 10X Fluorescent Assay Buffer and 90% (v/v) molecular biology grade water. 200 µl of 2 µg/ml H33258 and 10 µl sample was added to each well and read at 355nm/excitation and

460nm/emission on a microplate fluorometer (Fluoroskan Ascent Microplate Fluoremeter, Thermo Scientific, Inc.).

5.2.8 *In Vitro Gene Expression of Osteogenic and Chondrogenic Genes*

Osteogenic and chondrogenic gene expression was evaluated using real-time quantitative polymerase chain reaction. After the two-week incubation with either ADSC or BMSC and osteogenic, chondrogenic or growth medium, scaffolds (N=4 per group) were rinsed twice with PBS, chopped into small pieces (1-1.5 mm³), placed in 1 ml RNAlater® (Invitrogen, Life Technologies, Grand Island, NY) and placed at 4°C for 24 hours and then -20°C for storage. Total RNA was extracted from the samples using an RNEasy Mini Kit (Qiagen, Inc.), following the manufacturer's protocol. Reverse transcriptase was carried out at 42°C for 50 minutes using the SuperScript First-Strand Synthesis kit (Invitrogen). Gene expression of alkaline phosphatase (ALP), type I collagen, osteocalcin, type II collagen, aggrecan and tata box binding protein (as an endogenous control) was quantified using a7500 Real-time PCR System (Applied Biosystems, Carlsbad, CA). The $\Delta\Delta C_T$ analysis method was used to analyze gene expression data [55]. Fold changes are reported relative to expression of the endogeneous control gene (tata box binding protein [56]) and expression of the control condition for each cell type (growth medium, no rhBMP-2).

5.2.9 *Statistics*

For calcium content and sGAG content, multiple linear regression, performed using SPSS software (SPSS for Windows, Rel 14.0. 2005, SPSS, Inc., Chicago, IL), was used to determine which factors had a significant effect on a given response variable. For qPCR data, student's t-tests were used to compare fold change expression between

experimental and control groups and between “BMP-2” and “No BMP-2” for each medium condition.

5.3 Results

5.3.1 Permeability Analysis

The scaffolds used for this chapter and subsequent chapters were manufactured using selective laser sintering (SLS), which directly prints PCL into a scaffold structure. This technique offers numerous advantages over the indirect casting technique used in Chapter 4. Several hundred virtually defect-free scaffolds can be manufactured in hours (as opposed to days for the casting method), no additional casting or solvent materials are needed, and post-processing is minimal. However, since the SLS machine’s resolution is lower than the machines utilized to build wax molds for indirect casting, the scaffolds used here had larger pore and strut sizes that influenced their mass transport values. The permeability results of the Group B designs, shown in Table 3, indicate that manufacturing via SLS enabled creation of two scaffolds with a relative high and low permeability. As is true for the Group “A” designs, the permeability values for the Group “B” designs are well above the threshold permeability value that has been postulated for bone growth to occur [57]. Furthermore, the computational and experimental permeability values for the high permeability “B” design used in this Aim are very similar to those for the high permeability “A” design from Aim I. The high permeability “B” scaffold also has similar porosity values and architectural features, confirming that the high permeability “B” scaffold is an appropriate substitution. The experimental values for the “A” designs are lower than the predicted computational values due to shrinkage of the PCL material that occurs during casting. The “B” SLS-manufactured scaffolds do not

undergo shrinkage, so the computational values are better predictors of the experimental permeability obtained from manufactured scaffolds. The advantages over indirect casting that are afforded by SLS manufacturing outweigh the restrictions on scaffold design resulting from the SLS machine's lower resolution. For the studies in this and subsequent chapters, the high permeability "B" scaffold is used since the work presented in Chapter 4 had shown that a relatively high permeability scaffold was best for bone regeneration.

	Sphere Diameter	Designed Porosity	Computational		Experimental	
			Permeability (m ²)	Normalized to Low Perm Design	Permeability (m ²)	Normalized to Low Perm Design
High Permeability A	1.01	0.7	6.44E-09	7.83	1.54E-09	5.25
Low Permeability A	1.01	0.5346	8.23E-10	1.00	2.93E-10	1.00
High Permeability B	2.15	0.63	5.34E-09	6.30	1.70E-09	---
Low Permeability B	2.02	0.54	8.47E-10	1.00	---	---

Table 5-3: Computational and experimental permeability values for scaffolds used in Aim 4 (High Permeability A and Low Permeability A) and used in Aim II (High Permeability B and Low Permeability B). Note that Low Permeability B is only shown for comparison's sake and was not utilized in these studies.

5.3.2 Calcium Content

The primary function of osteoblasts is to produce a calcified collagen I matrix [58], so assessing mineralization of non-osteoblastic cells such as ADSC and BMSC is a way to determine their progress down an osteogenic lineage. Before assessing cells seeded in PCL constructs, ADSC and BMSC were cultured in monolayer and exposed to osteogenic medium to assess their innate mineralization potential. These results appear in Appendix B and prove that both cell types mineralized in response to osteogenic medium. Comparison of high and low passage cells showed a better mineralization response in low passage cells, but measurable mineralization was still observed at the higher passage. The extent of mineralization in the 3D constructs was analyzed using a calcium assay, with the results shown in Figure 2. Calcium deposition is evidence that the collagen matrix has

been laid down and mineralization has begun. While osteogenic gene expression and alkaline phosphatase production vary over time, mineralization typically increases once onset commences, making it a simple indicator of osteogenic progression. When rhBMP-2 was present on the scaffolds, the ADSC produced more mineral when in osteogenic or chondrogenic medium, and significantly more calcium content was observed for cells in osteogenic medium, compared to both chondrogenic and growth medium. Constructs cultured in chondrogenic medium produced more calcium when rhBMP-2 was present on the scaffolds, while there was no difference in mineralization for the two growth medium conditions. For the osteogenic medium conditions, more calcium was measured in the absence of rhBMP-2, suggesting that the osteogenic medium supplements were affecting mineralization more so than the conjugated rhBMP-2.

The mineralization of BMSC seeded in PCL scaffolds was also measured and the results are displayed in Figure 2B. With rhBMP-2 present on the scaffolds, more

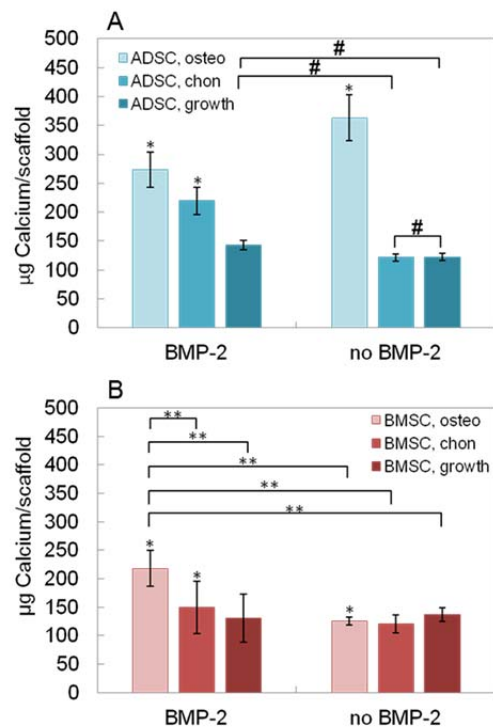


Figure 5.2: Calcium content as measured by cresolphthalein complexone methodology. (A) Calcium content in ADSC maintained in osteogenic (osteo), chondrogenic (chon) or growth medium. # not significant. All other comparisons are significant, $p < 0.01$. (B) Calcium content in BMSC maintained in osteogenic (osteo), chondrogenic (chon) or growth medium. ** $p < 0.01$. Asterisks indicate significant ($p < 0.05$) between groups with BMP-2 and without BMP-2 for a given medium condition.

mineralization was observed when the constructs were cultured in osteogenic medium, compared to chondrogenic or growth medium, which was also the case for the ADSC. When rhBMP-2 was not present on the scaffolds, there was no difference in mineralization across all medium conditions. These results suggest that while rhBMP-2 alone did not influence mineralization, when it was used in combination with soluble osteogenic factors, an increase in calcium content was observed.

5.3.3 sGAG Content

To quantify cartilaginous matrix production, sulfated-glycosaminoglycan (sGAG) content was measured using a DMMB assay. Maintenance in chondrogenic medium resulted in significant increases in sGAG content for ADSC, regardless of the presence of

rhBMP-2 on the scaffold, as shown in Figure 3A. For a given medium condition, the

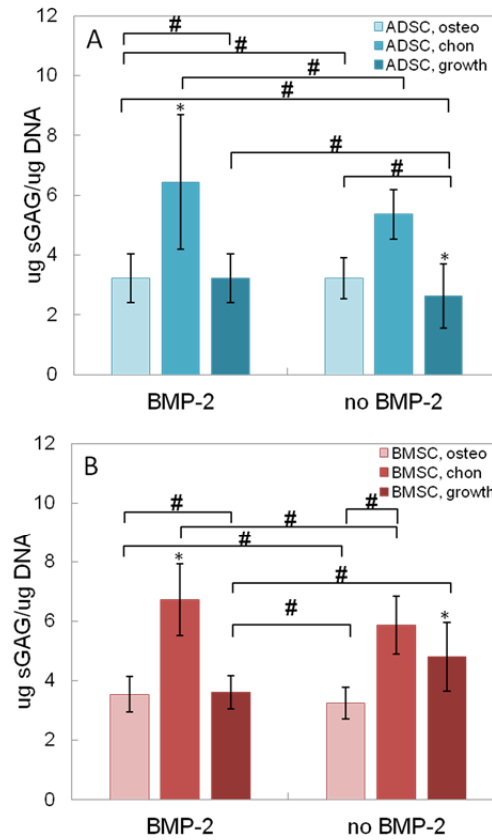


Figure 5.3: Sulfated-glycosaminoglycan (sGAG) content as measured by dimethylmethylene blue. (A) sGAG content in ADSC maintained in osteogenic (osteo), chondrogenic (chon) or growth medium. (B) sGAG content in BMSC maintained in osteogenic (osteo), chondrogenic (chon) or growth medium. # $p > 0.05$ (not significant). All other comparisons are significant, $p < 0.05$. Asterisks indicate significant ($p < 0.05$) between groups with BMP-2 and without BMP-2 for a given medium condition.

incorporation of rhBMP-2 on the scaffold did not significantly influence sGAG content in ADSC-seeded constructs. BMSC-seeded constructs displayed similar behavior.

Constructs cultured in chondrogenic medium had significantly more sGAGs than those in osteogenic or growth medium and rhBMP-2 did not effect sGAG production for a given medium condition. These results suggest that the supplements present in chondrogenic medium contributed to sGAG production and not the rhBMP-2 conjugated on the scaffolds.

5.3.4 *Osteogenic and chondrogenic gene expression*

Real-time quantitative PCR was used to analyze osteogenic and chondrogenic gene expression. Although gene expression is temporal (see Figure 2.2), we chose to analyze gene expression at two weeks because this is a typical pre-implantation culture period [59-61] and analysis at this time point gives us a snapshot of where in the differentiation process the cells are before implantation. Collagen I is the major organic component of the bone matrix and collagen fiber deposition is necessary before matrix mineralization can occur. Peak collagen I gene expression typically occurs early in the differentiation process (prior to day 10), although this can vary depending on the cell type. For ADSC at two weeks, collagen 1 expression was downregulated for all experimental groups relative to the control condition (constructs in growth medium without rhBMP-2 conjugated), as shown in Figure 4A. There was no difference in expression between constructs with or without rhBMP-2 in osteogenic medium. There was also no difference between constructs with or without rhBMP-2 in chondrogenic medium. For BMSC, collagen expression was upregulated relative to control (growth medium, no rhBMP-2) for all experimental groups except for constructs with rhBMP-2 cultured in growth medium, (Figure 4D). Like ADSC, there was no difference in expression between constructs with and without rhBMP-2 in osteogenic medium and in chondrogenic medium. The BMSC demonstrated greater overall collagen I expression, but it is likely that the medium components and not the conjugated rhBMP-2 produced this effect.

Alkaline phosphatase (ALP) is expressed in high levels in osteoblasts and pre-osteoblasts and is responsible for calcium phosphate mineral formation. ALP is typically expressed after collagen I expression has peaked, as the matrix is prepared for mineral deposition. In our studies, ALP gene expression was analyzed at two weeks for all experimental groups. The ADSCs cultured in osteogenic medium showed upregulated ALP gene expression relative to controls (Figure 4B), which is consistent with the calcium content results discussed previously. Constructs in chondrogenic medium had downregulated expression. These groups also had the highest sGAG content, so at this point in time the cells may be differentiating more toward cartilage than bone.

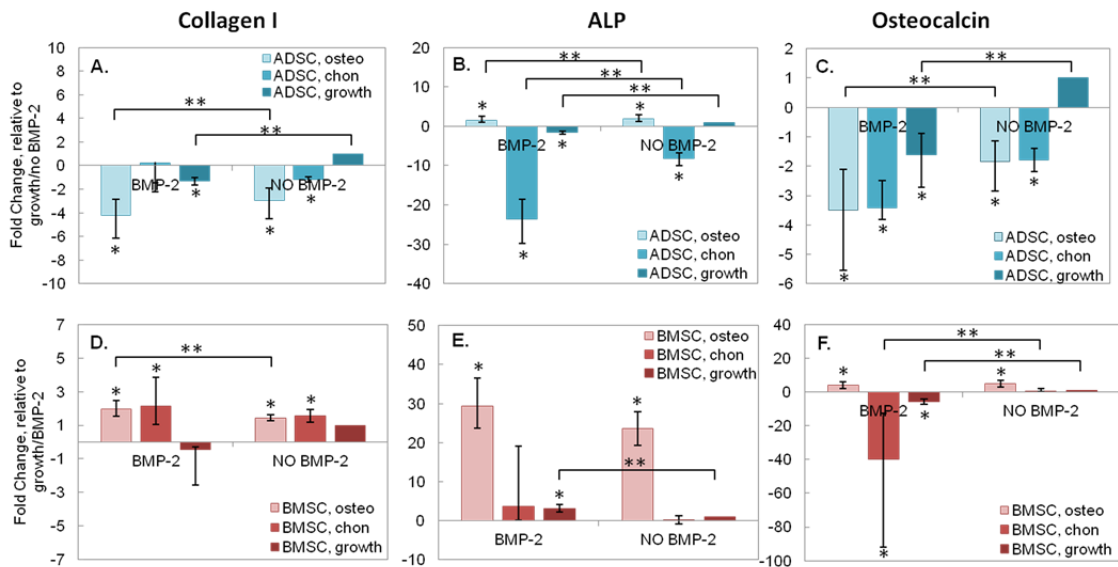


Figure 5.4: Expression of the osteogenic genes collagen 1 (panels A and D), alkaline phosphatase (panels B and E) and osteocalcin (panels C and F). Fold change values were calculated using the $\Delta\Delta C_T$ method and are reported as fold changes relative to control (growth medium, no BMP-2 for a given cell type). *p<0.05 relative to control. **p<0.01.

Incorporating rhBMP-2 on the scaffold when ADSC constructs were in growth medium led to decreased expression relative to controls. The BMSC cultured in osteogenic medium showed strong upregulation of ALP expression relative to controls, as shown in

Figure 4E. Expression in these groups was also greater than expression in the chondrogenic medium conditions, both of which showed no upregulation compared to controls. ALP expression in constructs conjugated with rhBMP-2 and cultured in growth medium was upregulated relative to controls, but this trend did not occur for osteogenic medium. The impact of the conjugated rhBMP-2 on ALP expression appears to depend on the additional medium factors present.

Once the bone matrix has been prepared for mineralization, osteocalcin begins depositing hydroxyapatite on the matrix. Osteocalcin gene expression is a later marker of mature bone formation, peaking after collagen I and ALP expression. In this study, ADSC osteocalcin expression at two weeks mirrored that of collagen I expression, with downregulation occurring for all groups relative to controls. The BMSC demonstrated upregulated osteocalcin expression when cultured in osteogenic medium, regardless of whether or not rhBMP-2 was present, which mirrors ALP expression in these groups. Expression was downregulated relative to control for BMSC in chondrogenic medium exposed to conjugated rhBMP-2.

Endochondral ossification has been proposed as the pathway through which mesenchymal stem cells produce bone in a tissue engineered environment [62, 63]. This hypothesis, along with an interest in studying how conjugated rhBMP-2 affects chondrogenic gene expression, prompted the examination of chondrogenic markers in this study. During osteogenesis, these cells have exhibited behaviors similar to those displayed during developmental endochondral ossification [64, 65]. While BMSC cultured in a high density three dimensional system is an accepted model for inducing chondrogenesis [49], markers of endochondral ossification, including hypertrophy,

collagen X expression and mineralization, have also been reported when this type of culture is used. Aggrecan expression of ADSC increased relative to control when constructs were cultured in osteogenic medium and contained conjugated rhBMP-2, as indicated in Figure 5A. This increase with rhBMP-2 present was not observed when the cells were in growth medium, suggesting that rhBMP-2 worked in tandem with factors in the osteogenic medium to increase aggrecan expression. For the constructs cultured in chondrogenic medium, there was a decrease in ADSC aggrecan expression

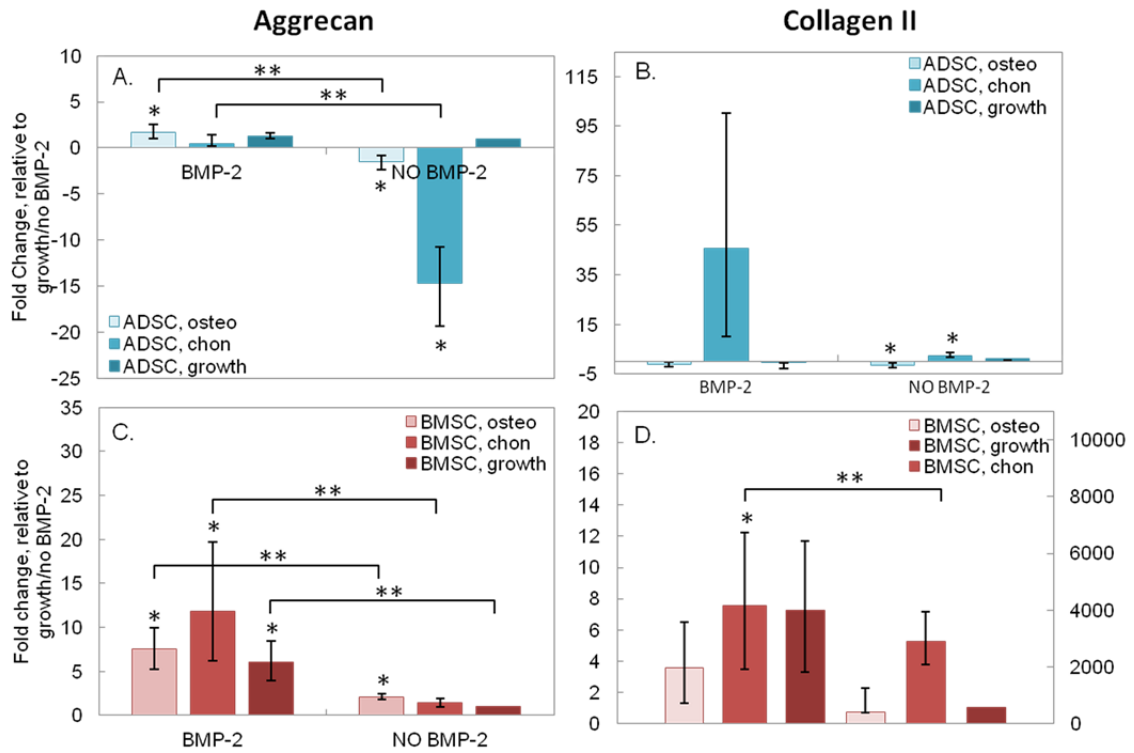


Figure 5.5: Expression of the chondrogenic genes aggrecan (panels A and C) and collagen type II (panels B and D). Note that in panel D, the “BMSC, chon, BMP-2” group adheres to the right-hand axis. Fold change values were calculated using the $\Delta\Delta C_T$ method and are reported as fold changes relative to control (growth medium, no BMP-2 for a given cell type). * $p < 0.05$ relative to control. ** $p < 0.05$.

relative to controls when rhBMP-2 was not present, but no change in expression when rhBMP-2 was there. Again, this suggests that rhBMP-2 works alongside medium components to augment aggrecan expression. Overall, BMSC aggrecan expression was

greater than for ADSC (Figure 5C). The presence of rhBMP-2 led to increased expression for all medium conditions compared to control. Furthermore, for all medium conditions, constructs with rhBMP-2 had greater aggrecan expression than constructs without rhBMP-2.

Collagen II is the primary component of cartilage extracellular matrix and its presence is an indication of chondrogenic differentiation. The ADSC showed upregulated collagen II expression relative to control when cultured in chondrogenic medium in constructs with conjugated rhBMP-2. Expression for this group was also greater than for any other medium condition, including ADSC without rhBMP-2 cultured in chondrogenic medium, suggesting that rhBMP-2 had a direct effect on collagen II expression, but only in the presence of additional chondrogenic factors. Collagen II expression was upregulated in BMSC for all constructs that had conjugated rhBMP-2, as well as in BMSC cultured in chondrogenic medium without rhBMP-2. There was no difference in expression between cells cultured with and without rhBMP-2 in chondrogenic medium. However, there was an increase in expression for cells cultured on constructs with rhBMP-2 (versus without) for growth and chondrogenic medium. This is strong evidence that for these two medium conditions, the rhBMP-2 was having the most effect on collagen II gene expression and not the soluble medium supplements.

The osteogenic and chondrogenic responses were not always consistent across the metrics analyzed, making it difficult to tease out the effects of medium versus rhBMP-2. The gene expression, calcium and sGAG data were pooled together as shown in Tables 4 and 5, and a qualitative approach was utilized to aid in analysis. For each experimental group, each metric was evaluated relative to the control condition (growth medium, no

rhBMP-2) for the particular cell type (results shown in Table 4). A “+” indicates significantly higher expression in the experimental groups, “-” indicates lower expression and “=” indicates no change in expression relative to control. The total number of positive osteogenic and chondrogenic responses were then tallied

		With Respect to "control" - growth medium/no BMP-2 for given cell type										
		Osteogenic Markers				Chondrogenic Markers						
Group	Calcium content	Col I exp	ALP Exp	BGLAP exp	sGAG content	ACAN exp	Col II exp	Col II/Col I (if > 1, marker of chon differentiation)		OSTEO	CHON	
with BMP-2	ADSC/growth	=	-	-	=	=	=	1.05	=	NONE	NONE	
	ADSC/chon	+	-	-	-	+	=	+	57.58	+	1/4	3/4
	ADSC/osteo	+	-	+	-	=	+	=	3.69	=	2/4	1/4
	BMSC/growth	=	=	+	-	=	+	+	7.43	+	1/4	3/4
	BMSC/chon	=	+	=	-	=	+	+	1546.84	+	1/4	3/4
	BMSC/osteo	+	+	+	+	-	+	+	2.74	=	4/4	2/4
Without BMP-2	ADSC/growth	N/A	N/A	N/A	N/A	N/A	N/A	N/A	N/A			
	ADSC/chon	=	-	-	-	+	-	=	2.70	+	0/4	2/4
	ADSC/osteo	+	-	+	-	=	=	=	2.10	+	2/4	1/4
	BMSC/growth	N/A	N/A	N/A	N/A	N/A	N/A	N/A	N/A			
	BMSC/chon	=	+	=	=	+	=	+	3.41	+	1/4	3/4
	BMSC/osteo	=	+	+	+	-	+	=	-1.14	-	3/4	1/4

Table 5-4: Qualitative assessment of the relative expression of osteogenic and chondrogenic markers. "+" indicates a significant increase relative to control (growth medium, no BMP-2), "-" signifies a decrease and "=" signifies no difference.

and reported in the last two columns of the table. For table 5, the same approach was taken except comparisons were made between “with BMP-2” and “without BMP-2.” From this analysis, the ADSC/chon/BMP-2, BMSC/growth/BMP-2, BMSC/chon/BMP-2 and BMSC/chon/no BMP-2 groups showed strong chondrogenic responses, while the BMSC/osteo/BMP-2 and BMSC/osteo/no BMP-2 group showed strong osteogenesis. Table 5 separates the effect of differentiation medium from the effect of rhBMP-2 and shows that rhBMP-2 specifically influenced expression of chondrogenic markers in the ADSC/chon, BMSC/growth, and BMSC/chon groups that had conjugated rhBMP-2, but not the BMSC/osteo/BMP-2 group.

		With Respect to no BMP-2, same medium										
		Osteogenic Markers				Chondrogenic Markers						
Group	Calcium content	Col I exp	ALP Exp	BGLAP exp	sGAG content	ACAN exp	Col II exp	Col II/Col I (if > 1, marker of chon differentiation)	OSTEO	CHON		
with BMP-2	ADSC/growth	=	-	-	=	=	=	1.05	=	NONE	NONE	
	ADSC/chon	+	-	-	-	=	+	+	57.58	+	1/4	3/4
	ADSC/osteo	-	=	=	-	=	+	=	3.69	=	0/4	1/4
	BMSC/growth	=	-	+	-	=	+	+	7.43	+	1/4	3/4
	BMSc/chon	=	=	=	-	=	+	+	1546.84	+	0/4	3/4
	BMSC/osteo	+	=	-	=	=	+	=	2.74	+	1/4	1/2

Table 5-5: Qualitative assessment of the relative expression of osteogenic and chondrogenic markers for groups with BMP-2 versus without BMP-2. "+" indicates a significant increase, "-" signifies a decrease and "=" signifies no difference.

5.4 Discussion

This study directly compared the effect of differentiation medium on the *in vitro* response of ADSC and BMSC seeded in rhBMP-2-conjugated PCL scaffolds. The results indicate that soluble medium factors influenced both osteogenesis and chondrogenesis, while conjugated rhBMP-2 had a greater effect on chondrogenesis. rhBMP-2 acted independently to induce chondrogenesis in BMSC cultured in growth medium, but worked in tandem with soluble chemical factors to increase chondrogenic marker expression of cells in chondrogenic medium. Across groups, the BMSC expressed more markers of differentiation and tended more toward chondrogenesis than osteogenesis. These results showcase the complexity of differentiation and are evidence that these two cell types behave differently from one another when exposed to soluble differentiation factors and conjugated rhBMP-2.

Inducing *in vitro* osteogenesis prior to *in vivo* implantation may improve the bone formation response of cells in tissue engineered constructs. The four osteogenic markers

assessed in this study were chosen based on their temporal distribution along the osteogenic differentiation pathway [66]. Collagen I gene expression is an early indicator of osteogenic differentiation, calcium content and alkaline phosphatase gene expression are slightly later indicators of osteogenesis, and osteocalcin gene expression is a mature bone marker. The two common methods to induce osteogenesis *in vitro* prior to implantation *in vivo* are chemically-induced osteogenesis and protein-induced osteogenesis. The former involves administering traditional, soluble osteogenic supplements such as beta-glycerophosphate, ascorbic acid and dexamethasone, which are collectively referred to as “osteogenic medium.” Protein-induced osteogenesis involves incorporating bone-specific growth factors, such as rhBMP-2, into the culture system, an approach that has grown in popularity due to its potential for *in vivo* translation.

In general, BMSC had a mildly greater tendency for osteogenesis *in vitro* compared to ADSC, as demonstrated by differences displayed between BMSC and ADSC in osteogenic medium. BMSC showed upregulation of all three osteogenic genes (compared to cells in growth medium), while the ADSC only showed an increase in ALP expression. The chemical supplements in osteogenic medium emerged as the primary factors affecting expression of osteogenic markers in both ADSC and BMSC. When in osteogenic medium, BMSC demonstrated greater expression of osteogenic genes without rhBMP-2 present versus with rhBMP-2. These expression levels were greater than for ADSC in osteogenic medium, regardless of rhBMP-2's presence, a trend that has also been reported by others [30, 67] and which suggests a greater innate osteogenic capacity of BMSC.

rhBMP-2's particular effect on osteogenesis was isolated by comparing constructs conjugated with rhBMP-2 and cultured in a particular medium to constructs cultured in the same medium without conjugated rhBMP-2. BMSC responded positively to rhBMP-2 by upregulating ALP when in growth medium. However, BMSC cultured in osteogenic medium did not display this same positive response to rhBMP-2 and a greater ALP response was actually observed in the absence of rhBMP-2. Furthermore, expression of ALP for this group was significantly higher than for BMSC exposed to rhBMP-2 in growth medium, suggesting a greater effect of soluble osteogenic supplements on ALP production. The only significant osteogenic effect that rhBMP-2 had on ADSC was an increase in mineralization for constructs also cultured in chondrogenic medium. Since such a response was not observed for ADSC in growth medium with rhBMP-2, the increased mineralization may have resulted from the inclusion of dexamethasone in the chondrogenic medium, which has been shown to augment mineralization when used in combination with rhBMP-2 [21]. These results are also in keeping with reported inconsistencies in the ability of human ADSC to respond osteogenically to rhBMP-2. In one study, there was no significant change in healing of *in vivo* bone defects for rhBMP-2 used in combination with ADSC versus rhBMP-2 alone [32]. *In vitro* studies have also demonstrated inconsistent osteogenic gene expression and no significant increase in mineralization of ADSC in response to rhBMP-2 [2]. Our findings support the hypothesis that rhBMP-2 may not influence the osteogenic fate of ADSC.

Stimulating endochondral ossification through chondrogenic priming has shown promise for inducing *in vivo* bone growth [62, 63]. This has primarily been done using traditional chondrogenic medium but there have been some studies investigating

osteocondral bone growth induced by BMPs [45, 46]. The work of this thesis investigated how the combination of differentiation medium and conjugated rhBMP-2 influenced *in vitro* expression of chondrogenic markers. Exposing cells to chemical medium components is the traditional method for inducing chondrogenesis *in vitro*, but rhBMP-2 has also shown particular effectiveness for inducing expression of chondrogenic markers in mesenchymal stem cells [68], often in the presence of TGF- β 1 [69, 70], a common proteinaceous component of chondrogenic medium. This combinatorial effect of rhBMP-2 and chondrogenic supplements increased chondrogenic marker expression by ADSC, but rhBMP-2 alone did not produce such an effect. These results show that ADSC were more sensitive to soluble factors than to conjugated rhBMP-2, which is contrary to the behavior demonstrated by BMSC. BMSC exposed to rhBMP-2 had high expression levels of chondrogenic markers when in chondrogenic medium, but also demonstrated upregulation of aggrecan and collagen II when cultured on rhBMP-2 conjugated scaffolds in growth medium or osteogenic medium. This suggests that conjugated rhBMP-2 had a significant effect on the upregulation of chondrogenic markers by BMSC and that BMSC were more sensitive to rhBMP-2 than ADSC. A similar finding was reported in a study comparing BMSC and ADSC taken from the same donor and induced to differentiate via traditional soluble factors [71].

The task of isolating the effects of soluble factors and incorporated growth factors is nontrivial but is important for adequately promoting osteogenesis within a tissue engineered construct. Growth factors can be tethered to constructs [8, 9, 37, 72], delivered in soluble form [2, 3] or expressed in cells after adenoviral transduction [33, 73] and these delivery methods all have their advantages and limitations. Dragoo et al

[28] found a similar rate and level of *in vitro* osteogenesis between ADSC transduced with rhBMP-2 and cells exposed to soluble rhBMP-2, suggesting that either of these methods is appropriate for delivering rhBMP-2. However, the particular advantage of using rhBMP-2 over osteogenic medium in that study was unclear because all groups were cultured in osteogenic medium yet no explicit comparisons were made to cells in osteogenic medium without rhBMP-2. A study using gelatin/ β -TCP scaffolds compared the osteogenic potential of ADSC and BMSC exposed to osteogenic medium or to rhBMP-2 encapsulated in microspheres [44]. The addition of rhBMP-2 increased Hounsfield bone density unit (HU) values at 4 and 6 weeks, compared to constructs only exposed to osteogenic medium. These findings emphasize the positive effect that the rhBMP-2 released from microspheres had on inducing bone formation, but there have also been studies citing little positive effect of rhBMP-2 over osteogenic medium alone [2]. It is difficult to make a definitive statement regarding the osteogenic effect of rhBMP-2 because the dose, delivery mode and additional external factors all influence how rhBMP-2 interacts with cells.

In the study presented in this Chapter, the effect of conjugated rhBMP-2 was isolated by assessing its osteogenic influence both in combination with and in the absence of soluble media supplements. Most instances of osteogenic marker expression were due to traditional osteogenic medium supplements, which may signal that the conjugated rhBMP-2 had difficulty impacting expression of osteogenic markers. These results are contrary to other studies that reported comprehensive upregulation of osteogenic markers when rhBMP-2 was conjugated to scaffolds using sulfo-SMCC [10, 37]. However, there are important differences between those studies and the one presented here. Electrospun

chitosan scaffolds with sulfo-SMCC-conjugated rhBMP-2 showed better growth factor retention and more ALP activity and mineralization over time, compared to constructs with adsorbed rhBMP-2 [37]. Differences between that study and the one presented here may have resulted from the choice of scaffolding materials and the mechanism of sulfo-SMCC conjugation. Conjugation via sulfo-SMCC is non-specific in that the crosslinker does not preferentially target certain amine groups to link with on the rhBMP-2. Thus, depending on how and where the rhBMP-2 is conjugated, its bioactivity may be compromised by an altered configuration or steric hindrance of the active site [72]. The electrospun, nanofibrous chitosan membrane may have retained growth factor bioactivity better than the sintered PCL scaffold due to lack of crowding within the chitosan fiber network. It may have also been more prone to *in vitro* degradation, which would result in release of rhBMP-2 that was no longer immobilized and thus free to interact with cells. In addition, the bioactivity assessment in the chitosan study utilized mouse osteoblastic cells (MC3T3s), which have already obtained a state of osteogenic readiness and do not show variations due to donor, age and harvest site that are seen with human ADSC and BMSC [74-77]. A true examination of the rhBMP-2's bioactivity in the system presented here would require analysis using a well-characterized model, such as ALP expression by C2C12 cells [5, 8, 10].

Studies have also utilized Traut's reagent to introduce sulfhydryl groups on the surface of polymers prior to using sulfo-SMCC. The potential inhibition of sulfo-SMCC active sites is diminished because the sulfo-SMCC interacts with sulfhydryls on the polymer and amines on the growth factor, instead of interacting with amines on both substrates. This alone may be responsible for the more favorable osteogenic response

observed when this method was used to conjugate rhBMP-2 to a collagen scaffold [10]. The alternative sulfo-SMCC crosslinking method further differed from our method because it covalently attached polyhistidine antibodies that then bound specifically to His-BMP-2. This eliminated the covalent linkage between the sulfo-SMCC and His-BMP-2 to ensure maintenance of the rhBMP-2's activity.

The examples above demonstrate the recent interest in using bioconjugate techniques to tether rhBMP-2 to scaffolds. Physical adsorption is the typical control condition for conjugation studies, since this method represents a more relevant *in vivo* condition than delivery of soluble rhBMP-2. However, soluble rhBMP-2 may be a more useful control for conjugation studies since it is likely the released growth factor that is responsible for a cellular response and not the growth factor that is still immobilized on the scaffold. From the literature discussed here, the key determinant of rhBMP-2's osteogenic potency is the availability of its active site. Thus, the most successful conjugation methods should enable cells to freely access the conjugated rhBMP-2's active site and/or promote steady release of the growth factor from the scaffold such that cells interact with the free form of the growth factor. The system used in this study may have had less bioavailable rhBMP-2 than other similar systems, which is why chemical supplements had a greater effect on osteogenesis.

5.5 Conclusion

The results of this study are indicative of the complexity of bone tissue engineering systems due to interactions between cells, growth factors and chemical differentiation factors. Isolating the effects of individual osteogenic factors is nontrivial but was achieved to some degree in this study. Overall, soluble chemical factors had a

greater effect on *in vitro* osteogenic marker expression than conjugated rhBMP-2, while the conjugated rhBMP-2 was successful in inducing markers of chondrogenesis. BMSC had a greater capacity to produce chondrogenic precursors in response to the conjugated rhBMP-2 compared to ADSC, and BMSC appeared to be more actively differentiating in the *in vitro* environment. The true end-goal of tissue engineering is not to decipher patterns of osteogenesis in an *in vitro* environment, but to evaluate bone growth *in vivo*. Chapter 6 takes the systems that were introduced here and examines their potential to induce bone growth *in vivo*. This Chapter also stimulated concern over the rhBMP-2 delivery capability of the sulfo-SMCC conjugation method. These concerns are addressed in detail later in this dissertation in an effort to determine the best mode of growth factor incorporation for this system.

5.6 Acknowledgements

This work was funded by NIAMS AR 053379. Thank you to Marta Dias for her assistance in obtaining computational permeability values. Thank you to Ram Rao for his assistance with the calcium assay and to Sitaram Chivukula for his assistance with *in vitro* assays, cell culture and experimental permeability measurements.

5.7 References

- [1] Wozney JM, Rosen V, Celeste AJ, Mitsock LM, Whitters MJ, Kriz RW, et al. Novel regulators of bone formation: molecular clones and activities. *Science* 1988. p. 1528-34.
- [2] Zuk P, Chou Y, Mussano F, Benhaim P, Wu B. Adipose derived stem cells and BMP-2: Part 2. BMP-2 may not influence the osteogenic fate of human adipose-derived stem cells. *Connective Tissue Research* 2011. p. 119-32.
- [3] Huang WB, Carlsen B, Wulur I, Rudkin G, Ishida K, Wu B, et al. BMP-2 exerts differential effects on differentiation of rabbit bone marrow stromal cells grown in two-dimensional and three-dimensional systems and is required for in vitro bone formation in a PLGA scaffold. *Experimental Cell Research*. 2004;299:325-34.
- [4] Hiraki Y, Inoue H, Shigeno C, Sanma Y, Bentz H, Rosen DM, et al. Bone Morphogenetic Proteins (BMP-2 and BMP-3) Promote Growth and Expression of the Differentiated Phenotype Of Rabbit Chondrocytes and Osteoblastic MC3T3-E1 Cells In Vitro. *Journal of Bone and Mineral Research*. 1991;6:1373-85.
- [5] Katagiri T, Yamaguchi A, Komaki M, Abe E, Takahashi N, Ikeda T, et al. Bone Morphogenetic Protein-2 Converts the Differentiation Pathway OF C2C12 Myoblasts into the Osteoblast Lineage. *Journal of Cell Biology*. 1994;127:1755-66.
- [6] Knippenberg M, Helder MN, Doulabi BZ, Wuisman P, Klein-Nulend J. Osteogenesis versus chondrogenesis by BMP-2 and BMP-7 in adipose stem cells. *Biochemical and Biophysical Research Communications*. 2006;342:902-8.
- [7] La W-G, Kang S-W, Yang HS, Bhang SH, Lee SH, Park J-H, et al. The Efficacy of Bone Morphogenetic Protein-2 Depends on Its Mode of Delivery. *Artificial Organs*. 2010;34:1150-3.
- [8] Pohl TLM, Boergermann JH, Schwaerzer GK, Knaus P, Cavalcanti-Adam EA. Surface immobilization of bone morphogenetic protein 2 via a self-assembled monolayer formation induces cell differentiation. *Acta Biomaterialia*. 2012;8:772-80.
- [9] Zhang HN, Migneco F, Lin CY, Hollister SJ. Chemically-Conjugated Bone Morphogenetic Protein-2 on Three-Dimensional Polycaprolactone Scaffolds Stimulates Osteogenic Activity in Bone Marrow Stromal Cells. *Tissue Engineering Part A*. 2010;16:3441-8.
- [10] Zhao Y, Zhang J, Wang X, Chen B, Xiao Z, Shi C, et al. The osteogenic effect of bone morphogenetic protein-2 on the collagen scaffold conjugated with antibodies. *Journal of Controlled Release*. 2010;141:30-7.
- [11] Basmanav FB, Kose GT, Hasirci V. Sequential growth factor delivery from complexed microspheres for bone tissue engineering. *Biomaterials*. 2008;29:4195-204.

- [12] Chong Y-I, Ahn K-M, Jeon S-H, Lee S-Y, Lee J-H, Tae G. Enhanced bone regeneration with BMP-2 loaded functional nanoparticle–hydrogel complex. *Journal of Controlled Release* 2007. p. 91-9.
- [13] Jeon O, Song SJ, Yang HS, Bhang S-H, Kang S-W, Sung MA, et al. Long-term delivery enhances in vivo osteogenic efficacy of bone morphogenetic protein-2 compared to short-term delivery. *Biochemical and Biophysical Research Communications*. 2008;369:774-80.
- [14] Kim HD, Valentini RF. Retention and activity of BMP-2 in hyaluronic acid-based scaffolds in vitro. *Journal of Biomedical Materials Research*. 2002;59:573-84.
- [15] Kim S, Kang YQ, Krueger CA, Sen ML, Holcomb JB, Chen D, et al. Sequential delivery of BMP-2 and IGF-1 using a chitosan gel with gelatin microspheres enhances early osteoblastic differentiation. *Acta Biomaterialia*. 2012;8:1768-77.
- [16] Raiche AT, Puleo DA. In vitro effects of combined and sequential delivery of two bone growth factors. *Biomaterials*. 2004;25:677-85.
- [17] Katagiri T, Yamaguchi A, Ikeda T, Yoshiki S, Wozney J, Rosen V, et al. The non-osteogenic mouse pluripotent cell line, C3H10T1/2, is induced to differentiate into osteoblastic cells by recombinant human bone morphogenetic protein-2. *Biochemical and Biophysical Research Communications* 1990. p. 295-9.
- [18] Takuwa Y, Ohse C, Wang EA, Wozney JM, Yamashita K. Bone Morphogenetic Protein-2 Stimulates Alkaline-Phosphatase Activity and Collagen Synthesis in Cultured Osteoblastic Cells, MC3T3-E1. *Biochemical and Biophysical Research Communications*. 1991;174:96-101.
- [19] Wang EA, Rosen V, Dalessandro JS, Bauduy M, Cordes P, Harada T, et al. Recombinant Human Bone Morphogenetic Protein Induces Bone Formation. *Proceedings of the National Academy of Sciences of the United States of America*. 1990;87:2220-4.
- [20] Yamaguchi A, Katagiri T, Ikeda T, Wozney JM, Rosen V, Wang EA, et al. Recombinant Human Bone Morphogenetic Protein-2 Stimulates Osteoblastic Maturation and Inhibits Myogenic Differentiation In Vitro. *Journal of Cell Biology*. 1991;113:681-7.
- [21] Luppen CA, Smith E, Spevak L, Boskey AL, Frenkel B. Bone morphogenetic protein-2 restores mineralization in glucocorticoid-inhibited MC3T3-E1 osteoblast cultures. *Journal of Bone and Mineral Research*. 2003;18:1186-97.
- [22] Torii Y, Hitomi K, Tsukagoshi N. Synergistic effect of BMP-2 and ascorbate on the phenotypic expression of osteoblastic MC3T3-E1 cells. *Molecular and Cellular Biochemistry*. 1996;165:25-9.
- [23] Long MW, Robinson JA, Ashcraft EA, Mann KG. Regulation of Human Bone Marrow-Derived Osteoprogenitor Cells by Osteogenic Growth Factors. *Journal of Clinical Investigation*. 1995;95:881-7.

- [24] Luu HH, Song W-X, Luo X, Manning D, Luo J, Deng Z-L, et al. Distinct roles of bone morphogenetic proteins in osteogenic differentiation of mesenchymal stem cells. *Journal of Orthopaedic Research*. 2007;25:665-77.
- [25] Mizuno H. Adipose-derived stem cells for tissue regeneration and repair: ten years of research and a literature review. *Journal of Nihon Medical School*2009. p. 56-66.
- [26] Chen QA, Yang ZL, Sun SJ, Huang H, Sun XJ, Wang ZG, et al. Adipose-derived stem cells modified genetically in vivo promote reconstruction of bone defects. *Cytotherapy*. 2010;12:831-40.
- [27] Panetta NJ, Gupta DM, Lee JK, Wan DC, Commons GW, Longaker MT. Human Adipose-Derived Stromal Cells Respond to and Elaborate Bone Morphogenetic Protein-2 during In Vitro Osteogenic Differentiation. *Plastic and Reconstructive Surgery*. 2010;125:483-93.
- [28] Dragoo JL, Choi JY, Lieberman JR, Huang J, Zuk PA, Zhang J, et al. Bone induction by BMP-2 transduced stem cells derived from human fat. *Journal of Orthopedic Research*2003. p. 622-9.
- [29] Noel D, Caton D, Roche S, Bony C, Lehmann S, Casteilla L, et al. Cell specific differences between human adipose-derived and mesenchymal-stromal cells despite similar differentiation potentials. *Experimental Cell Research*. 2008;314:1575-84.
- [30] Kim D, Monaco E, Maki A, de Lima AS, Kong HJ, Hurley WL, et al. Morphologic and transcriptomic comparison of adipose- and bone-marrow-derived porcine stem cells cultured in alginate hydrogels. *Cell and Tissue Research*. 2010;341:359-70.
- [31] Zuk P, Chou Y-F, Mussano F, Benhaim P, Wu BM. Adipose-derived Stem cells and BMP2: Part 2. BMP2 may not influence the osteogenic fate of human adipose-derived stem cells. *Connective Tissue Research*. 2011;52:119-32.
- [32] Chou Y-F, Zuk PA, Chang T-L, Benhaim P, Wu BM. Adipose-Derived stem cells and BMP-2: Part 1. BMP2-treated adipose derived stem cells do not improve repair of segmental femoral defects. *Connective Tissue Research*2011. p. 109-18.
- [33] Schek RM, Wilke EN, Hollister SJ, Krebsbach PH. Combined use of designed scaffolds and adenoviral gene therapy for skeletal tissue engineering. *Biomaterials*. 2006;27:1160-6.
- [34] Saito E, Liao E, Hu W, Krebsbach P, Hollister S. Effects of designed PLLA and 50:50 PLGA scaffold architectures on bone formation in vivo. *Journal of Tissue Engineering and Regenerative Medicine*2011.
- [35] Minamide A, Yoshida M, Kawakami M, Okada M, Enyo Y, Hashizume H, et al. The effects of bone morphogenetic protein and basic fibroblast growth factor on cultured mesenchymal stem cells for spine fusion. *Spine*. 2007;32:1067-71.

- [36] Liu Y, Huse RO, de Groot K, Buser D, Hunziker EB. Delivery mode and efficacy of BMP-2 in association with implants. *Journal of Dental Research*. 2007;86:84-9.
- [37] Park YJ, Kim KH, Lee JY, Ku Y, Lee SJ, Min BM, et al. Immobilization of bone morphogenetic protein-2 on a nanofibrous chitosan membrane for enhanced guided bone regeneration. *Biotechnology and Applied Biochemistry*. 2006;43:17-24.
- [38] Draenert F, Nonnenmacher A-L, Ka¨mmerer P, Goldschmitt J, Wagner W. BMP-2 and bFGF release and in vitro effect on human osteoblasts after adsorption to bone grafts and biomaterials. *Clinical Oral Implants Research*2012. p. 1-8.
- [39] Gharibjanian NA, Chua WC, Dhar S, Scholz T, Shibuya TY, Evans GRD, et al. Release Kinetics of Polymer-Bound Bone Morphogenetic Protein-2 and Its Effects on the Osteogenic Expression of MC3T3-E1 Osteoprecursor Cells. *Plastic and Reconstructive Surgery*. 2009;123:1169-77.
- [40] Liu H-W, Chen C-H, Tsai C-L, Lin IH, Hsiue G-H. Heterobifunctional poly(ethylene glycol)-tethered bone morphogenetic protein-2-stimulated bone marrow mesenchymal stromal cell differentiation and osteogenesis. *Tissue Engineering*. 2007;13:1113-24.
- [41] Liu H-W, Chen C-H, Tsai C-L, Hsiue G-H. Targeted delivery system for juxtacrine signaling growth factor based on rhBMP-2-mediated carrier-protein conjugation. *Bone*. 2006;39:825-36.
- [42] Jeon O, Song SJ, Kang S-W, Putnam AJ, Kim B-S. Enhancement of ectopic bone formation by bone morphogenetic protein-2 released from a heparin-conjugated poly(Llactic- co-glycolic acid) scaffold. *Biomaterials*2007. p. 2763-71.
- [43] The Efficacy of Bone Morphogenetic Protein-2 Depends on its Mode of Delivery. *Artificial Organs*2010. p. 1150-3.
- [44] Weinand C, Nabili A, Khumar M, Dunn J, Ramella-Roman J, Jeng J, et al. Factors of Osteogenesis Influencing Various Human Stem Cells on Third-Generation Gelatin/b-Tricalcium Phosphate Scaffold Material. *Rejuvenation Research*2011. p. 185-94.
- [45] Yu YY, Lieu S, Lu C, Colnot C. Bone morphogenetic protein 2 stimulates endochondral ossification by regulating periosteal cell fate during bone repair. *Bone*. 2010;47:65-73.
- [46] Noel D, Gazit D, Bouquet C, Apparailly F, Bony C, Ponce P, et al. Short-term BMP-2 expression is sufficient for in vivo osteochondral differentiation of mesenchymal stem cells. *Stem Cells*. 2004;22:74-85.
- [47] Retting KN, Song B, Yoon BS, Lyons KM. BMP canonical Smad signaling through Smad1 and Smad5 is required for endochondral bone formation. *Development*. 2009;136:1093-104.

- [48] Kang H. Hierarchical Design and Simulation of Tissue Engineering Scaffold Mechanical, Mass Transport, and Degradation Properties: University of Michigan; 2010.
- [49] Kemppainen JM, Hollister SJ. Differential effects of designed scaffold permeability on chondrogenesis by chondrocytes and bone marrow stromal cells. *Biomaterials*. 2010;31:279-87.
- [50] Jeong CG, Hollister SJ. Mechanical, Permeability, and Degradation Properties of 3D Designed Poly(1,8 Octanediol-co-Citrate) Scaffolds for Soft Tissue Engineering. *Journal of Biomedical Materials Research Part B-Applied Biomaterials*. 2010;93B:141-9.
- [51] Li CM, Vepari C, Jin HJ, Kim HJ, Kaplan DL. Electrospun silk-BMP-2 scaffolds for bone tissue engineering. *Biomaterials*. 2006;27:3115-24.
- [52] Ter Brugge PJ, Jansen JA. In vitro osteogenic differentiation of rat bone marrow cells subcultured with and without dexamethasone. *Tissue Engineering*. 2002;8:321-31.
- [53] Kim SS, Park MS, Jeon O, Choi CY, Kim BS. Poly(lactide-co-glycolide)/hydroxyapatite composite scaffolds for bone tissue engineering. *Biomaterials*. 2006;27:1399-409.
- [54] Jeong CG, Hollister SJ. Mechanical and biochemical assessments of 3D poly (1,8 octanediol-co-citrate) scaffold pore shape and permeability effects on in vitro chondrogenesis using primary chondrocytes. *Tissue Engineering Part A* 2010. p. 3759-68.
- [55] Schmittgen TD, Livak KJ. Analyzing real-time PCR data by the comparative C-T method. *Nature Protocols*. 2008;3:1101-8.
- [56] Fink T, Lund P, Pilgaard L, Rasmussen JG, Duroux M, Zachar V. Instability of standard PCR reference genes in adipose-derived stem cells during propagation, differentiation and hypoxic exposure. *Bmc Molecular Biology*. 2008;9.
- [57] Hui PW, Leung PC, Sher A. Fluid conductance of cancellous bone graft as a predictor for graft-host interface healing. *Journal of Biomechanics*. 1996;29:123-32.
- [58] Ecarotcharrier B, Glorieux FH, Vanderrest M, Pereira G. Osteoblasts Isolated From Mouse Calvaria Initiate Matrix Mineralization in Culture. *Journal of Cell Biology*. 1983;96:639-43.
- [59] Kasten P, Vogel J, Luginbuhl R, Niemeyer P, Tonak M, Lorenz H, et al. Ectopic bone formation associated with mesenchymal stem cells in a resorbable calcium deficient hydroxyapatite carrier. *Biomaterials*. 2005;26:5879-89.
- [60] Kasten P, Vogel J, Luginbuhl R, Niemeyer P, Weiss S, Schneider S, et al. Influence of platelet-rich plasma on osteogenic differentiation of mesenchymal stem cells and ectopic bone formation in calcium phosphate ceramics. *Cells Tissues Organs*. 2006;183:68-79.

- [61] Leong DT, Abraham MC, Rath SN, Lim T-C, Chew FT, Hutmacher DW. Investigating the effects of preinduction on human adipose-derived precursor cells in an athymic rat model. *Differentiation*. 2006;74:519-29.
- [62] Farrell E, Both SK, Odoerfer KI, Koevoet W, Kops N, O'Brien FJ, et al. In-vivo generation of bone via endochondral ossification by in-vitro chondrogenic priming of adult human and rat mesenchymal stem cells. *Bmc Musculoskeletal Disorders*. 2011;12.
- [63] Farrell E, van der Jaqt O, Koevoet W, Kops N, van Manen C, Hellingman C, et al. Chondrogenic priming of human bone marrow stromal cells: a better route bone repair? *Tissue Engineering Part C*2009.
- [64] Reddi AH. *Cell Biology and Biochemistry of Endochondral Bone Development. Collagen and Related Research*. 1981;1:209-26.
- [65] Hellingman CA, Koevoet W, Kops N, Farrell E, Jahr H, Liu W, et al. Fibroblast Growth Factor Receptors in In Vitro and In Vivo Chondrogenesis: Relating Tissue Engineering Using Adult Mesenchymal Stem Cells to Embryonic Development. *Tissue Engineering Part A*. 2010;16:545-56.
- [66] Owen TA, Aranow M, Shalhoub V, Barone LM, Wilmig L, Tassinari MS, et al. Progressive development of the rat osteoblast phenotype in vitro: reciprocal relationships in expression of genes associated with osteoblast proliferation and differentiation during formation of the bone extracellular matrix. *Journal of Cell Physiology*1990. p. 420-30.
- [67] Vishnubalaji R, Al-Nbaheen M, Kadalmani B, Aldahmash A, Ramesh T. Comparative investigation of the differentiation capability of bone-marrow- and adipose-derived mesenchymal stem cells by qualitative and quantitative analysis. *Cell and Tissue Research*2012. p. 419-27.
- [68] Wang EA, Israel DI, Kelly S, Luxenberg DP. Bone Morphogenetic Protein-2 Causes Commitment and Differentiation in C3H10T1/2 and 3T3 Cells. *Growth Factors*. 1993;9:57-&.
- [69] Freyria AM, Mallein-Gerin F. Chondrocytes or adult stem cells for cartilage repair: The indisputable role of growth factors. *Injury-International Journal of the Care of the Injured*. 2012;43:259-65.
- [70] Melhorn AT, Niemeyer P, Kaschte K, Muller L, Finkenzeller G, Hartl D, et al. Differential effects of BMP-2 and TGF- β 1 on chondrogenic differentiation of adipose derived stem cells. *Cell Proliferation*2007. p. 809-23.
- [71] Afizah H, Yang Z, Hui JHP, Ouyang HW, Lee EH. A comparison between the chondrogenic potential of human bone marrow stem cells (BMSCs) and adipose-derived stem cells (ADSCs) taken from the same donors. *Tissue Engineering*. 2007;13:659-66.
- [72] Masters KS. Covalent Growth Factor Immobilization Strategies for Tissue Repair and Regeneration. *Macromolecular Bioscience*. 2011;11:1149-63.

- [73] Peterson B, Zhang J, Iglesias R, Kabo M, Hedrick M, Benhaim P, et al. Healing of critically sized femoral defects, using genetically modified mesenchymal stem cells from human adipose tissue. *Tissue Engineering*. 2005;11:120-9.
- [74] Tsuchida H, Hashimoto J, Crawford E, Manske P, Lou J. Engineered allogeneic mesenchymal stem cells repair femoral segmental defect in rats. *Journal of Orthopaedic Research*. 2003;21:44-53.
- [75] Mendes SC, Tibbe JM, Veenhof M, Both S, Oner FC, van Blitterswijk CA, et al. Relation between in vitro and in vivo osteogenic potential of cultured human bone marrow stromal cells. *Journal of Materials Science-Materials in Medicine*. 2004;15:1123-8.
- [76] Pilgaard L, Lund P, Duroux M, Fink T, Ulrich-Vinther M, Soballe K, et al. Effect of oxygen concentration, culture format and donor variability on in vitro chondrogenesis of human adipose tissue-derived stem cells. *Regenerative Medicine*. 2009;4:539-48.
- [77] Osyczka AM, Damek-Poprawa M, Wojtowicz A, Akintoye SO. Age and Skeletal Sites Affect BMP-2 Responsiveness of Human Bone Marrow Stromal Cells. *Connective Tissue Research*. 2009;50:270-7.

CHAPTER 6 In Vivo Bone Regeneration by Human Adipose Derived Stem Cells and Bone Marrow Stromal Cells on PCL Scaffolds Conjugated with rhBMP-2

6.1 Introduction

Bone tissue engineering, using specifically designed scaffolds and recombinant human bone morphogenetic protein-2 (rhBMP-2), is an attractive alternative to traditional bone repair methods. This technology has the potential to replace autografts, eliminating the graft harvesting surgery and thus reducing patient morbidity. However, safety concerns and questions surrounding rhBMP-2's optimal mode of use have limited its widespread adoption in the clinic. rhBMP-2 is FDA-approved for lumbar spinal fusion, but distal diffusion of the protein away from the implantation site and over-stimulation of bone growth led to adverse events in patients after off-label use [1-3]. Chemical conjugation may address these issues by improving rhBMP-2's retention on scaffolds and enabling controlled release [4-6]. There are conflicting reports of soluble rhBMP-2's osteogenic effect on various cell types and few reports detailing how chemically conjugated rhBMP-2 affects cells. In particular, there is a need to assess the potential of human adipose derived stem cells (ADSC) and bone marrow stromal cells (BMSC) to respond to conjugated rhBMP-2. These cells are the most likely candidates for incorporation into a clinically relevant tissue engineered bone repair solution, yet their behavior in response to rhBMP-2 delivered in different manners may vary and warrants further characterization.

Researchers have been studying the osteogenic effects of rhBMP-2 *in vitro* and *in vivo* since the growth factor was shown to induce bone formation in animals when implanted in both orthotopic and ectopic sites [7]. The ability of rhBMP-2 to induce unspecialized mesenchymal host cells to produce bone is partially due to the cells' previous attainment of chondro-osteogenic competence. While not fully differentiated, such cells have achieved a state of osteogenic readiness after receiving specific signals during embryonic and/or post-fetal development. In a tissue engineering environment, some control over signaling is attained through the scaffold design and by utilizing external factors (such as rhBMP-2) that direct cells to undergo osteogenesis and make bone *in vivo*. The challenge is determining the optimal combination of factors, cells and scaffolding material that results in robust and reliable bone formation.

ADSC and BMSC are both multipotent, adult stem cell types that have shown promise for bone applications. There are conflicting reports on the importance of pre-implantation osteoinduction of these cells for stimulating *in vivo* bone growth. Culturing cells in differentiation medium *in vitro* before implantation is a well-established way to induce osteogenesis [8-10]. Some studies utilizing small animal cranial defect models show better healing when ADSC are cultured in osteogenic medium before implantation (versus cells that have not been osteoinduced) [11, 12], while other studies indicate that ADSC that have not been pre-osteinduced still have the capacity for healing versus controls [13]. Endochondral ossification has been reported after *in vitro* chondrogenic priming of mesenchymal stem cells [14], demonstrating that priming with osteogenic supplements is not the only method of inducing bone growth *in vivo*. Bone induction by rhBMP-2 alone may be more practical and clinically relevant than *in vitro* pre-

differentiation. Successful bone growth using ADSC was observed when rhBMP-2 was adsorbed onto beta-TCP scaffolds [15] or introduced via adenoviral transduction of the cells [16]. In the latter study, no significant difference was observed between constructs with rhBMP-2-producing cells versus constructs impregnated with a collagen/rhBMP-2 gel, suggesting that the cells may not perform better than rhBMP-2 alone. This is in accordance with other studies that have reported no significant effect of ADSC on bone growth [17, 18]. Variability in the *in vivo* bone regeneration capacity of BMSC has also been reported [19]. Furthermore, issues with poorly controlled rhBMP-2 delivery highlight that the mode of rhBMP-2 attachment to a scaffold is significant and may affect rhBMP-2's diffusion from the scaffold and ability to stimulate osteogenesis. Thus it is important to fully characterize a given conjugation method in terms of both its *in vitro* and *in vivo* effect on cells.

The inconsistencies regarding the osteogenic response of ADSC and BMSC in the presence of rhBMP-2 may be due to the variability of these cells' osteogenic capacity [20, 21] and the inherent complexity of *in vivo* systems. This complexity makes it difficult to determine what factor(s) is responsible for a bone healing response. The *in vitro* study of Aim 2 (Chapter 5) represented an initial screening of osteogenic factors that could be used to promote *in vivo* bone growth, but *in vitro* findings do not always translate to an *in vivo* setting [21]. Bone defect animal models are popular in the field of bone tissue engineering because they are a more realistic representation of a clinical setting, compared to ectopic models. However, these models are particularly complex because the host's innate healing response complicates the task of isolating which external factors have osteogenic effects. In this study, a well-characterized subcutaneous

in vivo mouse model [22, 23] was used to reduce variability associated with orthotopic models to more effectively study the particular effects of pre-implantation differentiation and conjugated rhBMP-2 on *in vivo* bone growth.

Poly- ϵ -caprolactone (PCL) scaffolds were chosen as the substrate on which to conjugate rhBMP-2 and seed cells. PCL is an FDA approved biodegradable polyester with mechanical and degradation properties that are appropriate for bone tissue engineering applications [24-27]. It is easily manufactured into regularly designed scaffolds via selective laser sintering (SLS), a technique that enables high volume production of defect-free scaffolds in a short amount of time (hours as opposed to days required by other techniques) [24, 28]. Growth factor incorporation into scaffolds has been accomplished using gel encapsulation [29, 30], physical adsorption [13] and direct conjugation [31-33]. The mode of growth factor delivery influences bone growth distribution and can determine how much rhBMP-2 is initially needed to produce an osteogenic effect. Using less rhBMP-2 and containing it within a scaffold is a way to mitigate potential adverse events [34]. Direct conjugation methods tether rhBMP-2 to a polymer material through either a covalent bond [6, 33] or electrostatic interactions with functional groups on the polymer [35-38]. Utilizing a covalent bond to tether the rhBMP-2 prevents burst release of the protein, reducing the initial amount needed and may also promote localized bone growth by retaining the growth factor on the scaffold for a prolonged period of time.

The goals of this study were to compare *in vivo* bone regeneration between BMSC and ADSC in response to conjugated rhBMP-2 and determine if *in vitro* behavior (reported in Chapter 5) translates to *in vivo* bone growth. Additionally, the role of

differentiation medium (osteogenic or chondrogenic) versus conjugated rhBMP-2 on *in vivo* bone growth of cell-seeded constructs is analyzed. The scaffold design used in this study was modeled after the high permeability scaffold design used previously (in Aim I) and adjusted accordingly for manufacturing by SLS. The crosslinker sulfo-succinimidyl-4-(N-maleimidomethyl)cyclohexane-1-carboxylate (sulfo-SMCC) [32] covalently linked rhBMP-2 to high permeability PCL scaffolds. This chemical conjugation method may have several advantages over adsorption: 1) the rhBMP-2 remains tethered to the scaffold, leading to more localized bone growth, 2) the growth factor may remain in an activated state for longer, leading to greater interaction with cells and thus a stronger osteogenic response, and 3) conjugating rhBMP-2 with high efficiency means less rhBMP-2 is required initially, which may mitigate concerns involving uncontrolled bone growth.

6.2 Materials and Methods

6.2.1 Scaffold Design and Fabrication

A cylindrical scaffold with regular internal architecture was designed as described in Chapter 5. The designed scaffold permeability, porosity and surface area were $7.69 \times 10^{-5} \text{ m}^2$, 63%, and 200.10 mm^2 , respectively. Scaffolds were manufactured out of PCL (with 4% hydroxyapatite incorporated as a flow agent) using a Formiga P 100 laser plastic sintering machine (EOS, Krailling, Germany). Time zero mechanical test specimens had an 8 mm diameter and a height of 16 mm. Scaffolds for *in vivo* experiments had a diameter of 4 mm and a height of 2 mm.

6.2.2 *rhBMP-2 Conjugation*

rhBMP-2 (Genscript, Inc., Piscataway, NJ) was conjugated to PCL scaffolds using the crosslinker sulfo-SMCC (Pierce, Thermo Scientific, Rockford, IL), as shown schematically in Figure 5.1 (Chapter 5). Amine groups were introduced onto the surface of the scaffolds by submerging the scaffolds in a 10% w/v solution of 1,6-hexanediamine in isopropanol under vacuum for 1 hour at 37°C. Scaffolds were then thoroughly washed in deionized, distilled water and dried under vacuum for 24 hours. For sulfo-SMCC conjugation, scaffolds were washed at room temperature in activation buffer (BuPH phosphate buffered saline, Pierce, Thermo Scientific, Rockford, IL) three times, under vacuum for 20 minutes each. A 4 mg/ml solution of sulfo-SMCC in activation buffer was then added to each scaffold for 1 hour, under vacuum at room temperature. Scaffolds were then washed twice in activation buffer and once in conjugation buffer (activation buffer containing 0.1M EDTA). A 50 µg/ml solution of rhBMP-2 in conjugation buffer (400 µl total volume) was then added to the scaffolds in an ultra low-attachment plate (Corning, Tewksbury, MA) for 18 hours at 4°C with gentle shaking. After the incubation with rhBMP-2, scaffolds were washed three times in deionized, distilled water and dried under vacuum for 24 hours.

6.2.3 *Cell Culture and Scaffold Cell Seeding for In Vivo Study*

Human adipose derived stem cells (ADSC) and bone marrow stromal cells (BMSC) (Lonza, Walkersville, MD) were cultured in either low glucose Dulbecco's Modified Eagle Medium (ADSC) or Modified Essential Medium Alpha (BMSC), supplemented with 10% fetal bovine serum and 5% penicillin/streptomycin (all reagents from Gibco, Carlsbad, CA). Cells were cultured until 80% confluency was reached (3-4

days) and then passaged repeatedly to amass required cell numbers to carry out experiments in scaffolds (cells at passage 5 or 6 were used in experiments). For each condition (see Table 1), 16 scaffolds were seeded, each with one million cells. The scaffolds were sterilized using two 30 minute washes in 70% ethanol and then thoroughly

	Cells	Medium	BMP-2?
1	ADSC	None	Yes
2	ADSC	Osteogenic	Yes
3	ADSC	Chondrogenic	Yes
4	ADSC	Osteogenic	No
5	ADSC	Chondrogenic	No
6	BMSC	None	Yes
7	BMSC	Osteogenic	Yes
8	BMSC	Chondrogenic	Yes
9	BMSC	Osteogenic	No
10	BMSC	Chondrogenic	No
11	None	None	Yes

Table 6-1: Experimental groups for implantation.

rinsed with PBS and placed in serum free medium for at least one hour prior to cell seeding. Just before seeding, the scaffolds were removed from the medium, placed in PBS to rinse, blotted dry on sterile gauze and then placed in a sterile Teflon mold, specifically designed for cell seeding. Cells were trypsinized, counted and resuspended in 5 mg/ml fibrinogen. 70 μ l of cells in fibrinogen were added to each scaffold, followed immediately by 7 μ l thrombin and then the Teflon mold containing the scaffolds was placed in a 37°C cell culture incubator for 30 minutes to induce gelation. Scaffolds were removed from the Teflon mold and placed in a low-attachment cell culture plate with 1.5 ml appropriate medium, depending on the experimental condition, according to the

experimental groups listed in Table 1. Osteogenic medium consisted of growth medium plus 10mM beta-glycerophosphate, 50 µg/ml ascorbic 2-phosphate and 10 nM dexamethasone. Chondrogenic medium consisted of growth medium plus 0.1 mM Non-essential amino acids, 50 µg/ml 2-phospho-L-ascorbic acid, 0.4 mM proline, 5 µg/ml insulin, 10ng/ml TGF-β and 0.1 µM dexamethasone. In this study, maintaining cells in differentiation medium is also referred to as “pulsed” (e.g. osteopulsed or chondrogenically-pulsed). Cell/scaffold constructs were maintained in culture for two weeks, with medium changes every three days.

6.2.4 *Subcutaneous Implantation Procedure for In Vivo Study*

Cell-seeded and control (no cells, conjugated rhBMP-2 only) scaffolds were implanted subcutaneously into the backs of NIH3-bg-nu-xid mice (Harlan Laboratories, Indianapolis, IN). For constructs that did not undergo *in vitro* differentiation prior to implantation (groups 1, 6 and 11), cells were trypsinized on the morning of the surgery and seeded into scaffolds as described in the previous section. Four scaffolds were implanted per mouse, with ten scaffolds implanted per group. After 8 weeks, mice were euthanized and scaffolds were removed, placed in zinc-buffered formalin (Z-Fix, Anatech, Ltd., Battle Creek, MI) overnight, in water for 24 hours and stored in 70% ethanol. This study was conducted in accordance with the regulations set forth by the University Committee on the Use and Care of Animals at the University of Michigan.

6.2.5 *Micro-computed Tomography (µCT) Analysis*

Explanted scaffolds were scanned in water with a high-resolution micro-computed tomography (µCT) scanner (GE Medical Systems, Toronto, Canada) at 75 kV and 75 mA, as described in Chapter 4. GEMS Microview software (GE Medical

Systems) was used to quantify bone growth into the scaffolds. To assess bone growth within the scaffold, a cylindrical region of interest (ROI) with fixed x and y dimensions of 6.0 mm and z-dimension of 4.0 mm was used. Bone volume (BV), tissue mineral density (TMD) and tissue mineral content (TMC) were determined, using a bone threshold value of 1100. To assess the amount and quality of bone grown at various radial distances into the scaffold, μ CT analysis was performed on each specimen using four concentric, hollow, cylindrical ROIs, with the same “z” dimensions as the entire scaffold ROIs and having outer diameters of 6.0, 4.5, 3.0, and 1.5 mm.

6.2.6 *Unconfined Compression Testing*

Implanted, fixed scaffolds were mechanically tested in unconfined compression using an MTS Alliance RT30 electromechanical test frame (1.0 mm/min, 0.5 lbf pre-load, MTS Systems Corp., Minneapolis, MN). Data were collected and analyzed using TestWorks4 software (MTS Systems, Corp.).

6.2.7 *Statistics*

Statistical differences between groups were determined with ANOVA using SPSS statistical software (IBM, New York, NY).

6.3 Results

6.3.1 *Micro-CT*

Scaffold bone volume analysis was completed for all implanted scaffolds and is summarized in Figure 1. Panels 1A and 1B display bone volumes for scaffolds with and without rhBMP-2, respectively. Scaffolds containing rhBMP-2 that were seeded with ADSC pulsed *in vitro* with osteogenic medium made more bone ($p < 0.05$) than rhBMP-2-

containing scaffolds that had ADSC pulsed with chondrogenic medium, BMSC pulsed with chondrogenic medium, or BMSC that were not pulsed. Because of high variability, no significant difference was observed between rhBMP-2-conjugated scaffolds that contained osteopulsed ADSC and rhBMP-2-conjugated scaffolds that contained either ADSC that hadn't been pulsed or osteopulsed BMSC. There was also no significant difference in bone volume between rhBMP-2-conjugated scaffolds with osteopulsed ADSC and BMP-2-conjugated scaffolds that contained no cells. The trends were similar

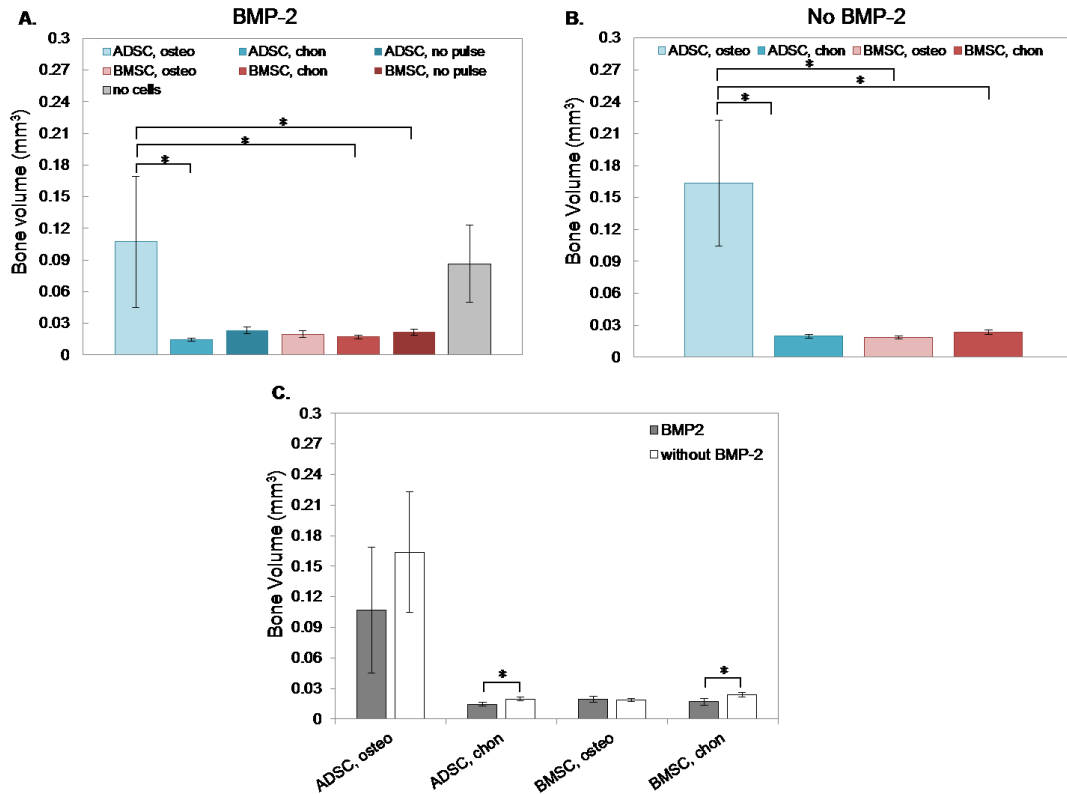


Figure 6.1: Bone volume as quantified by micro-CT. A) Bone volume in scaffolds conjugated with rhBMP-2. B) Bone volume in scaffolds without rhBMP-2. C) Comparison between scaffolds with and without rhBMP-2.

with scaffolds that did not contain rhBMP-2. Scaffolds containing osteopulsed ADSC had significantly more bone ($p < 0.05$) than chondrogenically-pulsed ADSC, osteopulsed BMSC and chondrogenically-pulsed BMSC. Comparing between scaffolds with rhBMP-

2 versus scaffolds without rhBMP-2, as shown in Figure 4C, significant differences ($p < 0.05$) occurred for chondrogenically-pulsed ADSC and chondrogenically-pulsed BMSC but not for either of the osteopulsed groups. The bone volumes reported for these groups are so low (less than 0.03 mm^3), so as to be considered negligible compared to the osteopulsed ADSC and no cells/rhBMP-2 groups. Thus, despite the statistical significance, the comparisons for the chondrogenically-pulsed groups are not particularly interesting.

Analysis of bone penetration into the scaffold is shown in Figure 2, scaffold groups with rhBMP-2 in 2A and scaffold groups without rhBMP-2 in 2B. The rhBMP-2-conjugated scaffolds with osteopulsed ADSC, the rhBMP-2-conjugated scaffolds without cells and the scaffolds with just osteopulsed ADSC (no rhBMP-2) showed maintenance of bone volume through to the core of the scaffold, as shown in Figure 2C. These data shed light on the pattern of bone growth within the scaffold region. We also looked at

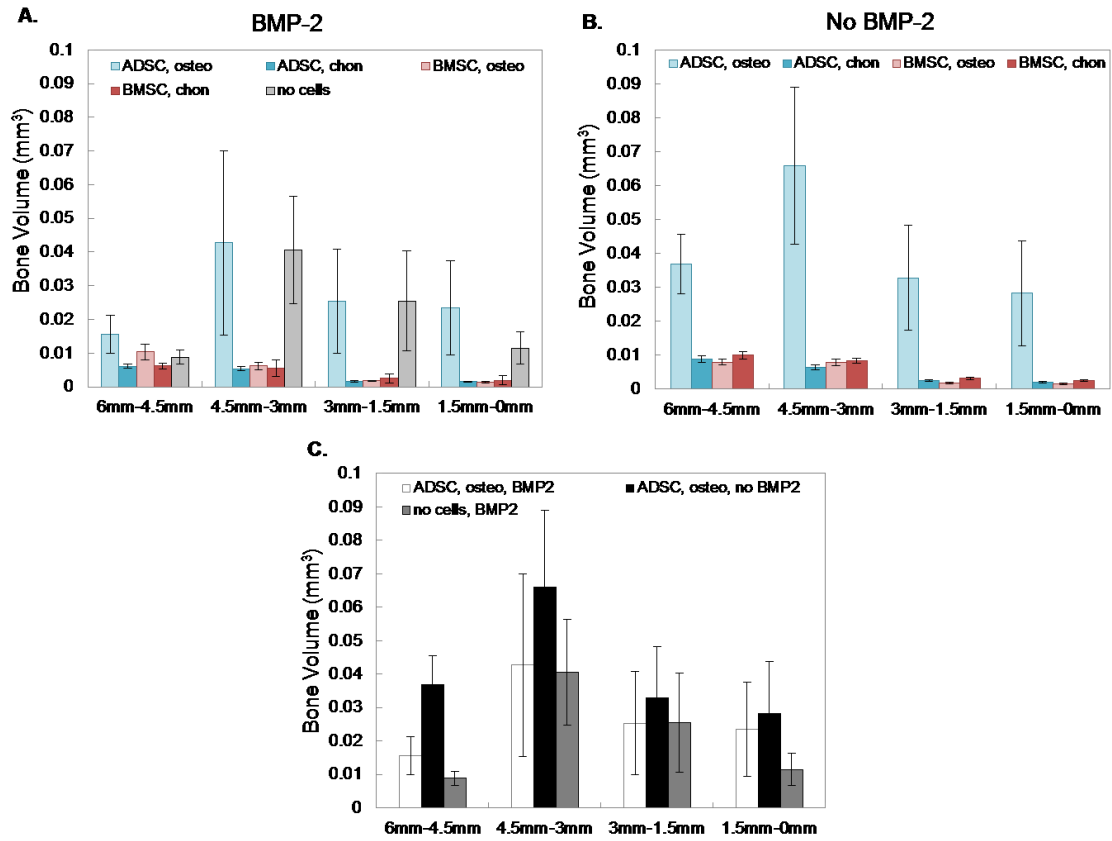


Figure 6.2: Penetration of bone into scaffold. Bone volume was measured in four cylindrical shell regions. A) Penetration of bone into scaffolds conjugated with rhBMP-2. B) Penetration of bone into scaffolds without rhBMP-2. C) Comparison of osteopulsed ADSC with and without rhBMP-2 and rhBMP-2-conjugated scaffolds without cells, which are the three groups that showed significant bone growth.

individual μ CT images slices to gather more information on how bone distribution throughout the scaffolds differed between the experimental groups, as seen in Figure 3. In the left panel of Figure 3 there are μ CT slices from three different rhBMP-2-conjugated scaffolds that contained ADSC that had not been pulsed *in vitro*. Only the PCL scaffold outline can be seen and there are virtually no mineralized areas. The next panel contains images from rhBMP-2-conjugated scaffolds that contained osteopulsed ADSC. In these samples, white areas of mineralization are distinct from the PCL scaffold. The mineralization follows the contours of the scaffold and appears to be evenly distributed

throughout the scaffold. This pattern of mineralization is also observed for scaffolds that only contained osteopulsed ADSC (no conjugated rhBMP-2), as shown in the next panel. Recall that there was no significant difference in total scaffold bone volume for the two groups with osteopulsed ADSC. There was also no difference between

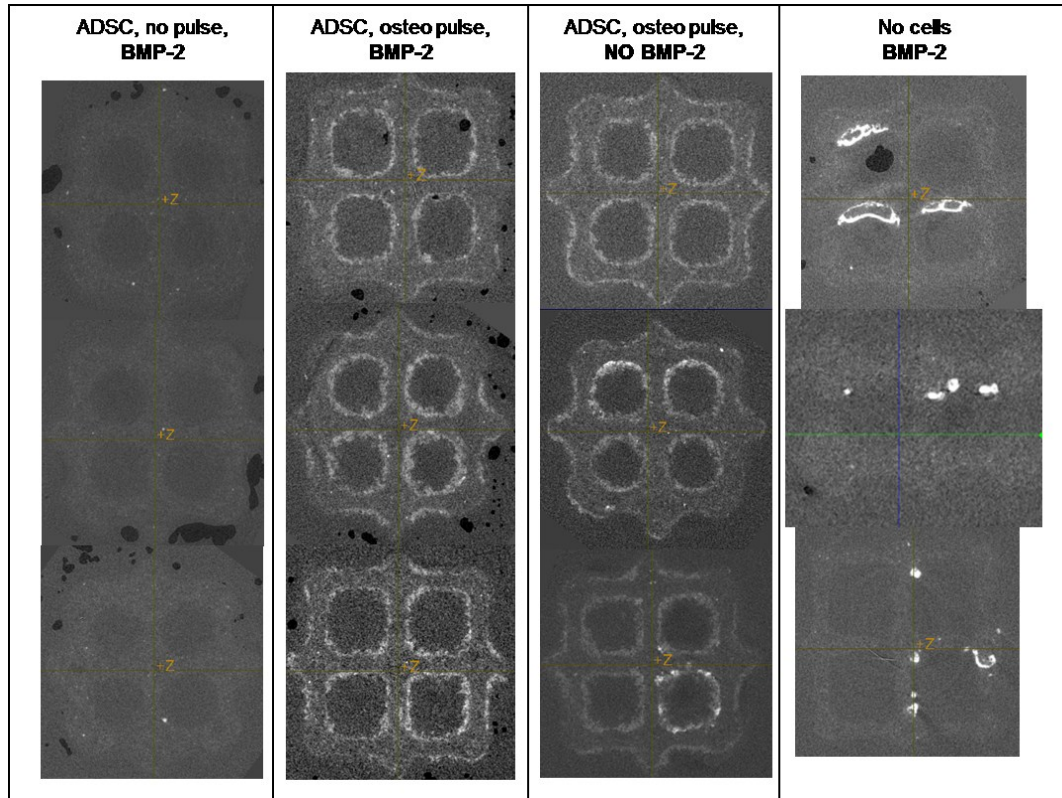


Figure 6.3: Micro-CT image slices through the center of PCL scaffolds. For each experimental groups listed along the top, images of central slices through three separate scaffolds are shown.

scaffolds with osteopulsed ADSC and scaffolds that only contained rhBMP-2. However, the distribution of the bone is very different for scaffolds with cells versus scaffolds containing only rhBMP-2, as shown in the right panel of Figure 3. When rhBMP-2 is present on the scaffold without cells, bone grows in dense nodules and is distributed randomly throughout the scaffold pore spaces.

6.3.2 *Mechanical Testing*

Mechanical testing was performed to determine the effect that newly formed bone tissue had on modulus and compressive strength of the constructs. The results, shown in Figure 4A, indicate an increase in modulus (approximately 1.7x) compared to native PCL scaffolds that were not implanted. This is a typical response resulting from soft tissue in-growth and was also observed in the Aim I for scaffolds implanted without cells for 4 weeks (~1.75x increase over native PCL scaffolds). There is no difference in modulus or 0.2% offset yield stress between groups, demonstrating that bone growth into the constructs was not sufficient to affect mechanical properties at eight weeks, even in constructs for which bone was quantifiable by μ CT.

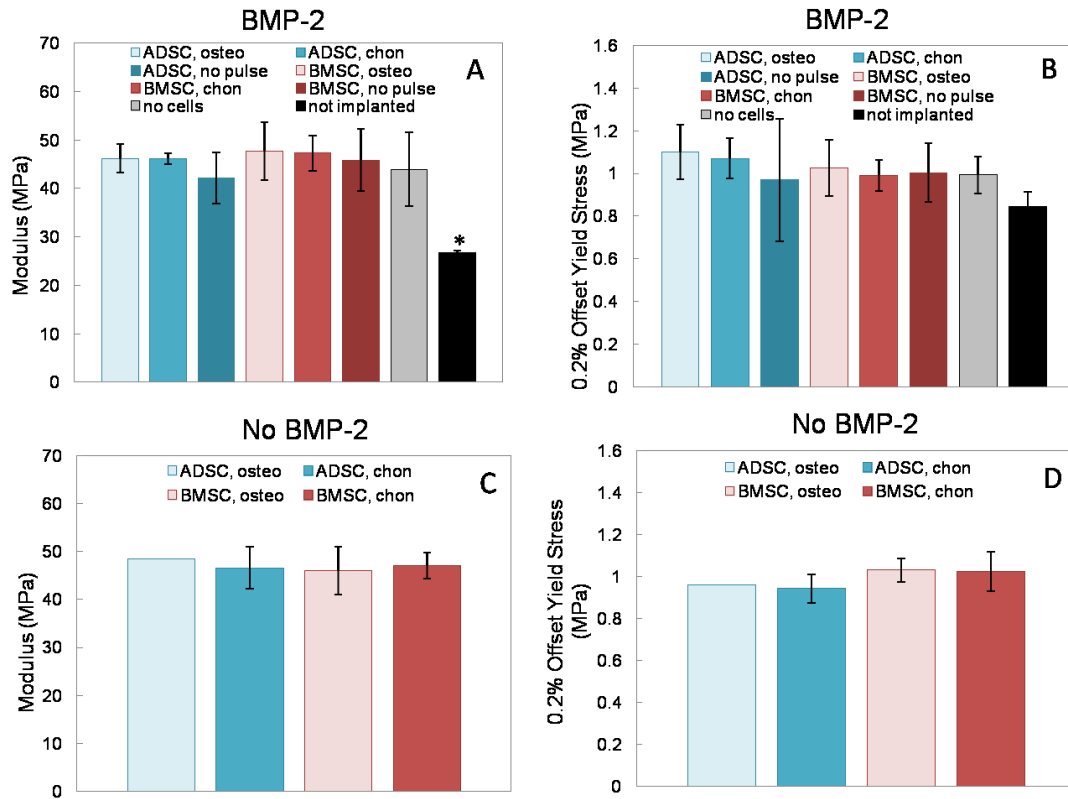


Figure 6.4: Mechanical properties of constructs, evaluated by unconfined compression testing. Panels A and C display modulus values for constructs with and without BMP-2, respectively. Panels B and D display 0.2% offset yield values for constructs with and without BMP-2, respectively. * $p < 0.05$ compared to all other groups.

6.4 Discussion

The ability to control and predict bone growth responses in a tissue engineering environment is imperative for translating research findings into reliable clinical products. The complexity introduced by the combination of multipotent stem cells with chemically-conjugated growth factors necessitates a rigorous examination of each factor in turn. This was the first time that the bone growth response of ADSC and BMSC was directly compared using this particular scaffolding system. The results showed a clear distinction between ADSC that received *in vitro* osteogenic supplements versus those that did not,

but no such difference between cells exposed to rhBMP-2 and cells that were not exposed to rhBMP-2. This suggests that the pre-culture with soluble osteogenic supplements was imperative for inducing bone growth in ADSC-seeded constructs. Constructs conjugated with rhBMP-2 and not seeded with cells grew the same amount of bone as constructs with osteogenically pulsed ADSC, but the bone was not evenly distributed throughout the scaffold like it was for ADSC constructs. This difference in bone tissue distribution may have been due to the pre-differentiation period that enabled the ADSC to settle into the scaffold environment, positioning them well for growing bone along the scaffold pores. In contrast, host fibroblasts were likely responsible for generating the bone seen on constructs that only had rhBMP-2. These cells would not have been encapsulated in the fibrin gel and would have had to penetrate from the surrounding tissue area into the scaffold pore area, giving them more freedom to exist anywhere within the scaffold space. This difference in tissue distribution has not been previously illuminated and is reason to further investigate ADSC as good candidates for bone regeneration.

The osteogenic effects of BMPs have been studied heavily since Marshall Urist first coined the term “bone morphogenetic protein” after observing bone growth following intramuscular implantation of demineralized bone matrix [39]. Subsequent publications detailed the isolation of BMPs from bone matrix [40] and their bone healing capacity [7, 40]. Specifically, BMP-2 garnered attention for inducing *in vivo* bone growth in cranial [41, 42] and segmental [43] defects. BMP-2’s specific osteogenic effect on osteoblastic and pre-osteoblastic cells has also been studied [44], as has its effect on multipotent cells from various sources [45], including BMSC [46]. It has been suggested that BMSCs are particularly sensitive to BMPs, including BMP-2, perhaps more sensitive

than mesenchymal cells from any other location in the body [47]. This claim has been substantiated in many *in vitro* studies utilizing BMSC and BMP-2 [48, 49], and *in vivo* where BMSC showed bone growth capacity in subcutaneous [14, 50, 51] and orthotopic [19, 30, 52] sites.

The results of the study presented here show negligible bone growth for BMSC, even those pre-differentiated *in vitro* and/or seeded onto rhBMP-2-conjugated scaffolds. There are several explanations for this behavior. The osteogenic capacity of BMSC varies considerably between donors and can lead to lack of bone growth despite promising *in vitro* results [21]. This variability has also led to inconsistencies between different *in vitro* experiments [53]. The mode of rhBMP-2 delivery is also a significant factor to consider. The covalent conjugation method used here may be impacting the BMSC's ability to interact with cellular receptors. It is possible that the rhBMP-2 is too tightly bound, negatively impacting its bioavailability. sulfo-SMCC typically links to an amine group on one entity and a sulfhydryl group on the other entity. However, since dimerized rhBMP-2 has no free sulfhydryl-containing cysteine groups, sulfo-SMCC used in this system links amines on PCL with amines on rhBMP-2. Growth factors like rhBMP-2 contain primary amines at the N-terminus and on lysine residues, but the crosslinker cannot differentiate between them and is free to interact with any free amine groups. This lack of specificity may stimulate the protein to adopt a configuration that blocks cells from interacting with its active site. The subcutaneous model used in this study could also be affecting the BMSC bone regeneration response. While constructs implanted in a defect site are exposed to factors that induce bone growth, including stem cells that migrate to the site

and osteogenic factors that are released during the bone healing response, a subcutaneous implant site does not provide these advantageous stimulants.

There was measurable bone growth when ADSC-seeded constructs were used in this study, but the results suggest that the conjugated-rhBMP-2 had little effect on this response. ADSC pulsed with osteogenic medium *in vitro* prior to implantation produced more bone than any of the BMSC groups. The presence of rhBMP-2 did not significantly influence bone growth in osteopulsed ADSC and failed to produce a significant bone growth response in any of the other cell-seeded constructs. Osteogenically pulsing ADSC has repeatedly been shown to improve their ability to make bone [11, 12], which is in accordance with the findings reported here. rhBMP-2 has also been shown to positively affect bone growth by ADSC [54, 55], but interpretation of such results may be hindered by the lack of appropriate controls. Only a few studies have compared bone growth by ADSC and rhBMP-2 to bone growth by rhBMP-2 alone, and these studies indicated no significant difference between the two groups [17, 56, 57], which is an agreement with the results presented here. The mixed results reported in the literature concerning the effects of osteogenic medium versus rhBMP-2 on *in vivo* bone growth by human mesenchymal stem cells are what initially prompted this study. As mentioned previously, one possible reason for the minimal cellular response to conjugated rhBMP-2 is that the rhBMP-2 was in an inactive form on the scaffold. Regardless of this possibility, we did observe bone growth for constructs containing only rhBMP-2 and previous work has shown bone growth and upregulation of osteogenic markers when using sulfo-SMCC to tether rhBMP-2 to materials [6, 37, 58, 59]. This suggests that the rhBMP-2 was released

from the scaffold at some point during the 8-week *in vivo* period and became available for cellular interaction.

This study presented no quantitative difference in total bone volume generated by ADSC-seeded constructs and constructs with rhBMP-2 alone, but the pattern of bone distribution throughout the scaffolds differed substantially between the two groups. Micro-CT images of ADSC-seeded constructs show mineralization that is localized to the contours of the scaffold pores. This mineralization was not only localized to the pores but was also evenly distributed throughout the scaffold. This is suggestive of bone formation by the ADSC themselves as opposed to recruited host cells, although probing for human-specific nuclear markers could prove this definitively. The same pattern is seen regardless of rhBMP-2's presence, which suggests that the combination of osteogenic medium and fibrin gel used for cell seeding retained the cells within the scaffold area and led to localized bone growth. Mineralized tissue that is evenly distributed may positively affect the mechanical properties of the construct by uniformly supporting the entire construct. Although bone volumes obtained in this study were too low to show an effect on mechanical properties, additional studies, perhaps in an orthotopic site where bone may grow more readily, could prove this point. A more uniform bone distribution resulting from scaffold-directed tissue growth may be particularly advantageous for reconstructing anatomically complex architectures [60].

Scaffolds containing only conjugated rhBMP-2 and no pre-seeded cells showed mineralization within the pore spaces and adjacent to the scaffold surface, but the tissue did not follow the scaffold pore contours like tissue generated in ADSC-seeded constructs. Instead, the bone for these constructs grew in dense nodules, randomly

distributed throughout the scaffold. Bone growth for these constructs was most likely due to fibroblasts infiltrating the scaffold area and responding to the rhBMP-2. While there was no significant difference in bone volume between ADSC with rhBMP-2 and ADSC without rhBMP-2, suggesting that the rhBMP-2 did not affect these cells' bone generation capacity, the host cells clearly showed a bone growth response to rhBMP-2. Several factors may be contributing to this observation. The animals used in this study were young (4-6 weeks) so their cells may have had more innate differentiation capacity, particularly in response to growth factors. Not only were the ADSC and BMSC older cells from adult donors, they had been passaged up to 5 times before implantation, which has been shown by others to reduce differentiation capacity [20, 61] and which resulted in decreased *in vitro* mineralization in preliminary studies of the ADSC and BMSC used here. The bone generated in scaffolds with only rhBMP-2 did not follow the scaffold contours like the bone in ADSC-seeded constructs. This is probably because the host cells that migrated into the rhBMP-2-only scaffolds were not encapsulated by the fibrin gel and could migrate more freely throughout the scaffold area.

Aside from pinpointing which factors affect bone growth *in vivo*, another important question that persists in the field of tissue engineering is how well *in vitro* results predict *in vivo* outcomes. *In vitro* studies offer a relatively easy, inexpensive way to evaluate a large number of tissue engineering variables including cell type, osteogenic factors and scaffolding system. However, while these studies seem attractive, their utility is not particularly valuable if the trends found *in vitro* do not carry over to even the simplest of *in vivo* models (those using mice and rats). Here, a well-established *in vivo* mouse model was used to collect data on bone growth due to various combinations of

cells, rhBMP-2 and pre-differentiation and determine if there were any consistencies in comparison to the *in vitro* results from Aim II. The results are somewhat mixed. The *in vitro* study indicated that BMSC were actively differentiating, but these cells generated very little bone *in vivo*. Similar behavior was reported previously [21] and may be due to the variability in these cells' innate osteogenic capacity or their inability to interact with the conjugated rhBMP-2, as mentioned above. ADSC pulsed with osteogenic medium mineralized the most of any group *in vitro* and also showed the most bone growth of the cell-seeded constructs *in vivo*. Furthermore, as in the *in vitro* studies, differentiation medium and not rhBMP-2 influenced bone growth the most.

Clearly, some of the *in vivo* results were consistent with *in vitro* findings, but there was also disagreement between the two studies. The lack of bone formation by BMSC was unexpected and not predicted by the *in vitro* results. The osteo-pulsed BMSC showed more signs of osteogenic differentiation *in vitro* than osteo-pulsed ADSC, but ADSC produced bone *in vivo*, while BMSC did not. It was noted in Chapter 5 that the BMSC tended toward expressing chondrogenic versus osteogenic markers *in vitro*, especially in response to conjugated rhBMP-2. The hypothesis was that this could lead to endochondral bone formation *in vivo*. While no bone at all was seen for these groups, it is possible that cartilage growth took place. Future studies should extend the *in vivo* time period and specifically analyze constructs for cartilage post-implantation.

Cellular responses to growth factors are complex, tightly regulated processes and predicting or ensuring a specific response *in vivo* is a challenge. As tissue engineers we attempt to eliminate as many of the unknowns as possible to create a more reliable, predictable environment. One way to do this is to engineer a growth factor delivery

method that helps control the amount and pattern of bone growth. Although the sulfo-SMCC conjugation method used in this thesis was chosen based on previous characterization [6], the generally low bone volumes for all experimental groups call into question the efficacy of this method and prompted a reevaluation of the method's efficacy in Chapter 7. Subsequent studies focus on evaluating the conjugation method's efficiency, release profile and bioactivity in comparison to two other attachment methods.

6.5 Conclusion

Tethering rhBMP-2 onto PCL scaffolds is a promising way to control delivery of the growth factor and promote localized bone growth. Evaluating the response of cells to conjugated rhBMP-2 as well as the influence of additional differentiation factors is important for designing a reliable system that best promotes bone growth. In this study, ADSC-seeded constructs that were pre-differentiated *in vitro* with osteogenic medium and constructs containing only conjugated rhBMP-2 produced the most bone *in vivo*. The presence of rhBMP-2 did not affect bone volumes generated in cell-seeded constructs, but the presence of cells affected the distribution of the bone. This finding suggests that incorporating cells into a scaffold system, as opposed to rhBMP-2 alone, may positively influence directed tissue growth and may lead to more uniform mechanical properties. The overall lower than expected bone volumes and lack of appreciable bone volume for BMSC-seeded constructs suggest that covalent rhBMP-2 conjugated to PCL via sulfo-SMCC may be too tightly bound and consequently, less bioactive. In Aim 4, presented in Chapter 7, the sulfo-SMCC method and two alternative conjugation techniques are discussed and evaluated in more detail in an effort to bring clarity to this issue.

6.6 Acknowledgements

This work was funded by NIAMS AR 053379. Thank you to Sitaram Chivukula for assistance with animal surgeries, cell culture and mechanical testing and to Colleen Flanagan for assistance with μ CT analysis.

6.7 References

- [1] Perri B, Cooper M, Lauryssen C, Anand N. Adverse swelling associated with use of rh-BMP-2 in anterior cervical discectomy and fusion: a case study. *Spine Journal*. 2007;7:235-9.
- [2] Shields LBE, Raque GH, Glassman SD, Campbell M, Vitaz T, Harpring J, et al. Adverse effects associated with high-dose recombinant human bone morphogenetic protein-2 use in anterior cervical spine fusion. *Spine*. 2006;31:542-7.
- [3] Smucker JD, Rhee JM, Singh K, Yoon ST, Heller JG. Increased swelling complications associated with off-label usage of rhBMP-2 in the anterior cervical spine. *Spine*. 2006;31:2813-9.
- [4] Pohl TLM, Boergermann JH, Schwaerzer GK, Knaus P, Cavalcanti-Adam EA. Surface immobilization of bone morphogenetic protein 2 via a self-assembled monolayer formation induces cell differentiation. *Acta Biomaterialia*. 2012;8:772-80.
- [5] Zhao Y, Zhang J, Wang X, Chen B, Xiao Z, Shi C, et al. The osteogenic effect of bone morphogenetic protein-2 on the collagen scaffold conjugated with antibodies. *Journal of Controlled Release*. 2010;141:30-7.
- [6] Zhang HN, Migneco F, Lin CY, Hollister SJ. Chemically-Conjugated Bone Morphogenetic Protein-2 on Three-Dimensional Polycaprolactone Scaffolds Stimulates Osteogenic Activity in Bone Marrow Stromal Cells. *Tissue Engineering Part A*. 2010;16:3441-8.
- [7] Urist MR, Delange RJ, Finerman GAM. Bone Cell Differentiation and Growth Factors. *Science*. 1983;220:680-6.
- [8] Monaco E, Bionaz M, Rodriguez-Zas S, Hurley WL, Wheeler MB. Transcriptomics Comparison between Porcine Adipose and Bone Marrow Mesenchymal Stem Cells during In Vitro Osteogenic and Adipogenic Differentiation. *Plos One*. 2012;7.
- [9] Zuk P, Zhu M, Ashjian P, De Ugartea D, Huang J, Mizuno H, et al. Human adipose tissue is a source of multipotent stem cells. *Molecular Biology of the Cell* 2002. p. 4279-95.
- [10] Ogawa R, Mizuno H, Watanabe A, Migita M, Shimada T, Hyakusoku H. Osteogenic and chondrogenic differentiation by adipose-derived stem cells harvested from GFP transgenic mice. *Biochemical and Biophysical Research Communications*. 2004;313:871-7.
- [11] Dudas JR, Marra KG, Cooper GM, Penascino VM, Mooney MP, Jiang S, et al. The osteogenic potential of adipose-derived stem cells for the repair of rabbit calvarial defects. *Annals of Plastic Surgery*. 2006;56:543-8.

- [12] Yoon E, Dhar S, Chun DE, Gharibjanian NA, Evans GRD. In vivo osteogenic potential of human adipose-derived stem cells/poly lactide-co-glycolic acid constructs for bone regeneration in a rat critical-sized calvarial defect model. *Tissue Engineering*. 2007;13:619-27.
- [13] Levi B, James AW, Nelson ER, Vistnes D, Wu B, Lee M, et al. Human Adipose Derived Stromal Cells Heal Critical Size Mouse Calvarial Defects. *Plos One*. 2010;5.
- [14] Farrell E, Both SK, Odoerfer KI, Koevoet W, Kops N, O'Brien FJ, et al. In-vivo generation of bone via endochondral ossification by in-vitro chondrogenic priming of adult human and rat mesenchymal stem cells. *Bmc Musculoskeletal Disorders*. 2011;12.
- [15] Mesimaki K, Lindroos B, Tornwall J, Mauno J, Lindqvist C, Kontio R, et al. Novel maxillary reconstruction with ectopic bone formation by GMP adipose stem cells. *International Journal of Oral and Maxillofacial Surgery*. 2009;38:201-9.
- [16] Peterson B, Zhang J, Iglesias R, Kabo M, Hedrick M, Benhaim P, et al. Healing of critically sized femoral defects, using genetically modified mesenchymal stem cells from human adipose tissue. *Tissue Engineering*. 2005;11:120-9.
- [17] Chou Y-F, Zuk PA, Chang T-L, Benhaim P, Wu BM. Adipose-Derived stem cells and BMP-2: Part 1. BMP2-treated adipose derived stem cells do not improve repair of segmental femoral defects. *Connective Tissue Research* 2011. p. 109-18.
- [18] Zuk P, Chou Y-F, Mussano F, Benhaim P, Wu BM. Adipose-derived Stem cells and BMP2: Part 2. BMP2 may not influence the osteogenic fate of human adipose-derived stem cells. *Connective Tissue Research*. 2011;52:119-32.
- [19] Tsuchida H, Hashimoto J, Crawford E, Manske P, Lou J. Engineered allogeneic mesenchymal stem cells repair femoral segmental defect in rats. *Journal of Orthopaedic Research*. 2003;21:44-53.
- [20] Hoemann CD, El-Gabalawy H, McKee MD. In vitro osteogenesis assays: Influence of the primary cell source on alkaline phosphatase activity and mineralization. *Pathologie Biologie*. 2009;57:318-23.
- [21] Mendes SC, Tibbe JM, Veenhof M, Both S, Oner FC, van Blitterswijk CA, et al. Relation between in vitro and in vivo osteogenic potential of cultured human bone marrow stromal cells. *Journal of Materials Science-Materials in Medicine*. 2004;15:1123-8.
- [22] Schek RM, Wilke EN, Hollister SJ, Krebsbach PH. Combined use of designed scaffolds and adenoviral gene therapy for skeletal tissue engineering. *Biomaterials*. 2006;27:1160-6.
- [23] Mitsak AG, Kemppainen JM, Harris MT, Hollister SJ. Effect of Polycaprolactone Scaffold Permeability on Bone Regeneration In Vivo. *Tissue Engineering Part A*. 2011;17:1831-9.

- [24] Williams JM, Adewunmi A, Schek RM, Flanagan CL, Krebsbach PH, Feinberg SE, et al. Bone tissue engineering using polycaprolactone scaffolds fabricated via selective laser sintering. *Biomaterials*. 2005;26:4817-27.
- [25] Rainer A, Giannitelli SM, Accoto D, De Porcellinis S, Guglielmelli E, Trombetta M. Load-Adaptive Scaffold Architecturing: A Bioinspired Approach to the Design of Porous Additively Manufactured Scaffolds with Optimized Mechanical Properties. *Annals of Biomedical Engineering*. 2012;40:966-75.
- [26] Sharaf B, Faris CB, Abukawa H, Susarla SM, Vacanti JP, Kaban LB, et al. Three-Dimensionally Printed Polycaprolactone and beta-Tricalcium Phosphate Scaffolds for Bone Tissue Engineering: An In Vitro Study. *Journal of Oral and Maxillofacial Surgery*. 2012;70:647-56.
- [27] Bionaz M, Mkrtschjan M, Kyrouac D, Hollister SJ, Wheeler MB. In Vitro Migration of Adipose-Derived Stem Cells From GFP Pigs Into Polycaprolactone Scaffolds Treated With FGF Or BMP2. *Reproduction Fertility and Development*. 2012;24:219-.
- [28] Jeong CG, Hollister SJ. A comparison of the influence of material on in vitro cartilage tissue engineering with PCL, PGS, and POC 3D scaffold architecture seeded with chondrocytes. *Biomaterials*. 2010;31:4304-12.
- [29] Chong Y-I, Ahn K-M, Jeon S-H, Lee S-Y, Lee J-H, Tae G. Enhanced bone regeneration with BMP-2 loaded functional nanoparticle–hydrogel complex. *Journal of Controlled Release* 2007. p. 91-9.
- [30] Minamide A, Yoshida M, Kawakami M, Okada M, Enyo Y, Hashizume H, et al. The effects of bone morphogenetic protein and basic fibroblast growth factor on cultured mesenchymal stem cells for spine fusion. *Spine*. 2007;32:1067-71.
- [31] Gharibjanian NA, Chua WC, Dhar S, Scholz T, Shibuya TY, Evans GRD, et al. Release Kinetics of Polymer-Bound Bone Morphogenetic Protein-2 and Its Effects on the Osteogenic Expression of MC3T3-E1 Osteoprecursor Cells. *Plastic and Reconstructive Surgery*. 2009;123:1169-77.
- [32] Park YJ, Kim KH, Lee JY, Ku Y, Lee SJ, Min BM, et al. Immobilization of bone morphogenetic protein-2 on a nanofibrous chitosan membrane for enhanced guided bone regeneration. *Biotechnology and Applied Biochemistry*. 2006;43:17-24.
- [33] Liu H-W, Chen C-H, Tsai C-L, Lin IH, Hsiue G-H. Heterobifunctional poly(ethylene glycol)-tethered bone morphogenetic protein-2-stimulated bone marrow mesenchymal stromal cell differentiation and osteogenesis. *Tissue Engineering*. 2007;13:1113-24.
- [34] Dickerman RD, Reynolds AS, Morgan BC, Tompkins J, Cattorini J, Bennett M. rh-BMP-2 can be used safely in the cervical spine: dose and containment are the keys! *Spine Journal*. 2007;7:508-9.

- [35] Liu H-W, Chen C-H, Tsai C-L, Hsiue G-H. Targeted delivery system for juxtacrine signaling growth factor based on rhBMP-2-mediated carrier-protein conjugation. *Bone*. 2006;39:825-36.
- [36] Jeon O, Song SJ, Kang S-W, Putnam AJ, Kim B-S. Enhancement of ectopic bone formation by bone morphogenetic protein-2 released from a heparin-conjugated poly(L-lactic-co-glycolic acid) scaffold. *Biomaterials* 2007. p. 2763-71.
- [37] Jeon O, Song SJ, Yang HS, Bhang S-H, Kang S-W, Sung MA, et al. Long-term delivery enhances in vivo osteogenic efficacy of bone morphogenetic protein-2 compared to short-term delivery. *Biochemical and Biophysical Research Communications*. 2008;369:774-80.
- [38] La W-G, Kang S-W, Yang HS, Bhang SH, Lee SH, Park J-H, et al. The Efficacy of Bone Morphogenetic Protein-2 Depends on Its Mode of Delivery. *Artificial Organs*. 2010;34:1150-3.
- [39] Urist MR. Bone - Formation By Autoinduction. *Science*. 1965;150:893-&.
- [40] Takagi K, Urist MR. THE REACTION OF THE DURA TO BONE MORPHOGENETIC PROTEIN (BMP) IN REPAIR OF SKULL DEFECTS. *Annals of Surgery*. 1982;196:100-9.
- [41] Sato K, Urist MR. Induced Regeneration Of Calvaria By Bone Morphogenetic Protein (BMP) In Dogs. *Clinical Orthopaedics and Related Research*. 1985:301-11.
- [42] Ono I, Gunji H, Kaneko F, Saito T, Kuboki Y. Efficacy of Hydroxyapatite Ceramic as a Carrier for Recombinant Human Bone Morphogenetic Protein. *Journal of Craniofacial Surgery*. 1995;6:238-44.
- [43] Yasko AW, Lane JM, Fellingner EJ, Rosen V, Wozney JM, Wang EA. The Healing of Segmental Bone Defects, Induced by Recombinant Human Bone Morphogenetic Protein (rhBMP-2) - A Radiographic, Histological and Biomechanical Study in Rats. *Journal of Bone and Joint Surgery-American Volume*. 1992;74A:659-70.
- [44] Yamaguchi A, Katagiri T, Ikeda T, Wozney JM, Rosen V, Wang EA, et al. Recombinant Human Bone Morphogenetic Protein-2 Stimulates Osteoblastic Maturation and Inhibits Myogenic Differentiation In Vitro. *Journal of Cell Biology*. 1991;113:681-7.
- [45] Katagiri T, Yamaguchi A, Ikeda T, Yoshiki S, Wozney J, Rosen V, et al. The non-osteogenic mouse pluripotent cell line, C3H10T1/2, is induced to differentiate into osteoblastic cells by recombinant human bone morphogenetic protein-2. *Biochemical and Biophysical Research Communications* 1990. p. 295-9.
- [46] Yamaguchi A, Yokose S, Ikeda T, Katagiri T, Wozney JM, Rosen V, et al. BMP-2 Induces Bone Marrow Stromal Cells to Differentiate into Osteoblasts and Decreases their Capacity to Support Osteoclast Formation. *Journal of Bone and Mineral Research*. 1993;8:S158-S.

- [47] Takagi K, Urist MR. The Role of Bone Marrow in Bone Morphogenetic Protein-Induced Repair of Femoral Massive Diaphyseal Defects. *Clinical Orthopaedics and Related Research*. 1982;224-31.
- [48] Huang WB, Carlsen B, Wulur I, Rudkin G, Ishida K, Wu B, et al. BMP-2 exerts differential effects on differentiation of rabbit bone marrow stromal cells grown in two-dimensional and three-dimensional systems and is required for in vitro bone formation in a PLGA scaffold. *Experimental Cell Research*. 2004;299:325-34.
- [49] Li CM, Vepari C, Jin HJ, Kim HJ, Kaplan DL. Electrospun silk-BMP-2 scaffolds for bone tissue engineering. *Biomaterials*. 2006;27:3115-24.
- [50] Kasten P, Vogel J, Luginbuhl R, Niemeyer P, Tonak M, Lorenz H, et al. Ectopic bone formation associated with mesenchymal stem cells in a resorbable calcium deficient hydroxyapatite carrier. *Biomaterials*. 2005;26:5879-89.
- [51] Kasten P, Vogel J, Luginbuhl R, Niemeyer P, Weiss S, Schneider S, et al. Influence of platelet-rich plasma on osteogenic differentiation of mesenchymal stem cells and ectopic bone formation in calcium phosphate ceramics. *Cells Tissues Organs*. 2006;183:68-79.
- [52] Noel D, Gazit D, Bouquet C, Apparailly F, Bony C, Poncelet P, et al. Short-term BMP-2 expression is sufficient for in vivo osteochondral differentiation of mesenchymal stem cells. *Stem Cells*. 2004;22:74-85.
- [53] van den Dolder J, de Ruijter AJE, Spauwen PHM, Jansen JA. Observations on the effect of BMP-2 on rat bone marrow cells cultured on titanium substrates of different roughness. *Biomaterials*. 2003;24:1853-60.
- [54] Dragoo JL, Choi JY, Lieberman JR, Huang J, Zuk PA, Zhang J, et al. Bone induction by BMP-2 transduced stem cells derived from human fat. *Journal of Orthopedic Research* 2003. p. 622-9.
- [55] Knippenberg M, Helder MN, Doulabi BZ, Wuisman P, Klein-Nulend J. Osteogenesis versus chondrogenesis by BMP-2 and BMP-7 in adipose stem cells. *Biochemical and Biophysical Research Communications*. 2006;342:902-8.
- [56] Zuk P, Chou Y, Mussano F, Benhaim P, Wu B. Adipose derived stem cells and BMP-2: Part 2. BMP-2 may not influence the osteogenic fate of human adipose-derived stem cells. *Connective Tissue Research* 2011. p. 119-32.
- [57] Yamagiwa H, Endo N, Tokunaga K, Hayami T, Hatano H, Takahashi HE. In vivo bone-forming capacity of human bone marrow-derived stromal cells is stimulated by recombinant human bone morphogenetic protein-2. *Journal of Bone and Mineral Metabolism*. 2001;19:20-8.

[58] Koo K, Yeo D, Ahn J, Kim B-S, Kim C-S, Im G-I. Lumbar posterolateral fusion using heparin-conjugated fibrin for sustained delivery of BMP2 in a rabbit model. *Artificial Organs*2012.

[59] Zhang Q, He Q-F, Zhang T-H, Yu X-L, Liu Q, Deng F. Improvement in the delivery system of bone morphogenetic protein-2: a new approach to promote bone formation. *Biomedical Materials*2012.

[60] Hollister SJ, Lin CY, Saito E, Schek RD, Taboas JM, Williams JM, et al. Engineering craniofacial scaffolds. *Orthodontics & craniofacial research*. 2005;8:162-73.

[61] Kretlow JD, Jin YQ, Liu W, Zhang WJ, Hong TH, Zhou GD, et al. Donor age and cell passage affects differentiation potential of murine bone marrow-derived stem cells. *Bmc Cell Biology*. 2008;9.

CHAPTER 7 Evaluating Three Methods of Attaching rhBMP-2 to Polycaprolactone Scaffolds

7.1 Introduction

Tethering recombinant human bone morphogenetic protein-2 (rhBMP-2) to polymer scaffolds may address problems with current attachment methods that require high amounts of rhBMP-2 and can result in uncontrolled protein delivery. Throughout this thesis, the chemical crosslinker, sulfosuccinimidyl-4-(N-maleimidomethyl)cyclohexane-1-carboxylate (sulfo-SMCC) has been used to covalently attach rhBMP-2 to PCL, a technique chosen based on previous characterization and demonstration of osteogenesis in rat mesenchymal stem cells [1]. However, while performing experiments for this thesis, issues with the previously used research methods were found. This discovery along with lower than anticipated bone volumes measured in Aim III were motivation to revisit the characterization of the sulfo-SMCC conjugation method. This Chapter presents conjugation efficiency, release profile and bioactivity analysis of the sulfo-SMCC conjugation method compared to heparin conjugation and physical adsorption, which are two other techniques for incorporating rhBMP-2 onto PCL.

The simplest method of attaching a growth factor to a scaffold is through physical adsorption, achieved by soaking the scaffold in an aqueous solution of the growth factor. Attachment is facilitated by electrostatic interactions between the scaffold material and

the growth factor. This method has been used to attach rhBMP-2 to a number of biologic and biomaterial substrates [1-6]. Its simplicity is attractive from a clinical standpoint, but compared to other methods of growth factor attachment, adsorption has been associated with lower bone volume [6], initial burst release of protein [7] and poor growth factor retention over time [4]. It is important to consider that many of the drawbacks associated with adsorption are specific for the material to which the rhBMP-2 is attached and generalizations about the adsorption method do not necessarily apply to all systems. Furthermore, in choosing an rhBMP-2 conjugation method, the potential drawbacks of adsorption should be balanced with the advantages it has over other conjugation methods, including reductions in cost, time, and protocol complexity. Nonetheless, new methods of growth factor conjugation have been developed to address shortcomings of the physical adsorption method.

Alternative methods of incorporating rhBMP-2 into tissue engineering systems range from gel encapsulation [8-10] to covalent linkage to scaffolds [4, 11-13]. Covalent conjugation involves using a chemical crosslinker that forms covalent bonds with functional groups on the scaffold material and functional groups on the growth factor. The motivation for using such methods is to create a very strong bond that is not hydrolysable so that the rhBMP-2 is only released when the scaffold material degrades. This retains the rhBMP-2 on the scaffold so that cells can continuously interact with it, localizing bone growth to the scaffold area and preventing uncontrolled diffusion of the rhBMP-2 to areas where bone growth is not desired. sulfo-SMCC is a water-soluble, heterobifunctional, amine to sulfhydryl cross linker that contains NHS-ester and maleimide reactive groups at opposite ends of a medium-length cyclohexane spacer arm

[14]. It has been used to link rhBMP-2 or peptides to aminolysed chitosan [4], collagen [15, 16] and PCL [1, 17], with positive bone growth and/or osteogenesis reported in all studies. Despite these positive results, when sulfo-SMCC was used with aminated PCL scaffolds in Chapter 6 (Aim III) of this thesis, little bone grew, which raised questions concerning a) the effectiveness of the rhBMP-2 conjugation, and b) the sulfo-SMCC-conjugated rhBMP-2's ability to stimulate bone growth. It is possible that the bioactivity of the rhBMP-2 could have been affected by the conjugation method, a concern that has been cited by others attempting chemical conjugation [13].

Heparin conjugation is another popular method that has been used to conjugate rhBMP-2 to materials. After heparin is covalently linked to a scaffold material using carbodiimide chemistry [18], it binds to rhBMP-2 through interaction of its acidic sulfate groups with basic residues of rhBMP-2's N-terminal heparin binding domain [19]. This specificity improves the bonding strength to slow release, orients the rhBMP-2 in a regular pattern and protects it from degradation to help retain rhBMP-2 activity [20], characteristics that do not occur when rhBMP-2 is simply adsorbed to a material. rhBMP-2 has been tethered via heparin to poly(l-lactic-co-glycolic acid) [18, 21, 22] and fibrin [23, 24]. Heparin conjugation accommodates attachment of many different growth factors, since conjugation is through electrostatic interactions and many growth factors contain specific heparin binding sites [20, 25, 26]. This capability could enable attachment of multiple growth factors to a single substrate. In this study, the heparin conjugation method was compared to sulfo-SMCC in terms of conjugation efficiency, release and alkaline phosphatase (ALP) production.

Growth factor conjugation methods are characterized by their ability to capture and retain growth factor on the scaffold and ability to promote a biologic response. Conjugation efficiency (also known as loading efficiency) refers to the percentage of the initial rhBMP-2 in solution that is successfully conjugated to the scaffold and can be quantified by ELISA or using a gamma radiation counter (if I¹²⁵-labeled rhBMP-2 is used) [7]. Release of the growth factor over time is also measured using these methods. Release is important to consider since one theory of conjugation involves retaining growth factor on the scaffold for an extended period of time to promote localized bone growth. The caveat to retaining rhBMP-2 on the scaffold is that the attached rhBMP-2 may not be bioactive [27, 28], in which case release of the growth factor is imperative for inducing a bone growth response. The burst release associated with adsorption may necessitate using a greater amount of rhBMP-2 initially. When large quantities of rhBMP-2 are used clinically, diffusion of released rhBMP-2 can lead to unwanted bone growth far from the defect site [29], which is why controlled delivery of lower doses is desired. Chemical conjugation techniques can control release to prevent this burst release.

A common metric used to evaluate the biological activity of conjugated rhBMP-2 is production of alkaline phosphatase (ALP), since many cell types have been shown to produce ALP during osteogenesis in response to rhBMP-2. Specifically, C2C12 myoblasts reliably produce ALP as they commit to the osteogenic lineage in response to rhBMP-2 [30]. Although we are ultimately interested in the response of ADSC and BMSC to rhBMP-2, these cells do not always behave in a straight forward manner and were thus not ideal for evaluating bioactivity of conjugated rhBMP-2. The C2C12 model

was chosen for these studies because it has been used extensively by others as an initial screening of rhBMP-2 bioactivity [11, 15].

In the study presented here, three conjugation methods – adsorption, sulfo-SMC and heparin – are employed to tether rhBMP-2 to PCL. Conjugation efficiency, release and biological activity via ALP production were analyzed in an effort to reevaluate the sulfo-SMCC conjugation method and compare its characteristics to those of two other popular growth factor conjugation techniques.

7.2 Materials and Methods

7.2.1 PCL Construct Manufacturing

PCL discs (2 cm² surface area) and cylindrical scaffolds (6.35 mm diameter, 4 mm height) with 2.15 mm spherical pores (see design complete specifications in Chapter 5) were manufactured of PCL by selective laser sintering (SLS) and are shown in Figure 1. Prior to sterilization, excess powder was blown off of the constructs and they were sonicated in 70% ethanol to remove any remaining un-sintered PCL.

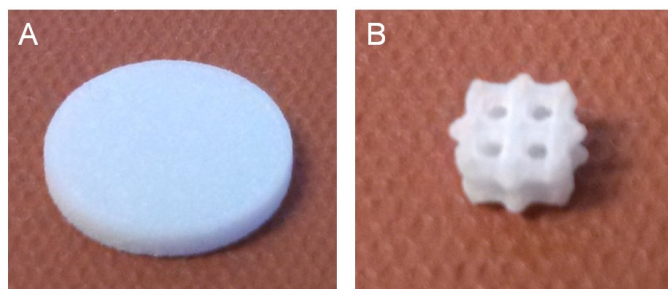


Figure 7.1: SLS-manufactured PCL disc (A) and porous scaffold (B).

7.2.2 rhBMP-2 Conjugation to PCL via Adsorption

For comparison of the three conjugation methods, 1 µg rhBMP-2 (Genscript, Inc., Piscataway, NJ) was attached to PCL discs. For reevaluation of previous characterization

of PCL scaffolds, 20 µg rhBMP-2 was used. For adsorption, discs or scaffolds were washed twice (20 minutes each) with “activation buffer” (BuPH phosphate buffered saline, Pierce, Thermo Scientific, Rockford, IL) and once with “conjugation buffer” (activation buffer with 0.1M EDTA). Constructs were placed in ultra-low-attachment culture plates (Corning, Tewksbury, MA) and 1 µg (discs) or 20 µg (scaffolds) rhBMP-2 in conjugation buffer was added. Constructs were incubated with rhBMP-2 for 18 hours at 4°C with gentle shaking. After the incubation with rhBMP-2, scaffolds were washed three times in deionized, distilled water (ddH₂O) and dried under vacuum for 24 hours.

7.2.3 rhBMP-2 Conjugation to PCL via sulfo-SMCC

For rhBMP-2 conjugation to PCL discs and scaffolds using the crosslinker sulfosuccinimidyl-4-(N-maleimidomethyl)cyclohexane-1-carboxylate (sulfo-SMCC, Pierce, Thermo Scientific, Rockford, IL), amine groups were first introduced onto the surface of the constructs by submerging the scaffolds in a 10% w/v solution of 1,6-hexanediamine in isopropanol under vacuum for 1 hour at 37°C. Constructs were then thoroughly washed in ddH₂O and dried under vacuum for 24 hours. For sulfo-SMCC conjugation, scaffolds were washed at room temperature in activation buffer (BuPH phosphate buffered saline, Pierce, Thermo Scientific, Rockford, IL) three times, under vacuum for 20 minutes each. A 4 mg/ml solution of sulfo-SMCC in activation buffer was then added to each scaffold for 1 hour, under vacuum at room temperature. Scaffolds were then washed twice in activation buffer and once in conjugation buffer (activation buffer containing 0.1M EDTA). A 50 µg/ml solution of rhBMP-2 in conjugation buffer (400 µl total volume) was then added to the scaffolds in an ultra low-attachment plate (Corning, Inc.) for 18 hours at 4°C with gentle shaking. After the incubation with

rhBMP-2, scaffolds were washed three times in ddH₂O and dried under vacuum for 24 hours. Figure 3.2 in Chapter 3 shows a schematic of this conjugation method.

7.2.4 *rhBMP-2 Conjugation to PCL via Heparin*

PCL discs were conjugated with rhBMP-2 using the heparin method, for comparison to the sulfo-SMCC and adsorption methods. Amine groups were introduced onto the discs as described above and the discs were then washed twice (20 minutes each) with PBS (-MgCl₂, -CaCl₂, Gibco) and once (15 minutes) with 2-(N-morpholino)ethanesulfonic acid (MES) buffer (Thermo Scientific, Rockford, IL). Heparin (10 mg/ml), 1-Ethyl-3-[3-dimethylaminopropyl]carbodiimide hydrochloride (EDC, 4 mg/ml) and sulfo-(N-hydroxysulfosuccinimide) (NHS, 11 mg/ml) were dissolved in MES buffer and reacted for 15 minutes. 2-mercaptoethanol (14 µl/ml) was added to quench the reaction and the pH was adjusted to 7.2-7.5. For heparin activation of the amine-functionalized discs, 0.5 ml of the 10 mg/ml heparin solution was added to each disc and left to react for 20-24 hours at room temperature. Following washing in deionized water, 1 µg rhBMP-2 in Dulbecco's Phosphate Buffered Saline (DPBS, Gibco) was added to each disc for 2 hours under vacuum at room temperature. Constructs were then washed and dried as described above. Figures 3.3b and 3.3c in Chapter 3 are visual representations of heparin activation and conjugation to a polymer, respectively.

7.2.5 *Conjugation Efficiency of Various Conjugation Methods*

Conjugation efficiency was determined for rhBMP-2 attached to discs using the sulfo-SMCC, heparin and adsorption methods and for rhBMP-2 attached to scaffolds via sulfo-SMCC and adsorption. An enzyme linked immunosorbent assay (ELISA) with an anti-BMP-2 antibody specific for *e. coli*-derived rhBMP-2 (Peprotech, Inc., Rocky Hill,

NJ) was used to measure the amount of rhBMP-2 initially added to each construct and the amount washed off in the three washes immediately following the conjugation/adsorption period. ELISA plates were coated with capture antibody overnight at room temperature, washed four times, blocked with 1% BSA and then washed again. Samples were appropriately diluted in Dulbecco's phosphate buffered saline (DPBS, Gibco, Inc., Grand Island, NY), added to the plate in triplicate along with rhBMP-2 standard, and the plates were incubated at room temperature for two hours. Plates were then washed, incubated with biotinylated detection antibody for two hours, washed again and incubated with avidin peroxidase for 30 minutes. After a final wash, 2,2'-Azino-bis(3-ethylbenzothiazoline-6-sulfonic acid) liquid substrate (Sigma-Aldrich Corp., St. Louis, MO) was added to produce the color change. Plates were read at 405 nm and 650 nm. For wavelength correction, optical density values at 650 nm were subtracted from those at 405 nm. rhBMP-2 concentration was determined from a logarithmic standard curve determined from standards. The amount of rhBMP-2 conjugated or adsorbed to the scaffold was calculated as the amount initially in the conjugation solution minus the amount washed off following the conjugation period.

7.2.6 Release of rhBMP-2 from PCL Constructs

Following conjugation or adsorption, constructs (N=3 per group) were placed in ultra low-attachment dishes and 1 ml of DPBS (Gibco, Inc., Grand Island, NY) was added. Plates were incubated at 37°C with gentle shaking. On days 1, 3, 7, 10 and 14 the DPBS was removed and frozen for later assessment by ELISA. The removed DPBS was replaced with fresh DPBS. ELISA was performed (as described above) on collected samples to determine the amount of rhBMP-2 that was released at each time point.

7.2.7 *C2C12 Myoblast Seeding for Alkaline Phosphatase Assays*

C2C12 cells were a generous gift of the Krebsbach lab. Cells were expanded in monolayer in growth medium consisting of high glucose Dulbecco's Modified Eagle Medium (DMEM), 10% fetal bovine serum (FBS) and 1% penicillin/streptomycin (all reagents from Gibco). When approximately 80% confluency was reached, cells were trypsinized (0.25% trypsin, Gibco) and then seeded at a density of 40,000 cells per disc. There were eight groups (N=4 per group): 1) PCL only, 2) PCL with adsorbed rhBMP-2, 3) amine-functionalized PCL with sulfo-SMCC conjugated, 4) amine-functionalized PCL with sulfo-SMCC-conjugated rhBMP-2, 5) amine-functionalized PCL with heparin conjugated, 6) amine-functionalized PCL with heparin-conjugated rhBMP-2, 7) tissue culture polystyrene (TCPS), and 8) TCPS with 1 µg/ml rhBMP-2 added to the culture medium. Constructs were maintained in growth medium for 3 days and then ALP production was analyzed.

7.2.8 *Alkaline Phosphatase Production of C2C12 Myoblasts Cultured on PCL Discs*

The ALP response of C2C12 cells was used to assess the bioactivity of rhBMP-2 conjugated to PCL discs. A quantitative assay was used to quantify ALP production, which was then normalized to total protein. After three days in culture, cells were removed from discs with 500 µl lysis buffer containing 10mM Tris Buffer, 0.2% IGEPAL (Sigma-Aldrich), and 2mM Phenylmethanesulfonyl fluoride (PMSF, Sigma-Aldrich) in ethanol, and frozen at -80°C until analysis. For ALP quantification, samples underwent three freeze (-80°C)/thaw (37°C) cycles to disrupt cell membranes. The samples were centrifuged (10,000 rpm, 10 minutes) and the supernatant was transferred to a new tube. The stock ALP standard solution consisted of 80 µl p-Nitrophenol solution

(Sigma-Aldrich) in 3.92. 0.02 N NaOH. Serial dilutions of the stock ALP standard were prepared to give seven standards ranging in concentration from 200 nM/ml to 0 nM/ml. The ALP stock solution consisted of one ALP substrate tablet (Sigma-Aldrich) dissolved in 5 ml deionized water. To make the ALP working solution, 4 ml of ALP stock solution was added to 4 ml of alkaline buffer solution (Sigma-Aldrich). Standards (200 µl) were added to a 96-well plate in triplicate along with 20 µl of each sample, in triplicate. 100 µl of ALP working solution was added to each sample well and the plate was incubated at 37°C with monitoring every 5 minutes until a color change occurred. 80 µl of 0.02 NaOH was added to each sample well to stop the reaction and the plate was read at 405 nm using a spectrophotometer (Thermo Multiskan Spectrum, Thermo Scientific, Inc.). Results are reported as ALP content per time per protein content.

7.2.9 Total Protein Quantification

Total protein was quantified using a BCA Protein Assay (Pierce, Thermo Scientific, Inc.) per the manufacturer's instructions. Protein was analyzed immediately following ALP quantification. Samples and bovine serum albumin standards were added in triplicate (25 µl) to a 96 well plate followed by 200 µl of BCA working reagent. The plate was incubated for 30 minutes at 37°C, cooled to room temperature and the absorbance was read at 562 nm.

7.2.10 Alkaline Phosphatase Staining of C2C12 Myoblasts Cultured on PCL Disc

In addition to quantifying ALP, discs were stained for ALP to visualize ALP generated by C2C12 cells. Following culture for 3 days, constructs were fixed in zinc-buffered formalin (Z-Fix, Anatech, Ltd., Battle Creek, MI) for 15 minutes and then

washed three times with DPBS. Discs were dried in air at room temperature for four hours and then frozen at -80°C. An ALP staining kit (Sigma-Aldrich) was used following the manufacturer's instructions with volumes adjusted for staining directly in 24-well culture dishes. Discs were counterstained with hematoxylin for viewing cell nuclei. Images of stained cells on discs were obtained at the Michigan Microscopy and Image Analysis Laboratory using a Leica DMIRB inverted microscope (Leica Microsystems, Buffalo Grove, IL).

7.2.11 Statistics

SPSS (IBM, New York, NY) statistical software was used to perform one-way ANOVA for determining significance between groups.

7.3 Results

7.3.1 BMP-2 Conjugation Efficiency and Release from Discs – Comparison of Three Conjugation Methods

PCL discs were used to compare the three rhBMP-2 attachment methods because they reduced complexity associated with a porous structure and facilitated cell culture without the need for a cell-encapsulation agent. Conjugation efficiency is displayed in Figure 2. Significantly less rhBMP-2 was attached to discs using adsorption compared to both the sulfo-SMCC and heparin methods. There was no difference in conjugation efficiency between adsorption and heparin, although the heparin trended toward greater efficiency than adsorption. Conjugation by sulfo-SMCC was nearly 99% effective with very little variability. Variability for adsorption was highest of the three methods.

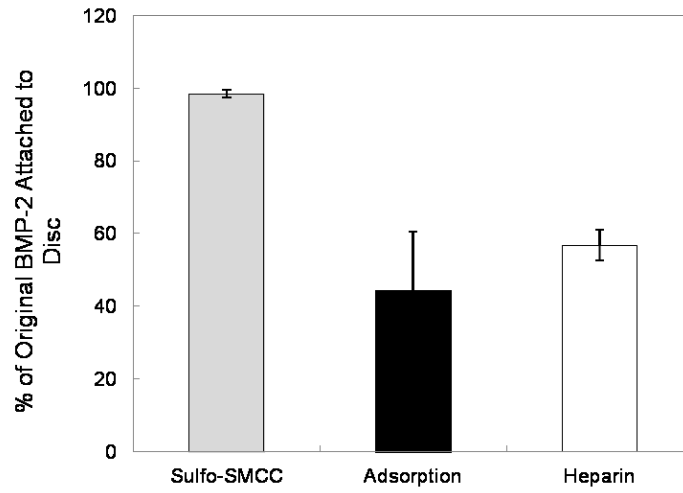


Figure 7.2: rhBMP-2 conjugation efficiency.

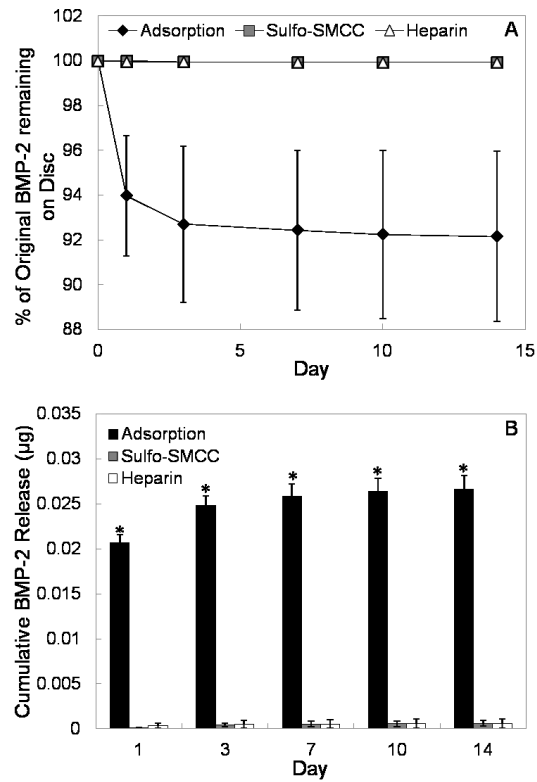


Figure 7.3: rhBMP-2 release from discs. A. Percent of initial rhBMP-2 remaining on discs over 14 days. B. Cumulative release over 14 days. * $p < 0.05$ versus other groups at each time point.

The release of conjugated rhBMP-2 over 14 days was also analyzed for each of the three attachment methods. The results are shown in Figure 3. The most dramatic release was observed for adsorption, with an average of 6% (0.02 μg) of the initially loaded rhBMP-2 released from adsorbed discs by Day 1. By Day 14, $92.16 \pm 3.81\%$ of the originally adsorbed rhBMP-2 remained on the discs. Both the sulfo-SMCC and heparin methods showed very little release over the course of the 14 day release period. This was expected for the sulfo-SMCC method since the sulfo-SMCC covalently bonds rhBMP-2 to PCL and release should only occur as the polymer degrades, which does not occur over a time period as short as 14 days.

7.3.2 BMP-2 Conjugation Efficiency and Release from Scaffolds

To confirm that the PCL scaffolds used in Aims II and III had been successfully conjugated with rhBMP-2 using sulfo-SMCC, the amount of rhBMP-2 conjugated to scaffolds using this method was quantified. Attachment via adsorption was also analyzed since it had been previously reported that conjugation with sulfo-SMCC yielded better results. Conjugation efficiency and release over 14 days were evaluated to compare the two attachment methods and these results are shown in Figure 4. Two conjugation efficiency experiments were performed to confirm reliability of the conjugation and ELISA procedures.

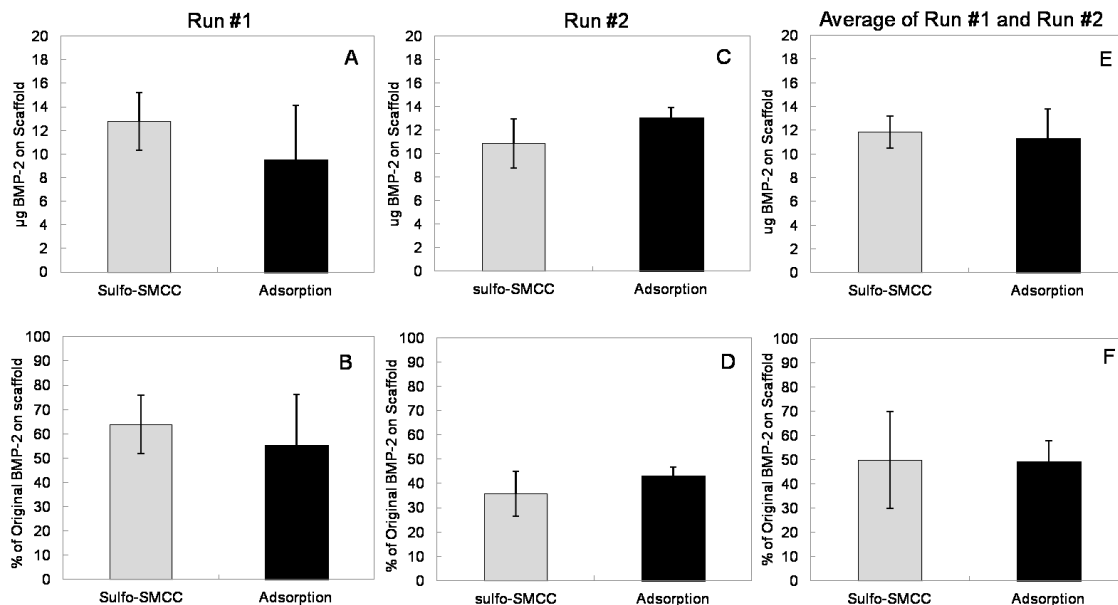


Figure 7.4: rhBMP-2 conjugation efficiency for PCL scaffolds. A and B display absolute and % of original BMP-2, respectively, for experiment 1, while C and D display these values for experiment 2. E and F display average values of the two experiments, absolute amount of BMP-2 in E and % of original BMP-2 in F.

The average conjugation efficiency was 49.78 ± 19.89 % for the sulfo-SMCC method (total N=6, N=3 for each of two separate experiments) and 49.10 ± 8.72 % for the adsorption method (total N=6, N=3 for each of two separate experiments). These values suggest little difference in conjugation efficiency between the two methods over the 18 hour conjugation/adsorption time period. The release profiles for the two methods appear

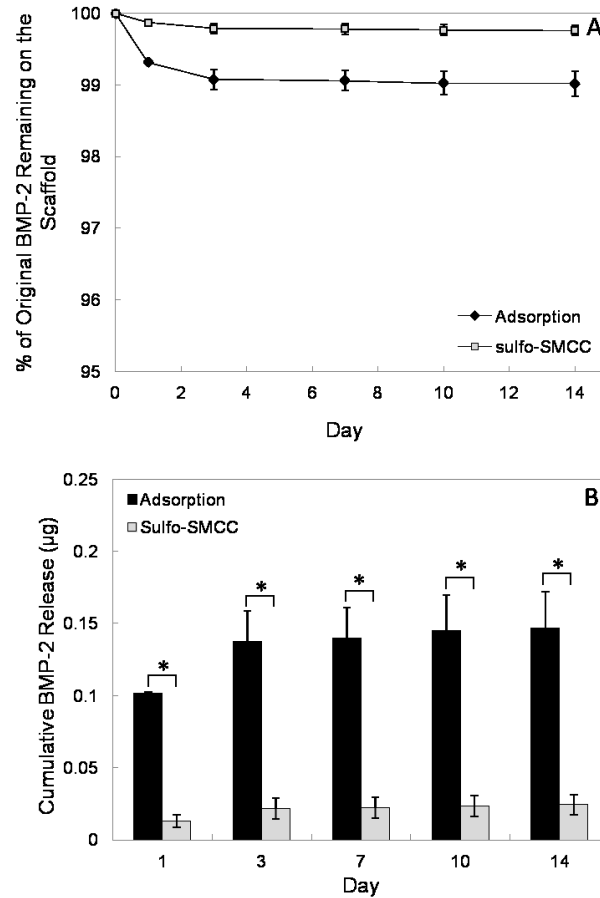


Figure 7.5: rhBMP-2 release from scaffolds. A. Percent of initial rhBMP-2 remaining on scaffolds over 14 days. B. Cumulative release over 14 days. * $p < 0.05$.

in Figure 5. Significant release occurred over days 1 and 3 for the adsorption method, but did not occur for rhBMP-2 conjugated using sulfo-SMCC. Furthermore, the cumulative release of rhBMP-2 from adsorbed scaffolds is significantly greater than from sulfo-SMCC-conjugated scaffolds at each time point. These data demonstrate that although similar conjugation efficiencies are obtained with either method, rhBMP-2 conjugated via sulfo-SMCC is bound more tightly to the scaffold, preventing initial release and resulting in less release over the fourteen days compared to adsorption. It should be noted that even with the adsorption method, 99% of the rhBMP-2 still remains on the scaffold after 14

days, which is much higher than any other reports of rhBMP-2 conjugation in the literature, as will be discussed later.

7.3.3 *Alkaline Phosphatase Production*

Alkaline phosphatase (ALP) production by C2C12 cells seeded on PCL discs was measured and is reported as ALP activity per micrograms protein per minute in Figure 6. The same experimental groups analyzed for conjugation efficiency and release (PCL/adsorbed BMP-2, PCL/sulfo-SMCC-conjugated BMP-2, PCL/heparin-conjugated BMP-2) were analyzed for ALP content. Negative controls for each condition consisted of the substrate material minus rhBMP-2 for each condition. A positive control consisted of unmodified PCL discs seeded with C2C12 cells and exposed to soluble rhBMP-2. Only two groups supported ALP production in response to rhBMP-2 and those were rhBMP-2 adsorbed on PCL and PCL plus soluble rhBMP-2. The results proved that the C2C12 cells were capable of producing ALP in response to rhBMP-2. The lack of ALP for the sulfo-SMCC- and heparin-conjugated rhBMP-2 suggests that even though the cells were exposed to the attached rhBMP-2, they were not able to interact with the growth factor in such a way that supported ALP production.

7.3.4 *Alkalkine Phosphatase Staining*

Discs were stained for ALP using a solution of naphthol AS-BI phosphate and fast red violet LB salt, which results in red staining of active ALP. Prior to applying the hematoxylin counterstain, intense red staining was evident for discs that had adsorbed rhBMP-2 (data not shown). This red staining did not appear for any other group,

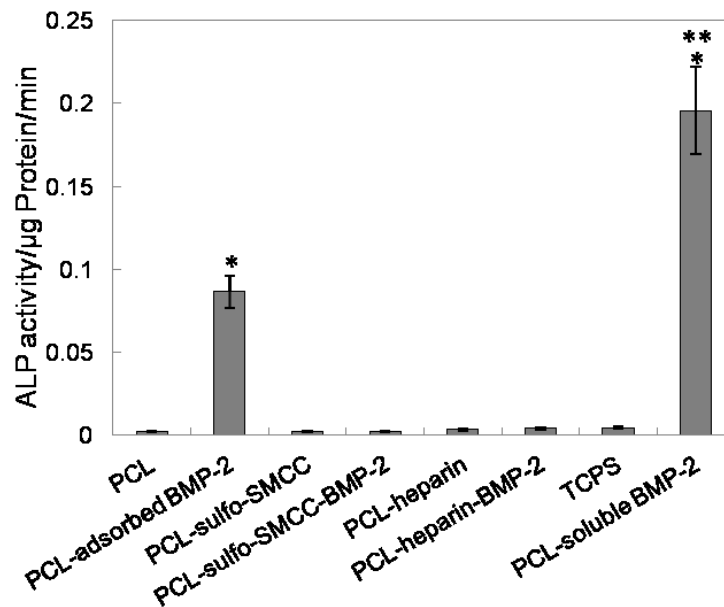


Figure 7.6: Alkaline phosphatase content. * $p < 0.05$ versus PCL, PCL-sulfo-SMCC, PCL-sulfo-SMCC-BMP-2, PCL-heparin, PCL-heparin-BMP-2, TCPS. ** $p < 0.05$ versus PCL-adsorbed-BMP-2.

mirroring the results of the quantitative assay. Microscopy was performed to obtain a closer look at the ALP staining and representative images are shown in Figure 7. Figure 7A shows an unmodified PCL disc seeded with C2C12 cells. The blurred areas resulted from imaging the three-dimensional, rough surface of the PCL disc. Cell nuclei are stained dark purple/black by hematoxylin, but no red ALP staining is present. Panel B shows an image of cells seeded on a PCL disc with adsorbed rhBMP-2. Again, cell nuclei are dark purple, and in this image, the arrows indicate the red staining of ALP. Panels C and D show PCL-sulfo-SMCC and PCL-sulfo-SMCC-rhBMP-2 discs, respectively. The cell density appears similar to the cell density for PCL and PCL with adsorbed rhBMP-2, suggesting that modification with sulfo-SMCC does not negatively impact cell attachment and retention. Compared to Panel B, there is no red staining in Panel D, which means no ALP was present in this sample. The same was true for Panel F, representing a

PCL disc conjugated with rhBMP-2 using heparin. The two heparin samples (Panels E and F) also have much less hematoxylin staining, indicative of lower cell attachment and retention.

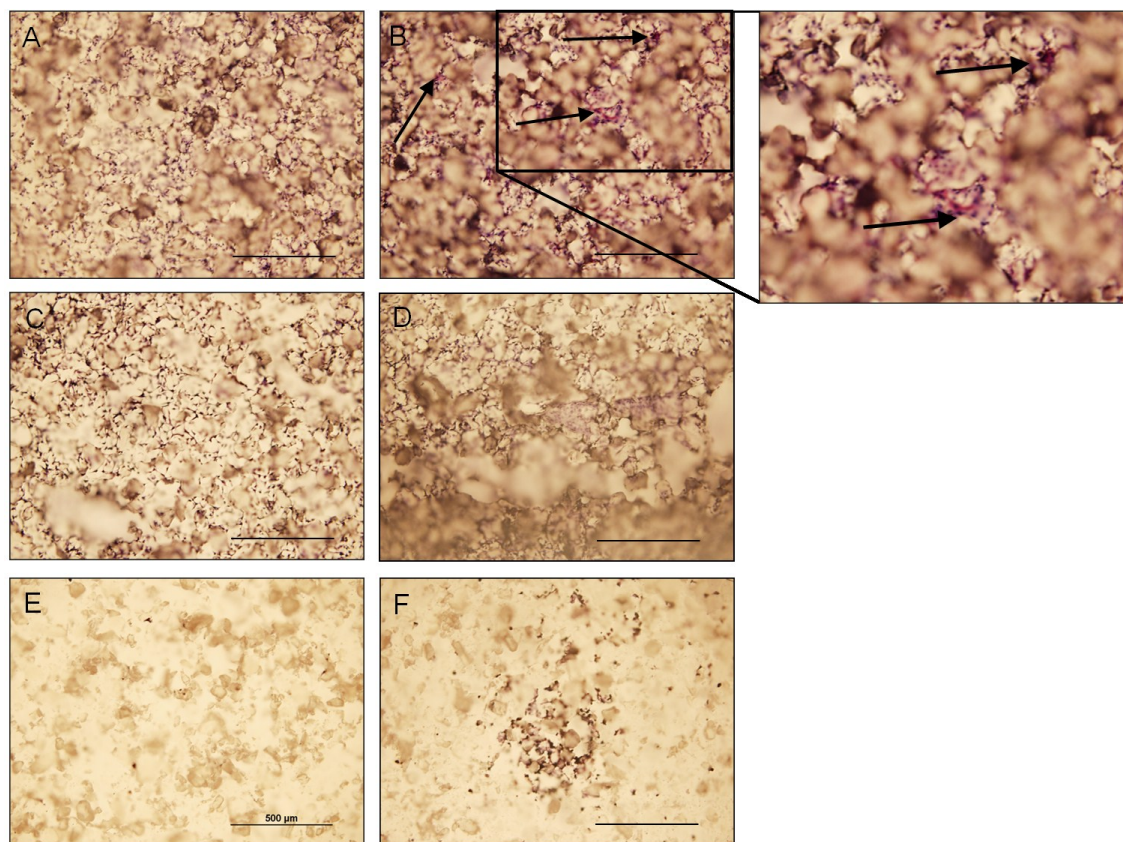


Figure 7.7: Day 3 alkaline phosphatase staining on discs seeded with C2C12 cells. A. PCL, B. PCL-adsorbed-BMP-2 (arrows show red ALP stain), C. PCL-sulfo-SMCC, D. PCL-sulfo-SMCC-BMP-2, E. PCL-heparin, F. PCL-heparin-BMP-2. Error bar = 500 µm.

7.4 Discussion

Conjugating rhBMP-2 to polymeric scaffolds has been proposed to control release of the growth factor and localize bone growth. The studies performed in Aims II and III and presented in Chapter 5 and 6, respectively, utilized the heterobifunctional cross-linker sulfo-SMCC to tether rhBMP-2 to PCL scaffolds, a method chosen based on previous work in the Scaffold Tissue Engineering Group [1]. However, when the conjugation efficiency and release study results that had been previously reported could not be repeated, issues with the previous experimental method were uncovered. This discovery, coupled with the small bone volumes generated in Aim III prompted a reexamination of the sulfo-SMCC conjugation technique. The results of this Chapter proved that rhBMP-2 could be successfully immobilized on porous PCL scaffolds using both sulfo-SMCC and adsorption. Comparison of rhBMP-2 attachment methods showed that the sulfo-SMCC method yielded the highest conjugation efficiency, but failed to induce C2C12 ALP production after three days *in vitro*, suggesting that the bioactivity of covalently immobilized rhBMP-2 was negligible. However, the bone growth observed on rhBMP-2-conjugated scaffolds in Aim III suggests recovery of bioactivity upon release of the rhBMP-2 from the scaffold.

Recombinant human BMP-2 can be generated from Chinese hamster ovary (CHO) cells [31] or *Escherichia coli* (*e. coli*) [32] and significant differences exist between the resulting recombinant protein. For instance, CHO-derived rhBMP-2 is glycosylated making it more soluble than *e. coli*-derived rhBMP-2. Antibody detection of rhBMP-2 is also specific to a particular derivation of the recombinant protein due to differences in tertiary structure, a distinction that is particularly relevant with respect to

immunoassays such as ELISA. This discrepancy came to light when attempts were made to replicate previously performed conjugation efficiency and release experiments for the constructs used in Aims II and III. We discovered that conjugated *e. coli*-derived rhBMP-2 had been incorrectly quantified using ELISA with an antibody against CHO-derived rhBMP-2. A correct ELISA protocol using an antibody against *e. coli*-derived rhBMP-2 was developed and the conjugation efficiency and release experiments were repeated and are presented in this Chapter.

There were two main goals of this study, the first being to characterize the three dimensional PCL scaffold system used in the previous two Chapters by determining the conjugation efficiency and release profile for PCL scaffolds conjugated with rhBMP-2 using sulfo-SMCC. The second goal was to compare the sulfo-SMCC method to two alternative methods for attaching rhBMP-2 to PCL, physical adsorption and heparin. Conjugation efficiency to discs was greater for the sulfo-SMCC method compared to physical adsorption, which agrees with previous reports of rhBMP-2 [4] and VEG-F [33] conjugation using sulfo-SMCC. This study reported even higher conjugation efficiency than other studies, which could be due to the surface roughness of the sintered PCL that was able to entrap sulfo-SMCC and rhBMP-2. The heparin method trended toward greater conjugation efficiency than adsorption but this was not significant, a finding that is in contrast to previous reports of the heparin method's superiority for conjugating rhBMP-2 [18, 23] and other growth factors [26, 34]. The amount of heparin that attached to amine groups on the PCL was not quantified in this study, so there may not have been enough heparin on the surface of the disc to facilitate complete rhBMP-2 coverage. Despite lower conjugation efficiency, the heparin method showed excellent retention of

rhBMP-2 over the 14 day release period, with a release profile comparable to sulfo-SMCC-conjugated discs. The strong bonding between heparin and rhBMP-2 is facilitated by a heparin binding site at the N-terminus of dimerized rhBMP-2 [35]. This specific interaction results in a linkage that is stronger than the electrostatic forces that are responsible for adsorption of rhBMP-2 to PCL and contributed to the very slow release of rhBMP-2 from heparin that was observed in this study.

The results of conjugating rhBMP-2 to three dimensional PCL scaffolds confirm that the sulfo-SMCC method used in Aims II and III successfully attached rhBMP-2 to the PCL scaffolds. There was no difference in conjugation efficiency between sulfo-SMCC and adsorption and both methods demonstrated that greater than 99% of the originally attached rhBMP-2 remained on the scaffolds after 14 days. Thus, even though the difference in release was significant between the two groups, adsorbed rhBMP-2 was retained much better than expected based on previous reports of adsorption [4]. The surface roughness of the sintered PCL used here (which can be seen in the images of Figure 7) may have improved adsorption of the protein, a phenomenon that has been reported previously [36]. From these results, we can be confident that there was rhBMP-2 on the scaffolds used in Aims II and III (~10 µg per scaffold) and that it remained on the scaffolds for the duration of the *in vitro* culture periods. Therefore, the reason for lower than expected bone volumes in Aim III is likely not due to an absence of immobilized rhBMP-2.

The scaffold conjugation results are contrary to the results obtained using PCL discs that showed significantly greater efficiency when the sulfo-SMCC method was used. Since the original intent of the study was not to compare between discs and

scaffolds, different original rhBMP-2 concentrations were used – 1 µg/ml for discs and 20 µg/ml for scaffolds (to mimic the conditions used in Aims II and III). While we could detect a freshly prepared 20 µg/ml solution of rhBMP-2 using ELISA, the solubility of non-glycosylated *e. coli*-derived rhBMP-2 is known to be low at neutral pH [37, 38], meaning the rhBMP-2 may have come out of solution and aggregated during the 18 hour conjugation procedure. This would have resulted in a lesser amount of soluble rhBMP-2 available for conjugation, lowering the proportion of the original amount that could attach to the scaffold. Mass transport differences resulting from architectural dissimilarity between the discs and scaffolds may have also had a significant effect on conjugation. Both constructs had the same surface area (2 cm²), but while 100% of the disc surface was freely exposed to the solution of rhBMP-2, only the outer surfaces of the scaffold were freely exposed. Fluid does not flow as freely through the inner pore areas of the scaffold as it does past the outer scaffold surfaces. The slower diffusion through the scaffold pores could limit both the amount of sulfo-SMCC crosslinker and the amount of rhBMP-2 that attaches to these surfaces, resulting in lower conjugation efficiency for scaffolds relative to discs.

Aside from a decrease in conjugation efficiency seen for sulfo-SMCC-conjugated scaffolds compared to discs, the relative difference between sulfo-SMCC-conjugated and adsorbed rhBMP-2 was also different for discs versus scaffolds. Discs had significantly greater conjugation efficiency for sulfo-SMCC, while for scaffolds, there was no difference in efficiency between adsorption and sulfo-SMCC. This discrepancy may have been due to the different rhBMP-2 concentrations utilized. The higher concentration employed for attachment to scaffolds may have caused a stronger concentration gradient

that drove adsorption at a rate that was similar to that of conjugation by sulfo-SMCC. In contrast, the 1 µg/ml concentration used for discs likely decreased the protein adsorption rate below that of the sulfo-SMCC reaction rate, resulting in better conjugation efficiency for sulfo-SMCC. Additional studies directly comparing conjugation efficiency between discs and scaffolds (using a constant rhBMP-2 concentration) are needed to pinpoint the reason behind the discrepancies.

The conjugation efficiency and release data indicate much greater attachment and much lower release than any other reports of attaching rhBMP-2 to scaffolds using sulfo-SMCC [4, 15] or heparin [18, 21, 22]. It is important to note that none of the previously described systems were identical to the PCL-based system used here and caution should be taken when directly comparing between dissimilar studies. Additionally, the conditions under which release is measured can vary from study to study. In this study, constructs underwent very gentle shaking on an orbital shaker, while other studies may vigorously shake the constructs, which could significantly affect release patterns. Nonetheless, there was some concern over the reliability of the values obtained from ELISA. Protein degradation during freeze/thaw cycles is a legitimate issue that is particularly relevant when working with very small amounts of protein. There was some concern that degradation of the rhBMP-2 occurred prior to performing the ELISA due to a freeze/thaw cycle. However, analysis of fresh (not frozen) released rhBMP-2 confirmed that this was not the case, confirming that the ELISA accurately measured the amount of rhBMP-2 in the collected buffer. Another possibility is that some of the unbound or released rhBMP-2 attached to the 24-well plates used for conjugation and release studies or to the microcentrifuge tubes used for collection. Ultra-low-attachment plates and lo-

bind Eppendorf tubes coated with 1% bovine serum albumin were used to prevent rhBMP-2 from adhering to plastic surfaces, although some attachment may have still occurred. Despite these concerns, our quantification technique went through several rounds of optimization and many precautions were taken to prevent protein loss, so we conclude that the rhBMP-2 was very tightly bound to the PCL. While tightly tethering growth factor to a scaffold is generally heralded as advantageous, the minimal release from the PCL may have negative consequences for rhBMP-2's bioactivity since it is often the released, free growth factor with which cells recognize and interact with to produce an osteogenic response.

One well established method for measuring the bioactivity of rhBMP-2 is to assess ALP production by C2C12 myoblasts in response to rhBMP-2 [11, 15, 20, 30]. An increase in ALP production is indicative of the second stage of osteogenesis, which also involves production of collagen I and osteocalcin and marks the point in differentiation where non-osteogenic cells become committed to the osteoblastic lineage. Although growth factor conjugation is intended as a positive improvement to the scaffold system, conjugating rhBMP-2 to a material involves manipulating the growth factor in a way that could negatively impact its bioactivity. The ALP assay showed that this was not the case for rhBMP-2 physically adsorbed to PCL, as the cells exhibited a strong ALP response when seeded on these constructs. The rhBMP-2 was available for interaction with cells, which is the first step toward inducing an osteogenic and eventual bone growth response. Neither the sulfo-SMCC-conjugated rhBMP-2 nor the heparin-conjugated rhBMP-2 induced a positive ALP response in C2C12. While only the results of one experiment are shown, this negative result was observed in multiple independent experiments and thus is

not likely due to random chance. The inability of C2C12 cells to express ALP when exposed to constructs with conjugated rhBMP-2 calls into question the utility of using either of these methods for attaching the growth factor to PCL.

Covalent conjugation techniques, including the sulfo-SMCC and carbodiimide chemistries used here, often rely on linkage to amines that are found in many different locations on the growth factor. rhBMP-2's N-terminal amines are attractive candidates for conjugation because they are distal to the protein's active site, so conjugation to these amines would not interfere with bioactivity. However, since the crosslinker cannot preferentially bind to specific amine groups, it may link to amines on the growth factor's abundant lysine groups, forcing the growth factor into a configuration that renders its active site sterically hindered or otherwise blocked [27, 28]. It is possible that conjugation to PCL using the sulfo-SMCC and heparin conjugation schemes negatively affected rhBMP-2's bioactivity, a concern that has been echoed by others attempting to conjugate rhBMP-2 to biomaterial scaffolds [13]. The lessened bioactivity and subsequent lack of ALP response could explain why conjugated rhBMP-2 had little effect on ADSC and BMSC in Aim II and may partially explain the lower than expected bone volumes reported in Aim III. This observation also challenges the belief that cells can interact with immobilized growth factors and suggests that a biologic response may only be triggered once the growth factor has been released from the scaffold.

Despite these concerns over conjugated rhBMP-2's bioavailability, the sulfo-SMCC and heparin methods have successfully promoted upregulation of ALP when used in other scaffold systems [15, 18]. Furthermore, the *in vivo* studies from Aim III showed some bone growth in scaffolds containing only conjugated rhBMP-2, meaning that at

least some of the rhBMP-2 became bioactive *in vivo* and induced a bone growth response. Historical accounts of protein and antibody binding report that there is typically only a small fraction of the bound protein in a biologically active conformation [28], so the assumption that cells are able to interact with immobilized growth factors may be invalid. The more likely mode of cellular interaction is through binding to a growth factor once it has been released from the polymer substrate and has assumed a normal conformation. According to the release study, an appreciable amount of adsorbed rhBMP-2 is released between days 1 and 3. This released rhBMP-2 was likely responsible for the positive ALP response that occurred for the adsorbed group, while the chemically conjugated discs that released very little rhBMP-2 between days 1 and 3 did not support C2C12 ALP production.

Since negligible rhBMP-2 was released over the three day time period of the *in vitro* ALP assay, the assay was insufficient to fully characterize the bioactivity of the sulfo-SMCC system. For a more complete picture, the *in vivo* results and rhBMP-2 release mechanisms must also be considered. Conjugated rhBMP-2 is likely released from the scaffold by degradation of PCL since PCL's ester linkages are weaker than the amide bonds formed between 1,6-hexanediamine and PCL and between sulfo-SMCC and rhBMP-2. The *in vivo* study was carried out for 8 weeks, allowing more time for hydrolysis of the ester linkages and subsequent release of rhBMP-2. The PCL constructs were also susceptible to enzymes (such as esterases) *in vivo* that may have accelerated the degradation of the outermost surface layers of PCL. Therefore, over the 8 week time course, the *in vivo* environment enabled rhBMP-2 to be released from the PCL and rendered in a form that cells could interact with to produce a bone growth response. This

highlights the differences between *in vitro* and *in vivo* systems and shows that even well-established characterization methods, such as the C2C12 ALP model, have their limitations.

7.5 Conclusions

These studies demonstrated differences in growth factor attachment and cellular response when rhBMP-2 is attached to SLS-manufactured PCL constructs using sulfo-SMCC, heparin or physical adsorption. In addition to differences between the three methods, differences were also observed when solid PCL discs were used versus three-dimensional, porous PCL scaffolds. Overall, conjugation by sulfo-SMCC led to high loading efficiency and less than 1% release over 14 days *in vitro*. However, both this method and the heparin method failed to induce ALP production by C2C12 myoblasts, indicating that the conjugated rhBMP-2 was not bioactive in its immobilized form. These results, along with the positive bone growth response at 8 weeks observed in Aim III, suggest that release of the sulfo-SMCC-conjugated rhBMP-2 restores its bioactivity and enables cells to interact with it. Retention of adsorbed rhBMP-2 was better than expected and led to successful production of ALP meaning either released rhBMP-2 and/or adsorbed rhBMP-2 remained bioactive and initiated osteogenesis in C2C12 cells. Future work includes reevaluating adsorption as a simple, viable rhBMP-2 attachment method, and modifying the chemical conjugation methods to optimize release and promote rhBMP-2 bioactivity.

7.6 Acknowledgements

Thank you to Sitaram Chivukula and Janki Patel for their assistance with scaffold conjugations and ELISA. This work was funded by NIAMS AR 053379.

7.7 References

- [1] Zhang HN, Migneco F, Lin CY, Hollister SJ. Chemically-Conjugated Bone Morphogenetic Protein-2 on Three-Dimensional Polycaprolactone Scaffolds Stimulates Osteogenic Activity in Bone Marrow Stromal Cells. *Tissue Engineering Part A*. 2010;16:3441-8.
- [2] Draenert F, Nonnenmacher A-L, Kämmerer P, Goldschmitt J, Wagner W. BMP-2 and bFGF release and in vitro effect on human osteoblasts after adsorption to bone grafts and biomaterials. *Clinical Oral Implants Research* 2012. p. 1-8.
- [3] Dong XL, Wang Q, Wu T, Pan HH. Understanding adsorption-desorption dynamics of BMP-2 on hydroxyapatite (001) surface. *Biophysical Journal*. 2007;93:750-9.
- [4] Park YJ, Kim KH, Lee JY, Ku Y, Lee SJ, Min BM, et al. Immobilization of bone morphogenetic protein-2 on a nanofibrous chitosan membrane for enhanced guided bone regeneration. *Biotechnology and Applied Biochemistry*. 2006;43:17-24.
- [5] Liu Y, Huse RO, de Groot K, Buser D, Hunziker EB. Delivery mode and efficacy of BMP-2 in association with implants. *Journal of Dental Research*. 2007;86:84-9.
- [6] Liu YL, Enggist L, Kuffer AF, Buser D, Hunziker EB. The influence of BMP-2 and its mode of delivery on the osteoconductivity of implant surfaces during the early phase of osseointegration (vol 28, pg 2677, 2007). *Biomaterials*. 2007;28:5399-.
- [7] Ziegler J, Mayr-Wohlfart U, Kessler S, Breitig D, Gunther KP. Adsorption and release properties of growth factors from biodegradable implants. *Journal of Biomedical Materials Research*. 2002;59:422-8.
- [8] Kim S, Kang YQ, Krueger CA, Sen ML, Holcomb JB, Chen D, et al. Sequential delivery of BMP-2 and IGF-1 using a chitosan gel with gelatin microspheres enhances early osteoblastic differentiation. *Acta Biomaterialia*. 2012;8:1768-77.

- [9] Basmanav FB, Kose GT, Hasirci V. Sequential growth factor delivery from complexed microspheres for bone tissue engineering. *Biomaterials*. 2008;29:4195-204.
- [10] Raiche AT, Puleo DA. In vitro effects of combined and sequential delivery of two bone growth factors. *Biomaterials*. 2004;25:677-85.
- [11] Pohl TLM, Boergermann JH, Schwaerzer GK, Knaus P, Cavalcanti-Adam EA. Surface immobilization of bone morphogenetic protein 2 via a self-assembled monolayer formation induces cell differentiation. *Acta Biomaterialia*. 2012;8:772-80.
- [12] He Q, Zhao Y, Chen B, Xiao Z, Zhang J, Chen L, et al. Improved cellularization and angiogenesis using collagen scaffolds chemically conjugated with vascular endothelial growth factor. *Acta Biomaterialia*. 2011;7:1084-93.
- [13] Karageorgiou V, Meinel L, Hofmann S, Malhotra A, Volloch V, Kaplan D. Bone morphogenetic protein-2 decorated silk fibroin films induce osteogenic differentiation of human bone marrow stromal cells. *Journal of Biomedical Materials Research Part A*. 2004;71A:528-37.
- [14] Sulfo-SMCC: A water soluble amine-to-sulphydryl crosslinker with a medium length cyclohexane spacer arm (8.3 angstroms). Thermo Fisher Scientific, Inc.; 2012.
- [15] Zhao Y, Zhang J, Wang X, Chen B, Xiao Z, Shi C, et al. The osteogenic effect of bone morphogenetic protein-2 on the collagen scaffold conjugated with antibodies. *Journal of Controlled Release*. 2010;141:30-7.
- [16] Zhang Q, He Q-F, Zhang T-H, Yu X-L, Liu Q, Deng F. Improvement in the delivery system of bone morphogenetic protein-2: a new approach to promote bone formation. *Biomedical Materials* 2012.
- [17] Shao Z, Zhang X, Pi Y, Wang X, Jia Z, Zhu J, et al. Polycaprolactone electrospun mesh conjugated with an MSC affinity peptide for MSC homing in vivo. *Biomaterials*. 2012;33:3375-87.
- [18] Jeon O, Song SJ, Kang S-W, Putnam AJ, Kim B-S. Enhancement of ectopic bone formation by bone morphogenetic protein-2 released from a heparin-conjugated poly(Llactic- co-glycolic acid) scaffold. *Biomaterials* 2007. p. 2763-71.

- [19] Rider C. Heparin/heparan sulphate binding in the TGF- β cytokine superfamily. *Biochemical Society Transactions* 2006. p. 458-60.
- [20] Zhao B, Katagiri T, Toyoda H, Takada T, Yanai T, Fukuda T, et al. Heparin potentiates the in vivo ectopic bone formation induced by bone morphogenetic protein-2. *Journal of Biological Chemistry*. 2006;281:23246-53.
- [21] La W-G, Kang S-W, Yang HS, Bhang SH, Lee SH, Park J-H, et al. The Efficacy of Bone Morphogenetic Protein-2 Depends on Its Mode of Delivery. *Artificial Organs*. 2010;34:1150-3.
- [22] Jeon O, Song SJ, Yang HS, Bhang S-H, Kang S-W, Sung MA, et al. Long-term delivery enhances in vivo osteogenic efficacy of bone morphogenetic protein-2 compared to short-term delivery. *Biochemical and Biophysical Research Communications*. 2008;369:774-80.
- [23] Koo K, Yeo D, Ahn J, Kim B-S, Kim C-S, Im G-I. Lumbar posterolateral fusion using heparin-conjugated fibrin for sustained delivery of BMP2 in a rabbit model. *Artificial Organs* 2012.
- [24] Chong Y-I, Ahn K-M, Jeon S-H, Lee S-Y, Lee J-H, Tae G. Enhanced bone regeneration with BMP-2 loaded functional nanoparticle-hydrogel complex. *Journal of Controlled Release* 2007. p. 91-9.
- [25] Ferrara N, Henzel WJ. Pituitary Follicular Cells Secrete a Novel Heparin-Binding Growth Factor Specific for Vascular Endothelial Cells. *Biochemical and Biophysical Research Communications*. 1989;161:851-8.
- [26] Cabric S, Sanchez J, Johansson U, Larsson R, Nilsson B, Korsgren O, et al. Anchoring of Vascular Endothelial Growth Factor to Surface-Immobilized Heparin on Pancreatic Islets: Implications for Stimulating Islet Angiogenesis. *Tissue Engineering Part A*. 2010;16:961-70.
- [27] Masters KS. Covalent Growth Factor Immobilization Strategies for Tissue Repair and Regeneration. *Macromolecular Bioscience*. 2011;11:1149-63.
- [28] Rusmini F, Zhong ZY, Feijen J. Protein immobilization strategies for protein biochips. *Biomacromolecules*. 2007;8:1775-89.

- [29] Dickerman RD, Reynolds AS, Morgan BC, Tompkins J, Cattorini J, Bennett M. rh-BMP-2 can be used safely in the cervical spine: dose and containment are the keys! *Spine Journal*. 2007;7:508-9.
- [30] Katagiri T, Yamaguchi A, Komaki M, Abe E, Takahashi N, Ikeda T, et al. Bone Morphogenetic Protein-2 Converts the Differentiation Pathway OF C2C12 Myoblasts into the Osteoblast Lineage. *Journal of Cell Biology*. 1994;127:1755-66.
- [31] Israel DI, Nove J, Kerns KM, Moutsatsos IK, Kaufman RJ. Expression and characterization of bone morphogenetic protein-2 in Chinese hamster ovary cells. *Growth factors (Chur, Switzerland)*. 1992;7:139-50.
- [32] Kuebler NR, Reuther JF, Faller G, Kirchner T, Ruppert R, Sebald W. Inductive properties of recombinant human BMP-2 produced in a bacterial expression system. *International Journal of Oral and Maxillofacial Surgery*. 1998;27:305-9.
- [33] Gerber HP, Vu TH, Ryan AM, Kowalski J, Werb Z, Ferrara N. VEGF couples hypertrophic cartilage remodeling, ossification and angiogenesis during endochondral bone formation. *Nature Medicine*. 1999;5:623-8.
- [34] Chung HJ, Kim HK, Yoon JJ, Park TG. Heparin immobilized porous PLGA microspheres for angiogenic growth factor delivery. *Pharmaceutical Research*. 2006;23:1835-41.
- [35] Ruppert R, Hoffmann E, Sebald W. Human bone morphogenetic protein 2 contains a heparin-binding site which modifies its biological activity. *European Journal of Biochemistry*. 1996;237:295-302.
- [36] Deligianni DD, Katsala N, Ladas S, Sotiropoulou D, Amedee J, Missirlis YF. Effect of surface roughness of the titanium alloy Ti-6Al-4V on human bone marrow cell response and on protein adsorption. *Biomaterials*. 2001;22:1241-51.
- [37] Hillger F, Herr G, Rudolph R, Schwarz E. Biophysical comparison of BMP-2, ProBMP-2, and the free pro-peptide reveals stabilization of the pro-peptide by the mature growth factor. *Journal of Biological Chemistry*. 2005;280:14974-80.
- [38] *Tissue Engineering*. 1st ed: Elsevier Academic Press; 2008.

CHAPTER 8 Conclusions and Future Directions

8.1 Conclusions

The work presented in this thesis represents significant contributions to the field of scaffold bone tissue engineering. Scaffold architecture has long been known to influence tissue growth and mechanical properties, but by isolating the variable of permeability, the particular effect of mass transport on bone growth could be evaluated. The discovery that higher scaffold permeability supported greater bone growth has led to additional studies to further optimize scaffold architecture for an appropriate balance of permeability and mechanical properties. The conjugation work undertaken for this thesis demonstrated the complexity that is introduced when rhBMP-2 is incorporated into a system. It also reinforced the importance of utilizing and optimizing correct characterization techniques prior to moving forward with more in-depth studies. Future work with rhBMP-2 conjugation will focus on better understanding the benefits and drawbacks to using adsorption versus chemical conjugation and optimizing rhBMP-2 incorporation for clinical use.

8.1.1 Polycaprolactone Scaffold Permeability Affects Bone Growth

Scaffold architecture is a significant variable to consider when designing constructs for bone repair. Architecture affects mechanical properties, tissue morphology,

mass transport and manufacturability. Advanced solid free form fabrication techniques enable creation of scaffolds with two levels of design specificity. First, computed tomography captures the anatomic shape of a bone defect needing repair and is used to render the macro scaffold architecture, creating a construct that fits precisely to the defect. Specifically designed internal architecture is then incorporated into the scaffold to provide mechanical support and promote scaffold-guided bone growth. This thesis looked at how internal scaffold architecture, specifically scaffold permeability, affects bone growth.

Permeability describes the flow of fluid through a porous medium and is an umbrella variable for other mass transport variables including porosity, pore size, tortuosity and interconnectivity. The scaffold permeability was altered in our scaffolds by changing the throat size (connection between pores). Both scaffold designs had permeability values above that of the threshold reported for bone in-growth to occur [1], but the higher permeability designs led to greater bone growth *in vivo*. Penetration of tissue into the center regions of the high permeability scaffolds increased mechanical properties from 4 to 8 weeks, an increase that was not seen for low permeability scaffolds. Isolating the particular effect of a single mass transport variable is complicated by the fact that many of these variables are intimately connected, so changing one parameter automatically changes others. Furthermore, there are manufacturability constraints that the scaffold design must meet. While every effort was made to hold all scaffold design variables except permeability constant between the two designs used in Aim I, surface area and porosity are intimately connected to permeability and so could not be held constant. Scaffold surface area has been positively correlated with bone

formation on osteoconductive materials such as ceramics [2], but the same conclusion cannot be made for materials like PCL that are not naturally osteoconductive. In fact, a lower surface area may be advantageous for scaffolds made of non-osteoconductive materials. This claim was substantiated by our experiments that showed less bone growth for low permeability scaffolds that not only had lower permeability than the high permeability designs, but also higher surface area.

8.1.2 Conjugated rhBMP-2 Promoted Expression of Chondrogenic Markers In Vitro While Soluble Factors Encouraged Osteogenic Marker Expression

Traditionally, differentiation of pluripotent cells is accomplished *in vitro* by exposing the cells to soluble, chemical factors in the cell culture medium. Osteogenic medium typically contains β -glycerophosphate, ascorbic acid and dexamethasone, while chondrogenic medium contains insulin, ascorbic acid, TGF- β , proline and dexamethasone. In this thesis, ADSC and BMSC were exposed to various combinations of differentiation medium and scaffold-conjugated rhBMP-2 in an effort to determine the effect on expression of osteogenic and chondrogenic markers. rhBMP-2 had a greater effect on chondrogenesis than osteogenesis, a finding that was elucidated by comparing constructs with and without rhBMP-2 cultured in the same medium. For ADSC, three out of the four chondrogenic markers analyzed were upregulated in the presence of rhBMP-2, but this was not observed for constructs in growth medium, suggesting that the conjugated rhBMP-2 and chondrogenic medium factors worked in tandem to promote expression. However, for BMSC, the rhBMP-2 had a chondrogenic effect that was independent of the soluble medium factors.

Although the conjugated rhBMP-2 did not have a large individual effect on osteogenesis, it did have a positive combinatorial effect on osteogenic markers when used in conjunction with osteogenic medium. This occurred for both ADSC and BMSC, although the response was more pronounced and consistent for BMSC. The finding that rhBMP-2 alone does not induce an osteogenic response from these cell types is not completely surprising. Others have also reported no effect of rhBMP-2 on BMSC expression of ALP [3] and no significant and consistent effect of rhBMP-2 on osteogenesis of ADSC [4]. These cells are sensitive to the particulars of the environment that they are in and may express some markers of differentiation but not others, so it is difficult to assess their behavior with only a few metrics. The chondrogenic and osteogenic markers chosen for analysis in this thesis were intended as initial probes into the differentiation tendencies of the cells when used in the PCL/conjugated rhBMP-2 environment. A time course study investigating alkaline phosphatase (ALP) production, mineralization and expression of a full panel of osteogenic genes would provide a more detailed, comprehensive expression profile. The conjugation method used here may have also had a deleterious effect on the cells' ability to respond positively to the rhBMP-2. Additional studies comparing soluble, adsorbed and conjugated rhBMP-2 will clarify if the conjugation is negatively affecting differentiation capacity.

8.1.3 BMSC Demonstrated More Evidence of In Vitro Differentiation than ADSC

One of the main goals of this thesis was to determine the relative behavior of ADSC and BMSC when exposed to rhBMP-2 conjugated to PCL scaffolds and cultured in various differentiation media. There has been a lot of research attempting to answer

this question and the results are conflicting, with some studies reporting better osteogenesis by BMSC [5, 6] and others showing an equal or stronger response by ADSC [7, 8]. The effect of rhBMP-2 versus soluble medium factors is also not straightforward but has important consequences for creating tissue engineered products that are feasible for the clinic. Preliminary work looking at mineralization of ADSC and BMSC proved that the cells mineralized in response to traditional osteogenic medium (Appendix B). In the three-dimensional environment, ADSC displayed greater mineralization than BMSC, which mirrored the 2D results, but this was not the case for osteogenic gene expression. Overall, BMSC displayed greater osteogenic and chondrogenic gene expression compared to ADSC, suggesting that the BMSC were more actively differentiating in response to both rhBMP-2 and soluble medium supplements. This finding led to a hypothesis that BMSC may have better potential for bone formation, but this was disproved by the *in vivo* study that showed better bone growth for ADSC. The disconnect between *in vitro* and *in vivo* findings demonstrates the importance of corroborating *in vitro* results with *in vivo* data.

8.1.4 *rhBMP-2 did not Significantly Affect In Vivo Bone Volume*

Just as the comparison between cell types is important, so is the direct comparison between the bone growth capacity of cells plus rhBMP-2 versus cells alone. In Aim III's *in vivo* study, ADSC that had been pre-differentiated *in vitro* with osteogenic medium produced the most bone of all the cell-seeded groups and there was no difference between constructs with conjugated rhBMP-2 versus constructs without conjugated rhBMP-2. This finding is in accordance with the *in vitro* data showing that soluble medium

components had a greater effect on osteogenic markers than conjugated rhBMP-2 did. Another important comparison is between bone growth induced by cells plus rhBMP-2 and rhBMP-2 alone. Many studies looking at bone growth induced by rhBMP-2 fail to include the important control of rhBMP-2 alone, without any pre-seeded cells. In this thesis, the total bone volume in ADSC-seeded constructs (pre-differentiated *in vitro* with osteogenic medium) did not differ significantly from constructs that only contained conjugated rhBMP-2. Pre-seeding cells into rhBMP-2-conjugated PCL constructs may not be required to induce bone formation, a finding that has important consequences for clinical feasibility. Incorporating cells into a construct necessitates an additional cell-harvesting procedure that the patient must endure and requires time and resources to pre-culture the cells, both of which complicate the clinical process. Eliminating these steps by using a construct that only has rhBMP-2 would decrease complexity and make implementation more straightforward.

8.1.5 ADSC Promoted Evenly-distributed Scaffold-Guided Tissue Growth In Vivo

The lack of quantitative difference between constructs with osteo-pulsed ADSC and constructs with only rhBMP-2 is motivation to investigate use of rhBMP-2 alone, since this would be a simpler and more feasible solution. However, there was a marked difference in the distribution and pattern of bone growth for constructs pre-seeded with cells, a difference that may improve the long-term viability of the construct. ADSC-seeded constructs showed scaffold-guided tissue growth that closely followed the scaffold pore contours and was evenly distributed through the scaffold both radially and in the z-direction. In contrast, constructs that only had conjugated rhBMP-2 showed

dense nodules of mineralized tissue that were sporadically distributed throughout the scaffold pores. Scaffold-guided tissue growth is particularly important for reconstructing delicate anatomical features such as those of the face [9], because the growing bone follows the complex shape of the implanted scaffold. Evenly distributed bone tissue may also encourage more controlled scaffold degradation and more uniform mechanical properties. The complexity of incorporating cells into a scaffold system should be carefully weighed with the benefit that scaffold guided tissue growth may bring to the bone reconstruction process.

8.1.6 *Not all In Vitro Trends Translated to In Vivo Results*

Characterizing the biologic response to a fixed scaffold variable like permeability is relatively straightforward and important for evaluating scaffold design criteria. However, there is less control over biologic variables such as cells and differentiation factors and their behavior is inherently less predictable. Therefore the conclusions resulting from studies in Aims II and III that combined scaffold, cells and growth factors are more complex but are also a more accurate representation of a complete tissue engineered system. These complexities increase further when moving from an *in vitro* to an *in vivo* system. In this study, some of the *in vivo* findings correlated with *in vitro* results while others did not. Soluble differentiation factors consistently affected osteogenesis more than conjugated rhBMP-2 regardless of the setting. However, ADSC produced far more bone than BMSC *in vivo* despite the fact that BMSC differentiated more actively *in vitro*, showing that cellular behavior *in vitro* did not always correlate with *in vivo* findings.

Despite the BMSC being more active *in vitro* overall, ADSC showed greater *in vitro* mineralization, a finding that mirrors the greater *in vivo* bone formation of ADSC compared to BMSC. Both mineralization and gene expression were analyzed *in vitro*, but gene expression is a complex, highly regulated process that also exhibits temporal variation, so absolute osteogenic behavior is difficult to decipher from gene expression alone. Thus, in the system used here, mineralization may be a better predictor of *in vivo* bone formation than gene expression. The significantly greater bone volume produced for ADSC-seeded constructs compared to BMSC-seeded constructs is an important distinction because this comparison has been made frequently, yet with inconsistent conclusions. BMSC are believed to respond more strongly to rhBMP-2 [10], and this was shown here *in vitro*, although this response tended toward chondrogenesis as opposed to osteogenesis. *In vivo*, the conjugated rhBMP-2 did not have a significant effect on bone growth, so the response of ADSC and BMSC depended on other factors. Previous studies have shown equal osteogenic capacity for ADSC and BMSC [11] as well as variability in the osteogenic capacity of BMSC [12]. Thus, when the effect of rhBMP-2 is eliminated, as it was in these studies, the ADSC's innate capacity for bone growth may have dominated, resulting in greater *in vivo* bone growth than for BMSC.

The lack of complete agreement between the *in vitro* and *in vivo* studies is likely due in part to the additional complexities that an *in vivo* system presents. It could also be due to a highly ambitious experimental plan that attempted to analyze two cell types and two differentiation mediums all in combination with rhBMP-2 conjugated to scaffolds using a method that had not been fully characterized previously. A more streamlined and focused research plan may have produced more straightforward and relevant results.

Nonetheless, the conclusions gleaned from these studies demonstrate the difficulty in predicting *in vivo* behavior from *in vitro* results.

8.1.7 Chemical Conjugation Method Affects rhBMP-2 Retention and Bioactivity

There are several criteria that must be met for a growth factor delivery method to successfully induce bone growth. The primary consideration is maintenance of the growth factor's bioactivity, but growth factor retention and release profile are also important. Less bone growth than expected was observed on scaffolds conjugated with rhBMP-2 using sulfo-SMCC, which stimulated several questions about rhBMP-2's bioactivity and retention on the scaffold when this conjugation method is used. Taking into consideration both the conjugation efficiency and release studies, the sulfo-SMCC method was superior to both the adsorption and heparin methods. The discrepancy in sulfo-SMCC conjugation efficiency between discs and scaffolds should be investigated more thoroughly using the same initial amount of rhBMP-2. While these studies were repeated several times, further studies should be conducted for both discs and scaffolds to determine if the difference is a true one or was due to variability in the conjugation and/or ELISA procedure.

The conjugation efficiency and release experiments proved that the sulfo-SMCC conjugation method successfully introduced and retained rhBMP-2 on the scaffolds implanted for *in vivo* studies, but questions still remained regarding whether the rhBMP-2 was biologically active. When rhBMP-2 is modified from its native form or incorporated into a scaffold system, its ability to induce a biologic response may be compromised. This may not be problematic as long as the conjugated rhBMP-2 is released and the

released rhBMP-2 is still bioactive. Analysis of rhBMP-2 bioactivity revealed that C2C12 myoblasts produced ALP when seeded on PCL discs adsorbed with rhBMP-2 but did not produce ALP when seeded on discs with sulfo-SMCC-conjugated rhBMP-2. This experiment did not specifically distinguish whether the rhBMP-2 inducing the response was still attached to the scaffold or had been released, but in the time period of 3 days, rhBMP-2 was released from adsorbed discs but not from sulfo-SMCC or heparin-conjugated discs. This suggests that the ALP response occurred when cells interacted with released, not scaffold-bound, BMP-2.

These findings have significant implications for the *in vivo* studies presented in this thesis. Due to the covalent linkage connecting rhBMP-2 to sulfo-SMCC conjugated PCL constructs, release can only occur upon PCL degradation, which is very slow *in vivo*. Thus the scaffolds implanted *in vivo* for 8 weeks likely retained most of the initially conjugated rhBMP-2, but since it was in an inactive form, it failed to induce a large bone formation response. The little bone formation that did occur on the constructs that only had conjugated rhBMP-2 (and no cells) suggests that over the 8 week *in vivo* period, some of the rhBMP-2 was released and induced a bone formation response. A dedicated *in vivo* release study would have to be performed to confirm that the rhBMP-2 was indeed released from the scaffold *in vivo*. The inactivity of the conjugated rhBMP-2 helps to explain why osteogenic medium induced ADSC to grow bone *in vivo* regardless of BMP-2's presence.

8.2 Future Work

8.2.1 *Incorporate Scaffold Architecture into Constructs for Specific Applications*

Aim I concluded that compared to low permeability, high scaffold permeability supported better penetration of bone into the scaffold and increased mechanical properties of the construct. The increase in mechanical properties was significant at eight weeks, but could be increased further with additional scaffold modifications. Future studies should evaluate a broader range of scaffold permeability values to determine if the base mechanical properties can be improved while still allowing for good tissue penetration. This is particularly important for load-bearing applications and when using a slowly-degrading material such as PCL that will impart mechanical strength to the construct for a long period of time.

Ongoing and future work on scaffold design optimization for bone tissue engineering focuses on using favorable scaffold architectures for specific clinical applications. To this end, internal architectures similar to the ones used in this thesis have been used in a modular scaffold for mandibular reconstruction. The high permeability designs can also be used for reconstructing other tissues requiring a large vascular supply. The lower permeability design was previously shown to support better cartilage growth by primary chondrocytes [13] and is being considered for integration with chondrocytes into scaffolds for cartilage reconstruction of the ears and trachea. We also wish to determine if scaffolds that have computationally optimized permeability values but irregular architectures offer any advantages for bone growth over high permeability scaffolds with regular architectures (like the scaffolds used in this thesis). The

computationally-designed scaffolds have the additional advantage of also being optimized for mechanical properties, but it remains to be determined if this two-way optimization improves bone growth.

To fully evaluate bone growth in defect sites and for specific applications, appropriate animal models are needed. The ectopic mouse model used throughout this thesis is appropriate for screening scaffold variables, but a more complex, defect model should be used to fully evaluate the biological response induced by scaffolds containing cells and growth factors. Rabbit femur and rat cranial models are popular and would be relatively easy to implement in our laboratory. The use of large animal models is imperative for translating research findings to the clinic. For mandibular reconstruction applications, porcine mandibular models are popular because of the shape similarity between pig and human mandibles. Our group has previously employed porcine models for both mandibular reconstruction and spinal fusion and future studies are planned for evaluating growth factor conjugation and scaffold mineralization in the context of these applications.

8.2.2 *Further Refine and Characterize Conjugation Methods*

The characterization of sulfo-SMCC, heparin and adsorption attachment methods presented in this thesis was intended as an initial comparison of the three methods. Additional characterization experiments should be performed to confirm the results already obtained, analyze release past 2 weeks and examine other features of osteogenesis such as mineralization and gene expression. *In vitro* release should be quantified for at least 8 weeks to mirror the time period of *in vivo* implantation. The

sulfo-SMCC and heparin release methods showed little release over two weeks, but may exhibit a gradual release if evaluated over a longer time period. Release *in vivo* is more complicated than *in vitro* release and may be accelerated due to the presence of enzymes such as hydrolases, so it is important to perform an *in vivo* release study in addition to an extended *in vitro* study. Unfortunately, evaluating *in vivo* release is more challenging because the indirect ELISA method is not transferrable to an *in vivo* setting, but release in this setting could be evaluated by optimizing a direct ELISA method that would involve direct detection of rhBMP-2 on the scaffold. Evaluating release of radio-labeled rhBMP-2 is another direct measurement technique that may offer improvements to the indirect ELISA method [14].

Despite its reputation for imparting uncontrolled, burst release, physical adsorption is very attractive from a clinical perspective because it is the simplest method for attaching rhBMP-2 to scaffolds. Chemical conjugation methods have the potential to increase loading efficiency and control release of rhBMP-2, but these methods involve more steps and take longer, which may compromise their clinical appeal. The goal is to optimize an attachment method such that it is easy to use but also encourages localized bone growth and sustained release. The original sulfo-SMCC conjugation method takes over three days to complete, but there are modifications that could be made to simplify the process. Studies are currently underway to investigate rhBMP-2 conjugation efficiency at various incubation time points and at both 4°C and room temperature. Efforts are also being made to conduct the entire conjugation procedure under sterile conditions to eliminate a post-conjugation sterilization step and mimic a clinical setting.

Here we analyzed rhBMP-2 bioactivity by ALP production of C2C12 myoblasts, an accepted and well characterized metric. This analysis should be expanded to include evaluation at various time points to coincide with rhBMP-2 release, and extension to other cell types such as ADSC and BMSC. Furthermore, time-dependent mineralization should be evaluated to give a more complete picture of rhBMP-2-induced osteogenesis. In addition to performing more bioactivity assessments, the conjugation system itself could be modified to promote better release and thus a greater biologic response. Instead of amine groups, sulfhydryl groups can be introduced onto the scaffold surface [15, 16], in which case the sulfo-SMCC would link these sulfhydryl groups to amine groups on the rhBMP-2. This conjugation conformation may enable the attached rhBMP-2 to remain biologically active, eliminating the need for rhBMP-2 to be released before it can interact with cells and induce an osteogenic effect.

8.2.3 *Perform Additional In Vivo Studies to Better Understand the Role of Cells*

The results of the *in vivo* studies showed no quantitative difference in bone volume between ADSC-seeded constructs that had been osteopulsed *in vitro* and constructs conjugated with rhBMP-2 but not seeded with cells. However, there was a marked qualitative difference in bone distribution, with pre-seeded cells stimulating scaffold-guided bone growth. The question remaining is does this scaffold-guided tissue growth provide additional benefit to the long-term viability of the construct? To answer this question, additional *in vivo* studies should be performed comparing ADSC-seeded constructs to constructs containing just adsorbed or sulfo-SMCC-conjugated rhBMP-2. These studies should be carried out to longer time points, and in orthotopic sites such that

a greater innate bone response is stimulated. This will enable better examination of mechanical properties and tissue morphology to highlight advantages of including cells in constructs.

Despite the potential benefit cells may have, incorporating them into a scaffold prior to *in vivo* implantation in a clinical setting requires additional time and effort to harvest and culture the cells, and introduces more opportunities for contamination. Our results suggest that conjugation of rhBMP-2 alone may be enough to stimulate osteogenesis of host cells at the defect site. Furthermore, unpublished work by our group showed little difference in the bone formation response of adsorbed rhBMP-2 versus conjugated rhBMP-2. Taken together, these findings warrant further investigation into the bone growth response of rhBMP-2 attached to scaffolds (either through adsorption or chemical conjugation) that are not seeded with cells. Combining a mineral coating with conjugated or adsorbed rhBMP-2 may further increase the scaffold's bone formation potential, and work has already begun to analyze the combination of mineralization and attached rhBMP-2. The studies reported here were performed ectopically, but future studies should be carried out using a defect model such that the natural bone healing response can augment bone growth induced by the conjugated rhBMP-2. The sulfo-SMCC and adsorption methods should be compared *in vivo* at various time points, which will provide insight into the temporal bioavailability of rhBMP-2 conjugated using each of the methods.

8.3 References

- [1] Hui PW, Leung PC, Sher A. Fluid conductance of cancellous bone graft as a predictor for graft-host interface healing. *Journal of Biomechanics*. 1996;29:123-32.
- [2] Mastrogiacomo M, Scaglione S, Martinetti R, Dolcini L, Beltrame F, Cancedda R, et al. Role of scaffold internal structure on in vivo bone formation in macroporous calcium phosphate bioceramics. *Biomaterials*. 2006;27:3230-7.
- [3] Reilly GC, Radin S, Chen AT, Ducheyne P. Differential alkaline phosphatase responses of rat and human bone marrow derived mesenchymal stem cells to 45S5 bioactive glass. *Biomaterials*. 2007;28:4091-7.
- [4] Zuk P, Chou Y, Mussano F, Benhaim P, Wu B. Adipose derived stem cells and BMP-2: Part 2. BMP-2 may not influence the osteogenic fate of human adipose-derived stem cells. *Connective Tissue Research* 2011. p. 119-32.
- [5] Sakaguchi Y, Sekiya I, Yagishita K, Muneta T. Comparison of human stem cells derived from various mesenchymal tissues - Superiority of synovium as a cell source. *Arthritis and Rheumatism*. 2005;52:2521-9.
- [6] Kim D, Monaco E, Maki A, de Lima AS, Kong HJ, Hurley WL, et al. Morphologic and transcriptomic comparison of adipose- and bone-marrow-derived porcine stem cells cultured in alginate hydrogels. *Cell and Tissue Research*. 2010;341:359-70.
- [7] Monaco E, Bionaz M, Rodriguez-Zas S, Hurley WL, Wheeler MB. Transcriptomics Comparison between Porcine Adipose and Bone Marrow Mesenchymal Stem Cells during In Vitro Osteogenic and Adipogenic Differentiation. *Plos One*. 2012;7.
- [8] Vishnubalaji R, Al-Nbaheen M, Kadalmani B, Aldahmash A, Ramesh T. Comparative investigation of the differentiation capability of bone-marrow- and adipose-derived mesenchymal stem cells by qualitative and quantitative analysis. *Cell and Tissue Research* 2012. p. 419-27.
- [9] Hollister SJ, Lin CY, Saito E, Schek RD, Taboas JM, Williams JM, et al. Engineering craniofacial scaffolds. *Orthodontics & craniofacial research*. 2005;8:162-73.
- [10] Yamaguchi A, Yokose S, Ikeda T, Katagiri T, Wozney JM, Rosen V, et al. BMP-2 Induces Bone Marrow Stromal Cells to Differentiate into Osteoblasts and Decreases their Capacity to Support Osteoclast Formation. *Journal of Bone and Mineral Research*. 1993;8:S158-S.

- [11] Noel D, Caton D, Roche S, Bony C, Lehmann S, Casteilla L, et al. Cell specific differences between human adipose-derived and mesenchymal-stromal cells despite similar differentiation potentials. *Experimental Cell Research*. 2008;314:1575-84.
- [12] Mendes SC, Tibbe JM, Veenhof M, Both S, Oner FC, van Blitterswijk CA, et al. Relation between in vitro and in vivo osteogenic potential of cultured human bone marrow stromal cells. *Journal of Materials Science-Materials in Medicine*. 2004;15:1123-8.
- [13] Kemppainen JM, Hollister SJ. Differential effects of designed scaffold permeability on chondrogenesis by chondrocytes and bone marrow stromal cells. *Biomaterials*. 2010;31:279-87.
- [14] Kempen DHR, Lu L, Hefferan TE, Creemers LB, Maran A, Classic KL, et al. Retention of in vitro and in vivo BMP-2 bioactivities in sustained delivery vehicles for bone tissue engineering. *Biomaterials*. 2008;29:3245-52.
- [15] Zhao Y, Zhang J, Wang X, Chen B, Xiao Z, Shi C, et al. The osteogenic effect of bone morphogenetic protein-2 on the collagen scaffold conjugated with antibodies. *Journal of Controlled Release* 2010. p. 30-7.
- [16] Gittens SA, Matyas JR, Zernicke RF, Uludag H. Imparting bone affinity to glycoproteins through the conjugation of bisphosphonates. *Pharmaceutical Research*. 2003;20:978-87.

APPENDIX A Mechanical Characterization and Non-linear Elastic Modeling of Poly(glycerol sebacate) for Soft Tissue Engineering

A.1 Introduction

Repairing damage to soft tissue due to trauma, disease or congenital defects is difficult due to the unique structural and nonlinear mechanical characteristics of these tissues. For cardiac tissue, most treatment options fail to regenerate damaged tissue and only aim to prevent further damage (Sabbah et al., 1994; Jain et al., 2007; Fujimoto et al., 2007; Batista et al., 1997), while for adipose tissue, current grafting techniques often suffer from suboptimal mechanical properties and volume loss due to resorption (Patrick, 2001; Flynn et al., 2008). Tissue engineering techniques utilizing specialized materials and scaffold designs may have the potential to address these problems for successful soft tissue reconstruction. However, a critical unanswered question is to what degree successful reconstruction depends on how closely the scaffold mechanical properties match soft tissue mechanical properties. Testing hypotheses concerning this question requires that we can characterize soft tissue properties with an appropriate nonlinear elastic constitutive model and engineer biomaterials with similar nonlinear elastic behavior. This scaffold engineering process remains a significant challenge in the field of soft tissue engineering due to the complex nonlinear elastic properties of these tissues.

Soft tissues from throughout the body can be modeled as “pseudoelastic”, which entails a nonlinear stress strain relationship with finite deformation under physiologic load (Fung, 1993; Humphrey, 2002). An ideal biomaterial for repairing or regenerating

these tissues should likewise display some degree of nonlinear elasticity. One of the simplest substrate for tissue engineering is a soft, gel-like material such as fibrin-thrombin gel, hydrogels or collagen gel. Fibrin has been used for cardiac (Huang et al., 2007; Ye et al., 2000), adipose (Ahmed et al., 2008) and cartilage (Fussenegger et al., 2003) applications and as a cell delivery vehicle for numerous tissue types (Bensaid et al., 2003). Fibrin has been characterized as a viscoelastic material, as have adipose and other soft tissues (Geerligs et al., 2008). However, this characterization fails to consider the nonlinear elastic properties of the tissue that are present due to the large strains experienced *in vivo*.

Collagen and hyaluronic acid (HA), which are both components of the extracellular matrix (ECM), have also been investigated for cardiac, blood vessel and adipose applications (Kofidis et al., 2002; Gentleman et al., 2006; Seliktar et al., 2000; Halbleib et al., 2003). Collagen is present in soft tissues such as skin, cartilage, myocardium and blood vessels and contains specific amino acid sequences that are recognized by cells (Lee and Mooney, 2001). It undergoes enzymatic degradation and its mechanical properties can be adjusted using chemical crosslinkers or by applying a cyclic strain (Seliktar et al., 2000). Collagen constructs can be fabricated into many different shapes including sponges, tubes and discs and are good for cell encapsulation and delivery. Gels have been fabricated with moduli ranging from 2-140 kPa (Seliktar et al., 2000; Roeder et al., 2002), which is in the range of blood vessels (120-1800 kPa) (Bergel, 1961) and myocardium (20-500 kPa) (Chen et al., 2008). Varying the stiffness of the gel has been shown to direct cell differentiation within collagen (Wang et al., 2010) and HA (Seidlits et al., 2010). HA, is a cell-friendly, elastic, non-immunogenic material with

well-characterized biocompatibility and biodegradability (Miyamoto et al., 2004) that can be manufactured into specific shapes using UV crosslinking and freeze-drying (Sakai et al., 2007). HA constructs have been manufactured to have moduli ranging from 1-500 kPa (Seidlits et al., 2010; Brigham et al., 2009). Increasing the degree of methacrylation of the HA increases the Young's modulus, as does the addition of collagen to the construct. Collagen/HA constructs have been produced to have Young's moduli of up to 800 kPa (Brigham et al., 2009), which is again in the range of soft tissues, as listed above. These features make collagen and HA attractive materials for tissue engineering. However, even with crosslinking and creating composites of the two materials, the Young's moduli of these gels are still quite low, which could jeopardize the longer-term mechanical integrity of such constructs. These materials may be best suited for cell encapsulation and delivery applications in combination with more robust scaffolds.

As described above, gels and protein based materials like collagen, elastin, and submucosa have merit for use as tissue engineering matrices. However, despite the fact that constructs made from such materials have been characterized as nonlinear elastic (Wu et al., 2006), systematic changes in these nonlinear properties are difficult to achieve. Furthermore, these materials do not allow for precise control of the internal architecture for enhancing mass transport (Radisic et al., 2005). Both of these design considerations are important for creating constructs to mimic the nonlinear elasticity and mass transport properties found in natural soft tissues. Three-dimensional scaffolds of polymeric or naturally-derived materials may be used to address these issues. A number of materials have been investigated as scaffolding materials for soft tissue applications. These include chitosan (Blan and Birla, 2007), collagen-chitosan (Zhu et al., 2009),

PLGA (Patrick et al., 2002) and PGA. Chitosan is a polysaccharide derived from sea crustaceans and scaffolds of chitosan are typically prepared via freeze-drying. The freeze-drying method creates a uniform pore distribution and allows for some control over pore size (Correia et al., 2011) and scaffold architecture. Techniques can be used in combination with freeze-drying to create regular architecture. Directional solidification was used to fabricate collagen scaffolds with regular, lamellar architecture (Von Heimburg et al., 2001), while a method of solid free form fabrication created chitosan constructs with regular lattice architectures (Geng et al., 2005). Particulate leaching and electrospinning, which produce scaffolds with either random porosity (particulate leaching and electrospinning) or uniaxial oriented porosity (electrospinning), are popular techniques for fabricating PLGA scaffolds, but solid free form fabrication techniques can also be used (Saito et al., 2010; Park et al., 2011; Roy et al., 2003). While the linear elastic moduli of these constructs may be ideal for certain applications, varying even the effective linear elastic properties of these scaffolds in a predictable, controllable manner is a challenge. Furthermore, the linear behavior of these materials makes it very difficult to create nonlinear elastic properties in scaffolds that reflect soft tissue nonlinear elasticity.

A more recently developed class of biomaterial elastomers does exhibit base nonlinear elastic behavior. These materials, including poly(1,8-octanediol-co-citrate) (POC) (Kang et al., 2006; Motlagh et al., 2007), poly(glycerol sebacate) (PGS) (Wang, 2008) and poly(glycerol dodecanoic acid) (PGD) (Migneco et al., 2009), can be engineered as scaffolds with effective nonlinear elastic behavior given their base nonlinear elastic behavior. Jeong et al manufactured 3D porous POC scaffolds for

chondrogenesis and characterized the mechanical properties using a nonlinear elastic Neo-Hookean model (Jeong and Hollister, 2010a, 2010b). Jeong et al also reported changes in nonlinear elastic behavior due to changes in POC synthesis conditions. Migneco et al similarly characterized the nonlinear elastic properties of PGD using a Neo-Hookean model (Migneco et al., 2009).

Compared to POC and PGD, less is known about the nonlinear behavior of PGS. PGS is a biodegradable, thermoset elastomer, introduced as an alternative to biodegradable polymers lacking the mechanical properties for success in soft tissue applications (Wang, 2008). PGS can be crosslinked either by exposure to UV light (Ifkovits et al., 2009) or by heat. Cross-linked PGS becomes a three-dimensional network of random coils, similar in structure to collagen and elastin, the major protein components of the extracellular matrix (Wang et al., 2002). PGS has been investigated for use in nerve, blood vessel and cartilage regeneration, and drug delivery (Sun et al., 2009; Sundback et al., 2005; Gao et al., 2007; Motlagh et al., 2006; Kempainen and Hollister, 2010). Previous work using PGS for cardiac applications focused on how fluid flow and oxygen perfusion affect cardiac regeneration (Radisic et al., 2006; Marsano et al., 2008; Engelmayer et al., 2008). Initial material studies did not characterize PGS as a nonlinear elastic material or the effect of curing conditions on nonlinear elastic behavior (Wang et al., 2002). Engelmayer et al. (2008) further characterized the mechanical properties of PGS scaffolds but did not address PGS's nonlinear behavior. Characterizing the nonlinear elasticity of this material will allow for the design of scaffolds that approximate the mechanical properties of the soft tissues for which they are being developed (Janz and Grimm, 1973; Humphrey, 2002).

Here we investigated the effect of curing time and temperature on the nonlinear elastic properties and maximum strain of PGS. We hypothesized that by changing the curing conditions of PGS, these properties could be tuned to match the properties of various soft tissues. First, we assessed bulk material nonlinear elastic properties by tensile testing solid specimens of PGS. To examine how porosity affects the nonlinear elastic response of the material, we characterized porous PGS constructs formed in the shape of tensile test bars, the first time that this has been achieved. PGS sponges made by salt fusion (Murphy et al., 2002) represent the simplest scaffolds and thus acted as our porous tensile testing constructs. The tensile data were fit to a Neo-Hookean model for quantitative comparisons to soft tissues (Janz and Grimm, 1973; Nardinocchi and Teresi, 2007).

A.2 Materials and Methods

A.2.1 PGS Synthesis and Tensile Specimen Fabrication

PGS was synthesized as previously described (Wang et al., 2002). Briefly, equimolar amounts of glycerol and sebacic acid were mixed at 120°C under nitrogen for 24 hours and then placed under 30 mTorr vacuum at 120°C for 48 hours as depicted in Figure 1. The resulting pre-polymer (pre-PGS) was cured in a Teflon mold, shaped according to ASTM standard D-412a for tensile testing vulcanized rubber and thermoplastic elastomers (International, 2002), under five combinations of time and temperature: 120°C for 48 hours (“120deg/48h”); 120°C for 72 hours (“120deg/72h”), 120°C for 96 hours (“120deg/96h”), 135°C for 48 hours (“135deg/48h”) and 150°C for 48 hours (“150deg/48”). Previous research (Wang et al., 2002) and preliminary work by our group indicate that the polymer will not cure at temperatures below 120°C, which

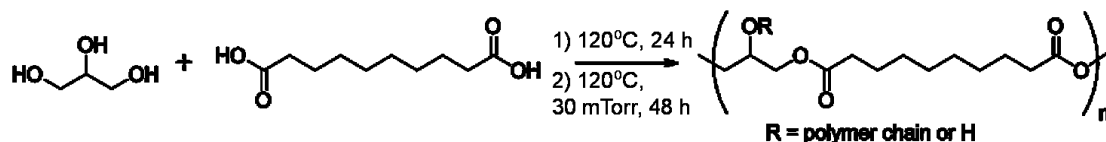


Figure A.1: Reaction scheme for poly(glycerol sebacate). The polymer is synthesized from glycerol and sebacic acid in a two-step process: 24 hours at 120°C followed by 48 hours at 120°C under 30 mTorr vacuum.

aided in the selection of curing conditions giving a range of PGS properties (tangential modulus and maximum strain) meaningful for soft tissue applications (Bergel, 1961; Watanabe et al., 2006). Three conditions are at a fixed temperature, varying only time, while three hold time fixed, varying temperature, enabling rigorous examination of the effects of time or temperature on the properties of the polymer. Porous tensile strips were made by packing 106-125 μm salt particles into the gage section of a Teflon mold and placing the mold in a humidity (95%) chamber overnight to fuse the salt (Murphy et al., 2002). A 5% w/v solution of PGS in Tetrahydrofuran (THF) was added to the fused salt until saturation was reached and the THF was evaporated. Pre-PGS was melted at 90°C and then added to the tabs of the tensile specimens to create solid portions for gripping the specimens during testing. The strips were cured under the same conditions as for solid specimens. After curing, the salt was leached out in reverse-osmosis water for 12 hours and the specimens were dried in a vacuum oven for three days. This salt fusion method yielded specimens with a gage section of interconnected pores (Murphy et al., 2002) and 84% porosity (see Section 3.4 for calculation), with solid tabs to enable tensile testing with a large scale mechanical testing system. Cylindrical sections of the gage sections were obtained using a 6 mm biopsy punch. The sections were gold-coated and their pore structure imaged using scanning electron microscopy (Hitachi S3200N Variable Pressure

Scanning Electron Microscope, Hitachi High Technologies America, Inc., Pleasanton, CA 94588).

A.2.2 Tensile Testing

Solid and porous PGS specimens were tested in tension to failure using an MTS RT/Alliance mechanical test frame (500 N load cell, MTS Systems, Corp., Eden Prairie, MN) to determine nonlinear elastic properties, tangential Young's tangential modulus (slope of the tangent to the stress-strain curve at 12.5% strain) and failure strain (N = 6 per curing condition, per tensile testing condition). Both solid and porous specimens were tested dry, at room temperature ("dry") and wet at 37°C ("wet") (to mimic *in vivo* conditions) at a loading rate of 50 mm/min, as per ASTM standard D-412a (International, 2002). For the "wet" tests, specimens were soaked in PBS for 24 hours, blotted dry, and tested in a custom built heating chamber that kept the specimens at 37°C for the duration of the tensile test. Additional solid, dry specimens were also tested at a loading rate of 120 mm/min to examine possible strain rate effects.

A.2.3 Swelling of PGS

The swelling percentage and cross-linking density of solid and porous PGS samples were measured using the method previously described by Chen et al. (2008). Solid and porous specimens of PGS cured under the five curing conditions (120deg/48h, 120deg/72h, 120deg/96h, 135deg/48h, 150deg/48h) were cut with a biopsy punch to yield cylinders with a diameter of 6 mm and a height of 1.5 mm (N = 3 per group). The samples were weighed to obtain initial dry weight, m_o , and then placed in THF. The specimens were weighed each day until no measureable weight increase was observed (this occurred on day 3). At this time, the equilibrium weight was measured, m_{eq} . The

specimens were then placed in a 25°C oven for one week after which the dry weight, m_d , was measured. Swelling percentage and crosslinking density were obtained from the swelling experiments for both solid and porous specimens of PGS cured under the five curing conditions. Swelling percentage was calculated as:

$$(m_{eq} - m_d)/m_d \quad (1)$$

Where m_{eq} is mass of the swollen network at equilibrium (after the polymer has been allowed to swell fully) and m_d is mass of the dried network after extraction of soluble materials (after drying in a vacuum oven at 25°C for one week). Crosslinking density was calculated for each sample using the following two equations (Chen et al., 2008):

$$v = \frac{\ln(1-v_2)+v_2+\chi v_2^2}{v_1(\frac{v_2}{2}-v_2^{\frac{1}{3}})} \quad (2)$$

$$v_2 = \left[1 + \left(\frac{m_{eq}-m_d}{m_d}\right) \left(\frac{\rho_2}{\rho_1}\right)\right]^{-1} \quad (3)$$

Where v is strand density, v_2 is the volume fraction of polymer at equilibrium swelling (obtained from swelling percentage), χ is the polymer-solvent interaction parameter, v_1 is the molar volume of solvent, and ρ_1 and ρ_2 are the densities of the polymer and solvent, respectively. Crosslinking density is equal to $v/2$.

A.2.4 Neo-Hookean Model Fitting

Stress-strain data from tensile tests performed on solid PGS were fit to a Neo-Hookean non-linear elastic model:

$$W(\lambda_1, \lambda_2, \lambda_3) = \frac{\mu_1}{2} (\lambda_1^2 + \lambda_2^2 + \lambda_3^2 - 3) \quad (4)$$

W is the strain energy function; λ_1 , λ_2 , and λ_3 are stretch ratios; and μ_1 is a material constant fit to experimental data. Matlab was used to fit μ_1 for each combination of curing

condition and testing condition, either dry or wet. R-squared values of the fits were used to assess how well the model fit the data. To validate the incompressibility assumption needed to use this model, the gage section volume change was assessed as PGS specimens were tested in tension. At various strain points (5%, 20%, 40%, 60%) the test was paused and the length, width and thickness of the specimen were measured using a digital caliper.

To aid in our analysis of the porous tensile testing results, we also estimated μ for the porous specimens, μ_{pr} , using a Voight model, as $v_s\mu_1$, where v_s is sponge volume fraction and μ_1 is the fitted Neo-Hookean parameter for solid PGS (Hashin, 1985). Sponge volume fraction was calculated by first determining the porosity, n , of the sponges, as v_v/v_T , where v_v = void volume, or volume of NaCl and v_T = total volume. The volume of NaCl can be calculated for a defined shape using the packing density and density of NaCl, defined as 0.84 and 2.16 g/cm³, respectively. For the gage sections of the tensile specimens, porosity (n) was calculated to be 0.84. Sponge volume fraction v_s , is then simply $(1-n)$, or 0.16.

A.2.5 Statistical Analysis

Multiple linear regression, performed using SPSS software (SPSS for Windows, Rel 14.0. 2005, SPSS, Inc., Chicago, IL), was used to determine which factors (curing condition, wet or dry testing, strain rate) had a significant effect on a given response variable (tangential modulus, Neo-Hookean constant, maximum strain, crosslinking density).

A.3 Results

A.3.1 Tensile Testing of Solid PGS

Representative stress-strain curves for solid and porous PGS specimens cured under the five curing conditions and tested dry at 50 mm/min are displayed in Figure 2, solid specimens in Figure 2a and porous specimens in Figure 2b. The shapes of the curves appear to be more nonlinear for porous specimens, although this was not the case for all curing conditions. The average tangential moduli taken at 12.5% strain are displayed in Figure 3. For solid specimens, the general trend was an increase in tangential modulus as curing time and temperature increased going from curing condition 120deg/48h to curing condition 150deg/48h. For the solid specimens tested dry, tangential modulus was significantly different between all groups except 120deg/48h and

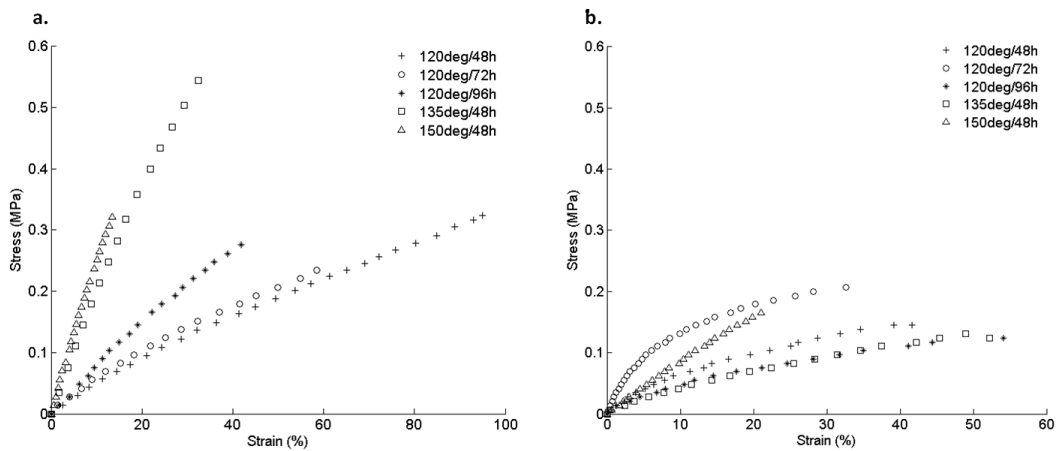


Figure A.2: Representative stress-strain curves for solid (a) and porous (b) specimens tested dry at 50 mm/min.

120deg/72h. For specimens tested wet, significant differences occurred between all curing conditions except between 120deg/48h and 120deg/72h and between 120deg/96h and 135deg/48h. Specimens cured at 120deg/48h and tested wet had a significantly

lower tangential modulus ($p \leq 0.01$) than their dry counterparts. This behavior was expected and was also true for specimens cured at 120deg/72h ($p \leq 0.01$) and 135deg/48h ($p \leq 0.05$).

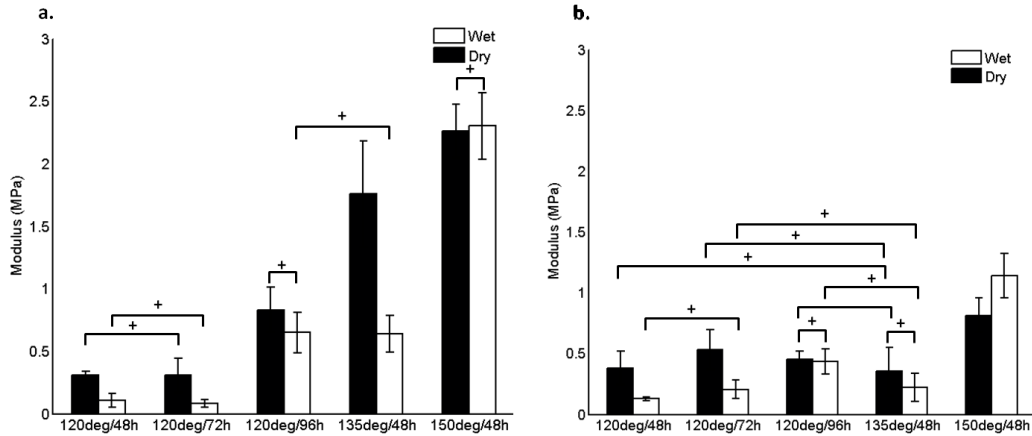


Figure A.3: Modulus for specimens tested at 50 mm/min. (a) Solid specimens tested dry and wet; (b) Porous specimens tested dry and wet. +no significance, all other comparisons significant at $p < 0.05$

The maximum strain for solid specimens, displayed in Figure 4a, decreased as curing time and temperature increased. This was only a general trend and not all differences between subsequent curing conditions were significant. For the dry specimens, increasing the temperature while keeping the curing time constant at 48 hours resulted in a significant decrease in maximum strain when the temperature was increased from 120°C to 135°C, but there was no difference going from 135°C to 150°C. Increasing curing time while keeping temperature constant at 120°C was significant only when the time was increased to 96 hours; no difference occurred when increasing curing time from 48 hours to 72 hours. For the specimens tested wet, we expected the overall maximum strain values to be higher than those for the dry specimens. However, only the 120deg/48h curing condition resulted in a significant increase in maximum strain for the wet testing condition versus the dry condition.

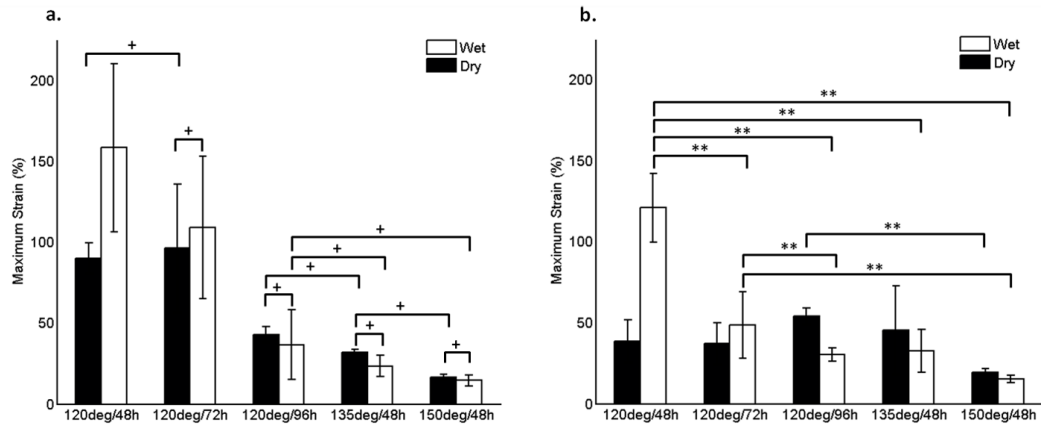


Figure A.4: Maximum (failure) strain for specimens tested at 50 mm/min. (a) Solid specimens tested dry and wet; +no significance. All other comparisons are significant at $p \leq 0.05$. (b) Porous specimens tested dry and wet. * $p \leq 0.05$, ** $p \leq 0.01$.

Strain rate effects on PGS mechanical properties were determined by testing solid samples at 120 mm/min for each of the five curing conditions (see Figure 5). Note that only significance *between* strain rates for a given curing condition is shown. There was a significant increase in tangential modulus for specimens tested at 120 mm/min, compared to 50 mm/min, for the 120deg/48h ($p \leq 0.01$) and 135deg/48h curing conditions ($p \leq 0.05$). For the maximum strain data, the only significant difference observed was for the

150deg/48h condition.

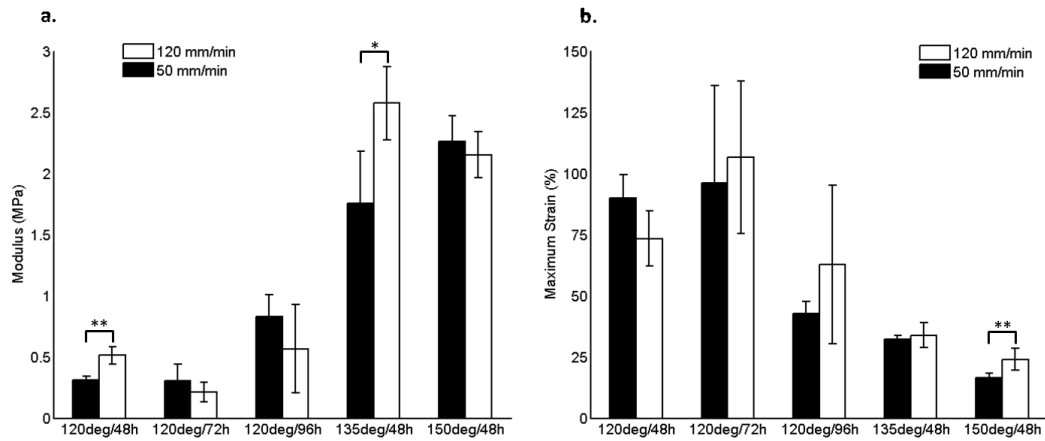


Figure A.5: Modulus (a) and maximum strain (b) of solid specimens tested at 50 mm/min and 120 mm/min. Only comparisons between strain rates are shown. * $p < 0.05$, ** $p < 0.01$.

A.3.2 Tensile Testing of Porous PGS

Tensile specimens with porous gage section were successfully manufactured. The gage sections had a porous, sponge-like architecture, as displayed in the scanning electron microscopy images in Figure 6. Porous specimens did not display the same trends as solid specimens, although there were some similarities between solid and

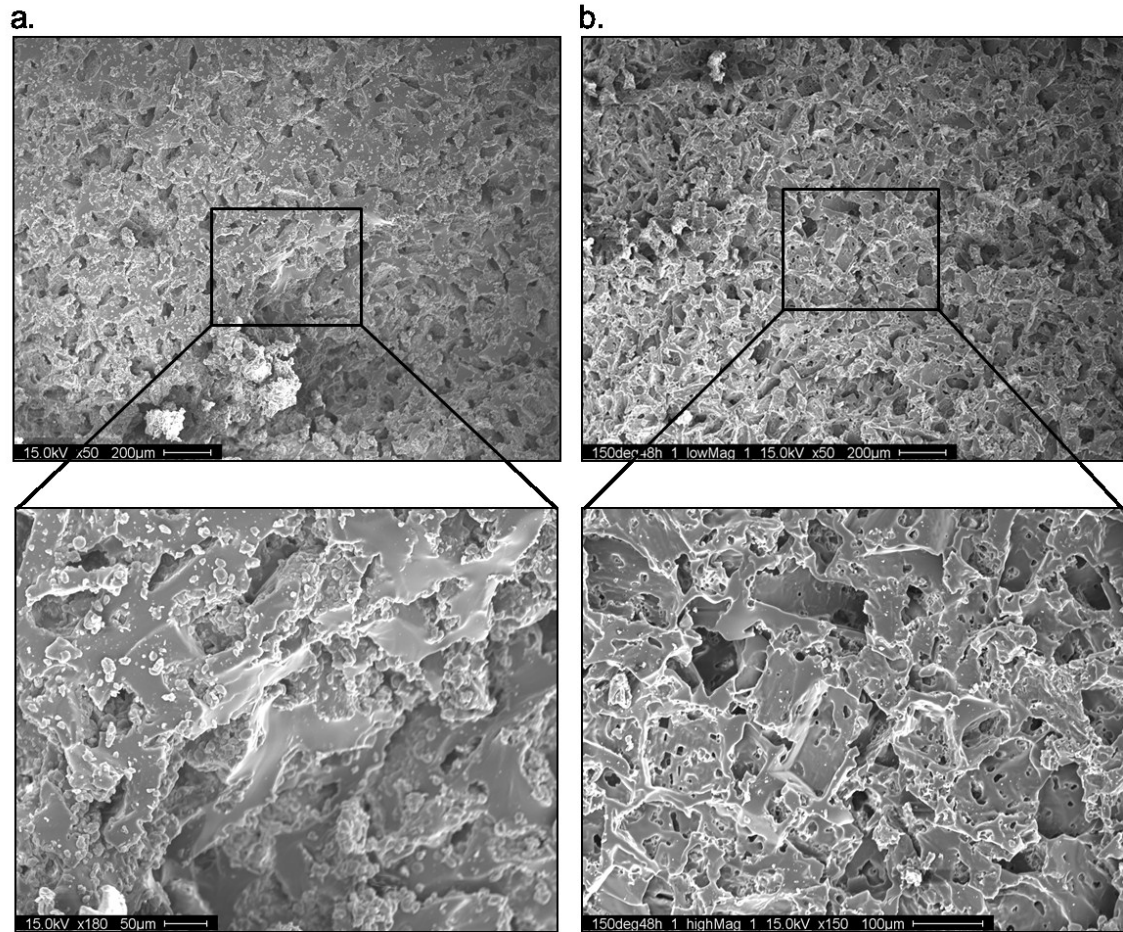


Figure A.6: Scanning electron microscopy (SEM) images of porous gage sections from PGS tensile testing specimens. Representative images from two curing conditions. (a) 120°C, 72h and (b) 150°C, 48h.

porous behavior. For both wet and dry testing conditions, the porous specimens cured at 150deg/48h had a significantly greater average tangential modulus than specimens cured under all other conditions (Figure 3b). No other significant differences occurred between curing conditions for specimens tested dry. For the wet testing condition, the 120deg/48h curing condition showed a significantly lower moduli than the 120deg/96h condition, suggesting that, like the solid specimens, the curing time must be increased beyond 48 hours for a difference in properties to be observed at a curing temperature of 120°C. The maximum strain data (Figure 4b) for porous specimens tested wet show more similarities to the solid data than the tangential modulus data. The 120deg/48h group displayed the

greatest maximum strain ($p \leq 0.01$ for all comparisons) and the 120deg/72h condition resulted in a greater maximum strain than both the 120deg/96h and the 150deg/48h groups. The porous specimens tested dry displayed few differences in maximum strain between groups (only 150deg/48h and 120deg/96h were significantly different).

Comparisons between porous and solid specimens (not displayed on figures) indicate that for specimens tested dry, solid specimens had significantly greater tangent moduli ($p \leq 0.01$) than their porous counterparts for every curing condition except 120deg/48h. For specimens tested wet, this was only true for conditions 135deg/48h and 150deg/48h.

A.3.3 Swelling Percentage and Crosslinking Density

The results from the swelling experiment are displayed in Figure 7, swelling percentage in 7a and crosslinking density in 7b. For the solid samples, swelling percentage decreased as curing time and temperature increased, except for the anomalous result seen for 120deg/48h. This trend persisted in general for the porous samples,

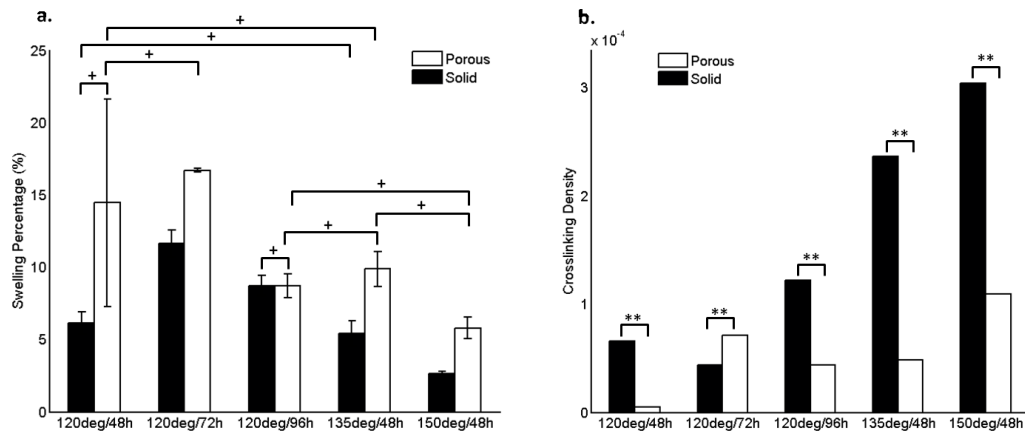


Figure A.7: Swelling percentage and crosslinking density. a. Swelling percentage of solid and porous specimens. + signifies no significance. Comparisons not marked as “not significant” are significant at $p \leq 0.01$ for all comparisons except 150deg/48h/porous v. 150deg/48h/Solid and 120deg/48h v. 120deg/96h (porous), which are significant at $p < 0.05$. b. Crosslinking density of solid and porous specimens. ** $n < 0.01$

although the 120deg/48h and 120deg/96h specimens had lower than expected values and the 120deg/48h group had a notably large standard deviation. Swelling percentage was significantly greater for the porous samples than for their solid counterparts for all curing conditions except 120deg/96h and 120deg/48h. For 120deg/72h, the porous samples had a greater swelling percentage than their solid counterparts, as expected, but also a greater crosslinking density, which was not expected. It is notable that for this condition, the average tangential modulus of porous specimens was greater than the average tangential modulus of solid specimens. This may have been due to a manufacturing defect seen in the samples in which a thin layer of solid PGS formed along the porous gage sections, increasing tangential modulus but not necessarily affecting swelling percentage. To account for this solid film, we recalculated the solid volume fraction of the tensile strip gage section to incorporate both the solid and porous sections. We then multiplied this value by the solid Neo-Hookean parameter to estimate the porous material response, as described below.

A.3.4 Neo-Hookean Model Fitting

Gage section volumes changed by less than 3%, validating incompressibility as assumed by the Neo-Hookean model. Stress vs. strain plots for solid and porous specimens tested dry at 50 mm/min are shown in Figure 8 and Figure 9, respectively. Values of μ_1 fit to the data (for both the dry and wet testing condition) are displayed in Figures 8f (solid) and 9f (porous) for the five conditions. R-squared values are also shown in 8f and 8l and show that for most samples, the Neo-Hookean model fit the data well. Regardless of testing condition (wet or dry), no differences in μ_1 occurred between solid and porous specimens cured at 120deg/48h and 120deg/96h. For 120deg/72h, the

porous samples had a significantly greater value of μ_1 than their solid counterparts, an anomaly which reflects the unexpected tangential moduli and crosslinking density data for samples cured under this condition. The values of μ_1 for the porous data were less than the values of μ_1 obtained for their solid counterparts for the 135deg/48h and

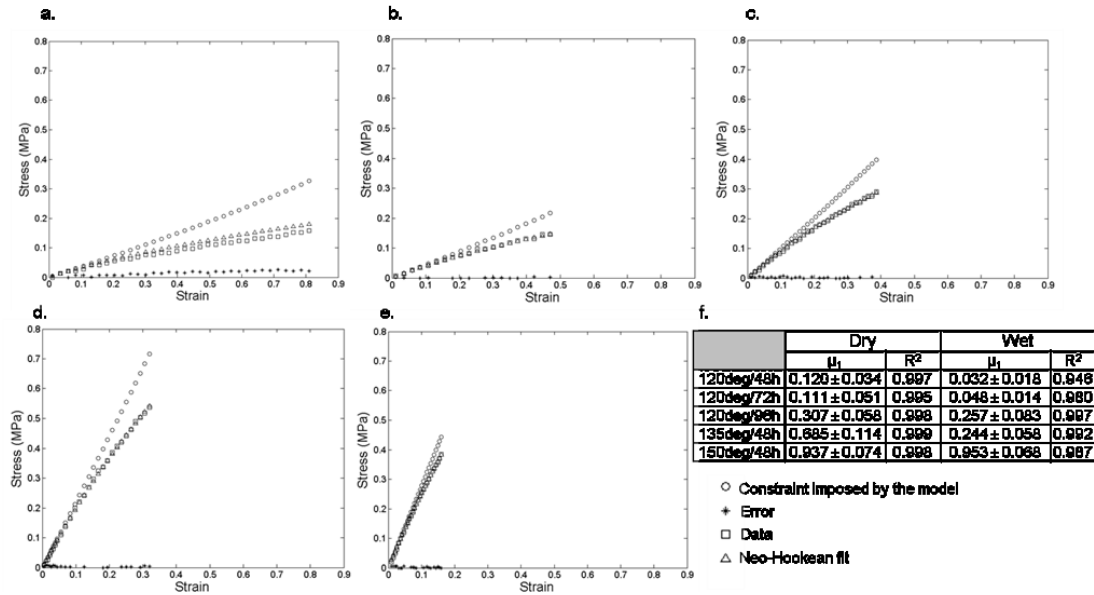


Figure A.8: Solid data fit to a nonlinear elastic Neo-hookean model. Representative fits are shown for specimens tested dry and cured at 120deg/48h (a), 120deg/72h (b), 120deg/96h (c), 135deg/48h (d) and 150deg/48h (e). Values of μ_1 (average \pm standard deviation) and R-squared values for each curing condition tested wet and dry are shown in (f).

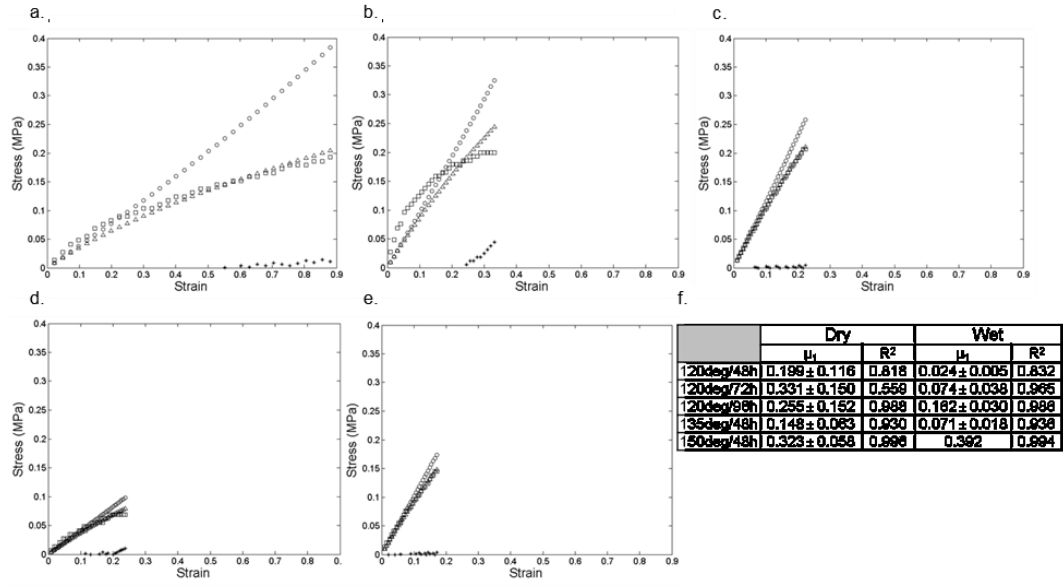


Figure A.9: Porous data fit to a nonlinear elastic Neo-hookean model. Representative fits are shown for specimens tested dry and cured at 120deg/48h (a), 120deg/72h (b), 120deg/96h (c), 135deg/48h (d) and 150deg/48h (e). Values of μ_1 (average \pm standard deviation) and R-squared values for each curing condition tested wet and dry are shown in (f).

150deg/48h curing conditions. Thus, as curing temperature increases to 135°C and 150°C, the differences between solid and porous behavior become more pronounced.

To aid in our analysis of the porous tensile testing results, we also calculated predicted μ for the porous specimens, μ_{pr} as $\nu_s \mu_1$, where ν_s is sponge volume fraction and μ_1 is the fitted Neo-Hookean parameter for solid PGS (see Section 3.4). These predicted μ values for the porous specimens act as a prediction for the experimentally obtained tangential moduli. The expected and actual moduli for the porous specimens cured under the five curing conditions and tested at 50 mm/min are shown in Table 1 for specimens tested dry and in Table 2 for specimens tested wet. The actual moduli of the porous specimens were greater than predicted for all conditions, although the percent difference between predicted and actual tangential modulus was considerably less for 135deg/48h and 150deg/48h, than for the three conditions cured at 120°C. As described

in the previous section, the manufacturing of porous samples resulted in the existence of a thin, solid layer of PGS along the gage section of all specimens. To account for this

Dry, 50 mm/min			$V_f = 0.16$		$V_f = 0.328$	
	μ_1 , solid	μ_1 , porous	μ_1 , porous, predicted	% Difference	μ_1 , porous, predicted	% Difference
120deg/48h	0.107	0.199	0.019	165%	0.039	134%
120deg/72h	0.114	0.331	0.018	180%	0.037	160%
120deg/96h	0.310	0.255	0.049	135%	0.101	86.7%
135deg/48h	0.684	0.148	0.110	29.7%	0.225	-41.2%
150deg/48h	0.945	0.323	0.150	73.2%	0.307	5.02%

Table A.1: Expected and actual moduli for the porous specimens cured under the five curing conditions and tested dry at 50 mm/min.

Wet, 50 mm/min			$V_f = 0.16$		$V_f = 0.328$	
	μ_1 , solid	μ_1 , porous	μ_1 , porous, predicted	% Difference	μ_1 , porous, predicted	% Difference
120deg/48h	0.032	0.024	0.005	129%	0.011	76.90%
120deg/72h	0.048	0.074	0.008	163%	0.016	130%
120deg/96h	0.257	0.162	0.041	119%	0.084	63.00%
135deg/48h	0.244	0.071	0.039	58.30%	0.08	-11.80%
150deg/48h	0.953	0.392	0.153	88.00%	0.313	22.60%

Table A.2: Expected and actual moduli for the porous specimens cured under the five curing conditions and tested wet at 50 mm/min.

solid film, an “effective solid volume fraction” was calculated to be 0.328. The solid layer accounted for approximately 20% of the gage section thickness and by incorporating this solid portion, the volume fraction of solid material more than doubled, from 0.16 to 0.328. Using this solid volume fraction estimate, the predicted μ_1 values dropped and were closer to the actual values obtained from fitting the data to the Neo-Hookean model, as shown in Tables 1 and 2.

A.4 Discussion

The characterization of PGS’s mechanical properties is an important step in examining its feasibility for soft tissue applications, since mechanical and architectural

properties of tissue engineered scaffolds will influence cell adhesions and tissue formation. PGS has been studied for many specific tissue applications, from cardiac tissue (Park et al., 2011; Marsano et al., 2010) to cartilage (Kemppainen and Hollister, 2010) and adipose tissue. Part of the appeal of using PGS is having the ability to tune its mechanical properties (Ifkovits et al., 2009; Marsano et al., 2010). Here we demonstrate the ability to tune both solid and porous construct properties through curing and show how these material responses can be modeled by a commonly used nonlinear elastic model for comparison to native soft tissue properties.

A.4.1 Tensile Testing of Solid and Porous PGS

It is important to examine the tensile behavior of a material being investigated for use in soft tissue regeneration as many soft tissues are subjected to tensile force. Previous work on the properties of PGS only examined one curing condition, or looked at the effect of varying the pre-polymer synthesis conditions, and did not characterize the nonlinear elastic behavior of PGS (Patrick et al., 2002; Engelmayr et al., 2008). It was shown that the tensile properties of PGS depended on pre-polymer synthesis temperature. We present the differences in bulk material tensile properties obtained by varying the time and temperature of polymer curing, which affects crosslinking and largely determines mechanical properties. A range of nonlinear elastic properties, tangential modulus and strain at break were obtained by altering only the curing condition. PGS cured at a lower temperature for a shorter amount of time yielded a tangential modulus of 0.11 MPa, close to that of blood vessels and myocardium (Bergel, 1961; Chen et al., 2008). When cured for longer at a higher temperature, a tangential modulus of 2.26 MPa was achieved, which is within the range for collagen that is found in tendon (Misof et al.,

1997). This ability to tune PGS's properties can be used in conjunction with other design variables to optimize scaffolds for particular soft tissue applications.

The relationships among tangential modulus and maximum strain for the solid specimens cured under the five curing conditions were expected since longer curing times and higher temperatures result in a stiffer, more crosslinked material. For the 50 mm/min strain rate, the moduli are significantly different for all of the curing conditions except between 120deg/48h and 120deg/72h. This lack of significant difference may be due to the fact that the material cured at 120°C for 48 hours was just barely cured, so increasing the time another 24 hours did not greatly affect the material's properties. While the tangential modulus values of solid PGS fell within the range of moduli observed for many soft tissues, these values were still not as low as those of adipose tissue (Stacey et al., 2009).

We tested solid PGS at two different strain rates (50 mm/min and 120 mm/min) to examine strain rate effects on PGS mechanical properties. Many soft biological tissues display some degree of viscoelasticity causing the tissue to become stiffer as strain rate increases (Kempainen and Hollister, 2010; Marsano et al., 2008; Janz and Grimm, 1973). The increase in tangential modulus between strain rates for the 120deg/48h and 135deg/48h conditions is similar to the rate dependent strain stiffening effect that is seen in some soft tissue responses (Fung, 1993). From these data, it appears as though PGS may demonstrate a degree of strain stiffening, and hence viscoelasticity, depending on the curing condition. However, the effect of strain rate on tangential modulus was not significant for the other three curing conditions, suggesting that the effect of curing condition on tangential modulus is greater than the effect of strain rate.

A scaffold for tissue regeneration will be porous, necessitating an examination of how porosity changes bulk material properties. As seen in Table 1, there was a difference between the predicted and experimental porous tangential moduli. This discrepancy can be attributed in part to the Voigt model used to calculate the tangential modulus. This model predicts the absolute upper bound on linear and nonlinear elastic properties for a composite material (Hashin, 1985), so the actual tangential modulus of a porous specimen is expected to be less than predicted. Tangential modulus was higher than predicted for all curing conditions and the relationship between the curing conditions was not as expected. Although specimens cured at 150°C for 48h (150deg/48h) had greater tangential moduli than specimens cured under any other conditions, as expected, there were no other significant differences between groups, meaning the porous data did not display the same trend as the solid data. These unusual results may be due to the manufacturing process. The porosity of the sponges is high and only a small amount of PGS actually exists in the scaffolds, since a 5% solution of PGS in THF is used to manufacture them. Taken together, these factors may diminish the effect of curing on the tangential modulus of porous specimens. We also noticed that there were greater differences in tangential moduli and more dependence on curing condition for porous specimens tested “wet”. Soaking the specimens in PBS to create this “wet” testing condition may have swelled the polymer network to elucidate differences between the curing conditions that were not apparent when testing the specimens at room temperature under dry conditions.

We found that a thin layer of PGS formed across the top of all porous specimens during curing. This may have had the greatest effect on tangential modulus, and could

explain the higher than predicted moduli and the lack of significant differences between groups. When a new solid volume fraction was calculated that accounted for this solid film, the difference between the predicted and actual values for μ_1 for the porous samples decreased for all curing conditions. Thus, accounting for the solid film along the porous gage sections resulted in more realistic predictions of μ_1 and shows that this solid film was most likely having a significant effect on the tensile properties of the porous specimens.

The porous moduli for the 120deg/72h, 120deg/96h, 135deg/48h and 150deg/48h conditions were significantly less than the respective solid moduli for these conditions, as expected. However, there is no significant difference between solid and porous moduli for specimens cured under the 120deg/48h condition. Again, we believe the manufacturing process for these particular porous scaffolds may explain why the tangential modulus values for porous specimens were not as low as predicted. According to Murphy et al., NaCl used for particulate leaching that was fused for 24 hours resulted in solvent cast PLG scaffolds with higher compressive moduli, compared to scaffolds made without salt fusion and scaffolds made with salt fused for less time (Murphy et al., 2002). The salt fusion process may increase the mechanical properties of the scaffolds compared to scaffolds manufactured without salt fusion and may explain why there is no significant difference between the solid and porous moduli for the 120deg/48h condition. Another possible explanation for why some of the porous specimens had higher moduli than their solid counterparts is that the degree of polymer curing was greater for these specimens due to the small diameter polymer connections between pores. We tested this hypothesis by curing (and tensile testing) solid PGS specimens with decreasing gage

section thicknesses, to mimic the decreased amount of polymer material in porous specimens. For the 120deg/72h condition, decreasing the gage section thickness by 25% resulted in a 28% increase in tangential modulus. These results are only preliminary but suggest that for certain curing conditions, the polymer material within the porous specimens may actually form more crosslinks, resulting in stiffer mechanical properties than are observed for solid specimens.

A.4.2 Swelling Percentage and Crosslinking Density

To further investigate why the tensile behavior of the porous specimens differed from what was predicted, a swelling experiment was performed to see if polymer crosslinking was altered. A higher crosslinking density means a lower swelling percentage, corresponding to a stiffer material in the case of elastomers such as PGS. The solid specimens displayed this relationship between swelling percentage and crosslinking density – greater swelling % corresponding to lower crosslinking density as curing time and temperature decreased. For the porous data, the behavior was not as straight forward, and is highlighted by two particularly notable anomalies. The first is that crosslinking density was significantly greater for porous samples cured at 120deg/72h, compared to their solid counterparts. This result mirrors the tensile testing results whereby the 120deg/72h curing condition resulted in a greater average tangential modulus value for porous compared to solid specimens. This increased crosslinking and subsequent increased tangential modulus may be due to a greater degree of polymer curing for the porous specimens due to the small diameter polymer connections between pores (as discussed in Section 5.1).

The second unexpected result was that the average swelling percentage for the porous 120deg/96h specimens was nearly identical to that of their solid counterparts. This is unexpected since the crosslinking density of the porous specimens is much lower than the solid specimens, as we expected. These particular samples may have had a more pronounced manufacturing artifact in the form of a thicker coating of solid PGS along the gage section. This would more greatly affect the swelling percentage measurement since this was based purely on observed changes in mass, as opposed to a formulaic calculation.

A.4.3 Neo-Hookean Modeling

We modeled the nonlinear elasticity of PGS since most soft tissues are modeled as incompressible nonlinear elastic materials. For instance, a nonlinear Neo-Hookean model has been used to represent the passive, isotropic ground matrix of myocardium, making this model appropriate for modeling PGS to determine if it behaves similarly to myocardium (Humphrey, 2002). Results demonstrated that PGS could be fit well with a nonlinear elastic Neo-Hookean model, since R-squared values were greater than 0.95 for most tests (see Figure 8). Out of the twenty conditions tested and modeled with the Neo-Hookean model, only five had R-squared values below 0.95 – 120deg/48h porous/dry, 120deg/72h porous/dry, 135deg/48h porous/dry, 120deg/48h porous/wet, and 135deg/48h porous/wet. These conditions may be better modeled using an Ogden model. In general though, these results demonstrate that the behavior of PGS can be modeled as a classic nonlinear elastic material, assuming isotropy and incompressibility.

The fits of the tensile data to the Neo-Hookean model illustrate how curing condition and strain rate affect PGS's mechanical properties. In the model, μ_1 is a

material constant that can be fit to experimental data to describe the shear modulus. The value of μ_1 increases as the material becomes more cross-linked and stiffer. We obtained a value for μ_1 for solid and porous specimens cured under each curing condition and tested at 50 mm/min, as shown in Figure 8. For the solid data the values of were significantly different between all curing conditions, except between 120deg/48h and 120deg/72h, paralleling the differences in tangential modulus obtained from analyzing the tensile tests (see Figure 3). For the porous data, μ_1 for 135deg/48h was significantly less than for conditions 120deg/72h and 150deg/48h, and μ_1 for 150deg/48h was greater than for 135deg/48h, also paralleling the tangential modulus data. When comparing values of μ_1 between solid and porous specimens for each curing condition, the solid values were always significantly greater than the porous values, except for the 120deg/48h and 120de/72h.

A.5 Conclusion

Poly(glycerol sebacate) can be cured under various conditions to produce materials with varying mechanical properties. These properties can be modeled using a non-linear elastic Neo-Hookean model that has also been used for modeling the isotropic ground substance of soft tissue nonlinear behavior. This will allow future studies designing PGS scaffolds to match the passive nonlinear elastic properties of soft tissues. Incorporating random porosity through salt fusion yields a scaffold that can be used to support cells. Introduction of porosity also decreases the nonlinear elastic properties of PGS. Future studies include comparing PGS properties to other biological tissue types and designing and characterizing PGS scaffolds for regenerating these tissues.

A.6 Acknowledgments

Thank you to Jessica M. Kemppainen for her assistance with PGS synthesis and curing. Anna Mitsak was funded by a National Science Foundation Graduate Research Fellowship.

A.7 References

- Ahmed, T.A., Dare, E.V., Hincke, M., 2008. Fibrin: a versatile scaffold for tissue engineering applications. *Tissue Eng. B* 14(2), 199-215.
- Batista, R.J.V., Verde, J., Nery, P., Bocchino, L., Takeshita, N., Bhayana, J.N., Bergsland, J., Graham, S., Houck, J.P., Salerno, T.A., 1997. Partial left ventriculectomy to treat end-stage heart disease. *Ann. Thorac. Surg.* 64, 628-634.
- Bensaid, W., Triffitt, J.T., Blanchat, C., Oudina, K., Sedel, L., Petite, H., 2003. A biodegradable fibrin scaffold for mesenchymal stem cell transplantation. *Biomater.* 24(14), 2497-2502.
- Bergel, D.H. 1961. The static elastic properties of the arterial wall. *J. Physiol.* 156, 445-57.
- Blan, N.R., Birla, R.K. 2007. Design and fabrication of heart muscle using scaffold-based tissue engineering. *J. Biomed. Mater. Res. A* 86A(1),195-208.
- Brigham, M.D., Bick, A., Lo, E., Bendali, A., Burdick, J.A. Khademhosseini, A. 2009. Mechanically robust and bioadhesive collagen and photocrosslinkable hyaluronic acid semi-interpenetrating networks. *Tissue Eng.* 15(00), 1-9.
- Chen, Q.Z., Bismarck, A., Hansen, U., Junaid, S., Tran, M.Q., Harding, S.E., Ali, N.N., Boccaccini, A.R. 2008. Characterisation of a soft elastomer poly(glycerol

- sebacate) designed to match the mechanical properties of myocardial tissue. *Biomater.* 29, 47-57.
- Engelmayr, G.C., Cheng, M., Bettinger, C.J., Langer, R., Freed, L.E. 2008. Accordion-like honeycombs for tissue engineering of cardiac anisotropy. *Nat. Mater.* 7, 1003-1010.
- Flynn, L.E., Prestwich, G.D., Semple, J.L., Woodhouse, K.A. 2008. Proliferation and differentiation of adipose-derived stem cells on naturally derived scaffolds. *Biomater.* 29, 1862-1871.
- Fujimoto, K.L., Tobita, K., Merryman, W.D., Guan, J., Momoi, N., Stolz, D.B., Sacks, M.S., Keller, B.B., Wagner, W.R. 2007. An elastic, biodegradable cardiac patch induces contractile smooth muscle and improves cardiac remodeling and function in sub-acute myocardial infarction. *J. Am. Coll. Cardiol.* 49, 2292-2300.
- Fung, Y.C. 1993. *Biomechanics: Mechanical Properties of Living Tissues*, second ed. Springer-Verlag, New York.
- Fussenegger, M., Meinhart, J., Hobling, W., Kullich, W., Funk, S., Bernatzky, G. 2003. Stabilized autologous fibrin-chondrocyte constructs for cartilage repair in vivo. *Ann. Plast. Surg.* 51(5), 493-498.
- Gao, J., Ensley, A.E., Nerem, R.M., Wang, Y. 2007. Poly(glycerol sebacate) supports the proliferation and phenotypic protein expression of primary baboon vascular cells. *J. Biomed. Mater. Res. A* 83A, 1070-1075.
- Geerligts, M., Peters, G.W.M., Ackermans, P.A.J., Oomens, C.W.J., Baaijens, F.P.T. 2008. Linear viscoelastic behavior of subcutaneous adipose tissue. *Biorheol.* 45, 677-688.

- Geng, L., Feng, W., Hutmacher, D.W., Wong, Y.S., Loh, H.T., Fuh, J.Y.H. 2005. Direct writing of chitosan scaffolds using a robotic system. *Rapid. Prototyp. J.* 11(2), 90-7.
- Gentleman, E., Nauman, E.A., Livesay, G.A., Dee, K.C. 2006. Collagen composite biomaterials resist contraction while allowing development of adipocytic soft tissue in vitro. *Tissue Eng.* 12(6), 1639-1649.
- Halbleib, M., Skurk, T., de Luca, C., von Heimburg, D., Hauner, H. 2003. Tissue engineering of white adipose tissue using hyaluronic acid-based scaffolds I: in vitro differentiation of human adipocyte precursor cells on scaffolds. *Biomater.* 24, 3125-3132.
- Hashin, Z. 1985. Large isotropic elastic deformation of composites and porous media. *Int. J. Solids Struct.* 21, 711-720.
- Huang, Y.C., Khait, L., Birla, R.K. 2007. Contractile three-dimensional bioengineered heart muscle for myocardial regeneration. *J. Biomed. Mater. Res. A* 80A, 719-731.
- Humphrey, J.D. 2002. *Cardiovascular solid mechanics: Cells, tissues, and organs.* Springer-Verlag, New York.
- Ifkovits, J.L., Devlin, J.J., Eng, G., Matens, T.P., Vunjak-Novakovic, G., Burdick, J.A. 2009. Biodegradable fibrous scaffolds with tunable properties formed from photocrosslinkable poly(glycerol sebacate). *ACS Appl. Mater. Interfaces* 1(9), 1878-1892.

- International, A. Standard Test Methods for Vulcanized Rubber and Thermoplastic Elastomers in Tension. 2002, ASTM Committee D11 on Rubber: West Conshocken, PA.
- Jain, A.R., Mallya, B.S.S., Gupta, V.M., Shah, D.S., Trivedi, B.R., Shastri, N.A., Mehta, C.B., Jain, K.A., Bhavasar, N.R., Naik, A.M., Shah, U.J., Gandhi, P.S., Goyal, R.K. 2007. Beneficial effects of endoventricular circular patch plasty in patients with left ventricular systolic dysfunction and left ventricular dyskinetic or akinetic apical segment. *Indian J. Thorac. Cardiovasc. Surg.* 23, 16-24.
- Janz, R.F., Grimm, A.E. 1973. Deformation of Diastolic Left Ventricle. Nonlinear Elastic Effects. *Biophys. J.* 13,689-704.
- Jeong, C.G., Hollister, S.J. 2010. Mechanical and biochemical assessments of 3D poly (1,8 octanediol-co-citrate) scaffold pore shape and permeability effects on in vitro chondrogenesis using primary chondrocytes. *Tissue Eng. A.* 16(12), 3759-3768.
- Jeong, C.G. and Hollister, S.J. 2010. Mechanical, permeability, and degradation properties of 3D designed poly(1,8 octanediol-co-citrate) scaffolds for soft tissue engineering. *J. Biomed. Mater. Res. B* 3B(1),141-149.
- Kang, Y., Yang, J., Khan, S., Anissian, L., Ameer, G.A. 2006. A new biodegradable polyester elastomer for cartilage tissue engineering. *J. Biomed. Mater. Res. A* 77(2), 331-339.
- Kemppainen, J.M., Hollister, S.J. 2010. Tailoring the mechanical properties of 3D-designed poly(glycerol sebacate) scaffolds for cartilage applications. *J. Biomed. Mater. Res. A* 94A(1), 9-18.

- Kofidis, T., Akhyari, P., Boublik, J., Theodorou, P., Martin, U., Ruhparwar, A., Fischer, S., Eschenhagen, T., Kubis, H.P., Kraft, T., Leyh, R., Haverich, A. 2002. In vitro engineering of heart muscle: Artificial myocardial tissue. *J. Thorac. Cardiovasc. Surg.* 124, 63-69.
- Lee, K.Y. and Mooney, D.J. 2001. Hydrogels for tissue engineering. *Chem. Rev.* 101(7), 1869-77.
- Marsano, A., Maidhof, R., Tandon, N., Gao, J., Wang, Y., Vunjak-Novakovic, G. 2008. Engineering of functional contractile cardiac tissues cultured in a perfusion system. 30th Annual International Conference of the IEEE Engineering in Medicine and Biology Society. 3590-3593.
- Marsano, A., Maidhof, R., Wan, L.Q., Wang, Y., Gao, J., Tandon, N., Vunjak-Novakovic, G. 2010. Scaffold stiffness affects the contractile function of three-dimensional engineered cardiac constructs. *Biotechnol. Prog.* 26, 1382-1390.
- Migneco, F., Huang, Y.C., Birla, R.K., Hollister, S.J. 2009. Poly(glycerol-dodecanoate), a biodegradable polyester for medical devices and tissue engineering scaffolds. *Biomater.* 30(33), 6479-6484.
- Misof K., Landis, W.J., Klaushofer, K., Fratzl, P. Collagen from the osteogenesis imperfecta mouse model (OIM) shows reduced resistance against tensile stress. *J. Clin. Invest.* 1997;100(1):40-5.
- Miyamoto, K., Sasaki, M., Minamisawa, Y., Kurahashi, Y., Kano, H., Ishikawa, S. 2004. Evaluation of in vivo biocompatibility and biodegradation of photocrosslinked hyaluronate hydrogels (HADgels). *J. Biomed. Mater. Res.* 70A, 550-9.

- Motlagh, D., Allen, J., Hoshi, R., Yang, J., Lui, K., Ameer, G. 2007. Hemocompatibility evaluation of poly(diols citrate) in vitro for vascular tissue engineering. *J Biomed Mater Res A* 82(4), 907-916.
- Motlagh, D., Yang, J., Lui, K.Y., Webb, A.R., Ameer, G.A. 2006. Hemocompatibility evaluation of poly(glycerol-sebacate) in vitro for vascular tissue engineering. *Biomater.* 27, 4315-4324.
- Murphy, W.L., Dennis, R.G., Kileny, J.L., Mooney, D.J. 2002. Salt fusion: An approach to improve pore interconnectivity within tissue engineering scaffolds. *Tissue Eng.* 8, 43-52.
- Nardinocchi, P. and L. Teresi. 2007. On the active response of soft living tissues. *J. Elast.* 88, 27-39.
- Park, H., Larson, B.L., Guillemette, M.D., Jain, S.R., Hua, C., Engelmayer, G.C., Freed, L.E. 2011. The significance of pore micro-architecture in a multilayered elastomeric scaffold for contractile cardiac muscle constructs. *Biomater.* 32, 1856-1864.
- Park, K.J., Shim, J.-H., Kang, K.S., Yeom, J., Jung, H.S., Kim, J.Y., Lee, K.H., Kim, T.-H., Kim, S.-Y., Cho, D.-W., Hahn, S.K. 2011. Solid free form fabrication of tissue-engineered scaffolds with a poly(lactic-co-glycolic acid) grafted hyaluronic conjugate encapsulating an intact bone morphogenetic protein-2/poly(ethylene glycol) complex. *Adv. Funct. Mater.* 21, 2906-2912.
- Patrick, C.W., Zheng, B., Johnston, C., Reece, G.P. 2002. Long-term implantation of preadipocyte-seeded PLGA scaffolds. *Tissue Eng.* 8(2), 283-293.

- Patrick, C.W. 2001. Tissue engineering strategies for adipose tissue repair. *The Anat. Rec.* 263, 361-366.
- Radisic, M., Park, H., Gerecht, S., Cannizzaro, C., Langer, R., Vunjak-Novakovic, G. 2006. Biomimetic approach to cardiac tissue engineering: oxygen carriers and channeled scaffolds. *Tissue Eng.* 12, 2077-2091.
- Radisic, M., Vunjak-Novakovic, G. 2005. Cardiac tissue engineering. *J. Serb. Chem. Soc.* 70, 541-556.
- Roeder, B.A., Kokini, K., Sturgis, J.E., Robinson, J.P., Voytik-Harbin, S.L. 2002. Tensile mechanical properties of three-dimensional type I collagen extracellular matrices with varied microstructure. *J. Biomech. Eng. – Trans. ASME.* 124(2), 214-22.
- Roy, T.D., Simon, J.L., Ricci, J.L., Rekow, E.D., Thompson, V.P., Parsons, J.R. 2003. Performance of degradable composite bone repair products made via three-dimensional fabrication techniques. *J. Biomed. Mater. Res.* 66(2), 283-291.
- Sabbah, H.N., Shimoyama, H., Kono, T., Gupta, R.C., Sharov, V.G., Scicli, G., Levine, T.B., Goldstein, S. 1994. Effects of Long-Term Monotherapy with Enalapril, Metoprolol, and Digoxin on the Progression of Left-Ventricular Dysfunction and Dilation in Dogs with Reduced Ejection Fraction. *Circ.* 89, 2852-2859.
- Saito, E., Kang, H., Taboas, J.M., Diggs, A., Flanagan, C.L., Hollister, S.J. 2010. Experimental and computational characterization of designed and fabricated 50:50 PLGA porous scaffolds for human trabecular bone applications. *J Mater Sci Mater Med.* 21(8), 2371-2383.

- Sakai, Y., Matsuyama, Y., Takahashi, K., Sato, T., Hattori, T., Nakashima, S., Ishiguro, N. 2007. New artificial nerve conduits made with photocrosslinked hyaluronic acid for peripheral nerve regeneration. *Biomed. Mat. Eng.* 17, 191-7.
- Seidlits, S.K., Khaing, Z.Z., Petersen, R.R., Nickels, J.D., Vanscoy, J.E., Shear, J.B., Schmidt, C.E. 2010. The effects of hyaluronic acid hydrogels with tunable mechanical properties on neural progenitor cell differentiation. *Biomaterials.* 31, 3930-3940.
- Seliktar, D., Black, R.A., Vito, R.P., Nerem, R.M. 2000. Dynamic mechanical conditioning of collagen-gel blood vessel constructs induces remodeling in vitro. *Ann. Biomed. Eng.* 28, 351-62.
- Stacey, D.H., Hanson, S.E., Lahvis, G., Gutowski, K.A., Masters, K.S. 2009. In vitro adipogenic differentiation of preadipocytes varies with differentiation stimulus, culture dimensionality, and scaffold composition. *Tissue Eng. A* 5(11), 3389-3399.
- Sun, Z.J., Chen, C., Sun, M.-Z., Ai, C.-H., Lu, X.-L., Zheng, Y.-F., Yang, B.-F., Dong, D.-L. 2009. The application of poly (glycerol-sebacate) as biodegradable drug carrier. *Biomater.* 30, 5209-5214.
- Sundback, C.A., Shyu, J.Y., Wang, Y., Faquin, W.C., Langer, R.S., Vacanti, J.P., Hadlock, T.A. 2005. Biocompatibility analysis of poly(glycerol sebacate) as a nerve guide material. *Biomater.* 26, 5454-5464.
- Von Heimburg, D., Zachariah, S., Kuhling, H., Heschel, I., Schoof, H., Hafemann, B., Pallua, N. 2001. Human preadipocytes seeded on freeze-dried collagen scaffolds investigated in vitro and in vivo. *Biomaterials* 22(5), 429-438.

- Wang, Y. 2008. Biorubber/Poly(glycerol sebacate). Encyclopedia of Biomaterials and Biomedical Engineering, second ed. Informa Healthcare USA, Inc., New York.
- Wang, Y.D., Ameer, G.A., Sheppard, B.J., Langer, R. 2002. A tough biodegradable elastomer. *Nat. Biotechnol.* 20, 602-606.
- Wang, L. and Stegemann, J.P. 2010. Thermogelling of chitosan and collagen composite hydrogels initiated with beta-glycerophosphate for bone tissue engineering. *Biomaterials.* 31(14), 3976-85.
- Watanabe, S., Shite, J., Takaoka, H., Shinke, T., Imuro, Y., Ozawa, T. et al. 2006. Myocardial stiffness is an important determinant of the plasma brain natriuretic peptide concentration in patients with both diastolic and systolic heart failure. *Eur. Heart J.* 27(7), 832-8.
- Williams, J.M., Adewunmi, A., Schek, R.M., Flanagan, C.L., Krebsbach, P.H., Feinberg, S.E., Hollister, S.J., Das, S. 2005. Bone tissue engineering using polycaprolactone scaffolds fabricated via selective laser sintering. *Biomaterials* 26, 4817-4827.
- Wu, X., Levenston, M.E., Chaikof, E.L. 2006. A constitutive model for protein-based materials. *Biomaterials* 27, 5315-5325.
- Ye, Q., Zund, G., Benedikt, P., Jockenhoevel, S., Hoerstrup, S.P., Sakyama, S., Hubbell, J.A., Turina, M. 2000. Fibrin gel as a three-dimensional matrix in cardiovascular tissue engineering. *Eur. J. Cardiothorac. Surg.* 17, 587-591.
- Zhu, Y., Liu, T., Song, K., Jiang, B., Ma, X., Cui, Z. 2009. Collagen-chitosan polymer as a scaffold for the proliferation of human adipose-derived stem cells. *J. Mater. Sci. Med.* 20, 799-808.